Development and Application of Quantitative ^{1}H NMR Spectroscopy and Chemometrics for Quality Determination of Red Fruit (*Pandanus conoideus*, Lam.) Oil

Dissertation zur Erlangung des naturwissenschaftlichen
Doktorgrades der Julius-Maximilians-Universität Würzburg

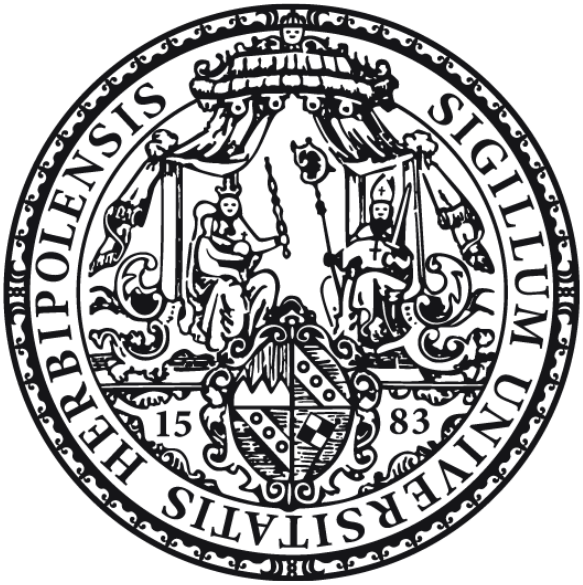

vorgelegt von

LILING TRIYASMONO

aus Wonogiri, Indonesien

Würzburg, 2022

Eingereicht bei der Fakultät für Chemie und Pharmazie am

_____

Gutachter der schriftlichen Arbeit

1. Gutachter:_____

2. Gutachter:_____

Prüfer des öffentlichen Promotionskolloquiums

1. Prüfer:_____

2. Prüfer:_____

3. Prüfer:_____

Datum des öffentlichen Promotionskolloquiums

_____

Doktorurkunde ausgehändigt am

_____

“Life is a journey, enjoy every period. Sometimes it's straight, turns, uphill and downhill. Our duty is just to get through to the end in the best way possible”

-To my family-

ACKNOWLEDGEMENTS

First and foremost, I would like to thank Allah, the almighty, for everything in my life.

I would also like to express my sincere gratitude and appreciation to:

Prof. Dr. Ulrike Holzgrabe

The Chairperson of Pharmaceutical and Medicinal Chemistry, Institute for Pharmacy and Food Chemistry of Julius-Maximilians University Würzburg, for the supervision of this work, her continuous support in all phases of my study, the trust she placed in me, the opportunity to prepare this work independently, and her encouragement in my studies. Without her guidance, this work could not have been completed.

I would also like to direct my gratitude and acknowledgements to the Rector of Lambung Mangkurat University 2014-2022 (Prof. Dr. Sutarto Hadi, M.Si., M.Sc) for financial support and the Institute for Pharmacy and Food Chemistry of Julius-Maximilians University Würzburg, for providing me with the research facilities.

Special thanks to the Dean of Mathematic and Natural Science Faculty of Lambung Mangkurat University (Abdul Gafur, Ph.D.) who gives me the permission to continue my study. I also wish to express my sincere thanks to Prof. Dr. rer.nat. RR. Endang Lukitaningsih and Prof. Dr. Abdul Rohman from Faculty of Pharmacy, Gadjah Mada University, for their willingness to provide a letter of recommendation so that I can continue my study, their patience in listening and always supporting me which very helpful during the process of completing this study.

Furthermore, special thanks to Dr. Curd Schollmayer, who always by my side when I had questions and who always willing to discuss and solving the problems with NMR spectroscopy. Dr. Jens Schmitz who always helps to facilitate and discuss on the titration work. Dr. Ludwig Höllein who always facilitates the IT work and the submission paper process.

I also wish to express my gratitude to all my friends, my colleagues in Würzburg (Adrian Leistener, Cristian Lombo, Dr. Christine Heinz, Emilie Hovah, Dr. Florian Geyer, Dr. Jonas Urlaub, Dr. Jonas Wohlfart, Joshua Weinmann, Laura Backer, Lukas Kirchner, Mohamed Marzouk, Nelson Masota, Nicolas Scheuplein, Rasmus Walther, Dr. Ruben Pawellek, Sebastian Schmidt, Sylvia Klapper, Theresa Lohr) Frau Möhler and Frau Weidinger for the peaceful and friendly academic atmosphere,have helped me to finish this research and also my colleagues in Banjarmasin (Dodon T Nugrahadi. M.Eng, Dr. Gunawan, Dr. Heri B Santoso, Khoerul Anwar M.Sc, Sri Cahyo Wahyono M.Si, Dr. Totok Wianto) which always provide moral support and encouragement, prayers and pleasant discussions during this PhD study period.

Finally, the greatest appreciation and honours are assigned to my beloved wife (Lisa Andina) and my son (Fatih Ahsan Maheswara) for their unconditional love, patience, understanding, and prayers. Your support was most valuable as I struggled to complete this study. Also thank you so much to my parents (Suwarmi & Hargiyanto), parents in law (Alm. Noor Salmah & Alm. Zulkifli), my brothers and sisters for their continuous moral support, prayers and encouragement.

TABLE OF CONTENTS

LIST OF ABBREVIATIONS

ATR	Attenuated Total Reflectance
AV	Acid value
DA	Discriminant Analysis
DNA	Deoxyribonucleic acid
DMSO	Dimethylsulfone
DTGS	Deuterium Triglycine Sulfate
EV	Ester value
FA	Fatty acid
FFA	Free fatty acid
FID	Free induction decay
FTIR	Fourier Transform Infrared
FT-NIR	Fourier Transform near Infrared
GLC	Gas Liquid Chromatography
HDL	High-Density Lipoprotein
IC_{50}	Half maximal inhibitory concentration
IV	Iodine value
LD_{50}	Lethal Dose resulting in 50% mortality
LDL-C	Lipoprotein-cholesterol
LOD	Limit of Detection
LOQ	Limit of Quantification
MUFA	Monounsaturated fatty acid
NOE	Nuclear Overhauser Effect

NMR	Nuclear Magnetic Resonance
Ph Eur	European Pharmacopoeia
PCA	Principal Component Analysis
PCR	Principal Component Regression
PLS	Partial Least Square
PLSR	Partial Least Square Regression
PUFA	Polyunsaturated fattyacid
RFO	Red fruit oil
RMSEC	Root Mean Square Error Calibration
RMSEP	Root Mean Square error Prediction
RMSEV	Root Mean Square error validation
TAG	Triacylglycerides
SV	Saponification value
Total UFA	Total Unsaturated Fattyacid
qNMR	quantitative Nuclear Magnetic Resonance

1. INTRODUCTION

Traditional medicine is the most widely used complementary and alternative medicine therapy worldwide[1]. Research from Pengpid S and Peltzer S[2] (2018) stated that 24.4% to 32.9% of the Indonesian population used traditional medicine every month. This population includes those who are older, live in urban and rural areas, are unhealthy, have chronic conditions, have experience symptoms of depression and sleep disorders. Therefore, Indonesia, which is widely known as the center of world biodiversity, has utilized one of its plant species, red fruit (*Pandanus conoideus*, Lam.), as one of the traditional medicinal substances.

1.1 Red Fruit Oil

Pandanus conoideus Lam. is an endemic plant in Papua, Indonesia, and Papua New Guinea. The local name of *Pandanus conoideus* is “red fruit”. This fruit has an unusual shape with 68-110 cm in length and a 10-15 cm diameter. It is red and contains a large amount of oil, known as Red Fruit Oil (RFO)[3]. **Fig. 1** shows an overview of red fruit trees, red fruit, crude red fruit oil, and red fruit oil products.

A B C D

Fig. 1 Red fruit trees (A), Red fruit (B), crude red fruit oil (C), and example of red fruit oil products (D).

Some species of the genus Pandanus are essential for people who live in the highlands of the Papua and West Papua Provinces, one of which is *Pandanus conoideus*, Lam. It is known by different local names in Indonesia, such as Pandan Seran (Maluku), saun (Seram), Sihu (Halmahera). At the same time, Papuan calls this plant Buah Merah, which means red fruit. People of Papua New Guinea also use this plant, commonly known as Marita (Pidgin)[4]. Red fruit grows at wider altitudes from the coast up to 1700 m above sea level[5]. Therefore, these plants spread almost all over Papua and West Papua territory. However, the tree can predominantly be found in Jayawijaya Mountains, Jayapura, Manokwari, Nabire, Timika, and Sorong (sub-district of Ayamaru)[6]. The botanical classification of the *Pandanus conoideus*, Lam.[7], is:

Kingdom : Plantae

Division : Spermatophyte

Class : Angiospermae

Subclass : Monocotyledonae

Order : Pandanales

Family : Pandanaceae

Species : *Pandanus conoideus,* Lam.

Traditionally, red fruit is used by Papuanese as an edible oil to increase energy and strengthen the immune system. RFO is a natural product obtained from extracted *Pandanus conoideus,* Lam. fruit. RFO contains active components such as phenols, carotenoids, tocopherols, and unsaturated fatty acids. RFO's reported characteristics differ from other Indonesian vegetable oils such as coconut and palm oil. RFO consist of by saturated fatty acid (10-20 %), monounsaturated fatty acid (oleic) (60-70 %), and polyunsaturated (2-10 %). The main components of red fruit oil and the nutritional content of RFO are presented in **Table 1**.

Table 1. Chemical and nutritional properties of RFO per 100 g sample[8]

Parameter	Value
Moisture (g)	0.70
Energy (kcal)	868
Protein (g)	<0.10
Lipid (g)	99.70
Carbohydrate (g)	5.10
Sodium (mg)	3
α-Carotene (µg)	130
β-Carotene (µg)	1.980
β-Cryptoxanthin (µg)	1.460
Water (g)	0.30
Calorific value (kcal)	899
Calorific value (kJ)	3695
α-Tocopherol (mg)	21.20

Recent studies indicate that the RFO is the most popular consumed in herbal commerce. This oil is used for medicinal purposes; the literature records some pharmacological studies with this RFO. Some of the benefits of red fruit oil are presented in **Table 2**.

The substantial pharmacological potential makes RFO a promising candidate for herbal products or functional food. Various RFO products are already on the market in Indonesia and abroad. However, multiple factors, such as geographical region, harvest time, and processing method, cause variability of the oil content of this red fruit[24]. Furthermore, quality assurance is required under regulations to ensure that RFO products have a qualified standard as an alternative to traditional medicine or functional food.

Table 2. The utilization of RFO

No	Study of activity	Technical information	References
1	Antioxidant activity		
	Natural Antioxidant	14.45 ppm	9,10
	Decreased oxidative DNA damage	50 µM benzo[a]pyrene + RFO, 500 µM tert-butylhydroperoxide + RFO, RFO at a dilution of 1: 10,000 for 24 h	11
2	Anticancer activity		
	Prevention of breast cancer development	LD_{50} 600 ppm, LD_{50} 0.25 µL/mL	12, 13, 14
	Prevention of colorectal cancer development	LD_{50} 200 ppm	12
	Prohibition of the growth of lung cancer cells	500 mg RFO/mL	8, 15
	Induction of apoptosis of servix cancer sells	upregulation of p53ser46 expression and downregulation of pAkt and mTOR	16
3	Antihyperchlolesteromic Activity		
	Reduction the low-density lipoproteincholesterol (LDL-C) in the blood	alloxan induction + RFO 0.12 mL	17
4	Hypoglycaemeic Activity		
	Reduction of blood glucose levels	RFO 45 mL, 0.5 %, 0.25 %	18, 19
5	Antiinflammatory activity		
	Inhibition inflamation of bowel diseases characterized by chronic inflamation to colorectal cancer	the inhibition rate was higher at 97% 24 hours after inflamation induction	20
6	Immunomodulatory activity	increase the percentage of CCR5 mRNA human blood imune cell by 13.54% on the HIV patient.	21
7	Hepatoteraphy activity		
	Recover liver damage	RFO 6% b/v	22
8	Natural pigments	heptadecene-(8)-carbonic acid (79.66%), hexadecanoid acid (5.62%), and 2,2-dimethyltetrahydrofuran (2.95%)	23

1.2. Quality assesment of oils

Oils are generally defined as triacylglycerides (TAG), liquid at room temperature. Based on their chemical properties, oils can be characterized by specifying values commonly known as fat parameters. The value of each parameter can be used as a basis for determining oil quality[25].

The chemical characteristics of edible fats and oils, including acid value (AV), saponification value (SV), ester value (EV), iodine value (IV), and fatty acid content, are critical parameters of interest. They determine the shelf-life quality and hence the economic value of oils. A list of chemical characteristics of edible fats and oils cited from the Ph Eur 10.0[26] standard methods is given in **Table 3**.

Table 3. Some chemical characteristics of edible fats and oils

Analysis	Abbreviation	Ph.Eur	Method	Determination of
Acid value	AV	2.05.01	Titration	Free fatty acid
Ester value	EV	2.05.02	(SV-AV)	Ester degree
Iodine value	IV	2.05.04	Titration	Unsaturated degree
Saponification value	SV	2.05.06	Titration	Average molecular weight
Fatty acid composition	-	2.04.22	GLC	Percentages of fatty acid (saturated, monounsaturated and polyunsaturated fatty acid)

The disadvantages of their determination which are e.g. described in international pharmacopoeias are the high consumption of solvents and other toxic chemicals and especially the poor specificity[27,28].

The AV measures the concentration of free fatty acids in fats and oils. The AV is determined by a titration based on the neutralization reaction of potassium hydroxide in ethanol. The values are usually expressed as a percent of free fatty acids calculated as oleic acid, lauric, ricinoleic, and palmitic acids and indicating the hydrolysis of the fat and/or oil. Therefore, free fatty acids are an essential quality indicator during oil processing and storage.

In order to measure SV, edible fats and oils are refluxed with a defined quantity of known potassium hydroxide, in an ethanol solution. Subsequently, non-reacted potassium hydroxides

are back titrated with standard hydrochloric acid. SV represents the average molecular weight of TAG. The higher SV measures the lower is the molecular weight of the TAG of fats and oils.

The IV characterizes the content of unsaturated fatty acids in TAG. When the mixture of edible fats and oils is added to a constant iodine bromide solution, the iodine molecules are added to the present double bonds of the TAG. The remaining iodine is titrated to the starch endpoint using the standard sodium thiosulfate. Therefore, IV is a valuable parameter for evaluating vegetable and fish oils. For example, olive oil contains monounsaturated fatty acids (18:1) and has an IV of 75–90, while soybean oil and corn oil are rich in polyunsaturated fatty acids (18:2); therefore, they have IV in the range from 120 to 140.

The composition of fatty acids (FA) is a valuable parameter in distinguishing edible fats and oils. Therefore, with GLC, the composition of fatty acids and oils from edible oils can be determined using a flame ionization detector (FID) and a capillary column. Therefore, the fatty acids have to be derivatized to give a methyl ester.

Different sophisticated instrumental techniques have been applied as an alternative to the classical indices SV, AV, EV, and IV. These techniques include pH-meters[29], chromatography, especially gas chromatography[30], high-performance liquid chromatography[31], high-performance size exclusion chromatography[27], and FTIR spectroscopy[32,33]. Generally, the results are in good accordance with the classical indices. In 2013, the German Society for Fat Science issued a standard method [DGF C VI 21a (13)] for using FT-NIR to determine polar compounds, polymerized triacylglycerols, acid value and anisidine value on frying fats and oils[34].

1.3 NMR Spectroscopy

1.3.1 Principle of NMR Spectroscopy

All spectroscopic techniques have the same principle, namely the difference in energy between the two states. This condition is also the main principle of nuclear magnetic resonance (NMR) spectroscopy. In NMR, there are two nuclear states with nuclear spin quantum numbers of 1/2,

commonly referred to as α- and β-states. The intervention of the atomic nucleus external magnetic field (Bo) will cause an energy difference between the two nuclei[33], as illustrated in **Fig 2**. The energy difference (ΔE) between the two states is:

$$\Delta E = \gamma \hbar B_0 \quad (1)$$

where γ is the gyromagnetic ratio for a given nucleus and ħ the reduced Planck's constant. Each nucleus has a different gyromagnetic ratio, for example, gyromagnetic ratios of proton (^{1}H) and carbon (^{13}C) are 42.58 MHz/T and 10.71 MHz/T, respectively.

If a nucleus is placed in the magnetic field, the spins of the nucleus align along the magnetic field B_0[33]. Since the possible orientation of N of the spins is affected by the spin quantum number $I = 2I + 1$, in the case of hydrogen with I= ½, 2 energy levels (E1 and E2) will be generated, which allow for two types of orientation, namely: parallel and anti-parallel. As can be seen in **Fig. 2**. This energy level is known as the Zeeman level[35].

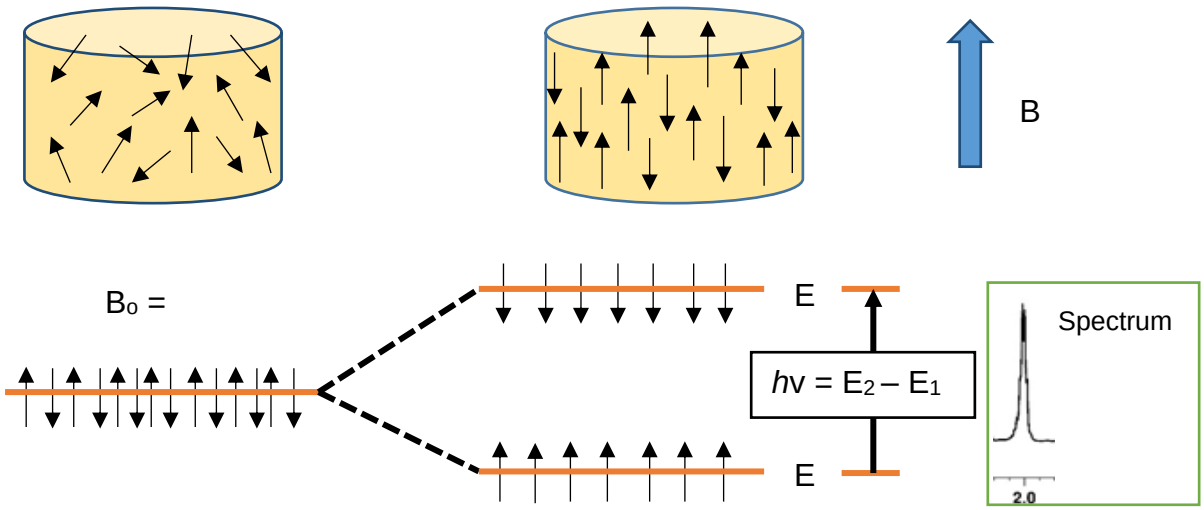

Fig. 2 Illustration of basic principle NMR: if a nucleus is in a magnetic field, resonance can absorb electromagnetic energy

A collection of nuclei of atoms with magnetic properties are distributed onto various energy levels defined by the orientation of their magnetic moments concerning an external magnetic field. This field is either homogeneous or inhomogeneous, depending on the NMR methodology. After reaching the so-called thermal equilibrium, nuclei are irradiated by a

second weak radiofrequency field. The excited nuclei give back their excess energy and return to low energy levels by two relaxation processes: interaction with the environment (lattice) or exchanging energy with neighboring nuclei at lower energy levels.

Furthermore, the rotating magnetization vector will produce a weak oscillating voltage in the surrounding coil to detect the voltage. Eventually, it will lead to the observed NMR signal. Relaxation of the bulk magnetization vector causes a loss of oscillatory voltage generating the NMR signal. It causes the NMR signal to decay over time, resulting in the observed independent free induction decay (FID). Furthermore, the final step of the processing of the NMR spectrum is the transformation of the time-dependent FID into a frequency-dependent spectrum. These two domains, time and frequency, are related by a simple function, and a frequency domain spectrum can be generated from a time domain signal by the Fourier transform[35].

1.3.2 Quantitative NMR

According to Holzgrabe[36] (2010), the most important fundamental relationship of qNMR is that the signal intensity (integrated signal area) I_x in the NMR spectrum is directly proportional to the number of nuclei N_x which are responsible for particular resonance:

$$I_x = K_s \cdot N_x \qquad (2)$$

where Ks is the spectrometer constant and remains the same for all resonances in a NMR spectrum. Furthermore, three main factors affect Ks, including (a) uniformity of pulse excitation over the entire spectral width. (b) the repetition time must be more than five times T1, and (c) the bandwidth decoupling, which causes an inherent distortion in intensity due to the nuclear overhauser effect (NOE).

There are two ways of quantifying analytes using NMR spectroscopy, including relative quantitation and absolute quantitation. First, the relative quantitation method is one of the easiest methods for NMR. Using the MX/MY molar ratio between the two compounds X and Y can be calculated by the equation:

$$\frac{M_x}{M_y} = \frac{I_x}{I_y} \cdot \frac{N_y}{N_x} \qquad (3)$$

K_S is not included in the formula because it will be the same for all the resonances in the spectrum, providing all the factors affect the optimized K_S. Similarly, the determination of the fraction of compound A in a mixture of components Z can also be calculated using the following formula:

$$\frac{M_A}{\sum_{i=1}^{Z} n_i} = \frac{I_A \cdot N_A}{\sum_{i=1}^{Z} I_i/N_i} \cdot 100\% \quad (4)$$

Second, there are two analytical procedures to determine the absolute concentration of analyte: (A) If all impurities (or other components) present in the NMR spectrum can be defined structurally and measured quantitatively, then the test is a fair difference from the value of 100%. This method is limited if the resonance of the impurity overlaps in the spectrum with the desired molecule or impurities (e.g., carbonates, moisture, an additive compound consisting of the same targeted signal) present in the sample. (B) In this procedure, provided the signals are separate, the purity of the principal component X can be calculated directly from the NMR spectrum using the following formula:

$$P_x = \frac{I_x}{I_{std}} \cdot \frac{N_{std}}{N_x} \cdot \frac{M_x}{M_{std}} \cdot \frac{m_{std}}{m} \cdot P_{std} \quad (5)$$

where, I, N, M, W and P are integral area, number of nuclei, molar mass, gravimetric weight and purity of analyte (x) and standard (std), respectively.

The quantitative inaccuracy of qNMR has been reported to be less than 2.0%, which is an acceptable limit for precision. Unlike other techniques, qNMR spectroscopy has certain acquisition and processing parameters and referencing techniques that need careful consideration in order to achieve a high degree of accuracy and precision. Sample preparation and experimental methods used may also introduce significant errors into quantitative NMR analysis, thereby reducing the accuracy and the precision of the resulting data. The analyst should therefore be well acquainted with acquisition (e.g., delay, pulse sequence, and acquisition time, T1) and processing parameters (phasing and baseline correction), referencing techniques and other analytical steps for careful optimization[36].

1.3.3 NMR method to determination of quality and main component oil

Nuclear magnetic resonance (NMR) is essential for studying dietary lipids, oils, and fats. Several studies have shown that low-resolution NMR has been successfully applied, including the determination of solid fat content in samples, melting point curves of semi-solid fats, or weight percentage of oil in foods[38,39].

Characteristics of the NMR instrument in the study of oils and fats depend on the purpose of the study. At a minimum, instruments with field strengths from 60 to 600 MHz have been used. Higher field strengths[40-43] provide better resolution, relatively minor signal overlap, and increased sensitivity. However, many studies indicate using medium-strength field instruments, such as 300 MHz[44-46], or even lower[47].

The sample preparation is relatively simple, because a certain amount of oil or fat is dissolved in a suitable deuterated solvent, in specific proportions, usually in a 5 mm diameter NMR tube. Deuterated chloroform is most commonly used as a solvent[48-52]. DMSO[53,54] and a mixture of deuterated dimethyl sulfoxide with $CHCl_3$[43-45].

Several previous studies demonstrated the use of various acquisition parameters. Among them; spectral acquisition is usually carried out at a controlled temperature between 20 ^{o}C and 30 ^{o}C[54,55]. Acquisition time ranges between 1.28 and 2.7 seconds[49,54], but appears in some recent authors to use a longer time, 5 - 7 s[45,56].

Recovery delays ranging from 1.5 to 53 seconds have previously been used[57-59], the majority at 2s[41,43,49,60]. However, some recent studies use a longer time[45,53,61]. The recovery delay depends on the relaxation time of T1 in the triglyceride molecule, which holds also true for the methylene proton of the glyceryl group. The longest T1 relaxation times are indicated by the proton of the terminal methyl group at 2.2 seconds. While the shortest T1 belongs to the four methylene protons on the glyceryl group at 0.36 seconds[57]. In addition, the relaxation delay time also considers T1 from the internal standard used[36]. Of note, T1 is dependent of the solvent used. The number of scans commonly used varies from 16 to 64, but depends on the purpose. The pulse width varies from 30^{o} to 90^{o} [42,43,62].

For NMR spectroscopy, the resonant position of the signal in the spectrum is called chemical shift. The chemical shift, intensity, and multiplicity contain helpful information on the different individual sample types of ^{1}H nuclei[63]. The chemical shift is referenced to ^{1}H signal of tetramethylsilane (TMS) being δ = 0.00 ppm.

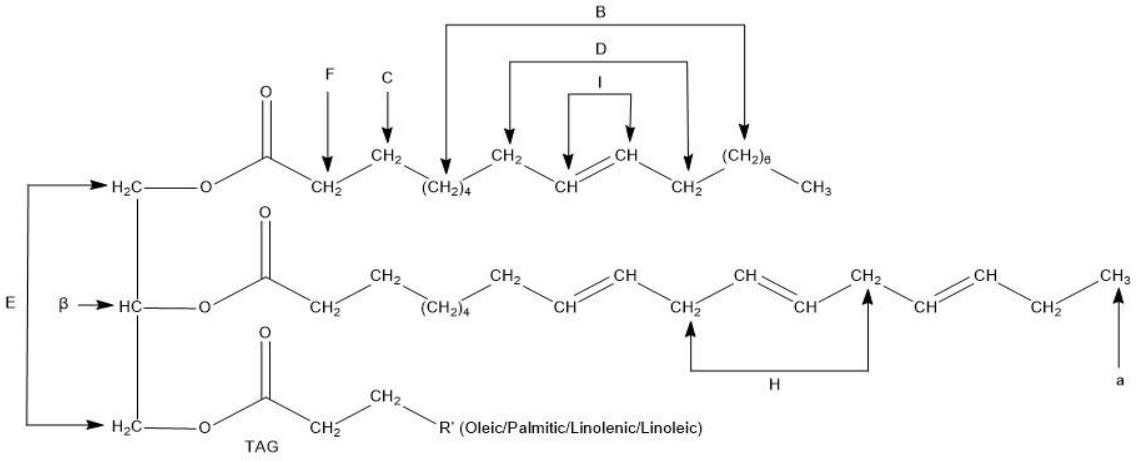

Fig. 3 Representative structures of TAG

As shown in **Fig. 3**, the triacylglycerol (TAG) structure is given, and **Table 4** shows the general proton signal chemical shifts of these compounds, the assignment of the protons to different functional groups, and the intensity of their typical relatives[56,61,65].

Table 4. Chemical shift assignment of the ^{1}H NMR signals of the main components of edible oils and fat

Signal	Functional group	Chemical shift (ppm)
A	(-C**H**$_3$) saturated, oleic and linoleic acyl chains	0.93-0.83
a	(-C**H**$_3$) linolenic acyl chains	1.03-0.93
B	(-(C**H**$_2$)n-) methylene groups	1.42-1.22
C	(–OCO-CH$_2$-C**H**$_2$-) β-methylene protons	1.70-1.52
D	(–C**H**$_2$-CH=CH-) allyl methylene protons	2.14-1.94
E	(–C**H**$_2$OCOR) methylene protons in the glyceryl group	4.32-4.10
F2	(–OCO-C**H**$_2$-) α-methylene protons	2.37-2.27
H	(=HC-C**H**$_2$-CH=) divinyl methylene protons	2.84-2.70
β	(-C**H**OCOR) methine proton at C2 of glyceride	5.26-5.20
I	(–C**H**=C**H**-) olefinic protons	5.37-5.27

^{1}H NMR experiments allow the determination of the parameters, such as average molecular weight and average number of double bonds of the sample, in a speedy and straightforward

way, using different approaches: some examples of determination quality parameters on oil and fats samples are given in **Table 5**.

Table 5 Some simple ^{1}H NMR analytical determination on oils and fats samples

Sample	NMR (MHz)	Parameter	References
Natural fat	60	Average molecular weight Iodine value	65
Butterfat	90	Average number of double bonds Average molecular weight Iodine value	66
Vegetable and Hydrogenated oils	300	Number of double-bond protons Average molecular weight Iodine value	57
Olive oil	400	Proportion of the several acyl groups	67
Leguminosae seed oils	500	Proportion of the several acyl groups	40
Edible vegetable oils	300	Proportion of the several acyl groups	68
Fish lipids	400	ω-3 polyunsaturated fatty acid proportion	69
Fish oils	500	ω-3 polyunsaturated fatty acid proportion	70
Fats and oils	300	Acid value, Saponification value, p-anisidin value, free fatty acid value	71
Kirk oil	400	Peroxide value	51
Walnuts oil	400	Unsaturated fatty acid compositions	46

1.4. FTIR Spectroscopy

1.4.1 Principle FTIR

Infrared (IR) spectroscopy is a technique based on the vibrations of the atomic bonds of a molecule. The IR spectrum is generally obtained by passing infrared radiation through the sample and determining how much radiation is absorbed[72]. Fourier-transform infrared (FTIR) spectroscopy is based on radiation interference between two partitions to produce an interferogram. The resulting signal is a function of the change in path length between the two partitions. Two distance and frequency domains, that mathematical methods can exchange, are called Fourier transforms[72]. The essential components of an FTIR spectrophotometer can be described as shown in **Fig. 4**.

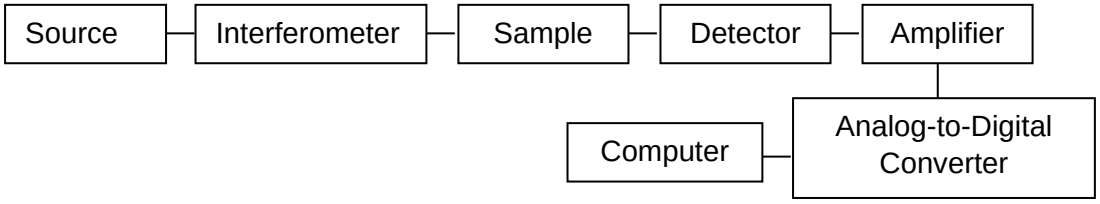

Fig. 4 Basic components of the FTIR spectrophotometer

Mid-region FTIR spectroscopy (4000-400 cm^{-1}) is a commonly used technique for analyzing organic compounds. This area generally uses Globar and Nernst light sources. The commonly used detector is Deuterium Triglycine Sulfate (DTGS). Currently, handling samples on FTIR spectrophotometers use the Attenuated Total Reflectance (ATR) technique. This ATR technique can obtain spectra of solids, liquids, semi-solids, and thin films. Besides being used for qualitative analysis, the ATR technique can also be used for quantitative analysis. The core of ATR is a crystal (infrared transparent material) with a high refractive index[73] (**Fig. 5**).

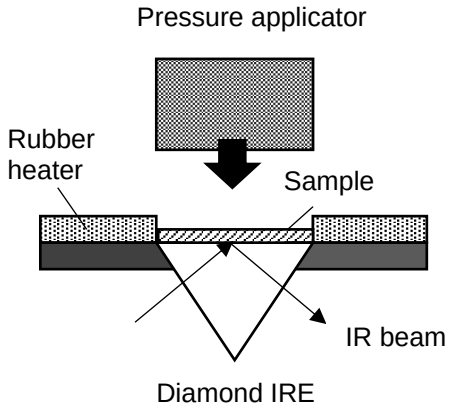

Fig. 5 Schematic overview of ATR with modified with permission from Shinzawa et al.[73]

The ATR description of the FTIR spectra of some edible oils provides essential information in determining the quality of these edible oils. This information is critical because every absorbance band that appears results from vibrations from the functional groups that make up the oil[74]. Consequently, oil analysis using the mid-region IR spectrum can provide information about bonds between atoms in the molecule and information regarding the various functional groups contained in the oil[75]. This absorption information is presented as a spectrum with wave

numbers in MIR spectroscopy or wavelengths in NIR spectroscopy on the x-axis and absorbance on the y-axis[75].

1.4.2 Quantitative FTIR

IR spectroscopy can also be used for quantitative analysis based on intensity or absorbance. The absorption of the IR spectrum band is directly proportional to the concentration of the corresponding functional group, as shown in the Lambert-Beer law ($A=\epsilon \cdot b \cdot c$)[76], where A is the measured absorbance, ϵ is the molar absorptivity coefficient, b is the path length, and c is the analyte concentration.

1.4.3 FTIR method to determination of quality and main component oil.

IR Spectroscopy technique, which is associated with multivariate calibration chemometrics such as partial least squares (PLS) and principal component analysis (PCA), can characterize vegetable oils, which allows characterizing differences between sample spectra[78]. For example, Rohman et al.[79] (2011) have distinguished RFO from canola oil and rice brain oil, all of which have similarities in the FTIR spectra profile, with the help of PLS chemometrics Discriminant Analysis (DA).

FTIR spectroscopy has also determined free fatty acid levels in olive oil copy by quantifying the band intensity at a wavenumber at 1710 cm^{-1}. In addition, after the sample is converted to a carboxylate anion, free fatty acid can be assessed at a wavenumber at 1570 cm^{-1}. Parameters related to the concentration of primary or secondary products of oil oxidation, such as peroxide value and anisidin value, can also be obtained from IR specta with a PLS combination within a specific calibration range. This technique has proven useful for monitoring the oxidation process as one of the parameters for the assessment of the oil quality[80].

The degree of unsaturation of the oil can also be determined using FT-IR spectroscopy according to the ratio absorbance of the aliphatic olefin group –C-H at 3007 cm^{-1} or from the absorbance of one band due to the vibration of -C=C- at 1500 cm^{-1} [80]. **Table 6** are given some examples of application FTIR for quantification on oil and fats sample.

Table 6 Some simple FTIR analytical determination on oils and fats sample using middle IR

Sample	Parameter	References
Fats and oils	Iodine value, Saponification value	32
Fats and oils	Peroxide value	81
Thermal stressed oil	Anisidine value and aldehyde	82
Edible oils and lard	Composition of concentrate	83
Palm oil	Iodine value	84
Edible oil	Oxidative stability	85
Frying oil	Quality parameters	86
Lubricant	Acid value	87
Edible oil	Trans content, IV, SV	88
Virgin coconut oil	Oxidative stability	89
Jatropa curcas seed Oil	Hydrolysis process	90
Red fruit oil	Iodine value, Acid value	91
Edible oil and mixtures	Fatty acid composition	78
Essential oils	Purity and quality	92

1.5 Chemometrics

Chemometrics is defined as applying mathematical and statistical methods in chemical measurements. Chemometrics in food and beverage analysis has been applied in many ways such as process monitoring and control, geographic origin determination of foodstuffs, food sources, and detection of adulteration[93]. Chemometrics in spectroscopy provides a way to develop multivariate calibrations from simple spectra to complex spectra[78]. In addition, the availability of more modern software on chemometrics can produce precise data models and more robust calibration models[74].

The chemometric method involves procedures for multivariate data analysis, which consists of a series of techniques used for data analysis with more than one variable[94]. The most common projection methods of multivariate data analysis used in olive oil studies, especially for classification and authentication, are Principal Component Analysis (PCA) and Partial Least Square (PLS).

1.5.1 PCA

Modern instruments efficiently do a multitude of measurements per unit of time. For example, if a spectroscopic sensor is used in situ to measure a spectrum at 300 wavelengths every 15 s, one hit will produce a 2406300 matrix of data, i.e. 72 000 values. However, this array's fraction of helpful information may be relatively low due to the multicollinearity. Therefore, data compression methods are used in chemometrics (unlike the traditional approach in which only

the results of some, essential measurements, are selected from the data) to provide a beneficial output[95]. **Fig 6** illustrates the equivalence between the experimental profile (^{1}H NMR spectra) and its graphical representation of the matrix.

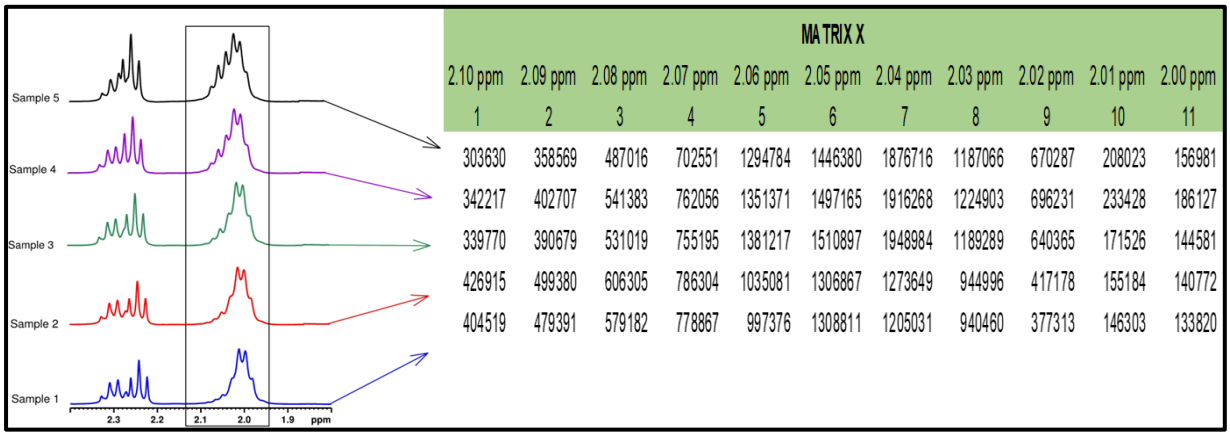

MATRIX X

2.10 ppm	2.09 ppm	2.08 ppm	2.07 ppm	2.06 ppm	2.05 ppm	2.04 ppm	2.03 ppm	2.02 ppm	2.01 ppm	2.00 ppm
1	2	3	4	5	6	7	8	9	10	11
303630	358569	487016	702551	1294784	1446380	1876716	1187066	670287	208023	156981
342217	402707	541383	762056	1351371	1497165	1916268	1224903	696231	233428	186127
339770	390679	531019	755195	1381217	1510897	1948984	1189289	640365	171526	144581
426915	499380	606305	786304	1035081	1306867	1273649	944996	417178	155184	140772
404519	479391	579182	778867	997376	1308811	1205031	940460	377313	146303	133820

Fig. 6 Graphical illustration of the equivalence between the collected experimental data (in this case, ^{1}H NMR spectra for 5 samples) and the data matrix X. Each row of the data matrix corresponds to the spectrum of a sample, whereas each column contains the value of a specific variable over all the individuals according to Biancolillo A and Marini F.[95]

New latent variables are used to represent the initial data in these methods. Two conditions must be fulfilled. First, the number of new variables should be much lower than the initial variables. Second, the loss caused by data compression should be commensurable with the noise. Data compression allows one to represent useful information in a more compact form convenient for visualization and interpretation.

The principal component analysis implies decomposition of the original 2D matrix X, i.e. representing it as a product of two 2D matrices **T** and **P**[96].

$$\mathbf{X} = \mathbf{T}\mathbf{P}^t + \mathbf{E} = \sum_{a=1}^{A} \mathbf{t}_a \mathbf{p}_a^t + \mathbf{E} \qquad (6)$$

In this equation, **T** is called the matrix of scores, **P** is the matrix of loadings, and **E** is the matrix of residuals (**Fig. 7**). The numbers of columns, **t**a in the matrix T and **p**a in the matrix **P**, are equal to the effective (chemical) rank of the matrix **X**. This value is designated by *A* and is called the number of principal components; naturally, it is smaller than the number of columns in the matrix **X**.

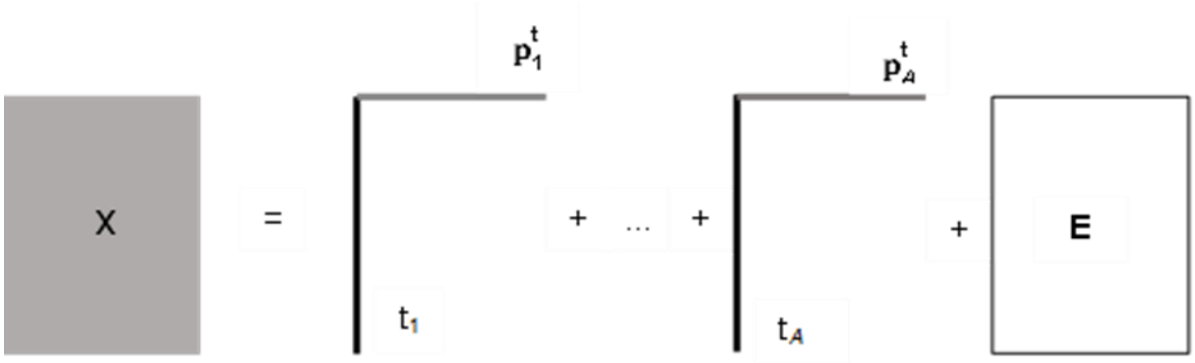

Fig. 7 Graphical view of the principal component analysis, adopted from and with permission Rodionova OY & Pomerantsev AL[97].

The principal component analysis is not only efficient in the problems of resolution, but is used to analyze any chemical data. In this case, the score T and loading P matrices can no longer be interpreted as the spectra, concentrations, and the number of principal components A, as the number of chemical components present in the system. Nevertheless, even formal analysis of the scores and loadings helps understand the data structure.

Since the scores represent a new set of coordinates along highly informative (relevant) directions, they may be used in two- or three-dimensional scatterplots (scores plots). This offers a straightforward visualization of the data, which can highlight possible trends in data, presence of clusters or, in general, of an underlying structure. A schematic representation of how PCA works is displayed in **Fig 8**.

Loading vector p1 of the first principal component (PC1) determines the direction of the new axis along which the data change more appreciably. The projections of all initial points on this axis form vector t1. The second principal component p2 is orthogonal to the first one, its direction (PC2) corresponding to the largest variation in the residuals (shown by segments perpendicular to the axis p1).

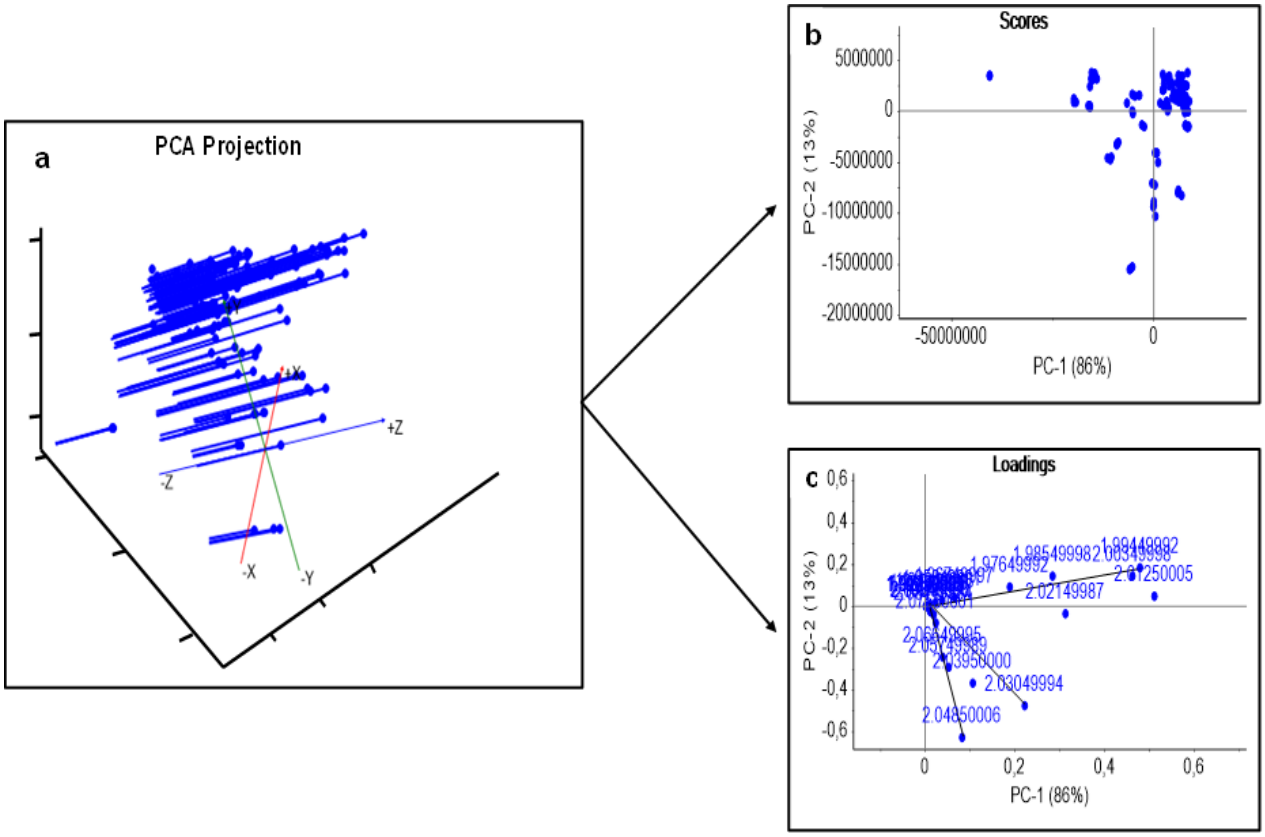

Fig. 8 Graphical illustration of the basics of PCA. The samples, here represented in a three-dimensional space (a), are projected onto a two-dimensional subspace spanned by the first two principal components. Inspection of the data set can be carried out by looking at the distribution of the samples onto the informative PC subspace (scores plot) (b) and interpretation can be then carried out by examining the relative contribution of the experimental variable to the definition of the principal components (loadings plot) (c) according to Biancolillo A and Marini F[95] and Rodionova OY & Pomerantsev AL[97]

When exploring the data by PCA, the attention is focused on score and loading plots. They bear information on the data structure. The proximity of two points implies their similarity, i.e. positive correlation. The points at a right angle are uncorrelated, while those in the opposite positions have a negative correlation. By using this approach in NMR and FTIR analysis, one can find out, for example, whether the linear section in the score plot corresponds to the regions of pure components in the spectrogram. The curved sections are regions of peak overlap, and the number of such sections corresponds to the number of components in the system. Whereas the score plot is used to analyze sample relationships, the loading plot is used to study the role of variables. By analyzing this plot similar to the scope plot, one can understand

which variables are interconnected or independent. A joint investigation of pair scores and loading plots also helps retrieve helpful information from the data[98].

1.5.2 PLS

Partial Least Squares Regression (PLSR) was proposed as an alternative method to calculate a reliable regression model in the presence of a variety of matrices, both simple and complex. PLS-regression, which uses a two-block predictive PLS model to model the relationship between two matrices, X and Y. In addition, PLS regression models give richer results than the traditional multiple regression approach.

Two blocks of data are used to solve problems of quantitative analysis. The first block **X** is the matrix of analytical signals (for example, spectra, chromatograms, and so on); the second block **Y** is the matrix of chemical parameters (for example, concentrations). The number of rows (I) in these matrices is equal to the number of samples, and the number of columns (J) in matrix X corresponds to the number of channels (wavelengths or chemicals shift) in which the signal is recorded. The number of columns (K) in matrix Y is equal to the number of chemical parameters, i.e. responses[95]. The purpose of calibration is to construct a mathematical model that would relate blocks X and Y and could be subsequently used to predict parameters y over a new row of analytical signals X. The simplest calibration model is one-dimensional regression (J=1, K=1).

$$y = a + bx \quad (7)$$

The second approach can be explained using Y=**C** and X=**S**. This approach currently prevails in chemometrics because it is more practically convenient. It directly predicts the required analytical parameter (for example, the concentration **C**) from the measured signal (spectrum **S**). In addition, modern regression methods (PCR, PLS) make it possible to handle data with errors in both blocks. PLS is the most widely used method for multivariate calibration in chemometrics. Therefore, an important distinction is that PLS implies simultaneous decomposition of matrices X and Y[98].

The projections are constructed in coordination in such a way as to maximize the correlation between the X-score and Y-score vectors. Therefore, the PLS regression describes much better complex relationships using a smaller number of the principal component. **Fig. 9** displayed operation data in basic PLS.

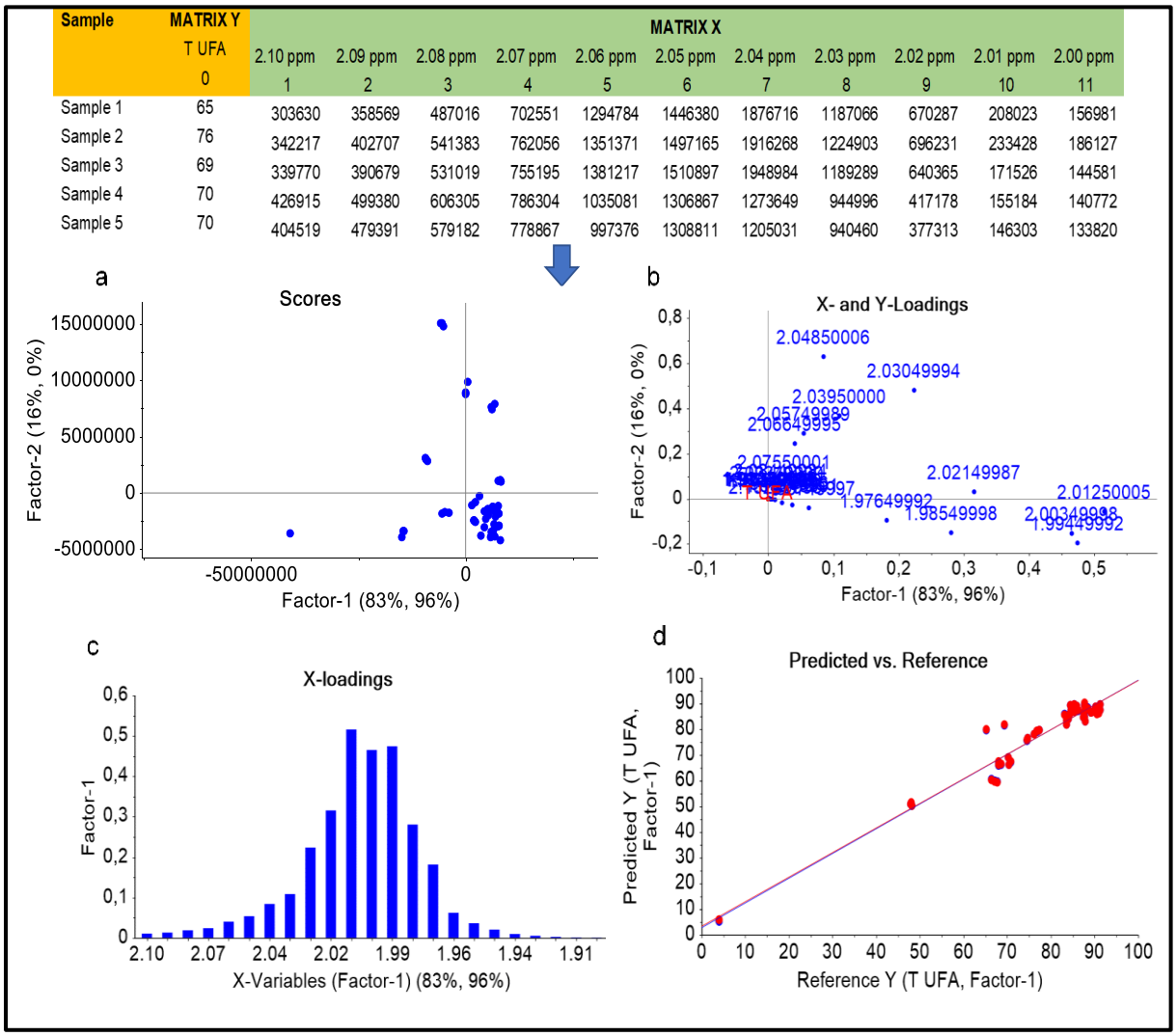

Fig. 9 Graphical illustration of the basics of PLS operation. The samples, represented in a two-matrix, are projected onto a low-dimensional subspace spanned by the two factors. Inspection of the data set can be carried out by looking at the distribution of the samples onto the informative scores plot (a), and interpretation can then be carried out by examining the relative contribution of the experimental variable to the definition of the X-and Y- Loading of Factor 1 (b). Plot of X-loading with axis X-Variables (PC1) of Factor 1 (c). Finally, PLS regression of predicted Y vs. reference Y can be determined by Factor 1 (d) according to Biancolillo A and Marini F.[95]

Furthermore, it should be emphasized that, for the calibration built by PLS to be accurate and reliable, the critical parameter is selecting several suitable latent variables to represent the exact data. For example, selecting a small number of components may risk not explaining all the relevant variances (underfitting). On the contrary, if it has too many (so that not only systematic information is captured but also noise), it can cause overfitting, i.e. the model is overfitting. As a result, it is very good at predicting the calculated sample but performs poorly on the new model. Therefore, an appropriate validation strategy is needed to reduce this risk, especially in selecting the optimal number of latent variables to lead to a minimum error during one of the validation stages. This validation model is commonly called cross-validation.

1.5.3 Validation multivariate analysis

Appropriate procedures for validating the chemometric model should be chosen to avoid model redundancy, as is the case when random noise is analyzed along with valuable data. Subsequently, the application of the most appropriate and optimal validation method uses a set of independent tests. In addition, this method makes it possible to estimate the new model to reliably estimate the predictive ability of the new model. Unfortunately, this is not always possible due to experimental and economic considerations, so the cross-validation method can be used.[96] In this validation method, a portion of samples is removed automatically from the model, simulating the remaining portion of data to subsequently estimate the model's quality with their aid. Thus, it is possible to obtain a real relative root mean square error of cross-validation[99]. If good results are obtained, the model is ready for practical use.

In principle, chemometrics relies on empirical models based on experimental measurements, which must then be able to fairly summarize data information, approximate the system being studied, and allow the prediction of one or more properties of interest. Therefore, many models can be calculated in principle on the same data. However, its performance can be affected by various factors, including the representative number of samples, the type of method itself, and algorithm[99]. Therefore, selecting the most appropriate model for the data under study and

verifying its reliability is very important, and the chemometric strategy for doing so is collectively referred to as validation[100].

Process validation requires an appropriate definition, which can be based on model parameters. However, in general, it is more likely to rely on the calculation of some residuals (i.e. the error criterion). In this context, to avoid over-optimism or bias, a correct validation strategy should involve estimating the model error on a different data set than the one used to calculate the model parameters. This method is usually achieved through external test sets or cross-validation.

Utilizing a second data with an entirely independent one as an evaluator of the model's performance to calculate the residuals is the best validation method to emulate. On the other hand, cross-validation based on repeated re-sampling of data set subsets for calibrating and testing can also be a feasible alternative, especially when the number of samples available is small and there is no possibility of constructing an external test set. Then, the predicted and residual values can be calculated on the the left-out samples. Finally, validation residual variance and standard error of cross validation (SECV) are computed. Generally, this method is more used for model selection (e.g., estimating the optimal number of components)[95].

References

1. Joos S, Glassen K, Musselmann B. 2012. Herbal medicine in primary healthcare in Germany: the patient's perspective. *Evid.-based Complement. Altern. Med*. 2012: 1-10. https://doi.org/10.1155/2012/294638
2. Pengpid S, Peltzer K. 2018. Utilization of traditional and complementary medicine in Indonesia: Results of a national survey in 2014–15. *Complement. Ther. Clin. Pract*. 33:156-163. https://doi.org/10.1016/j.ctcp.2018.10.006
3. Rohman A, Sugeng R, Che Man YB. 2012. Characterizaton of red fruit (Pandanus conoideus Lam) oil. *Int. Food Res. J.* 19 (2): 563-567.
4. Arumsari NI, Riyanto S, Rohman A. 2013. Some Phsico-chemical Properties of Red Fruit Oil (*Pandanus coneideus*, Lam.) from Hexane and Chloroform Fractions, *J.Food Pharm. Sci*. 1: 30-34.
5. Murtiningrum, Sarungallo ZL, Mawikere NL. 2012. The exploration and diversity of red fruit (*Pandanus conoideus,* Lam.) from Papua based on its physical characteristics and chemical composition. *J. Biol. Diversity.* 13(3): 124–29.
6. Budi M, Paimin FR. 2004. Red fruit (Pandanus conoideus Lam). *Penebar Swadaya* 3-26, 47-56, 67-68.
7. Wijaya H, Pohan HG. 2009. Kajian teknis standar minyak buah merah (*Pandanus conoideus* Lam). Prosiding PPI Standardisasi. Jakarta: Indonesia. 1-12.
8. Surono IS, Nishigaki T, Endaryanto A, Waspodo P. 2008. Indonesian biodiversities from microbes to herbal plants as potential functional food. *J. Fac. Agric. Shinshu Univ*. 44(1-2): 23-27.
9. Sangkala SA, Jura MR, Tangkas IM. 2014. Antioxidant activity test of red fruit (Pandanus baccari L) extractsi Poso area Central Sulawesi. *J. Akad. Kim*. 3 (4): 198-205.

10. Rohman A, Riyanto S, Yuniarti N, Saputra WR, Utami R, Mulatsih W. 2010. Antioxidant activity, total phenolic, and total flavaonoid of extracts and fractions of red fruit (*Pandanus conoideus,* Lam.). *Int. Food Res. J*. 17: 97-106.
11. Xia N, Schirra C, Hasselwander S, Förstermann, Li H. 2018. Red fruit (*Pandanus conoideus* Lam.) oil stimulates nitric oxide production and reduces oxidative stress in endothelial cells. *J. Funct. Foods*. 51: 65–74.
12. Moeljopawiro S, Anggelia MR, Ayuningtyas D, Widaryanti B, Sari Y, Budi IM. 2007. The effect of red fruit extract on breast and colorectal cancer cell lines. *Berkala Ilmiah Biologi* 6(2): 121 – 130.
13. Astirin OP, Harini M, Handajani NS. 2009. The effect of crude extract of Pandanus conoideus Lamb. var. yellow fruit on apoptotic expression of the breast cancer cell line (T47D). *Biodiversitas* 10 (1): 44-48.
14. Siagian R. 2015. Effect of red fruit (*Pandanus conoideus*) on the growth of breast cancer. *J. Agromed Unila*. 2(4): 500-503.
15. Nishigaki T, Hirose K, Waspodo I, Shigematsu H. 2010. Antitumor Effects of *Pandanus conoideus* in *in vitro* and *in vivo* Studies. *Laporan Penelitian*. Bogor: Balai Besar Industri Agro.
16. Achadiyani, Septiani L, Faried A, Bolly HM, Kurnia D. 2016. Role of the Red Fruit (*Pandanus conoideus* Lam.) Ethyl Acetate Fraction on the Induction of Apoptosis vs. Downregulation of Survival Signaling Pathways in Cervical Cancer Cells. *Eur. J. Med. Chem*. 13: 1-9.
17. Agnesa OS, Waluyo J, Prihatin J, Lestari SR. 2017. Potensi buah merah (Pandanus conoideus Lam.) dalam menurunkan kadar LDL darah tikus putih. *Bioeksperimen* 3 (1): 48-57.
18. Astuti Y, Dewi LLR. 2007. The effect of red fruit extract (*Pandanus conoideus* L.) to the blood glucose level. *Mutiara Medika* 7(1): 01-06.

19. Priyono SH. 2008. Kajian konservasi buah merah melalui kultur jaringan tanaman; ekstrasi, fraksinasi buah, uji antioksidan, dan uji antidiabetik. *J. Tek. Ling*. 9(3): 227-234.
20. Khiong K, Adhika OA, Chakravitha M. 2009. Inhibition of NF-κB pathway as the therapeutic potential of red fruit (*Pandanus conoideus* Lam.) in the treatment of inflammatory bowel disease. *JKM (Jurnal Kedokteran Maranatha)*. 9 (1): 69–75.
21. Tambaip T, Karo MB, Hatta M, Dwiyanti R, Natzir R, Massi MN, Islam AA, Djawad K. 2018. Immunomodulatory Effect of Orally Red Fruit (*Pandanus conoideus*) Extract on the Expression of CC Chemokine Receptor 5 mRNA in HIV Patients with Antiretroviral Therapy. *J. Immunol. Res*. 11: 15-21. https:// 10.3923/rji.2018.15.21
22. Wati A, Herman H, Sari DP. 2013. Uji hepatoterapi ekstrak etanol buah merah (Pandanus conoideus Lam.) asal kabupaten jayawijaya papua dengan parameter SGPT terhadap tikus putih jantan. *Jurnal Bionature*. 14 (2): 100-104.
23. Satriyanto B, Widjanarko SB, Yunianta. 2012. Heat stability of red fruit extract color as potential source of natural pigments. *Jurnal Teknologi Pertanian* 13(3): 157-168.
24. Sarungallo ZL, Hariyadi P, Andarwulan N & Purnomo EH. 2015. Characterization of chemical properties, lipid profile, total phenol and tocopherol content of oils extracted from nine clones of red fruit (Pandanus conoideus). *J. Natural Sci*. 49(2): 237–250.
25. Endo Y. 2018. Analytical Methods to Evaluate the Quality of Edible Fats and Oils: The JOCS Standard Methods for Analysis of Fats, Oils and Related Materials and Advanced Methods. *J. Oleo Sci*. 1: 67(1):1-10. https://doi: 10.5650/jos.ess17130
26. European Pharmacopoeia, 10th ed. 2020. European Department for the Quality of Medicines. Strasbourg. France: chapt. 2.5.1, 2.5.2, 2.5.4, 2.5.6.
27. Kamal-Eldin A, Pocorny J. 2005. In Handbook AOCS: Analysis of Lipid Oxidation, AOCS Press.
28. Shahidi F. 2005. In Handbook of Food Analytical Chemistry: Quality Assurance of Fats and Oils. John Wiley & Sons. 565-575.

29. Tubino M, Aricetti JA. 2013. A green potentiometric method for the determination of the iodine number of biodiesel. *Fuel* 103:1158–1163.
30. Xiea WQ, Chai X-S. 2016. An efficient method for determining the acid value in edible oils by solvent-assisted headspace gas chromatography**.** *Anal. Methods* 8: 5789-5793
31. Dobarganes, Velasco. 2002. Analysis of lipid hydroperoxides. *Eur. J. Lipid Sci. Technol*. 104: 420–428.
32. Van de Voort FR, Sedman J, Emo G, Ismail AA. 1992. Rapid and Direct Iodine Value and Saponofication Number Determination of Fats and Oils by Attenuated Total Reflactance/Fourier Transform Infrared Spectroscopy, *J. Am. Oil Chem. Soc*. 69(11): 1118-1123.
33. Guill'en MD, Cabo N. 2002. Fourier Transform Infrared Spectra Data versus Peroxide and Anisidine Values to Determine Oxidative Stability of Edible Oils. *Food Chem.* 77: 503-510. https://doi.org/10.1016/S0308-8146(01)00371-5
34. Gertz C, Fiebig HJ, Hancock JNS. 2013. FT-near infrared (NIR) spectroscopy screening analysis of used frying fats and oils for rapid determination of polar compounds, polymerized triacylglycerols, acid value and anisidine value [DGF C-VI 21a (13)]. *Eur. J. Lipid Sci. Technol.* 115: 1193-1197. https://doi.org/10.1002/ejlt.201300221
35. Günther H. 2013. NMR Spectroscopy: Basic Principles, Concepts, and Applications in Chemistry, Third Edition. Wiley-VCH, Weinheim, Germany
36. Holzgrabe U. 2010. Quantitative NMR spectroscopy in pharmaceutical applications. Prog. *Nucl. Magn. Reson. Spectrosc.* 57: 229–240. https://doi.org/10.1016/j.pnmrs.2010.05.001
37. Guillén MD, Ruiz A. 2001. High resolution ^{1}H nuclear magnetic resonance in the study of edible oils and fats. *Trends Food Sci. Technol.* 12(9): 328-338. https://doi.org/10.1016/S0924-2244(01)00101-7
38. Duynhoven JV, Gribnau MCM, Goudappel GJ, Shukla VKS. 1999. Solid fat content determination by NMR. *Inform.* 10: 479–484.

39. Aursand M, Rainuzzo JR, Grasladen H. 1993. Quantitative high-resolution ^{13}C and ^{1}H nuclear magnetic resonance of ω-3 fatty acids from white muscle of atlantic salmon (Salmo Salar). *J. Am. Oil Chem. Soc*. 70: 971–981.
40. Ketshajwang KK, Holmback J, Yeboah SO. 1998. Quality and compositional studies of some edible leguminosae seed oils in Botswana. *J. Am. Oil Chem. Soc*. 75: 741–743
41. Thoss V, Murphy PJ, Marriott R, Wilson T. 2012. Triacylglycerol composition of British bluebell (Hyacinthoides non-scripta) seed oil. *RSC Advances 2*(12): 5314–5322. https://doi.org/10.1039/c2ra20090b
42. Sarpal AS, Silva SR, Silva PRM, Monteiro TV, Itacolomy J, Cunha VS, Daroda RJ. 2015. Direct Method for the Determination of the Iodine Value of Biodiesel by Quantitative Nuclear Magnetic Resonance (q^{1}H NMR) Spectroscopy. *Energy and Fuels 29*(12): 7956–7968. https://doi.org/10.1021/acs.energyfuels.5b01462
43. Ingallina C, Cerreto A, Mannina L, Circi S, Vista S, Capitani D, Marini F. 2019. Extra-virgin olive oils from nine italian regions: An ^{1}H NMR-chemometric characterization. *Metabolites* 9(4): 1-12. https://doi.org/10.3390/metabo9040065
44. Moya MCM, Mendoza D, Ame´zquita FJ, Peris V, Bosch F. 1999. Study of the formation of carbonyl compounds in edible oils and fats by ^{1}H-NMR and FTIR. *J. Mol. Struct.* 482–483: 557–561.
45. Skiera C, Steliopoulos P, Kuballa T, Holzgrabe U, Diehl B. 2012. ^{1}H NMR approach as an alternative to the classical p-anisidine value method. *Eur. Food Res. Technol.* 235(6): 1101–1105. https://doi.org/10.1007/s00217-012-1841-5
46. Hama JR, Fitzsimmons-Thoss V. 2022. Determination of Unsaturated Fatty Acids Composition in Walnut (Juglans regia L.) Oil Using NMR Spectroscopy. *Food Anal. Methods* 15(5): 1226–1236. https://doi.org/10.1007/s12161-021-02203-0
47. Parker T, Limer E, Watson AD, Defernez M, Williamson D, Kemsley EK. 2014. 60 MHz ^{1}H NMR spectroscopy for the analysis of edible oils. TrAC - *Trends Anal. Chem*. 57: 147.158. https://doi.org/10.1016/j.trac.2014.02.006

48. Chen D, Liu Y, Hartman DR. 1999. Examination of fat oxidation products by FT-NMR and FTIR. *American Laboratory* 31: 15–18, 20.
49. Guillén MD, Ruiz A. 2003. Rapid simultaneous determination by proton NMR of unsaturation and composition of acyl groups in vegetable oils. *Eur. Food Res. Technol.* 105(11): 688–696. https://doi.org/10.1002/ejlt.200300866
50. Nieva-Echevarría B, Goicoechea E, Manzanos MJ, Guillén MD. 2014. A method based on ^{1}H NMR spectral data useful to evaluate the hydrolysis level in complex lipid mixtures. *Food Res. Int*. 66: 379–387. https://doi.org/10.1016/j.foodres.2014.09.031
51. Hafer E, Holzgrabe U, Wiedemann S, Adams KM, Diehl B. 2020. NMR Spectroscopy: Determination of Peroxide Value in Vegetable and Krill Oil by Using Triphenylphosphine as Tagging Reagent. *Eur. Food Res. Technol.* 122(5). https://doi.org/10.1002/ejlt.201900442
52. Qian J, Zhao C, Zhu H, Tong J, Zhao X, Yang H, Guo H. 2021. NMR detection of fatty acids content in walnut oil and compared with liquid chromatography. *J. Food Meas. Charact*. 15(3): 2716–2726. https://doi.org/10.1007/s11694-021-00813-0
53. Sacco A, Brescia MA, Liuzzi V, Reniero F, Guillou C, Ghelli S, Van Der Meer P. 2000. Characterization of Italian olive oils based on analytical and nuclear magnetic resonance determinations. *J. Am. Oil Chem. Soc*. 77(6): 619–625. https://doi.org/10.1007/s11746-000-0100-y
54. Almoselhy RIM, Allam MH, El-Kalyoubi MH, El-Sharkawy AA. 2014. ^{1}H NMR spectral analysis as a new aspect to evaluate the stability of some edible oils. *Ann. Agric. Sci*. 59(2): 201–206. https://doi.org/10.1016/j.aoas.2014.11.006
55. Castejón D, Fricke P, Cambero MI, Herrera A. 2016. Automatic ^{1}H-NMR screening of fatty acid composition in edible oils. *Nutrients 8*(2). https://doi.org/10.3390/nu8020093
56. Nieva-Echevarría B, Goicoechea E, Manzanos MJ, Guillén MD. 2015. Usefulness of ^{1}H NMR in assessing the extent of lipid digestion. *Food Chem.* 179: 182–190. https://doi.org/10.1016/j.foodchem.2015.01.104

57. Miyake Y, Yokomizo K, Matsuzaki N. 1998. Rapid determination of iodine value by ^{1}H nuclear magnetic resonance spectroscopy. *J. Am. Oil Chem. Soc.* 75: 15-19.

58. Mahanta BP, Sut D, Kemprai P, Paw M, Lal M, Haldar S. 2020. A ^{1}H-NMR spectroscopic method for the analysis of thermolabile chemical markers from the essential oil of black turmeric (Curcuma caesia) rhizome: application in post-harvest analysis. *Phytochem. Anal.* 31(1): 28–36. https://doi.org/10.1002/pca.2863

59. Ravaglia LM, Pizzotti ABC, Alcantara GB. 2019. NMR-based and chemometric approaches applicable to adulteration studies for assessment of the botanical origin of edible oils. *J. Food Sci. Technol.* 56(1): 507–511. https://doi.org/10.1007/s13197-018-3485-3

60. Mannina L, Marini F, Gobbino M, Sobolev AP, Capitani D. 2009. NMR and chemometrics in tracing European olive oils: the case study of Ligurian samples. *Talanta* 80: 2141–2148. https://doi.org/10.1016/j.talanta.2009.11.021

61. Guillén M, Carton I, Goicoechea E, Uriarte PS. 2008. Characterization of cod liver oil by spectroscopic techniques. New approaches for the determination of compositional parameters, acyl groups, and cholesterol from ^{1}H Nuclear Magnetic Resonance and Fourier transform infrared spectral data. *J. Agric. Food Chem.* 56(19): 9072–9079

62. Satyarthi JK, Srinivas D, Ratnasamy P. 2009. Estimation of Free Fatty Acid Content in Oils, Fats, and Biodiesel by ^{1}H NMR Spectroscopy. *Energy & Fuels* 23 (4): 2273-2277

63. Eads TM, Croasmun WR. 1998. ^{1}H NMR applications to fats and oils. *J. Am. Oil Chem. Soc.* 65: 78–83.

64. Knothe G, Kenar JA. 2004. Determination of the fatty acid profile by ^{1}H-NMR spectroscopy. *Eur. J. Lipid Sci. Technol.* 106(2): 88–96. https://doi.org/10.1002/ejlt.200300880

65. Johnson LF, Schoolery JN. 1962. Determination of unsaturation and average molecular weight of natural fats by nuclear magnetic resonance. *Anal. Chem.* 34: 1136–1139.

66. Nielsen LV. 1976. Studies on the relationship between unsaturation and iodine value of butterfat by high resolution nuclear magnetic resonance (NMR). *Milchwissenschaft* 31: 598–602.

67. Sacchi R, Addeo F, Paolillo L. 1997. ^{1}H and ^{13}C NMR of virgin olive oil. An overview. *Mag. Res. Chem*. 35: S133–S145.

68. Miyake Y, Yokomizo K, Matsuzaki N. 1998. Determination of unsaturated fatty acid composition by high-resolution nuclear magnetic resonance spectroscopy. *J. Am. Oil Chem. Soc.* 75: 1091–1094.

69. Sacchi R, Medina I, Aubourg SP, Addeo F, Paolillo L. 1993. Proton nuclear magnetic resonance rapid and structure-specific determination of ω-3 polyunsaturated fatty acids in fish lipids. *J. Am. Oil Chem. Soc.* 70: 225–228.

70. Igarashi T, Aursand M, Hirata Y, Gribbestad IS, Wada S, Nonaka M. 2000. Nondestructive quantitative determination of docosahexaenoic acid and ω−3 fatty acids in fish oils by high-resolution ^{1}H nuclear magnetic resonance spectroscopy. *J. Am. Oil Chem. Soc.* 77: 737-748. https://doi.org/10.1007/s11746-000-0119-0

71. Skiera C, Steliopoulos P, Kuballa T, Diehl B, Holzgrabe U. 2014. Determination of free fatty acids in pharmaceutical lipids by ^{1}H NMR and comparison with the classical acid value. *J. Pharm. Biomed. Anal.* 93: 43–50. https://doi.org/10.1016/j.jpba.2013.04.010

72. Stuart B. 2004. Infrared Spectroscopy: Fundamental and Aplication, John Wiley & Sons, Ltd: 18-34.

73. Shinzawa H, Genkawa T, Kanematsu W. 2012. Pressure-induced association of oleic acid (OA) under varying temperature studied by multiple-perturbation two-dimensional (2D) IR correlation spectroscopy. *J. Mol. Struct*. 1028: 164-169.

74. Ma K. 2000. Peroxide value and Trans analyses by Fourier Transform Infrared (FTIR) Spectroscopy, Dissertation, Ph.D, Department of Food Science and agriculture Chemistry, MacDonald Campus of MacGill University, Montreal, Canada : 9-10, 19-20

75. Reid LM, O'Donnel CP, Downey G. 2006. Recent technological advances for the determination of food authenticity, *Trend Food Sci. Technol.* 17: 334-353.

76. Mackie DM, Jahnke JP, Benyamin MS, Sumner JJ. 2016. Simple, fast, and accurate methodology for quantitative analysis using Fourier transform infrared spectroscopy, with bio-hybrid fuel cell examples. *MethodsX.* 3: 128-138. https://doi.org/10.1016/j.mex.2016.02.002
77. Smith BC. 1996. Fundamental of Fourier Transform Infrared Spectroscopy, New York, CRC Press.
78. Jović O, Smolić T, Primožič I, Hrenar T. 2016. Spectroscopic and Chemometric Analysis of Binary and Ternary Edible Oil Mixtures: Qualitative and Quantitative Study. *Anal. Chem.* 88(8): 4516–4524. https://doi.org/10.1021/acs.analchem.6b00505
79. Rohman A, Che Man YB, Riyanto S. 2011. Authentication analysis of red fruit (*Pandanus Conoideus*, Lam.) oil using FTIR spectroscopy in combination with chemometrics, *Phytochem. Anal.* 22 (5): 462-467.
80. Yildiz G, Wehling RL, Cuppett SL. 2001. Method for determining oxidation of vegetable oils by near-infrared spectroscopy. *J. Am. Oil Chem. Soc.* 78 (5): 495–502.
81. Van de Voort FR, Ismail A, Sedman A, Dubois J, Nicodemo T. 1994. The Determination of Peroxide Value by Fourier Transform Infrared Spectroscopy. *J. Am. Oil Chem. Soc.* 71(9): 921-926.
82. Dubois J, van de Voort FR, Sedman J. 1996. Quantitative Fourier transform infrared analysis for anisidine value and aldehydes in thermally stressed oils. *J. Am. Oil Chem. Soc.* 73: 787–794. https://doi.org/10.1007/BF02517956
83. Guillen MD, Cabo N. 1997. Characterization of Edible Oils and Lard by Fourier Transform Infrared Spectroscopy. Relationships between Composition and Frequency of Concrete Bands in the Fingerprint Region. *J. Am. Oil Chem. Soc.* 74: 1281-1286
84. Che Man YB, Setiowaty G, van de Voort FR. 1999. Determination of Iodine Value of Palm Oil by Fourier Transform Infrared Spectroscopy. *J. Am Oil Chem. Soc. 76*: 693-699.

85. Guillen MD, Cabo N. 2000. Some of The Most Significant changes in the Fourier Transform Infrared Spectra of Edible Oil under oxidative Condition, *J. Sci. Food Agric.* 80: 2028-2036.
86. Innawong B, Mallikarjunan P, Irudayaraj J, Marc JE. 2004. The determination of fryingoil quality using Fourier transform infrared attenuated total reflectance. *Int. J. Food Sci. Tech.* 37(1): 23-28.
87. Li D, Sedman J, García-González LD, van de Voort FR. 2009. Automated Acid Content Determination in Lubricants by FTIR Spectroscopy as an Alternative to Acid Number Determination. *J. ASTM Int.* 6: 1-12.
88. Li H, van de Voort FR, Sedman J, Ismail AA. 1999. Rapid Determination of cis and trans Content, Iodine Value, and Saponification Number of Edible Oils by Fourier Transform Near-Infrared Spectroscopy *J. Am. Oil Chem. Soc.* 76(4): 491-497.
89. Rohman A, Che Man YB, Ismail A, Hashim P. 2011. Monitoring the oxidative stability of virgin coconut oil during oven test using chemical indexes and FTIR spectroscopy. *Int. Food Res. J.* 18*:* 303-310.
90. Salimon J, Abdullah BM, Salih N. 2011. Hydrolysis optimization and characterization study of preparing fatty acids from Jatropha curcas seed oil. *Chem. Cent. J.* 5(67): 1-9. https://doi.org/10.1186/1752-153X-5-67
91. Triyasmono L, Riyanto S, Rohman A. 2013. Determination of iodine value and acid value of red fruit oil by infrared spectroscopy and multivariate calibration. *Int. Food Res. J.* 20(6): 3259–3263.
92. Agatonovic-Kustrin S, Ristivojevic P, Gegechkori V, Litvinova TM, Morton DW. 2020**.** Essential Oil Quality and Purity Evaluation via FT-IR Spectroscopy and Pattern Recognition Techniques. *Appl. Sci.* 10: 7294. https://doi.org/10.3390/app10207294
93. Bortoleto GG, Pataca LCM, Bueno MIMS. 2005. A new application of X-ray scattering using principal component analysis – classification of vegetable oils. *Anal. Chim. Acta* 539: 283-287.

94. Diaz TG, Meras ID, Casas JS, Franco MFA. 2005. Characterization of virgin olive oils according to its triglycerides and sterols composition by chemometric methods. *Food Control* 16: 339-347.

95. Biancolillo A, Marini F. 2018. Chemometric Methods for Spectroscopy-Based Pharmaceutical Analysis. *Front. Chem.* 1: 6: 576. https://doi.org/10.3389/fchem.2018.00576

96. Wold S, Esbensen K, Geladi P. 1987. Principal component analysis. *Chemom. Intell. Lab. Syst.* 2(1–3): 37-52p. https://doi.org/10.1007/978-0-387-87811-9_2

97. Rodionova YO, Pomerantsev LA. 2006. "Chemometrics: achievements and prospects", *Russ. Chem. Rev.* 75 (4): 271–287.

98. Brereton RG, Jansen J, Lopes J, Marini F, Pomerantsev A, Rodionova O. 2018. Chemometrics in analytical chemistry—part II: modeling, validation, and applications. *Anal. Bioanal. Chem.* 410: 6691–6704. https://doi.org/10.1007/s00216-018-1283-4

99. Stone M. 1974. Cross-Validatory Choice and Assessment of Statistical Predictions. J. *R. Stat. Soc.* 36: 111-147.

100. Westad F, Marini F. 2015. Validation of chemometric models—a tutorial. *Anal. Chim. Acta* 893: 14–24. https://doi.org/10.1016/j.aca.2015.06.056

2. AIM OF THE THESIS

This doctoral thesis aims to develop and apply a quantitative ^{1}H NMR method for determining the quality of RFO, including AV, EV, IV, and SV, as well as their unsaturated fatty acids content. In addition, this study also combines chemometrics with ^{1}H NMR data for quality assurance and RFO authentication. The purpose of this work can be described in detail as follows:

1. To develop, optimize, and apply a ^{1}H NMR quantitative method for simultaneously determining oil quality parameters (AV, EV, IV, and SV). The optimization carried out includes solvent effects, determination of T1, internal standards used, determination of appropriate acquisition parameters, and method validation so that the quantitative ^{1}H NMR method is obtained for an alternative for determining oil quality parameters that is faster, and more efficient without losing accuracy and precision.
2. To apply chemometrics to the ^{1}H NMR and FTIR spectra for visualization grouping, prediction and authentication of RFO based on the quality parameters of the degree of unsaturation and the acid value so that a fast and accurate grouping model is achieved to determine the quality and authenticity of RFO products.
3. To develop a ^{1}H NMR quantification technique with internal standards to determine the value of monounsaturated fatty acids, polyunsaturated fatty acids, and total unsaturated fatty acids of RFO. Subsequently, to apply chemometrics directly to ^{1}H NMR RFO spectra data for visualization grouping, prediction, and authentication of RFO products based on their unsaturated fatty acid composition, to obtain a fast, efficient and robust choice of quality assurance and authentication analysis methods of RFO.

3. RESULTS

3.1 Simultaneous determination of the Saponification Value, Acid Value, Ester Value, and Iodine Value in commercially available Red Fruit Oil (*Pandanus conoideus*, Lam.) using ^{1}H qNMR spectroscopy

Liling Triyasmono, Curd Schollmayer, Jens Schmitz, Emilie Hovah, Cristian Lombo, Sebastian Schmidt, Ulrike Holzgrabe

Food Anal. Method (2022), 1-13

https://doi.org/10.1007/s12161-022-02401-4

Abstract

Red Fruit Oil (RFO) can be extracted from fruits of *Pandanus conoideus,* Lam., an endogenous plant of Papua, Indonesia. It is a commonly used essential original traditional medicine. By applying a newly developed quantitative ^{1}H NMR (qNMR) spectroscopy method for quality assessment, a simultaneous determination of the saponification value (SV), acid value (AV), ester value (EV), and iodine value (IV) in RFO was possible. Dimethyl sulfone ($DMSO_2$) was used as an internal standard. Optimization of NMR parameters, such as NMR pulse sequence, relaxation delay time, and receiver gain, finally established the ^{1}H NMR-based quantification approach. Diagnostic signals of the internal standard at δ = 2.98 ppm, SV at δ = 2.37-2.20 ppm, AV at δ = 2.27-2.20 ppm, EV at δ = 2.37-2.27 ppm, and IV at δ = 5.37-5.27 ppm, respectively, were used for quantitative analysis. The method was validated concerning linearity (R^2 = 0.999), precision (less than 0.83%), and repeatability in the range 99.17-101.17%. Furthermore, this method was successfully applied to crude RFO, crude RFO

with palmitic and oleic acid addition, and nine commercial products. The qNMR results for the respective fat values are in accordance with the results of standard methods, as can be seen from the F- and t-test (< 1.65 and < 1.66, respectively). The fundamental advantages of qNMR, such as its rapidity and simplicity, make it a feasible and existing alternative to titration for the quality control of RFO.

Keywords: quantitative ^{1}H NMR, Saponification Value, Acid Value, Ester Value, Iodine Value, Red Fruit Oil

Introduction

The demand for speed and effectiveness of analytical methods, thereby resulting in high accuracy and precision, has increasingly become priority in recent years. One of the most promising methods for overcoming these challenges is quantitative nuclear magnetic resonance (qNMR) (Yu et al. 2018). The guidance on the use of qNMR and its application for quantitative purposes was reviewed by Holzgrabe (2010) and Beyer et al. (2010a) by depicting the quantitative analysis of oversulfated chondroitin sulfate and dermatan sulfate in heparin glycosaminoglycans. This has become the required method in the USP, as well as the use of qNMR for purity control of pharmaceutical grade L-alanine and determination of several lipid parameters with internal calibration for iodine, peroxide, and acid values.

Although the cost of NMR equipment is relatively high and requires operator experience, the qNMR method has many outstanding advantages. In addition to the ^{1}H NMR's ability to provide structural information, the proportionality of signal intensity with the number of cores allows quantification if recorded with the proper experimental NMR parameters (Beyer et al. 2010a; Holzgrabe 2010). Furthermore, a reliable non-destructive analysis enabling a rapid, simple, and simultaneous analysis of different analytes in one sample is possible (Hollis 1963; Jungnickel and Forbes 1963). Of note, it is not even necessary to have a refence substance (Holzgrabe 2010). Therefore, these inherent advantages make ^{1}H NMR a powerful tool for quantification. Between 1991 and 2015, qNMR was used in more than 1,750 publications in the field of food science (Lachenmeier et al. 2016) which indicates its potential.

Conventionally, the saponification value (SV) and acid value (AV) are determined by an acid-base titration method; the ester value (EV) is calculated from both these values. Such titration methods are dependent on observing the visual endpoint, which might be challenging, especially in the case of red fruit oil (RFO) where the solution is already colour red. The iodine value (IV) is generally used to estimate the degree of unsaturation of oil and fat. This determination is based on the reaction of double bonds within fatty acids and monoiodine bromide. This reaction consists of several steps and is also time-consuming. Potentiometric pH metrics, chromatography, and FTIR have been used to overcome these problems (Bernárdez et al. 2005; Triyasmono et al. 2013; Tubino and Aricetti 2013). However, some of these methods still have weaknesses because they require chemical modification of the sample for analysis, as described by Guillen et al. (2003). However, some qNMR methods have recently been reported for the characterization and quality assessment of lipids and oils (Guillén and Ruiz 2003a, b; Skiera et al. 2014; Hafer et al. 2020).

Red fruit oil (RFO) which is extracted from the fruit of the Pandanus conoideus, Lam. plant. This fruit is red, 68 to 110 cm long, 10 to 10 cm in diameter, and contains large oil. The plant is endogenous in Papua, Indonesia and is a commonly used traditional medicine. The oil has large quantities of monounsaturated fatty acids, mainly oleic acid (60-70%) (Rohman et al. 2012), which supposedly account for beneficial impacts on human well-being, for example, forestalling cardiovascular infections, decreasing plasma triacylglycerol (TAG), or expanding cholesterol levels of high-density lipoprotein (HDL) levels (García-González et al. 2008). Testimonies of the effectiveness of RFO have been published, among others, inhibiting tumor growth and killing cancer cells could be observed (Khiong et al. 2009).

The substantial pharmacological potential makes RFO a promising candidate for herbal products or functional food. Today, various RFO products are already available on the market in Indonesia and abroad. However, multiple factors, such as geographical region, harvest time, and processing method, cause this red fruit's oil content and composition (Sarungallo et al. 2015). Therefore, the required RFO quality control is carried out at all stages of the

production cycle, including incoming raw materials, during processing stages, and control of product output (Kleymenova et al. 2021). The quality assurance of RFO has to be ensured by the determination of SV, AV, EV, and IV (Endo Y 2018), which are given in a certificate so that certified RFO products will be guaranteed quality and increase the competitiveness of their products.

This study aimed to develop a qNMR method for simultaneously determining the SV, AV, EV, and IV of RFO. Experimental NMR conditions were systematically optimized, including relaxation delay time, pulse angle, and receiver gain. Method validation includes linearity, precision, repeatability, limit of detection (LOD), and limit of quantitation (LOQ) based on the guidelines of the International Conference on Harmonization (ICH) (ICH 2005). Furthermore, the results obtained by the qNMR method were compared with the compendial methods (titration) of the European Pharmacopoeia (Ph. Eur. 10 2020).

Material and Methods

Chemicals

Deuterated chloroform ($CDCl_3$, 99.8 % D) was purchased from Eurisotop (Saarbrücken, Germany). Tetramethylsilane (TMS) and hexa deuterium dimethyl sulfoxide (DMSO-d_6, 99.9 % D) from Deutero (Kastellaun, Germany), dimethyl sulfone ($DMSO_2$, TraceCERT®, 99.99 %) internal standard for quantitative NMR grade, palmitic acid, and oleic acid standards from Merck (Darmstadt, Germany). Furthermore, for titration, 0.1 M NaOH, 0.1 M sodium thiosulfate, 0.5 M HCl, and 0.5 M ethanolic KOH were purchased from VWR (BDH Chemicals) (Darmstadt, Germany). Ethanol, petroleum ether, chloroform, iodine monobromide, KI, and starch were purchased from Merck (Darmstadt, Germany); they all were of analytical grade and complied with the requirements of the international standard ISO 660:2009.

Apparatus

Quantitative ^1H NMR experiments were performed by using a Bruker AVANCE III 400MHz spectrometer operating at 400.13 MHz (Bruker BioSpin GmbH, Rheinstetten, Germany);

using an inverse probe NMR tube Boro 400-5-7 (Deutero, Kastellaun, Germany). The analytical balances AT21 Comparator (FACT) and AB204-S (Mettler Toledo, Gießen, Germany) were used. Titrations were carried out using a Titroline 6000/7000 instrument (SI Analytics, Mainz, Germany); lithium chloride was applied to the ethanol electrode, pH electrode (SI Analytics N6480 Eth, Mainz, Germany).

Sample extraction

The fruits of *Pandanus conoideus,* Lam. were collected from different regions (Nabire and Jayawijaya) of Papua, Indonesia. Furthermore, the RFO was obtained using the solvent extraction method by Sarungallo et al. (2015). Briefly, the fruits were cut into small pieces and subsequently subjected to a commercial blender containing ethanol and water (1:1, w/v). Next, approximately 12 g of the pulp of the red fruit was macerated with 80 ml of a solvent mixture of chloroform and methanol (2:1, v/v) and stirred at room temperature for 1 hour. The resulting solution was filtered, evaporated, 16 ml of a 0.88 % aqueous NaCl solution was added, and then the aqueous and the organic layers were separated. The organic layer will remain red, and the aqueous layer will be colorless and slightly cloudy. Finally, the organic layer was evaporated at 40 ^{o}C, fined in dark bottles, dried with nitrogen gas and stored at -20 ^{o}C until analysis.

Comercial products collection

Nine samples from different manufacturers of commercial products of RFO were purchased from a traditional herbal market in Jakarta, Indonesia, including one sample of BMOP (Griya An-Nur/ Exp date: 03.2023), Golden Red (Basmallah Food/ Exp date: 11.2022), MBM (PRIMA SOLUSI/ Exp date: 10.2022), Pro Jep (HERBAL 21/ Exp date: 06.2022), Red Oil papua (FIRA HERBALINDO/ Exp date: 07.2022), REDOTEN (SERIBU PULAU INDONESIA/Exp date: 07.2022), Redwin (Natures/ Exp date: 03.2023), Sari Buah Merah (athaku Herbalife/ Exp date: 12.2021), Sari Buah Merah (Loh Jinawi / Exp date: 10.2022).

NMR-experiments

833.33 mg of each RFO sample and 3.33 mg of $DMSO_2$ were dissolved in a solvent mixture $CDCl_3$ and DMSO-d_6 (5:1, v/v) containing ^{0}.1% TMS and were diluted to 2.0 ml. After mixing for 1 minute, 600 µL of each sample was analyzed by NMR spectroscopy in triplicate.

The ^{1}H NMR experiments were measured at 300.11 ± 0.10 K with a 30° flip angle, 32 scans, no rotation, and an acquisition time of 6.81s, followed by a relaxation delay of 9s. The receiver gain was set to 4, and for processing a line broadening factor of 0.3 Hz was applied. The resulting digital resolution was 0.15 Hz with a spectral width of 30.00 ppm (time-domain size 163k). Phase and baseline corrections were performed manually with TopSpin version 4.0 (Bruker BioSpin GmbH, Rheinstetten, Germany). All offset signals are referenced to the TMS signal (δ= 0.00 ppm).

Longitudinal relaxation time (T1) Determination

250 mg of each RFO sample and 1.0 mg $DMSO_2$ were dissolved in a 600µL of a mixture of $CDCl_3$ and DMSO-d_6 (5:1, v/v). After mixing for 1 min, 600 µL of each sample was analyzed by NMR spectroscopy. The relaxation delays of all of these protons were determined by the inversion recovery pulse sequence method, using the T1 cal Bruker program. An arrayed experiment was set with different values of relaxation delay, ranging from 0.05 to 17 s.

Determination of SV, AV, EV and IV by qNMR

The following signals were used for quantitative analysis: $DMSO_2$ (δ= 2.98 ppm), SV (δ= 2.37-2.20 ppm), AV (δ= 2.27-2.20 ppm), EV (δ= 2.37-2.27 ppm), and IV (δ= 5.37-5.27 ppm). The acquisition was carried out under the conditions mentioned above. Based on the calculation formula of quantitative NMR discussed by Holzgrabe 2010, Bharti and Roy 2012 and development by Skiera et al. 2014. Furthermore, the results were calculated according to the equation below:

$$SV_{NMR} = \frac{M_{KOH}}{m_s} \cdot \frac{m_{DMSO_2} \cdot P_{DMSO_2}}{M_{DMSO_2}} \cdot \frac{N_{DMSO_2}}{N_s\,(2)} \cdot \frac{I_{\alpha\text{-}CH_2\,(total)}\,(2.37\text{-}2.20\ ppm)}{I_{DMSO_2}\,(2.98\ ppm)} .1000 \qquad (1)$$

$$AV_{NMR} = \frac{M_{KOH}}{m_s} \cdot \frac{m_{DMSO_2} \cdot P_{DMSO_2}}{M_{DMSO_2}} \cdot \frac{N_{DMSO_2}}{N_s\,(2)} \cdot \frac{I_{\alpha\text{-}CH_2\,(acid)}\,(2.27\text{-}2.20\ ppm)}{I_{DMSO_2}\,(2.98\ ppm)} \cdot 1000 \quad (2)$$

$$EV_{NMR} = \frac{M_{KOH}}{m_s} \cdot \frac{m_{DMSO_2} \cdot P_{DMSO_2}}{M_{DMSO_2}} \cdot \frac{N_{DMSO_2}}{N_s\,(2)} \cdot \frac{I_{\alpha\text{-}CH_2\,(ester)}\,(2.37\text{-}2.27\ ppm)}{I_{DMSO_2}\,(2.98\ ppm)} \cdot 1000 \quad (3)$$

$$IV_{NMR} = \frac{M_{Iod}}{m_s} \cdot \frac{m_{DMSO_2} \cdot P_{DMSO_2}}{M_{DMSO_2}} \cdot \frac{N_{DMSO_2}}{N_s\,(2)} \cdot \frac{I_{\text{-}CH=CH\text{-}}\,(5.37\text{-}5.27\ ppm)}{I_{DMSO_2}\,(2.98\ ppm)} \cdot 100 \quad (4)$$

m_s denotes the sample weight in mg, *P* the purity, M the molecular weight in g/mol, N_s the number of protons, and I the ^{1}H NMR integral area according to Skiera et al. (2014).

Method validation

The validation process requires testing for linearity, precision, accuracy (repeatability), LOD, and LOQ according to International Conference on Harmonization (ICH) guidelines (ICH 2005). For determining the linearity, precision, and accuracy of this method, five solutions containing 50, 100, 150, 200, 250 mg of RFO and 1.0 mg of $DMSO_2$, respectively, were prepared in 600 µl of a solvent mixture of $CDCl_3$ and DMSO-d_6 (5:1, v/v) containing 0.1% of TMS. For the determination of LOD and LOQ, a six-series limited concentration solution containing 0, 2, 4, 6, 8, 10 mg of RFO, 1.0 mg of $DMSO_2$ was prepared and dissolved in 600 µl of solvent mixture $CDCl_3$ and DMSO-d_6 (5:1, v/v) containing 0.1% of TMS. Each final solution was analyzed by NMR spectroscopy in triplicate.

Linearity. Linearity was assessed by measuring five different concentration solutions of RFO, as described above. The regression curve is presented y = a + bx, with the mass ratio representing and the integral values, respectively. The correlation coefficients of quantitative protons were quantified at δ = 2.37-2.20 ppm, at δ = 2.27-2.20 ppm, at δ = 2.37-2.27 ppm, and at δ = 5.37-5.27 ppm.

Precision. The RSD of repeatability expressed precision. As described above, the repeatability was tested using five different concentration solutions which were measured in triplicate. In addition, the multivariate test was carried out to see all selected quantitative proton contributions of the RFO.

Accuracy. The accuracy of qNMR was evaluated by a recovery, using five different concentration solutions were determined in triplicate, as described above. Accuracy is calculated by means of the following equation: Recovery (%) = [(m_x-m_0/m_s] x 100%, where m_x is the weight of the calculated sample, m_0 is the weight of the calculated blank sample, and m_s is the weight of the sample taken.

Limit of detection and Limit of quantitation. LOD and LOQ were calculated based on the standard deviation of the y-intercept response and the slope of the calibration curve. A linear calibration curve is assessed by measuring six concentrations of RFO limited of range, as described above. It can be expressed in a model such as y = a + bx. This model is used to compute the sensitivity b and the LOD and LOQ. Therefore, LOD and LOQ can be expressed as LOD = $3.3S_a$/b, LOQ = $10S_a$/b, respectively, with S_a being the standard deviation of y-intercepts of the response and b being the slope of the calibration curve.

Determination of SV, AV, EV and IV by Titration

The SV was determined according to the Ph. Eur. 10.0 (2020). In brief: 2.0 g of RFO was dissolved in 25.0 ml of 0.5 M ethanolic potassium and refluxed for 30 min. The hot solution has to be titrated immediately with 0.5 M aqueous hydrochloric acid (HCl) solution using a potentiometric endpoint detection. A blank test was carried out. The SV was calculated using the equation SV = [28.05 x (n_2-n_1)]/m, with m being the sample weight, n_2 being the volume of 0.5 M aqueous HCl solution used for titration of the blank samples, and n_1 being the volume of 0.5 M aqueous HCl solution used for titration of the sample. The presumed SV for RFO is 200-300 mg KOH/g.

The AV was determined according to the Ph. Eur. 10.0 (2020). In brief: 250 mg of RFO were dissolved in 50 ml of a mixture of ethanol and diethyl ether (1:1, v/v) and titrated with an aqueous 0.1 M potassium hydroxide solution using potentiometric endpoint detection. The AV was calculated using the equation AV = (5.610 x n)/m, with m being the sample weight and n being the volume of 0.1 M potassium hydroxide solution used for titration of the sample.

The EV was determined according to Ph. Eur. 10.0 (2020). In brief: The EV was calculated according to the equation EV = SV-AV.

The IV was determined according to the Ph. Eur. 10.0 (2020). In brief: 0.25 g RFO was placed in a dry 250 ml iodine flask. 15.0 ml of chloroform was added, followed by a slow addition of 25.0 ml of iodine monobromide solution; the flask was closed. The solution was allowed to stand in the dark for 30 minutes, shaking frequently. Then, 10.0 ml of 100 g/l potassium iodide solution and 100 ml of water was added and the solution was titrated with 0.1 M sodium thiosulphate, using the starch solution as an indicator, which were added towards the end of the titration. A blank test was carried out. IV was calculated using the equation IV = [1,269 x (n_2-n_1)]/m, with m being the sample weight, n_2 being the volume of 0.1 M sodium thiosulphate solution used for titration blank sample, and n_1 being the volume of 0.1 M sodium thiosulphate solution used for titration of the sample. The presumed IV for RFO is 60-100 g I_2/100g.

Comparison of the results with Titration Methods

To compare the qNMR and titration methods, an F test, t-test, and a regression test were applied. The F test was used to assess the same precision and the t-test to assess the consistency between the two methods. A regression test was considered to evaluate the correlation and accuracy of qNMR with the titration method. The data was processed using Microsoft® Excel® 2019 MSO (Version 2204 Build 16.0.15128.20158) 64-bit software.

Results and Discussion

The main components of RFO are mixed triglycerides formed from different fatty acids. Minor components are mono- and di-glycerides, sterols, vitamins, fatty acids, and others (Rohman et al. 2012; Sarungallo et al. 2015). In general, the RFO NMR spectra have a pattern similar to vegetable oils (Beyer et al. 2010a). The assignment of the ^{1}H NMR spectra can be seen in **Fig. 1**.

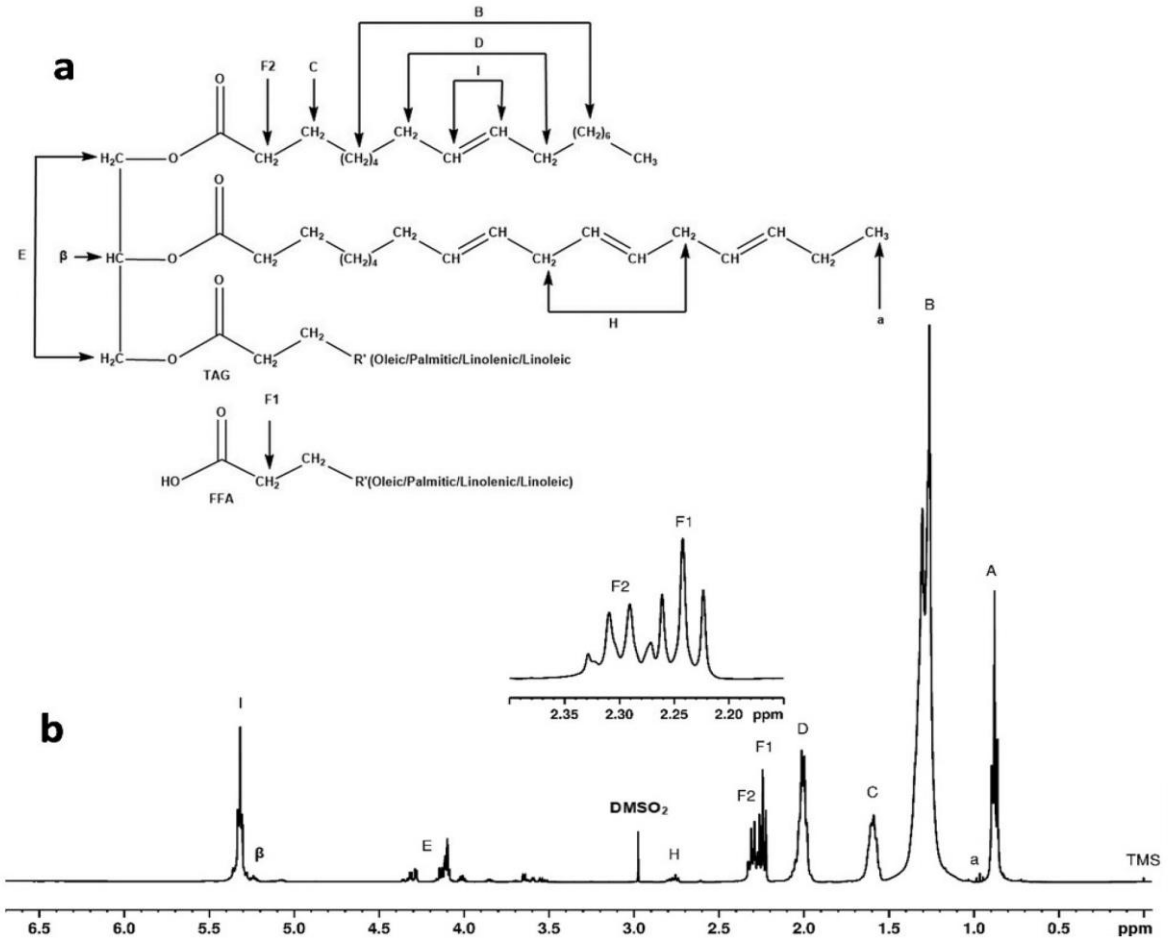

Fig. 1 a Representative structures of triacylglyceride (TAG) and free fatty acid (FFA) and **b** ^{1}H NMR spectrum of RFO dissolved in a mixture of $CDCl_3$ and DMSO-d_6 (5:1 v/v) containing TMS 0.1% with enlargement signal at δ= 2.20-2.37 ppm (F1 and F2).

Selection of solvents

A prerequisite for quantitative NMR spectroscopy is an unambiguous assignment of separated signals; hence choosing an appropriate solvent is important and was adopted from Skiera et al (2014). A good signal separation was achieved using a mixture of $CDCl_3$ and DMSO-d_6 (5:1, v/v), because the specific protons of the methylene α-CH_2 group at δ = 2.37-2.20 ppm (F1 and F2) are clearly visible. The beneficial effect of adding DMSO-d_6 to $CDCl_3$ is due to the NMR complex formation between DMSO and the fatty acid moiety (Abraham et al. 2006; Beyer et al. 2010b).

Selection of an appropriate internal standard

Selecting a proper internal standards is of great significance in qNMR experiments. $DMSO_2$ was used in this procedure because its signal at δ= 2.98 ppm does not overlap with sample and/or solvent components (see **Fig. 1b**). It is close to the analyte's resonance, thus minimizing the impact of pulse resonance (Fulmer et al. 2010; Giraudeau et al. 2014). Furthermore, $DMSO_2$ can be easily obtained with high purity and has good stability and solubility in the solvent system (Wells et al. 2004).

Assignment of the ^{1}H NMR spectra

The ^{1}H NMR spectrum of RFO consists of eleven signal groups appearing in spectral regions between δ= 0.50 and 5.50 ppm (Guillén and Ruiz 2003a, b; Beyer et al. 2010a) (see **Fig 1**). The signals are divided into eleven groups (A, a, B, C, D, E, F1, F2, H, I, and β) and are shown in **Table. 1**.

Table. 1 Assignment of signals of ^{1}H NMR spectra from RFO. Signal number are given in **Fig. 1;** TAG δ= 0.83- 5.50 ppm, FFA δ= 0.83-5.50 ppm

Signal	Functional group	Chemical shift (ppm)	
		TAG	FFA
A	(-C**H**$_3$) saturated, oleic and linoleic acyl chains	0.93-0.83	0.93-0.83
a	(-C**H**$_3$) linolenic acyl chains	1.03-0.93	1.03-0.93
B	(-(C**H**$_2$)n-) methylene groups	1.42-1.22	1.42-1.22
C	(–OCO-CH$_2$-C**H**$_2$-) β-methylene protons	1.70-1.52	1.70-1.52
D	(–C**H**$_2$-CH=CH-) allyl methylene protons	2.14-1.94	2.14-1.94
E	(–C**H**$_2$OCOR) methylene protons in the glyceryl group	4.32-4.10	-
F1	(–OCO-C**H**$_2$-) α-methylene protons	-	2.27-2.20
F2	(–OCO-C**H**$_2$-) α-methylene protons	2.37-2.27	-
H	(=HC-C**H**$_2$-CH=) divinyl methylene protons	2.84-2.70	2.84-2.70
β	(-C**H**OCOR) methine proton at C2 of glyceride	5.26-5.20	5.26-5.20
I	(–C**H**=C**H**-) olefinic protons	5.37-5.27	5.37-5.27

The α-CH_2 of both RFO and the FFA at δ= 2.27-2.20 ppm (F1) and δ= 2.37-2.20 ppm (F2) are of specials interest in addition to F1/2 the glyceride protons at δ= 4.32 - 4.10 ppm.

Selection of quantitative signals

Acidic hydrolysis using aqueous sulfuric acid was performed with RFO sample to confirm the assignment of signals F1 and F2 which were used to assess the SV, AV, and EV. Hydrolyzed RFO yields free fatty acids (FFA) (Salimon et al. 2011). As can be seen in **Fig. 2b**, upon hydrolysis α-CH_2 (F2) of the TAG disappeared, whereas the α-CH_2 (F1) of the FFA increases. The E signal of the methylene protons TAG at δ = 4.32 - 4.10 ppm disappeared after hydrolysis. Interestingly, the signals of the free glycerol are not visible because acidic conditions can catalyze the dehydration reaction of glycerol to form acrolein and other products, such as acrylic acid (Chai et al. 2007). Furthermore, the acrolein proton signal will resonate in the downfield region; CHO signal at δ= 9.51 ppm, CH_2= group at δ = 6.26 ppm and δ = 6.11 ppm relative to TMS. This signal moved slightly, depending on the solvent and pH used (De las Heras et al. 2020). As happened in the hydrolyzed RFO spectra, acrolein gave a signal at δ = 6.52 ppm and δ = 6.37 ppm from protons of the CH_2= group with the enlarged spectra of these regions (see **Fig. 2b**), while CHO signal overlaps with other signals at δ = 9.00 ppm.

The triplets of the α-CH_2 signals of the FFA are slightly high field shifted in comparison to the corresponding signal of TAG which is a multiplet. This is in accordance with the data reported by Nieva-Echevarría et al. (2014) and Kan et al. (1964).

Comparison of ^{1}H NMR spectra between RFO, oleic acid, and palmitic acid standards were carried out to confirm the signal I (-CH=CH-) assignment to IV calculation because there is a linear relation between IV and the number of olefinic protons (Miyake et al.1998). The -CH=CH- signals resonate at δ = 5.37-5.27 ppm in both RFO and oleic acid (see **Fig 2a** and **d**).

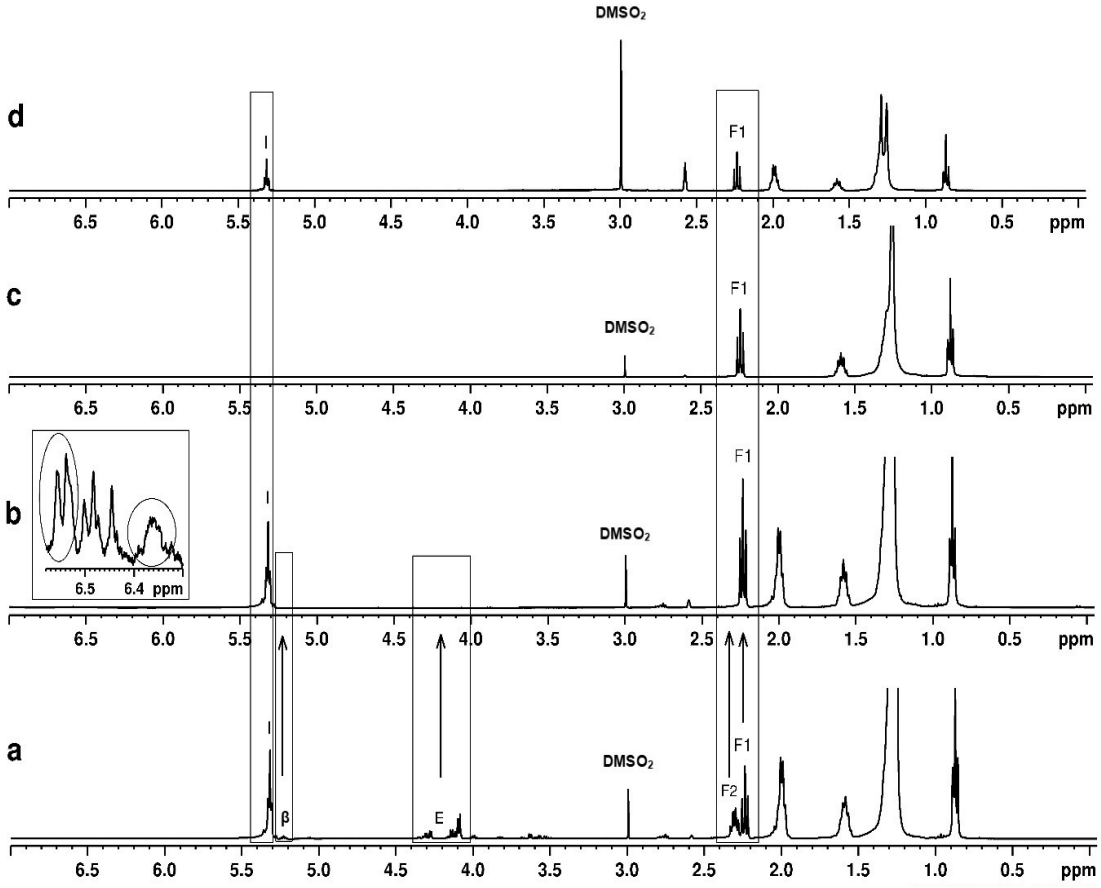

Fig. 2 Stacked Plot ^{1}H NMR Spectra 0.00 – 7.00 ppm (from bottom to top) of **a** RFO (100 mg), **b** hydrolyzed RFO (85 mg) with enlargement region of 6.20 – 6.80 ppm, **c** palmitic Acid standard, and **d** oleic Acid standard

The integrals of the signals F1 and F2, corresponding to α-CH_2 of both FFA and TAG at δ = 2.37-2.20 ppm, can be used for the quantification of SV: F1 correlated to α-CH_2 FFA at δ = 2.27-2.20 ppm for the determination of AV, F2 corresponding to α-CH_2 TAG at δ= 2.37-2.27 ppm for the quantification of EV, and signal I correlated to -CH=CH- signals at δ = 5.37-5.27 ppm can be used for the determination of IV, respectively.

Optimization of the measuring and processing parameters

It is indispensable to know the relaxation time T1 for each signal when quantifying because of a complete relaxation of all signals to achieve more than 99.3% of the equilibrium magnetization is required (Holzgrabe 2010). An inversion recovery experiment revealed T1 times as follows: $DMSO_2$ proton 2.748 s (the longest T1); α-CH2 FFA 0.524 s; α-CH2 TAG

0.287 s; and -CH=CH- 1.583 s (see **Fig. 3**). All the T1 signals of RFO measured are similar to T1 triolein and other edible oils (Miyake et al.1998). Hence, for 90^{o} flip angle, a relaxation delay of 13 s is reasonable. To shorten the analysis time, a flip angle of 30^{o} was applied, resulting in a delay of 9 s.

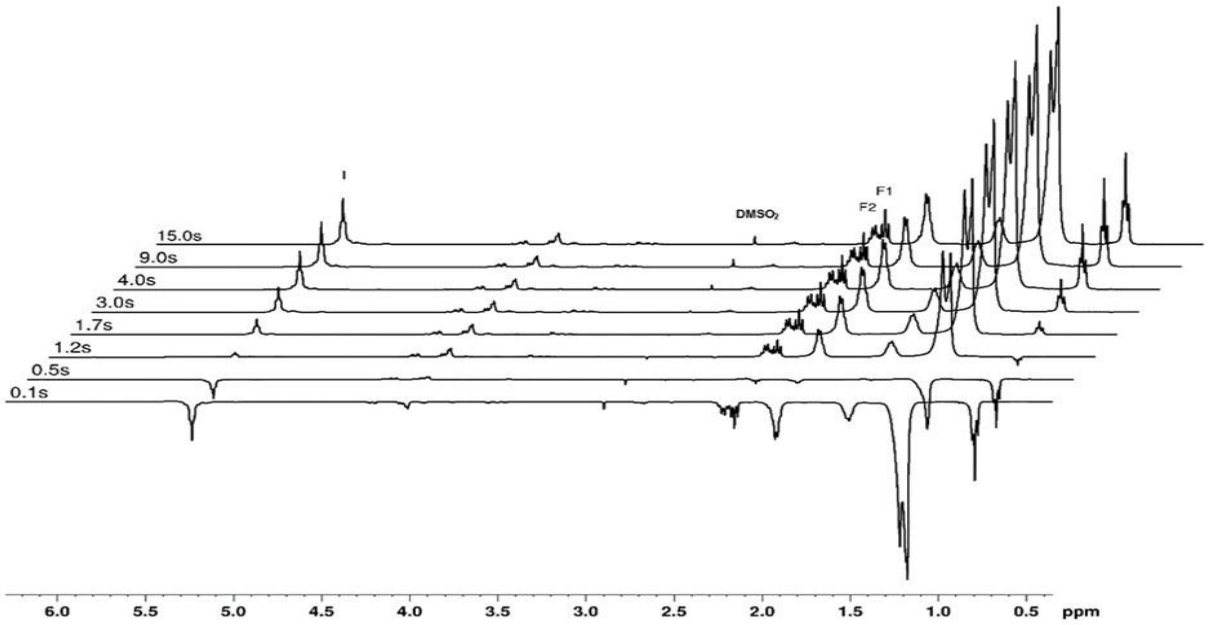

Fig. 3 400 MHz ^{1}H NMR; an inversion-recovery pulse sequence of experiments used to measure the values of T1 for the protons of RFO in $CDCl_3$: DMSO-d_6 (5:1, v/v), flip angle 180^{0} - τ - 90^{0} was applied

Choosing an appropriate NMR receiver gain (RG) can maximize the signal-to-noise ratio. Hence, the RG was varied between 4, 5, 5.65, and 6.35 (Torres and Price 2016). **Fig. 4** shows that the S/N value of the selected signal has a value of 1000, indicating that the sensitivity is acceptable (Holzgrabe 2010). However, the optimal S/N of each signal is appearing within the range of RG 4 to 5.

Furthermore, a suitable processing of the spectrum is essential to ensure reproducibility and traceability. The phase correction was done manually, and the baseline correction was carried out by the polynomial ABSG resulting in a narrow full width at half maximum (FWHM) value for the selected signal (TMS: 0.81 ± 0.07 Hz; $DMSO_2$: 0.84 ± 0.09 Hz). Therefore, the spectra appear to have sharp and symmetrical signals as desired (Deborde et al. 2019).

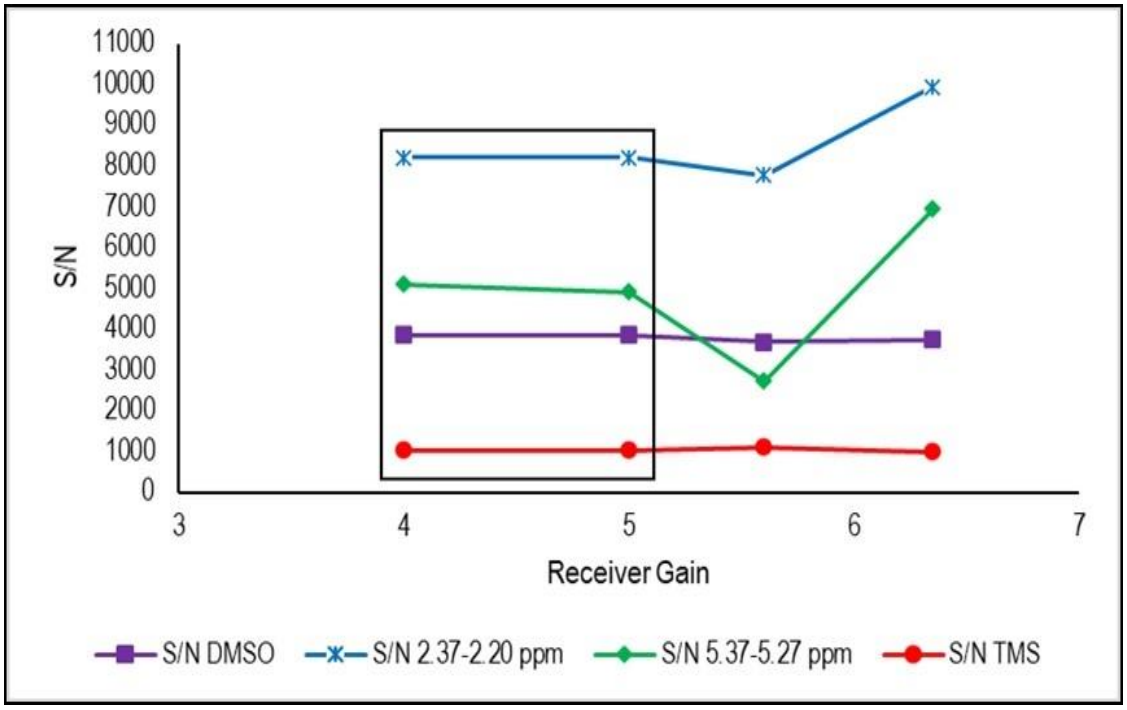

Fig. 4 Relationship between Receiver Gain and S/N

Method validation

The linearity was examined with the obtained integrals of the signals at δ = 2.37-2.20 ppm; δ = 2.27-2.20 ppm; δ = 2.37-2.27 ppm; and δ = 5.37-5.27 ppm. They were plotted versus the series of RFO concentrations. Linear regression was processed using Microsoft® Excel® 2019 MSO (Version 2204 Build 16.0.15128.20158) 64-bit software. As shown in **Table 2**, linearity was represented by the linear regression equation and its coefficient of determination (R^2) being 0.999 for all selected signals.

Table 2 Linearity test results of the qNMR method

Signal NMR (ppm)	Linear regression		RSD (%)
	Equation	R^2	
2.37-2.20	y = 0.11x - 0.02	0.999	0.52
2.27-2.20	y = 0.06x + 0.08	0.999	0.69
2.37-2.27	y = 0.05x - 0.11	0.999	0.60
5.37-5.27	y = 0.10x + 0.05	0.999	0.47

A multivariate test was carried out to see all selected integral contributions of the RFO signal to the precision and repeatability of the chosen measurement method. The Principal Component Regression (PCR) test indicates that the reference concentration of the RFO sample was proportional to the RFO determined by ^{1}H NMR, indicated by $R^2 > 0.999$ during calibration and 0.999 during validation. Additionally, precision was also demonstrated by small root mean square error (RMSE) values, RMSE Calibration of 0.77, and RMSE Validation of 0.90. The results of the model prediction test also show a linear relationship between the concentration measured by ^{1}H NMR and the prediction indicated by $R^2 > 0.999$ and RMSE Prediction 0.78. As shown in **Table 3**, the mean recoveries of the five samples were in the range of 99.17–101.17%, with RSD% less than 0.83% (González et al. 2010). The recovery calculation is based on the principle of an external standard method. Taken together, the NMR method can be regarded as precise and accurate

Table 3 Precision and recovery of five serial amounts of RFO

Weight taken (mg)	Recovery (%)	RSD (%)	Average Recovery (%)	Average RSD (%)
	100.91	0.64		
50	101.50	1.05	101.17	0.83
	101.12	0.79		
	99.12	0.63		
100	98.82	0.84	99.17	0.59
	99.56	0.31		
	99.51	0.35		
150	99.64	0.25	99.92	0.34
	100.60	0.42		
	100.53	0.38		
200	100.13	0.09	100.23	0.16
	100.04	0.03		
	100.43	0.30		
250	99.97	0.02	99.96	0.23
	99.49	0.36		

LOD and LOQ were determined by calculating the standard deviation of the y-intercept response and the slope of the calibration curve of six limited concentrations of RFO (ICH

2005). Furthermore, as shown in **Table 4**, the LOD is in the same range of 0.35-0.38 mg for all selected signals, and the LOQ for all selected signals has a similar value of 1.37-1.58 mg, except for signals at δ= 2.27-2.20 ppm that are below 4.78 mg, respectively. All LOQ values are comparable to the minimum S/N of 150 for achieving an RSD of less than 1% (Ph. Eur. 10.0. 2020).

Table 4 LOD and LOQ based on the calibration curve of SV, AV, EV and IV, respectively

Signal NMR (ppm)	Signal Correlation	Range (mg)	Calibration curve R^2	Calibration curve Equation	LOD (mg)	LOQ (mg)
2.37-2.20	SV	0-10	0.995	y = 90.88x + 5.93	0.37	1.58
2.27-2.20	AV		0.995	y = 90.88x + 5.93	0.37	1.58
2.37-2.27	EV		0.995	y = 31.12x + 1.23	1.46	4.78
5.37-5.27	IV		0.996	y = 108.98x - 0.27	0.35	1.37

These data demonstrated that the established qNMR approach was precise, accurate, and sensitive enough for the simultaneous quantitative determination of SV, AV, EV, and IV.

Quantification of SV, AV, EV, and IV of RFO with palmitic acid and oleic acid addition

One of the principal methods that can be used to obtain absolute quantitative data is the standard addition method (Beyer et al. 2010a; Holzgrabe 2010). For this purpose, the standard addition method was carried out by adding palmitic acid and oleic acid to RFO, respectively. Furthermore, the difference of the selected signal integral and its application to quantify SV, AV, EV, and IV can be assessed.

Fig. 5a displays the palmitic acid addition effect of linear increase integral signal at δ = 2.37-2.20 (R^2 0.994) and δ = 2.27-2.20 (R^2 0.998), meanwhile the integral signal at δ = 2.37-2.27 and δ = 5.37-5.27 are constant. **Fig**. **5b** shows a linear increase in SV (R^2 0.993; RSD 0.61) and AV (R^2 0.996; RSD 0.16) upon adding palmitic acid, while EV and IV remain.

Upon addition of oleic acid, a linear increase in SV (R^2 0.958; RSD 0.43), AV (R^2 0.964; RSD 0.56), and IV (R^2 0.970; RSD 0.38) of the sample in comparison to RFO was observed when using the integral increase in the RFO signal at δ = 2.27-2.20 and δ = 5.37-5.27 ppm (see

Fig. 5c and **d**). These results prove that adding oleic acid an unsaturated fatty acid, affects SV, AV, and IV due to an increase in the number of α-CH_2 signals of FFA and the signal of double bonds -CH=CH- in RFO. As expected, the calculated EV remains constant. Accordingly, this result also proves that the EV calculation can be directly read from the ^{1}H NMR RFO spectra on the α-CH_2 TAG signal at δ = 2.37-2.27 ppm. This is in stark contrast to the standard titration approach where it is calculated by EV = SV-AV. Taken together, the standard addition method gives reliable results for SV, AV, EV and IV using the qNMR method.

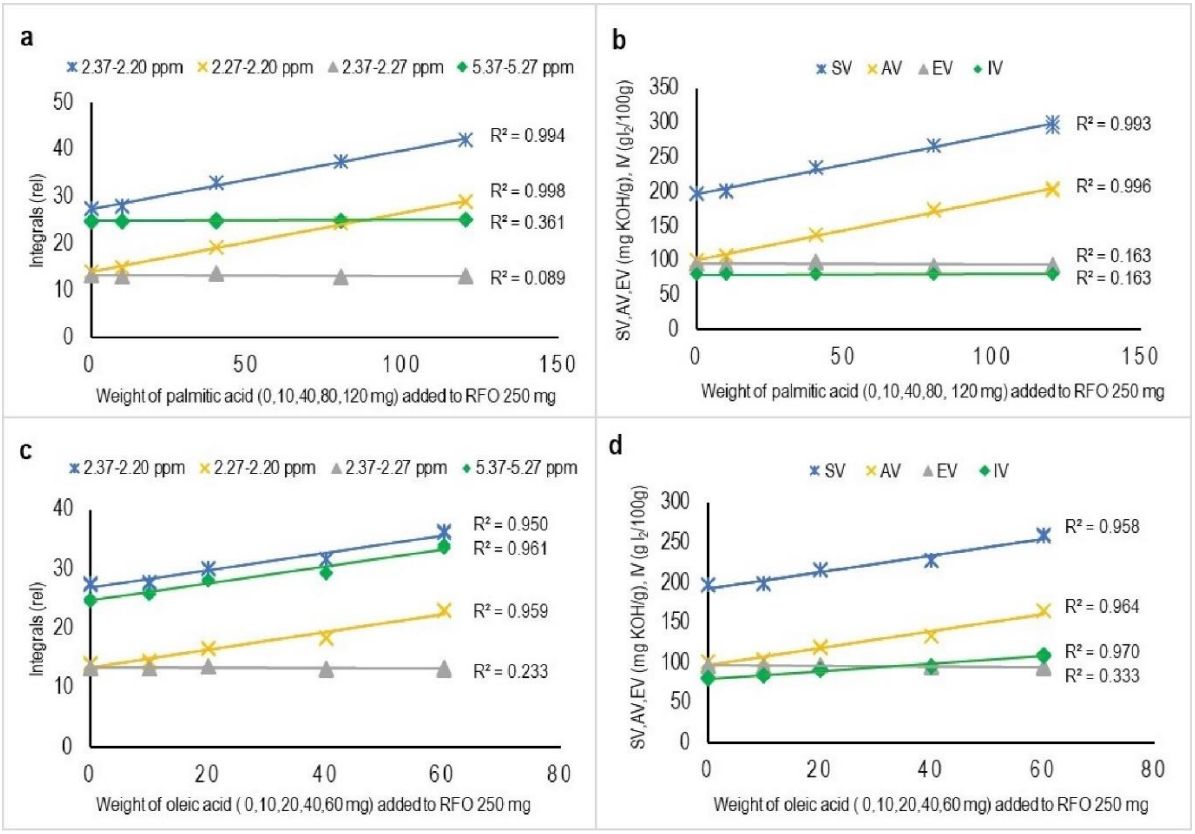

Fig. 5 a Correlation between RFO with palmitic acid addition versus Integral of ^{1}H NMR RFO (δ= 5.37-5.27 ppm, δ= 2.37-2.27 ppm, δ= 2.27-2.20 ppm, δ= 2.37-2.20 ppm) and **b** Correlation between RFO with palmitic acid addition versus SV, AV, EV, and IV by qNMR calculation. **c** Correlation between RFO with oleic acid addition versus integral of ^{1}H NMR RFO (δ= 5.37-5.27 ppm, δ= 2.37-2.27 ppm, δ= 2.27-2.20 ppm, δ= 2.37-2.20 ppm) and **d** correlation between RFO with oleic acid addition versus SV, AV, EV, and IV by qNMR calculation

Comparison with the Titration method

SV, AV, EV, and IV were determined for 17 RFO samples. This sample series contains 4 crude RFO with palmitic acid (10, 40, 80, and 120 mg), 4 crude RFO with oleic acid (10, 20, 40, and 80 mg), and 9 commercial product samples of RFO. Subsequently, SV, AV, EV and IV were determined using both the standard titration method (Ph. Eur. 10.0) and the qNMR method. An F-test and a Student's t-test were applied to evaluate significant differences between the two methods. The results displayed in **Table 5** are similar for both analysis methods. The values determined for commercials RFO products differ significantly: AV (9 – 100), EV (94 – 107) and IV (66- 80), respectively, indicating different qualities. Especially the broad range of the AV limit is an indicator for ongoing hydrolysis processes. Interestingly, the SV is similar (194 – 198) for all products. These SV results indicate that the fatty acids in commercial samples of RFO have a similar mean molecular weight. The range of 190 to 200 points towards a substantial amount of oleic, stearic, and palmitic acid, which is typical for RFO. Several SV values from the NMR calculation do not precisely match if compared with summarizing AV_{NMR} plus EV_{NMR}. A random error may cause this condition of the integration technique (Torres et al. 2017). However, the differences are not significant (RSD< 0.66).

Table 5 The SV, AV, EV and IV of RFO samples determined by qNMR and Titration methods (*n*=3)

Sample[a]	SV (mg KOH/g)		AV (mg KOH/g)		EV (mg KOH/g)		IV (g I_2/100 g)	
	qNMR	Titration	qNMR	Titration	qNMR	Titration (SV-AV)	qNMR	Titration
1	194.71 ± 0.56	194.50 ± 0.58	100.29 ± 0.71	100.54 ± 0.80	94.42 ± 0.20	93.96 ± 0.66	76.33 ± 0.83	75.53 ± 0.33
2	198.96 ± 1.38	199.69 ± 0.30	61.93 ± 0.48	61.65 ± 0.67	137.02 ± 0.90	138.03 ± 0.37	66.46 ± 0.37	66.37 ± 0.43
3	199.46 ± 0.41	199.76 ± 0.23	45.72 ± 0.59	45.30 ± 0.23	155.62 ± 0.96	154.46 ± 0.29	69.58 ± 0.79	70.08 ± 0.37
4	191.11 ± 0.76	191.63 ± 0.42	83.87 ± 0.83	84.00 ± 0.21	107.24 ± 0.18	107.63 ± 0.22	77.35 ± 0.35	77.50 ± 0.32
5	197.32 ± 0.33	197.51 ± 0.32	71.23 ± 0.80	73.40 ± 0.10	126.11 ± 0.78	124.11 ± 0.22	82.84 ± 0.25	81.44 ± 0.68
6	191.19 ± 0.47	191.92 ± 0.70	60.48 ± 0.51	60.87 ± 0.73	130.72 ± 0.13	131.05 ± 0.04	79.24 ± 0.96	79.67 ± 0.94
7	187.60 ± 0.03	186.86 ± 0.01	9.05 ± 0.09	9.36 ± 0.03	178.55 ± 0.12	177.51 ± 0.04	89.01 ± 0.30	86.99 ± 0.77
8	192.64 ± 0.35	191.40 ± 0.23	84.22 ± 0.30	83.02 ± 0.10	107.40 ± 1.63	108.38 ± 0.24	77.19 ± 0.49	77.26 ± 0.19
9	196.81 ± 1.16	196.75 ± 0.45	100.82 ± 0.57	101.19 ± 0.44	95.99 ± 0.64	95.55 ± 0.55	80.59 ± 0.53	80.39 ± 0.43
10	201.62 ± 0.97	202.12 ± 0.59	107.16 ± 0.96	110.34 ± 0.03	93.97 ± 0.72	91.78 ± 0.62	80.66 ± 0.41	80.37 ± 0.28
11	235.56 ± 0.69	231.46 ± 0.06	137.42 ± 0.08	137.75 ± 0.06	98.14 ± 0.77	93.71 ± 0.00	81.20 ± 0.56	80.62 ± 0.48
12	266.93 ± 0.56	268.42 ± 0.20	174.12 ± 0.20	175.52 ± 0.25	92.82 ± 0.36	92.89 ± 0.05	80.41 ± 0.09	81.06 ± 0.64
13	299.59 ± 1.07	300.07 ± 0.31	205.32 ± 0.08	202.46 ± 1.34	95.90 ± 1.16	97.62 ± 1.04	81.70 ± 0.35	80.79 ± 0.65
14	198.50 ± 1.15	200.70 ± 0.53	103.02 ± 1.17	105.35 ± 0.98	95.48 ± 0.04	95.35 ± 1.21	83.87 ± 0.13	82.84 ± 0.25
15	216.09 ± 0.76	216.91 ± 0.52	118.68 ± 0.80	118.32 ± 0.79	97.41 ± 0.18	98.59 ± 1.31	91.23 ± 0.33	91.94 ± 0.21
16	228.05 ± 0.73	231.23 ± 0.40	132.88 ± 0.21	135.16 ± 0.74	95.18 ± 0.52	96.06 ± 1.02	95.80 ± 0.02	96.83 ± 0.21
17	259.56 ± 0.54	258.86 ± 0.79	164.83 ± 0.46	169.12 ± 0.39	94.40 ± 1.34	89.74 ± 0.59	109.23 ± 0.81	108.90 ± 0.55

[a] 1-8 are commercial product RFO; 9 is crude RFO; 10-13 are crude RFO with palmitic acid (10, 40, 80, 120 mg); 14-17 are crude RFO with oleic acid (10, 20, 40, 80 mg)

Table 6 Statistics F-test, Student's t-test, and RSD results for four quality parameters of RFO calculated from qNMR method versus titration method

Parameter	F-Test	F-critical value	P(T<=t) one-tail	t critical one-tail	P(T<=t) two-tail	t critical two-tail	RSD (%)
SV	0.47	1.65	0.47	1.66	0.94	1.99	1.74
AV	0.47		0.47		0.93		1.65
EV	0.48		0.44		0.89		2.15
IV	0.50		0.46		0.92		0.90

As can be seen from **Table 6**, the t-test showed the consistency of both methods, and the F-test stated that both methods are of similar precision. Considering that both methods produce almost identical results for SV, AV, EV, and IV, a regression correlation was applied to calculated SV, AV, EV, and IV directly from ^{1}H NMR. The following equation was obtained for calculation of SV (y = 0. 986x + 2.426); AV (y = 0. 989x + 0.270); EV (y = 0.987 + 2.170); and IV (y = 0.994x + 0.782). Based on this result, it can be stated that qNMR could develop into a method for determining SV, AV, EV, and IV parallel to the conventional methods.

Conclusions

In this work, a qNMR method using the internal standard $DMSO_2$ with optimized conditions was developed (Solvent $CDCl_3$ and DMSO-d_6 (5:1 v/v) containing 0.1% TMS; acquisition parameters: 163 K, SW 30.00 ppm, AQ 6.81 s, digital resolution 0.15 Hz, d1 9 s and pulse angle 30^{o}) and successfully demonstrated the advantages of feasible detection speed, selectivity, linearity, precision, and accuracy in the quantitative analysis of four simultaneous oil quality parameters (SV, AV, EV, and IV) in crude RFO, a mixture of crude RFO with palmitic and oleic acid addition and its commercial products.

The NMR results were in good correlation with those determined by the compendial titration method. Furthermore, SV, AV, EV, and IV successfully can be determined directly from ^{1}H NMR spectra. In addition, the quantitative ^{1}H NMR method is simple, rapid, demands for less chemical reagents, and does not require complex preparation steps. Therefore, it represents an interesting alternative for routine quality control of RFO and commercial products.

Data availibility

The authors declare that all data supporting the findings of this study are available within the article.

References

Abraham RJ, Byrne JJ, Griffiths L & Perez M (2006) ^{1}H chemical shifts in NMR: Part 23, the effect of dimethyl sulphoxide versus chloroform solvent on ^{1}H chemical shifts. Magn. Reson. Chem 44(5):491–509. https://doi.org/10.1002/mrc.1747

Bharti SK and Roy R (2012) Quantitative ^{1}H NMR spectroscopy. TrAC Trends Analyt Chem 35: 5-26. https://doi.org/10.1016/j.trac.2012.02.007

Bernárdez L, Pastoriza G, Sampedro JJ, Herrera R, Cabo ML (2005) Modified method for the analysis of free fatty acids in fish. J. Agric.Food Chem 53(6):1903–1906. https://doi.org/10.1021/jf040282c

Beyer T, Diehl B, Holzgrabe U (2010a) Quantitative NMR spectroscopy of biologically active substances and excipients. Bioanal. Rev 2(1):1-22. https://doi.org/10.1007/s12566-010-0016-8

Beyer T, Schollmayer C & Holzgrabe, U (2010b) The role of solvents in the signal separation for quantitative ^{1}H NMR spectroscopy. J.Pharm. Biomed. Anal 52(1):51–58. https://doi.org/10.1016/j.jpba.2009.12.007

Chai SH, Wang HP, Liang Y, & Xu BQ (2007) Sustainable production of acrolein: Investigation of solid acid–base catalysts for gas-phase dehydration of glycerol. Green Chem 9(10):1130–1136. https://doi.org/10.1039/b702200j

Deborde C, Fontaine J. X, Jacob D, Botana A., Nicaise V, Richard-Forget F,Molinié R (2019) Optimizing 1D ^{1}H-NMR profiling of plant samples for high throughput analysis: extract preparation, standardization, automation and spectra processing. Metabolomics 15(28):1-12. https://doi.org/10.1007/s11306-019-1488-3

De las Heras E, Zuriarrain-Ocio A, Zuriarrain J, Bordagaray A, Dueñas MT, & Berregi I (2020) Quantitative determination of acrolein in cider by ^{1}H NMR spectrometry. Foods, 9(12):1-10. https://doi.org/10.3390/foods9121820

Endo Y (2018) Analytical Methods to Evaluate the Quality of Edible Fats and Oils: The JOCS Standard Methods for Analysis of Fats, Oils and Related Materials and Advanced Methods. J Oleo Sci, 1;67(1):1-10. https://doi: 10.5650/jos.ess17130

European Pharmacopoeia, 10th ed (2020) European Department for the Quality of Medicines. Strasbourg. France: 2.5.1, 2.5.2, 2.5.4, 2.5.6

Fulmer GR, Miller AJM, Sherden NH, Gottlieb HE, Nudelman AB, Stoltz M, Bercaw JE, Goldberg KI NMR (2010) Chemical shifts of trace impurities: Common laboratory solvents, organics, and gases in deuterated solvents relevant to the organometallic chemist. Organometallics 29(9):2176–2179. https://doi.org/10.1021/om100106e

García-González DL, Aparicio-Ruiz R, Aparicio R (2008) Virgin olive oil - Chemical implications on quality and health. Eur. J. Lipid Sci. Tech 110(7):602-607. https://doi.org/10.1002/ejlt.200700262

Giraudeau P, Tea I, Remaud GS, Akoka S (2014) Reference and normalization methods: Essential tools for the intercomparison of NMR spectra. J. Pharm. Biomed. Anal 93:3-16. https://doi.org/10.1016/j.jpba.2013.07.020

González AG, Herrador MÁ, Asuero AG (2010) Intra-laboratory assessment of method accuracy (trueness and precision) by using validation standards. Talanta 82(5):1995–1998. https://doi.org/10.1016/j.talanta.2010.07.071

Guillén[a] MD, Ruiz A (2003a) ^{1}H nuclear magnetic resonance as a fast tool for determining the composition of acyl chains in acylglycerol mixtures. Eur. J. Lipid Sci. Tech 105(9):502–507. https://doi.org/10.1002/ejlt.200300799

Guillén MD, Ruiz A (2003b) Rapid simultaneous determination by proton NMR of unsaturation and composition of acyl groups in vegetable oils. Eur. J. Lipid Sci. Tech 105(11):688–696. https://doi.org/10.1002/ejlt.200300866

Hafer E, Holzgrabe U, Wiedemann S, Adams KM, Diehl (2020) NMR Spectroscopy: Determination of Peroxide Value in Vegetable and Krill Oil by Using Triphenylphosphine as Tagging Reagent. Eur. J. Lipid Sci. Tech 122(5):1-11. https://doi.org/10.1002/ejlt.201900442

Hollis D (1963) Quantitative Analysis of Aspirin, Phenacetin, and Caffeine Mixtures by Nuclear Magnetic Resonance Spectrometry. Anal. Chem 35(11):1682–1684. https://doi.org/10.1021/ac60204a043

Holzgrabe U (2010) Quantitative NMR spectroscopy in pharmaceutical applications. Prog. Nucl. Magn. Reson. Spectrosc 57:229–240. https://doi.org/10.1016/j.pnmrs.2010.05.001

International Conference on Harmonization (ICH) of Technical Requirements for the Registration of Pharmaceuticals for Human Use (2005) Validation of analytical procedures: Text and Methodology. ICH-Q2(R1) Geneva:1-13

Jungnickel JL, Forbes JW (1963) Quantitative Measurement of Hydrogen Types by Integrated Nuclear Magnetic Resonance Intensities. Anal. Chem 35(8): 938–942.https://doi.org/10.1021/ac60201a005

Kan RO (1964) A Correlation of Chemical Shifts with Inductive Effect Parameters. J Am Oil Chem Soc 86(23):5180–5183. https://doi.org/10.1021/ja01077a029

Khiong K, Adhika OA, Chakravitha M (2009) Inhibition of NF-κB Pathway as the Therapeutic Potential of Red Fruit (Pandanus Conoideus Lam.) in the Treatment of Inflammatory Bowel Disease. Jurnal Kedokteran Maranatha 9(1):69–75

Kleymenova, NL, Nazina, LI, Bolgova, IN, Pegina, AN, & Orlovseva, OA (2021) Quality control in the production process of sunflower oil. *IOP Conference Series: Earth and Environmental Science*. IOP Publishing Ltd. https://doi.org/10.1088/1755-1315/845/

Lachenmeier D, Schönberger T, Ehni S, Schütz B, Spraul M (2016) A discussion about the potentials and pitfalls of quantitative nuclear magnetic resonance (qNMR) spectroscopy in food science and beyond. In Proceedings of the XIII International Conference on the Applications of Magnetic Resonance in Food Science: p. 77. https://doi.org/10.1255/mrfs.15

Miyake Y, Yokomizo K, Matsuzaki N (1998) Determination of unsaturated fatty acid composition by high-resolution nuclear magnetic resonance spectroscopy. J Am Oil Chem Soc 75:1091–1094

Nieva-Echevarría B, Goicoechea E, Manzanos MJ, Guillén MD (2014) A method based on ^{1}H NMR spectral data useful to evaluate the hydrolysis level in complex lipid mixtures. Food Res. Int 66:379–387. https://doi.org/10.1016/j.foodres.2014.09.031

Rohman A, Sugeng R, Che Man YB (2012) Characterizaton of red fruit (Pandanus conoideus Lam) oil. Int. Food Res. J 19(2):563–567

Salimon J, Abdullah BM, Salih N (2011) Hydrolysis optimization and characterization study of preparing fatty acids from Jatropha curcas seed oil. Chem. Cent. J 5(67):1-9. https://doi.org/10.1186/1752-153X-5-67

Sarungallo ZL, Hariyadi P, Andarwulan N, Purnomo EH (2015) Characterization of chemical properties, lipid profile, total phenol and tocopherol content of oils extracted from nine clones of red fruit (Pandanus conoideus). Kasetsart J. Natural Sci 49(2):237–250

Skiera C, Steliopoulos P, Kuballa T, Diehl B, Holzgrabe U (2014) Determination of free fatty acids in pharmaceutical lipids by ^{1}H NMR and comparison with the classical acid value. J. Pharm. Biomed. Anal 93:43–50. https://doi.org/10.1016/j.jpba.2013.04.010

Torres AM, Price WS (2017) Common problems and artifacts encountered in solution-state NMR experiments, Concepts. Magn. Reson. Part A: Bridging Education and Research 45A(2):1-16. https://doi.org/10.1002/cmr.a.21387

Triyasmono L, Riyanto S, Rohman A (2013) Determination of iodine value and acid value of red fruit oil by infrared spectroscopy and multivariate calibration. Int. Food Res. J 20(6):3259–3263

Tubino M, Aricetti JA (2013) A green potentiometric method for the determination of the iodine number of biodiesel. Fuel 103:1158–1163. https://doi.org/10.1016/j.fuel.2012.10.011

Wells RJ, Cheung J, Hook JM (2004) Dimethylsulfone as a universal standard for analysis of organics by QNMR. Accredit. Qual. Assur 9(8):450–456. https://doi.org/10.1007/s00769-004-0779-0

Yu C, Zhang Q, Xu PY, Bai Y, Shen WB, Di B, Su MX (2018) Quantitative determination and validation of octreotide acetate using ^{1}H-NMR spectroscopy with internal standard method, Magn. Reson. Chem. 56(1):37–45. https://doi.org/10.1002/mrc.4665

Acknowledgements

The authors would like to thank the supporting finance of Lambung Mangkurat University (Grant No. 3894/UN8/KP/2019). The authors warmly thank Dr. Jonas Urlaub, Nicolas Scheuplein, Joshua Weinnmann, Lukas Kichner, and Alexander Becht for their technical support during the study as well as Dr. Ludwig Höllein for editorial support during writing and preparation for submission this publication.

Funding

Open Access funding enabled and organized by Projekt DEAL. This study was financed in part by the Lambung Mangkurat University (Grant No. 3894/UN8/KP/2019).

Author Information

Authors and Affiliations

Institute for Pharmacy and Food Chemistry, University of Würzburg, 97074 Würzburg, Germany

Liling Triyasmono, Curd Schollmayer, Jens Schmitz, Emilie Hovah, Cristian Lombo, Sebastian Schmidt, Ulrike Holzgrabe

Department of Pharmacy, Faculty of Mathematics and Natural Sciences, Lambung Mangkurat University, 70713 Banjar Baru, Indonesia

Liling Triyasmono

Author contributions

Conceptualization: Liling Triyasmono and Ulrike Holzgrabe; Investigation: Liling Triyasmono, Curd Schollmayer, Jens Schmitz, Emilie Hovah, Cristian Lombo, Sebastian Schmidt; Methodology: Liling Triyasmono, Curd Schollmayer, Jens Schmitz, Emilie Hovah, Cristian Lombo, Sebastian Schmidt; Formal analysis: Liling Triyasmono and Curd Schollmayer; Visualization: Liling Triyasmono, Curd Schollmayer, Cristian Lombo; Writing—original draft: Liling Triyasmono; Writing-review & editing: Jens Schmitz, Sebastian Schmidt, Ulrike Holzgrabe; Resources: Ulrike Holzgrabe; Supervision: Ulrike Holzgrabe.

Corresponding author

Correspondence to Ulrike Holzgrabe.

Ethics declarations

Ethics approval

This article does not contain any studies with human participants or animals performed by any of the authors.

Conflict of interest

Liling Triyasmono declares that he has no conflict of interest. Curd Schollmayer declares that he has no conflict of interest. Jens Schmitz declares that he has no conflict of interest. Emilie Hovah declares that she has no conflict of interest. Cristian Lombo declares that he has no conflict of interest. Sebastian Schmidt declares that he has no conflict of interest. Ulrike Holzgrabe that she has no conflict of interest.

3.2 Chemometric analysis applied to ^{1}H NMR and FTIR data for a quality parameter distinction of Red Fruit (*Pandanus conoideus*, Lam.) Oil products[1]

[1] This chapter was accepted for publication in *Phytochem. Anal.* (2022). For details see chapter 7.1 List of publications

Liling Triyasmono, Curd Schollmayer, Ulrike Holzgrabe

Abstract

Introduction: Red fruit oil (RFO) is a natural product extracted from *Pandanus conoideus* Lam. fruit, a native plant from Papua, Indonesia. Nowadays, recent studies indicate that RFO is popularly consumed as herbal medicine. Furthermore, the quality of RFO must be assured.

Objectives: This study aimed to develop chemometric analysis applied to ^{1}H NMR and FTIR data for a quality parameter distinction of Red Fruit Oil (RFO), especially on the degree of unsaturation and the amount of free fatty acids (FFA), which are important quality parameters.

Materials and methods: Forty samples consisting of one crude RFO, thirty-three commercial RFOs, and three oils as blends, including olive oil, virgin coconut oil, and black seed oil, were analyzed by ^{1}H NMR and FTIR spectroscopy. After appropriate preprocessing of the spectra, the PCA and PLSR were used for model development.

Results: The essential signals for modeling the degree of unsaturation are the signal at δ= 5.37–5.27 ppm (^{1}H NMR) and the band at 3000-3020 cm^{-1} (FTIR). The FFA profile is represented by the signal at δ= 2.37-2.20 ppm (^{1}H NMR) and the band at 1680-1780 cm^{-1} (FTIR), respectively. PCA allows the visualization grouping of both methods with > 98% for the degree of unsaturation and > 88% full PC for FFA values. In addition, the PLSR model

provides an acceptable coefficient of determination (R^2) and errors in calibration, prediction, and cross-validation.

Conclusion: Chemometric analysis applied to ^{1}H NMR and FTIR spectra of RFO successfully classified and predicted product quality based on the degree of unsaturation and FFA values.

Keywords: ^{1}H NMR, FTIR, PCA, PLSR, Red fruit oil, degree of unsaturation, free fatty acid value

Abbreviations

RFO, Red Fruit Oil, PCA, Principal component analysis, PLS, Partial least Square, RMSEC, Root mean square error calibration, RMSEV, Root mean square error validation, RMSEP, Root mean square Prediction, FFA, Free fatty acid, TAG, Triacylglycerol, OR, Crude RFO (Original RFO), BSO, Black Seed Oil (Habattusauda), OVO, Olive Oil, VCO, Virgin Coconut Oil, ORCO, Crude RFO plus VCO, ORVO, Crude RFO plus Olive Oil, Crude RFO plus Black Seed Oil (Habbatusauda), AT, ATHAKU, BMO, Buah Merah Oil Papua, BMP, Buah Merah Papua, FR, Fira Herbalindo Buah Merah, GR, Golden Red, JW, Jaya Wijaya, KF, KF Minyak Buah Merah, KP, King Pandanus, LJ, Loh Jinawi, PG, Premium Gold, PR , Pro Jep Buah Merah, RD, REDOTEN, AH, Agro Herbal Husada, BMPro, BMPro Minyak Buah Merah, BMW, Buah Merah Wamena, CH, Cahaya Minyak Buah Merah, DIO, DioDes Minyak Buah Merah, EZA, Essensa Naturale Buah Merah, HM, Herbal Food Buah Merah, HP, Herbal Produk Buah Merah, MBM, Minyak Buah Merah, MHJ, Mahesa Herbal Jogja, OF, Oil Fit, PCI, PCI Buah Merah, PI, Papua Indonesia Minyak Buah Merah, PS, Planta Sehat, PT, Papua Tropika MBM, ROP, Red Oil Papua, RW, Redwin, SBM, Sari Buah Merah Made, THM, Tani Home Industri Buah Merah, TN, Tamba Sanjiwani Natur, RF, FIRA PAPUA.

1 INTRODUCTION

Red fruit oil (RFO) is a natural product extracted from Pandanus conoideus Lam. fruit, a native plant from Papua, Indonesia, and Papua New Guinea. The oval fruits of this tree are some 40-110 cm long, 5-25 cm in diameter, and have a weight of 3-8 kg. This fruit has a specific organoleptic: red color with a slightly chelating neutral taste. Traditionally, red fruits are used by Papuanese as an edible oil to increase energy and strengthen the immune system. Nowadays, recent studies indicate that RFO is popularly consumed as herbal medicine. It is used for medicinal purposes, as the literature records some pharmacological studies on RFO, such as inhibiting tumor growth and killing cancer cells,[1,2] increasing the number of anti-inflammatory and immune cells,[3] and antioxidant activity.[4] RFO contains active components such as phenols, carotenoids, tocopherols, and unsaturated fatty acids. RFO's reported characteristics differ from other Indonesian vegetable oils such as coconut and palm oil. RFO is dominated with monounsaturated fatty acid (MUFA) 60-70%, 10-20 %, saturated fatty acid (SFA) (10-20%), and polyunsaturated (PUFA) 2-10%.[5,6]

The quality of RFO must be assured. One of the oil quality parameters used to assess and classify is the degree of unsaturated lipids and the free fatty acid (FFA) value.[5,7] The conventional method for assessing the degree of unsaturated fatty acids is the determination of the iodine value (IV) and for quantification the amount of FFA is the acid value (AV). Unfortunately, the classical IV and AV methods have several drawbacks: time-consuming, the necessity for sample pretreatment, large sample size, large amounts of organic solvents, harmful chemicals, and the lack of specificity, which usually depends on a visual endpoint.

To overcome these obstacles, several fast and non-destructive instrumental methods have been proposed for food analysis of the complex mixture, i.e. high-resolution techniques such as nuclear magnetic resonance (NMR) and Fourier transform infrared (FTIR) spectroscopy. These methods can provide qualitative and quantitative information in one experiment. The NMR and FTIR spectra, e.g., provide information on the product's composition and quality characteristics.[8,9]

To accomplish the quality assurance, chemometrics is applied directly to the spectral data. These methods are particularly suitable for areas such as food investigations,[10] plant extracts,[11] drug and degradation products,[12,13] and oil authentication and characterization.[14,15] In the case of successful classification or diagnosis, multiple variables must be considered simultaneously. Using principal component analysis (PCA) samples can be correctly visualization the grouping (96%) and the discrimination between classes can be sufficient to characterize the geographical origin of the oil. The exploratory data analysis mainly consists of PCA, summarizing information in large-scale spectrum sets. Another form of data pattern research is Partial Least Squares Regression (PLSR), which aims to detect and predict similarities between samples.[16]

The present study aimed to build a model for RFO to guarantee the authenticity of this product using fast and easy-to-automate methodologies, compare different spectroscopic techniques and investigate whether the synergy among them is able to improve the efficiency of the classification and regression models, especially for the classification of commercial samples of RFO.

2 EXPERIMENTAL PROCEDURES

2.1 Materials

Hexa deuterium dimethyl sulfoxide (DMSO-d_6, 99.9 % D), tetramethylsilane (TMS) and NMR tube Boro 400-5-7 were purchased from Deutero (Kastellaun, Germany), deuterated chloroform ($CDCl_3$, 99.8 % D) and dimethyl sulfone ($DMSO_2$), internal standard NMR grade, were purchased from Merck (Darmstadt, Germany).

2.2 All Samples

A total of 40 different oils were used in this study, 33 samples thereof were RFO commercial product from different factories purchased from the local traditional herbal market, Jakarta, Indonesia. One crude RFO sample was obtained from solvent extraction,[17] three samples were crude RFO mixed with other oils, and three different samples, including olive oil (OVO),

coconut oil (VCO) and black seed oil (BSO) were the standard oil for additional RFO Products (Table 1). Furthermore, the sample was grouped into two components: calibration and prediction.

TABLE 1 List of the investigated sample

No	Sampel code	Type	Specification	Quantity	Replication number code
1	OR	crude RFO	Calibration	3	61,62,63
2	ORCO	modified RFO with VCO	Calibration	3	64.65.66
3	ORVO	modified RFO with OVO	Calibration	3	67,68,69
4	ORSO	modified RFO with BSO	Calibration	3	112,113,114
5	OVO	modifying oil (olive oil)	Calibration	3	70,71,72
6	VCO	modifying oil (coconut oil)	Calibration	3	115,116,117
7	BSO	modifying oil (black seed oil)	Calibration	3	118,119,120
8	AT	commercial	Calibration	3	4,5,6
9	BMO	commercial	Calibration	3	7,8,9
10	BMP	commercial	Calibration	3	10,11,12
11	FR	commercial	Calibration	3	28,29,30
12	GR	commercial	Calibration	3	31,32,33
13	JW	commercial	Calibration	3	40,41,42
14	KF	commercial	Calibration	3	43,44,45
15	KP	commercial	Calibration	3	46,47,48
16	LJ	commercial	Calibration	3	49,50,51
17	PG	commercial	Calibration	3	76,77,78
18	PR	commercial	Calibration	3	82,83,84
19	RD	commercial	Calibration	3	91,92,93
20	AH	commercial	Prediction test	3	1,2,3
21	BMPro	commercial	Prediction test	3	13,14,15
22	BMW	commercial	Prediction test	3	16,17,18
23	CH	commercial	Prediction test	3	19,20,21
24	DIO	commercial	Prediction test	3	22,23,24
25	EZA	commercial	Prediction test	3	25,26,27
26	HM	commercial	Prediction test	3	34,35,36

TABLE 1 continued

No	Sampel code	Type	Specification	Quantity	Replication number code
27	HP	commercial	Prediction test	3	37,38,39
28	MBM	commercial	Prediction test	3	52,53,54
29	MHJ	commercial	Prediction test	3	55,56,57
30	OF	commercial	Prediction test	3	58,59,60
31	PCI	commercial	Prediction test	3	73,74,75
32	PI	commercial	Prediction test	3	79,80,81
33	PS	commercial	Prediction test	3	85,86,87
34	PT	commercial	Prediction test	3	88,89,90
35	RF	commercial	Prediction test	3	94,95,96
36	ROP	commercial	Prediction test	3	97,98,99
37	RW	commercial	Prediction test	3	100,101,102
38	SBM	commercial	Prediction test	3	103,104,105
39	THM	commercial	Prediction test	3	106,107,108
40	TN	commercial	Prediction test	3	109,110,111

For producing model blends, binary mixtures of OVO, VCO, and BSO in crude RFO were prepared by adding BSO, OVO, and VCO to the crude RFO up to a total amount sample of 250.0 mg (1:1.5 w/w), respectively.

2.3 NMR spectroscopy

A total of 833.33 mg oil and 3.33 mg $DMSO_2$ was weighed into a 2.0 ml reaction tube. After the addition of a solvent mixture of $CDCl_3$ and DMSO-d_6 (5:1, v/v) containing 0.1% TMS up to 2.0 ml, the tube was closed and vortexed, and 600 µL of this solution was placed into a 5-mm-diameter inverse probe NMR tube (Boro 400-5-7, Deutero, Kastellaun, Germany). The sample analyzed by NMR spectroscopy (Avance III HD 400 MHz, Bruker BioSpin GmbH, Rheinstetten, Germany). The experiments were carried out at 300 K, a spectral width of 30.0 ppm (time-domain size 163k), relaxation delay of 9 s, number of scans of 32, acquisition time of 6.41 s, pulse width of 30°, pulse sequence of 30 zg, no rotation. The receiver gain was set to 4, and a line broadening factor of 0.3 Hz was applied for processing.[18] Previously,

measurements of the full spin-lattice relaxation (T1) of the protons in the sample were carried out according to Holzgrabe.[19] and Triyasmono et al.[18] The total acquisition time was 15 min.

The spectra were acquired using TopSpin 4.0 (Bruker BioSpin GmbH, Rheinstetten, Germany); a manual phase and baseline corrections were applied. All offset signals are referenced to the TMS signal (δ= 0.00 ppm). Each sample was measured in triplicate.

2.4 FTIR spectroscopy

An FT/IR-6100 spectrometer (JASCO Deutschland GmbH, Pfungstadt, Germany) equipped with an attenuated total reflectance (ATR) unit was used to obtain FTIR spectra. An oil droplet was placed on diamond cell ATR, and the absorbance spectra were recorded. The samples were scanned at room temperature at a resolution of 4 cm^{-1} in the wavenumber range 4000–600 cm^{-1}. The sample and background spectra are set at an average of over 32 scans. A new background spectrum was obtained after each measurement. The ATR was cleaned with isopropanol before a new sample was applied. All spectra were measured in triplicate and used for statistical analysis.

2.5 Pre-processing and multivariate data analysis

Data preprocessing of the ^{1}H NMR spectra was carried out using Amix 3.9.15 (Bruker BioSpin GmbH, Rheinstetten, Germany) to reduce by bucketing spectral regions of equal width of 0.009 ppm. After the bucketing spectra were obtained, they were converted into txt format to build the data matrix (Figure S1-S11 Supplementary Materials 1). The final range used for PCA and PLS was δ= 5.37–5.27 ppm and δ= 2.37-2.20 ppm.

The data preprocessing of FTIR spectra was performed as a baseline correction. Additionally, the scattering effects were removed by means of second-order smoothing polynomials through 25 points (Savitzky-Golay method).[20,21] Finally, the resulting spectra were converted into JCAMP format to build a data matrix. The final FTIR spectral range of interest was limited to 2990 to 3020 cm^{-1} and 1680-1780 cm^{-1}.

Unscrambler X 11.0 (CAMO Software AS., Oslo, Norway) was used for the individual analysis of both spectral methods using PCA and PLS. First, PCA methods were applied to attain delineate classes rules according to the degree of unsaturation and FFA value of commercial products. In addition, PLS methods were applied to predict the value of the degree of unsaturation and FFA composition of RFO commercial products.

The unsupervised pattern recognition models PCA and supervised pattern PLS were built on all replicates of all samples, as shown in Table 1. The calibration models were built using nineteen samples (in triplicate), including crude RFO, three modified RFO, three other oil (BSO, OVO, and VCO), and 15 commercial RFO. Furthermore, twenty-one commercial samples (in triplicate) other than those used as calibrations were used to test their class identities. The leave-one-out cross-validation procedure was used to verify the calibration and prediction model. Finally, the total calibration, validation, and prediction errors (RMSEC, RMSEV, and RMSEP) for each model sample were evaluated.[22]

3 RESULTS AND DISCUSSION

3.1 Spectral data for multivariate analysis

For multivariate data analysis, it is mandatory to have a sample preparation that generates reproducible spectra. Figure 1 shows the results of bucketing processes demonstrating a good performance for the alignment of RFO ^{1}H NMR spectra.[10,23,24]

Because the ^{1}H NMR spectrum contains several thousand points and is therefore variable, data reduction or clustering is usually used to reduce the dimension of the data. By bucketing, the spectrum is divided into spectral regions, or buckets (also called bins), and the total area in each bucket is calculated to represent the original spectrum. Finally, to make all spectra comparable, the overall sample concentration variation must be taken into account, as was the case with the ^{1}H NMR spectra of the sample. The clustering of spectra of 0.009 ppm bucket gave satisfactory results, especially the reliability of the chemical shift, and the signal intensity was the same as the original spectra for each sample. It is obtained from the sum of the

intensities in each set of buckets so that the area under each signal in the spectral region is used instead of the individual intensities.[23,25] As a result, the chemical shift variability around the signal and misalignment could be overcome. Thus, the resulting data matrix variables will slightly vary each iteration for further chemometric analysis processes.

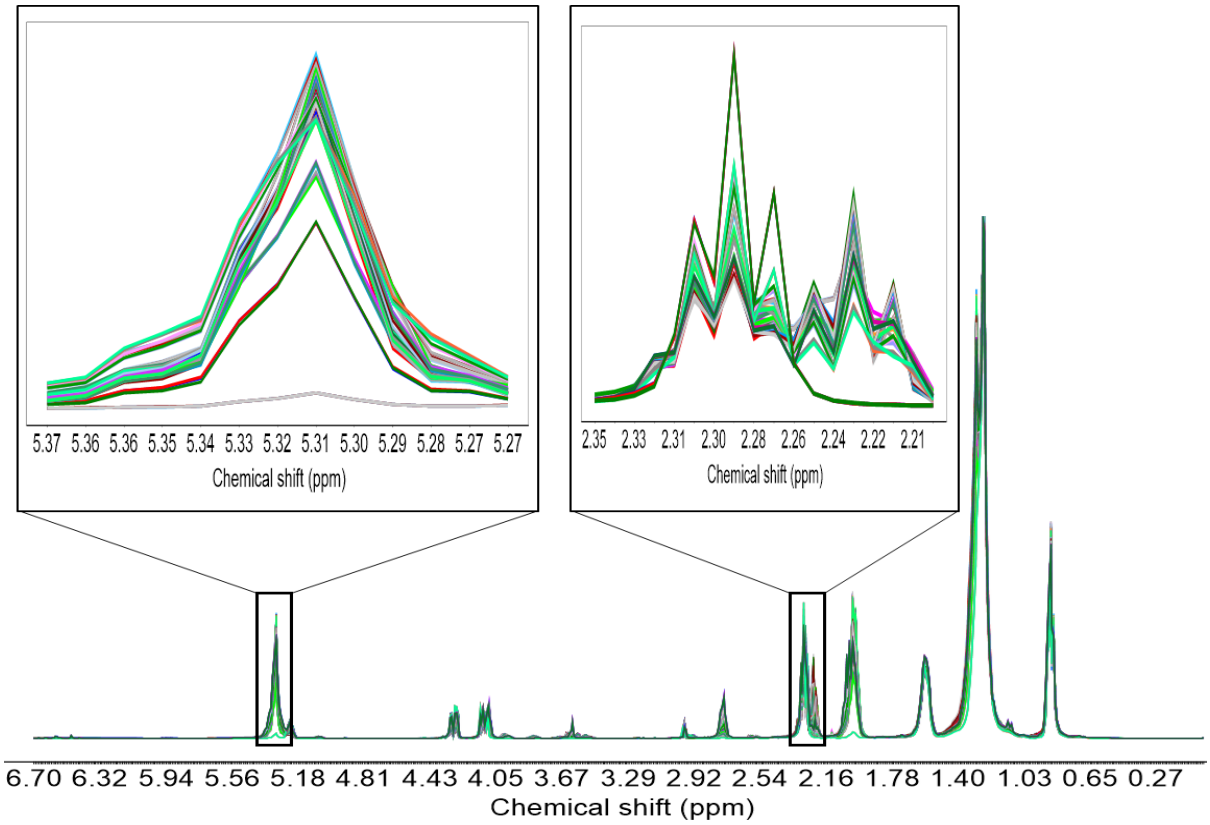

FIGURE 1 Reduced ^{1}H NMR spectra of all samples with an enlarged spectral range of δ= 5.37-5.27 ppm and δ= 2.37-2.20 ppm. The spectra are color-coded according to the brand

Furthermore, in FTIR spectra, preprocessing procedures also showed a good performance for alignment without derivative transformation and data loss with constant range wavenumber. With an interval of 4 cm^{-1} selected, it displays the level of smoothness of the data obtained during the measurement. The meaning of 4 cm^{-1} is that the spectrum is expected to be obtained at intervals of approximately 2 cm^{-1} to increase signal resolution (sharper spectra) without losing time[26]. This result proved that good resolution was obtained between the peak band at 1740 cm^{-1} and 1710 cm^{-1}, as well as at 3007 cm^{-1} and 2920 cm^{-1}, as can be seen in

Figure 2. All vibrational bands of sample spectra were obtained clearly at the same wavenumber. Therefore, the resulting data matrix variable will be reliable.

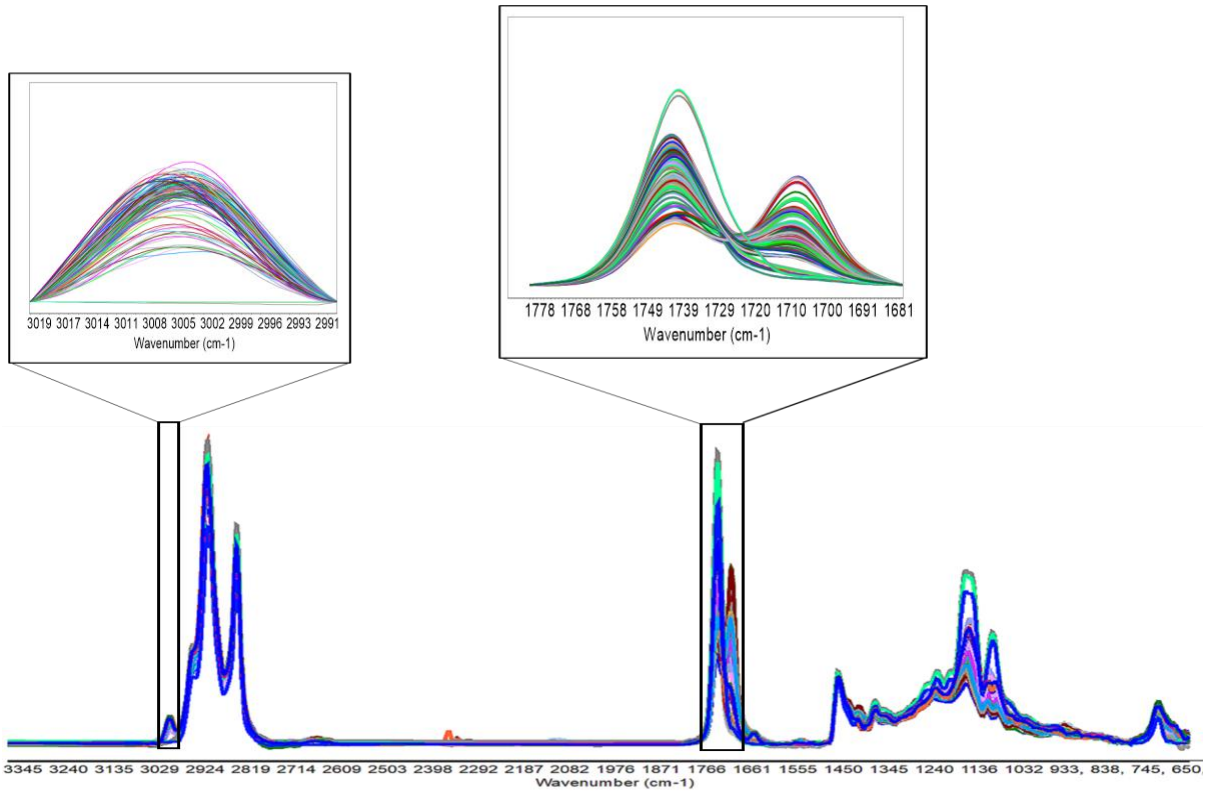

FIGURE 2 Reduced FTIR spectra of all samples with an enlarged spectral range of the band at 1780 – 1680 cm^{-1} and 3020 – 2990 cm^{-1}. The spectra are color-coded according to the brand

Generally, the spectra produced by these two processing methods have a similar profile in all samples. However, differences in some parts of the intensity on the ^{1}H NMR and absorbance on the FTIR spectra can be observed, especially in the signals/bands selected for analysis.

Finally, two different matrices were considered for both data:

1) ^{1}H NMR matrix consists of two segments; the degree of unsaturation (-CH=CH-) and FFA value (α-CH_2) signals. Thus, the final ^{1}H NMR data matrix contains 120 rows (samples) and 13 columns variables for the degree of unsaturation and 120 rows (sample) and 18 columns for FFA values, respectively. (i.e., relative intensity at different chemical shifts, respectively).

2) FTIR matrix consists of two segments; the degree of unsaturation (the C-H stretching band of the double bond) and FFA value (C=O) bands. Therefore, the final FTIR data matrix contains 120 rows and 33 columns for the degree of unsaturation, 120 rows and 105 columns for FFA values (i.e., absorbance samples at different wavenumber, respectively).

3.2 Evaluation of correlation selected signal (-CH=CH-) ^{1}H NMR and FTIR spectra

Both spectral data (^{1}H NMR and FTIR) consist of triacylglycerol (TAG) and FFA signals once these compounds are predominantly found in the intact material analysis.[5,27] The set of signals at δ= 5.37 - 5.27 ppm arises largely from the ^{1}H nuclei attached to carbons in the close neighborhood of a double bond.[28] This signal is related to the degree of unsaturation bonds in a triglyceride, regardless of whether these are located within monounsaturated or polyunsaturated chains. Since the FTIR spectra were acquired from precisely the same collection of samples used in the ^{1}H NMR analysis, an avenue exists for exploring the correlations between the two datasets. In addition, the C-H stretching band of the double bond in the FTIR spectra occurs in the range of 3000 to 3020 cm^{-1}.[29] Figure 3 shows a multivariate regression showing significant correlations between the ^{1}H NMR and FTIR datasets points (all PLS model analyses presented in Figure S1- Supplementary Materials 2).

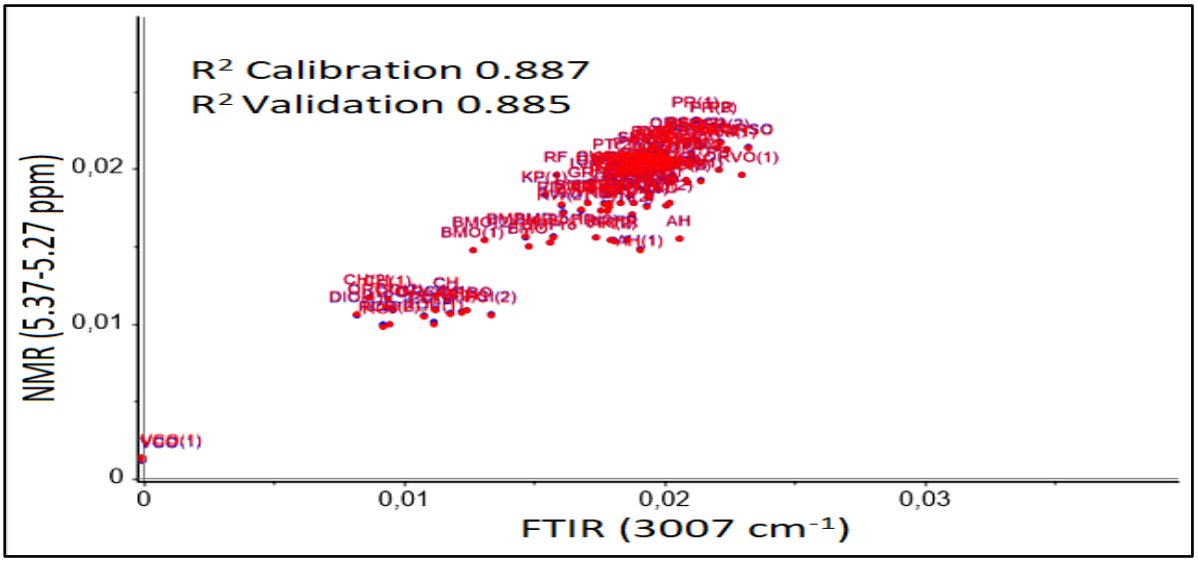

FIGURE 3 PLS calibration model for the relationship between ^{1}H NMR and FTIR spectra of the selected signal

The relevant ^{1}H NMR and FTIR spectral features are -C<u>H</u>=C<u>H</u>-. Even though the FTIR feature has a low intensity, both spectra show relatively strong variations with differences in each product's -C<u>H</u>=C<u>H</u>- bond content. According to Parker et al.,[28] these findings can be used as additional information: with a strong correlation between the two spectra; the signal -C<u>H</u>=C<u>H</u>- of NMR and the C-H stretching band of the double bond in the FTIR can be one of the signals that determines the difference between the respective oil products, especially regarding the degree of unsaturation.

3.3 Evaluation of correlation selected signal α-CH_2 of ^{1}H NMR and C=O FTIR spectra

It is well-known that C=O at 1710 cm^{-1} can be assigned to -COOH (acid) and C=O at 1740 cm^{-1} to -COOR (ester). The two bands are related to the FFA and TAG system, respectively. Interestingly, a strong correlation can be formed for the α-CH_2 signal of the NMR at δ= 2.37-2.20 ppm and the C=O band resonance of the IR at 1680 to 1780 cm^{-1}. The multivariate regression analysis states that both signals have a closed correlation ($R^2 > 0.97$ and $R^2 > 0.94$) (Figure 4 and all PLS model analyses presented in Figure S2 and S3- Supplementary Materials 2).

However, there are different interpretations of the relationship between the two bands, especially in the OVO, VCO, and OR samples. Namely, is for the band C=O (1710 cm^{-1}) with a signal α-CH_2 at δ = 2.37-2.20 ppm, which indicates the position of OVO and VCO had the lowest intensity, whereas OR had the highest intensity (Figure 4A). On the other hand, the C=O band (1740 cm^{-1}) indicates that the OVO and VCO have the highest intensity, while OR has the lowest intensity (Figure 4B). These results indicate that TAG OVO and VCO composition is more significant than FFA. In contrast, OR shows that the composition of FFA is higher than TAG. These results confirm that the C=O band at 1710 cm^{-1} is an acid (FFA) while the C=O band at 1740 cm^{-1} is an ester (TAG).[30]

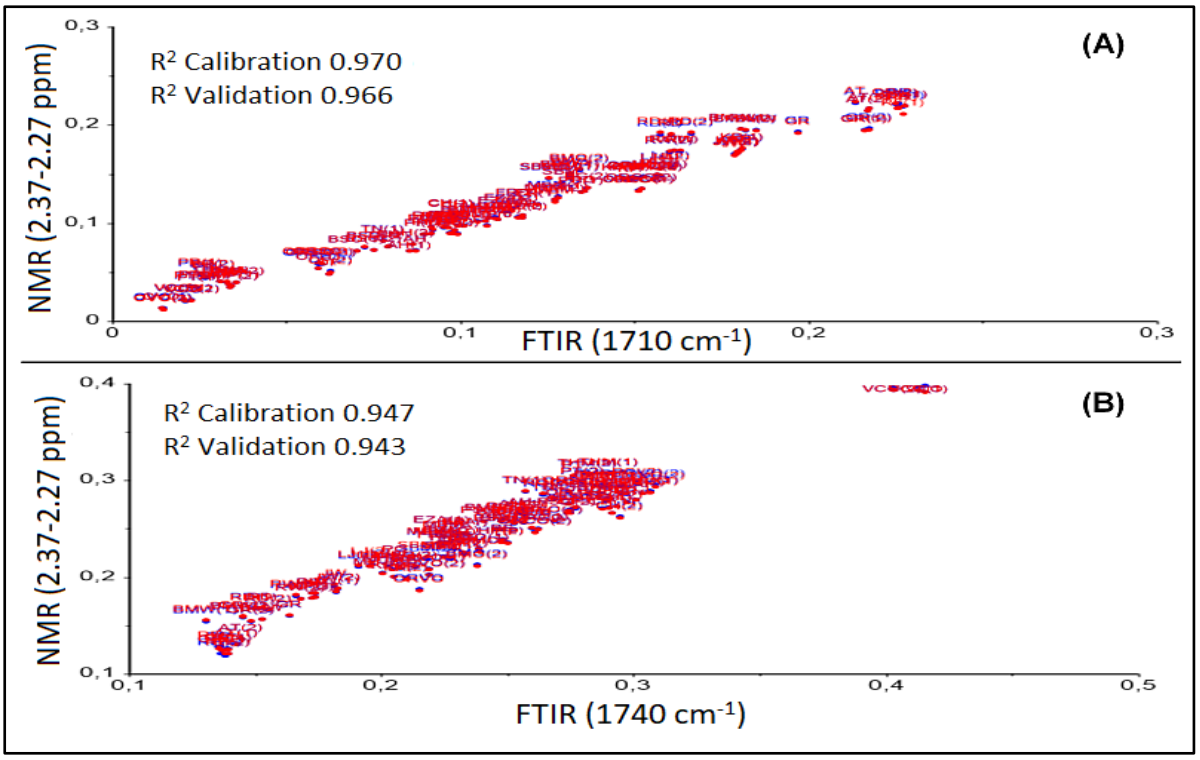

FIGURE 4 PLS calibration model for the relationship between ^{1}H NMR and FTIR spectra of the selected signal. (A) band 1710 cm^{-1} (B) band 1740 cm^{-1}

Parker et al. 's[28] have not shown any correlation between the C=O band (FTIR) and the α-CH_2 signal (^{1}H NMR) due to the absence of a heat map in the Pearson correlation statistic. However, our findings indicate a strong correlation between the α-CH_2 signal on ^{1}H NMR and the C=O band on FTIR. These results can be obtained because the two signals in each spectrum have good resolution and a relatively substantial intensity difference (see Figure 1 and Figure 2). In addition, these two functional groups are adjacent in the structure of the constituent FFA and TAG.[21,27] Therefore, these two signals/bands are essential in differentiating oil products based on the amount of FFA.

3.4 PCA Projection for the degree of unsaturation profile distinction

The PCA projection is carried out on the matrix data of the ^{1}H NMR and FTIR spectra related to the degree of unsaturation to predict the RFO product profile. The first PCA was performed on a calibration matrix of 57 spectra from 19 calibration samples. The presence of BSO, OVO, and VCO as a comparison and modifier of crude RFO in calibration modeling illustrates the

effect of adding these types of oil to crude RFO in matrix variables (see Materials & methods). Finally, the PCA calibration results are used to project 63 spectra from 21 samples of RFO products (prediction test). Based on the ability of PCA to determine the similarity between the calibration data model and the prediction data,[31] the RFO samples will be grouped according to the similarity of the variables. They will show the projection pattern due to changes in the variables caused by these modifications, which are also helpful for authentication.

The PCA of ^{1}H NMR data presents the separation of the RFO products into four main regions (Figure 5 and all PCA model analyses are displayed in Figure S4-Supplementary Materials 2). Most RFO products are on the positive side of the PC2 and PC1 axes (red circle), including OVO and ORVO. On the most negative side of the PC1 axis, there are VCO products (outliers/black circle) because it is a type of oil different from RFO (slight/no double bond), while BSO is located at the most negative PC2 (green circle), because of a lot of double bonds. Furthermore, this PCA projection can be used for RFO delineating classes based on the closeness of the degree of unsaturation category.

Accordingly, PCA Calibration and Projection plots indicate four products of RFO from the prediction set (ROP, CH, DIO, AH, and BMPro); three products from the calibration set (ORCO, BMO, and FR) are located in the negative PC1 (yellow circle) that are close to VCO, indicating a profile very similar to the VCO (especially a high amount of saturated lipid). In addition, there are four RFO products in the prediction set, which are similar to one calibration modification product (ORCO). Therefore, these results indicate that the products (ROP, CH, DIO, and PCI) are estimated to contain VCO.

On the other hand, there are two RFO products of the prediction test (HM and SBM) and two products of the calibration set (PR and ORSO) located on the negative side of the PC2 axis (green circle), where the products are projected close to the BSO profile indicating a lot of double bonds. In addition, there is one RFO product (SBM) in the prediction set, similar to one calibration modification product (ORSO). These results can denote that the product (SBM) is projected to contain BSO. Examination of PC1 and PC2 loading of the ^{1}H NMR data shows

that this separation occurs because the spectral domain at δ= 5.37 - 5.27 ppm (-CH=CH-) has different relative intensities; thus, the signal represents an important limitation of this method.

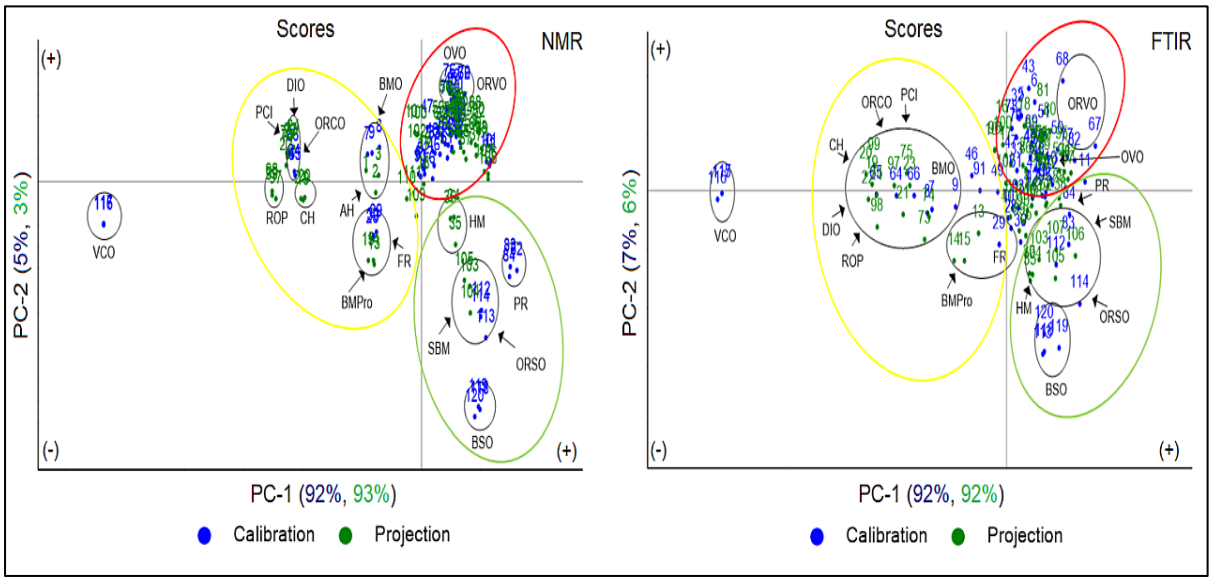

FIGURE 5 Projected twenty-one RFO commercial products based on principal components PC 1 and PC 2 with the selected signal at 5.37-5.27 ppm (–CH=CH-) of the nineteen ^{1}H NMR spectra calibration set (57 spectra) (NMR) and with the selected band at 3000-3020 cm^{-1} (the C-H stretching band of the double bond) of the nineteen FTIR spectra calibration set (57 samples) (FTIR). The replication number code indicates the label point for each sample (see Materials and methods). (green circle: ORSO projected sample group; yellow circle: ORCO projected sample group; red circle: ORVO projected sample group). (AH: Agro Herbal Husada, BMO: Buah Merah Oil Papua, BMPro: Minyak Buah Merah, BSO: Black Seed Oil, CH: Cahaya, DIO: DioDes Minyak Buah Merah, FR: Fira Papua, ORCO: Crude RFO plus VCO, ORSO: Crude RFO plus BSO, ORVO: Crude RFO plus OVO, PCI: PCI Buah Merah, PR: Pro Jep Buah Merah), ROP: Red Oil Papua, SBM: Sari Buah Merah, OVO: Olive Oil, VCO: Virgin Coconut Oil)

The treatment of FTIR data appears to have similarities in the projection of the sample product based on the degree of unsaturation. However, in Figure 5 FTIR, the PCA score plot shows a marked separation in which VCO is located in the most negative PC1, and BSO is in the most negative PC2, while most of the products are found in plots PC1, PC2 are positive (all PCA

model analyses presented in Figure S5- Supplementary Materials 2). At least the FTIR PCA plot results are similar to the ^{1}H NMR. Separation of the same products with a close profile to VCO can also be detected. For example, four products of the prediction test (ROP, CH, DIO, and PCI) are projected to ORCO (yellow circle), and the separation of products prediction test (SBM) close to the BSO profile is projected to ORSO (green circle). However, some projected overlapping products and different locations between replications can still be seen. The FTIR data loading assessment of PC1 and PC2 indicated that an absorption band at about 3000 - 3020 cm^{-1} (the C-H stretching band of the double bond) was responsible for this separation.

Chemometric analysis for both data sets showed projected differences in the degree of unsaturation between the RFO products. The total projection of the two data sets also indicates satisfactory results by producing 98% PC total separation into four region (black, yellow, red, and green circles) depending on the degree of unsaturation, as already described. Unfortunately, PCA projections on FTIR show a more considerable grouping variability, for example, the distance differences between product replication of BMPro and PCI in the yellow circle sample group and of ORSO, PR in the green circle sample group, respectively. The lower reproducibility observed in the FTIR results depends on the manual placement of the sample in the ATR, as has been discussed by Jovic et al.[32] Therefore, the triple clustering projection for FTIR shows unsatisfactory results. It is important to emphasize that replicate clustering is preferable when ^{1}H NMR is used.

3.5 PCA Projection for free fatty acid value profile distinction

Furthermore, PCA Projection predicts the RFO product profile based on the FFA value. As mentioned above, the presence of oil other than RFO, including BSO, OVO, and VCO, aims to compare and modify crude RFO to indicate changes in the sample matrix caused by the intervention of each oil. A total of 57 spectra from 19 samples were used as a data calibration matrix for projecting 21 RFO samples (see Materials and methods). The PCA data for ^{1}H NMR and FTIR presents a separation of the RFO products into four regions.

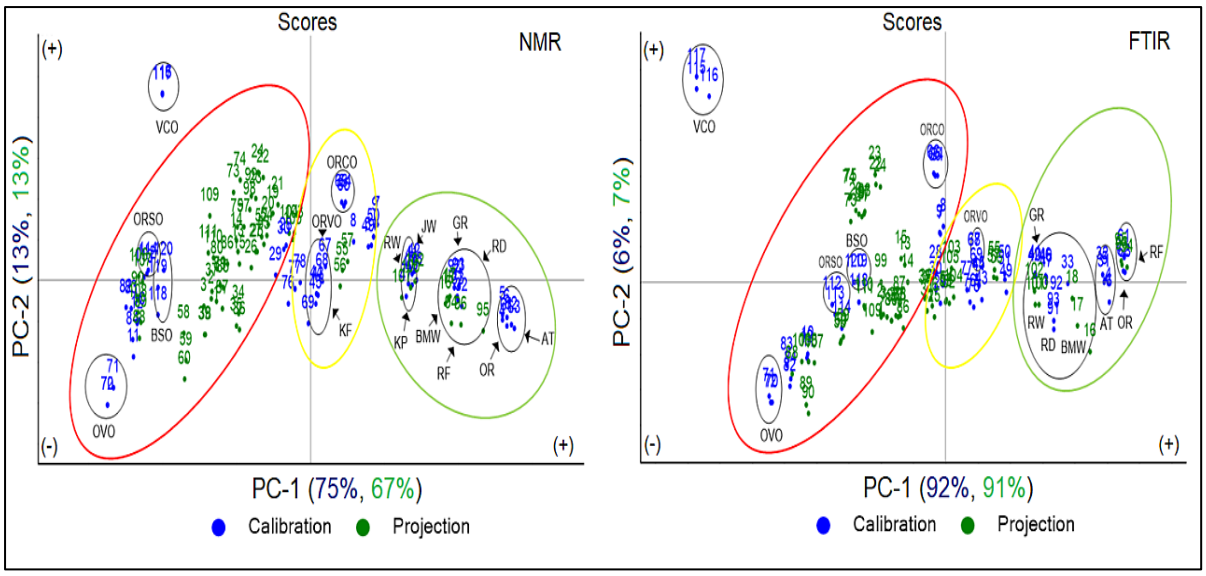

FIGURE 6 Projected twenty-one RFO commercial products based on principal component PC 1 and PC 2 with the selected signal at 2.37-2.227 ppm (α-CH_2) of the nineteen ^{1}H NMR spectra calibration set (57 spectra) and with the selected band at 1690-1780 cm^{-1} (C=O) of the nineteen FTIR spectra calibration set (57 spectra). The replication number code indicates the label point for each sample (see Materials and methods). (green circle: PC-1 positif projected sample group; yellow circle: PC-1 middle projected sample group; red circle: PC-1 negatif projected sample group). (AT: Athaku, BSO: Black seed oil, JW: Jaya Wijaya, KF: KF Minyak Buah Merah, KP: King Pandanus, GR: Golden Red, OR: Crude RFO, ORCO : Crude RFO plus VCO, ORVO: Crude RFO plus OVO, OVO: Olive Oil, RD: Redoten, RF: Fira Papua, VCO: Virgin Coconut Oil)

On the other hand, the PCA pattern projection from FTIR shows a pattern similar to NMR (Figure 6 and all PCA model analyses presented in Figure S6 and S7- Supplementary Materials 2). The 3 RFOs, including OR, AT, and RF (green circle), also lie at the farthest positive PC1, while the PC2 is positive. Meanwhile, most RFO products are projected along PC2 (negative to positive) in the red circle. Another similarity was also shown in the projections of VCO (farthest positive PC2) and OVO (farthest negative PC2) in the red circles .

The modified RFO also has a similar projection to the ^{1}H NMR data. The projected ORSO samples were identical to BSO (PC1 and PC2 were negative) in the red circles. As for the

ORCO projection, the FTIR pattern is better than the ^{1}H NMR pattern (PC1 negative and PC2 positive) because it is located in the same quadrant plot as the VCO, while ORSO in the NMR plot score is in the yellow circle. It means that the FTIR spectral pattern for ORCO can show the effect of adding VCO to the variable matrix pattern to be used as a reference for authentication.

Interestingly, the ORVO projections for both PCA patterns also show a similar location at the midpoint of the plot score (PC1 and PC2 are positive) in the yellow circle. However, they are not projected the same as OVO (red circle). These results show that the addition of OVO to crude RFO does not necessarily change the pattern of the variable matrix that is close to the OVO pattern. Accordingly, the results illustrate that the difference matrix variables used do not directly affect the projection pattern. This condition depends on the FFA amount of both. Furthermore, the FTIR projection pattern on the selected matrix variable shows a better projection pattern with a full PC of 98%, while ^{1}H NMR can project a full PC of 88%.

3.6 PCA for the degree of unsaturation grouping

In the visualization grouping approach, PCA builds three rules based on the degree of unsaturation content with three different oil products with RFO as standard, namely BSO, OVO, and VCO. When an RFO product has a low degree of unsaturation, it will approach VCO. An RFO product with a high degree of unsaturation identical to OVO is an original RFO product because, based on the characterization results,[5,6] the main content of RFO is oleic acid. In contrast, an RFO product with a higher degree of unsaturation will approach the BSO position because it has more unsaturated fatty acids than OVO. Furthermore, a visualization grouping PCA model can be obtained based on the value of the degree of unsaturation for the entire RFO product[27], according to previously reported by Triyasmono et al.[18] Figure 7 shows that both spectral data sets can be classified into 6 categories (IV : < 10; 40 - 60; 60-70; 70-80 and > 90) .

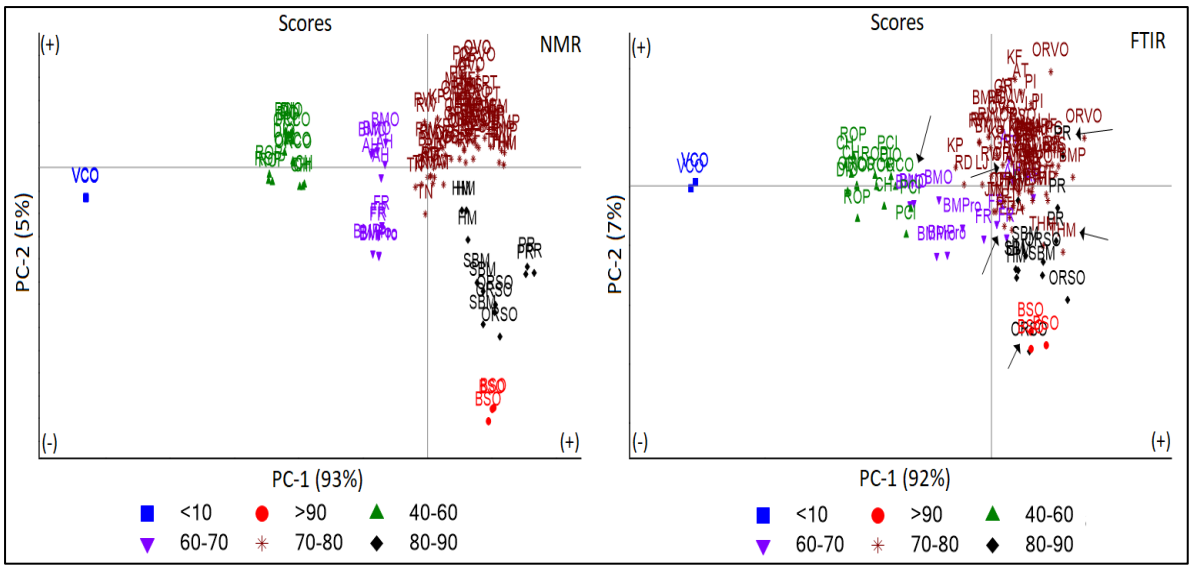

FIGURE 7 Plot scores of all samples (120 spectra) on the main components PC1 and PC2 on the selected signal ^{1}H NMR spectra and selected band FTIR based on the degree of unsaturation category (The point label according to the abbreviation section)

Both ^{1}H NMR and FTIR data presented satisfactory results with 98% total PC and 99% total PC of the classified products, respectively (all PCA model analyses presented in Figure S8 and S9- Supplementary Materials 2). For FTIR data, there are five types of classified products that overlap with the others (AH, BMO, FR, THM, and PR) (Figure 7 FTIR). As for the prediction of ^{1}H NMR, the observations were excellent because 100% of the samples were classified correctly. Furthermore, these results show that most products can be grouped at 70-80 degrees of unsaturation, as well as OVO, which indicates that most RFO products have a monounsaturated fatty acid component. On the other hand, four products (ROP, CH, DIO, and PCI) and ORCO are close to VCO, so it is suspected that there VCO components are added. Therefore, it affects to decrease the degree of unsaturation, and it is classified as lower than crude RFO (40-60).

In comparison, three products (SBM, PR, and FR) and ORSO are close to BSO, so it is suspected that BSO was added to the product component, causing an increased degree of unsaturation. Therefore, it is grouped as higher than crude RFO (80-90). Based on the fact that there are still miss-grouping in the FTIR data, even though 99% total PC of the samples

can be distinguished based on different variables. Finally, the best triplicate for ^{1}H NMR data implies a perfect visualization grouping based on the RFO product's unsaturation degree.

3.7 PCA for free fatty acid value grouping

Furthermore, for the classification approach based on its FFA value, the PCA model is based on the acid number possessed by each sample because the amount of FFA depends on the acid value of each sample. The FFA in each product is either occurring naturally or due to degradation. Meanwhile, the presence of BSO, OVO, and VCO independently and crude RFO modifiers can be used to compare the distribution pattern classification due to changes in the variable matrix (see Materials and methods). Figure 8 depicts the PCA visualization grouping of all total samples into seven categories according to acid values based on Triyasmono et al.[18] reported (AV: < 10; 40 - 60; 60-70; 70-80, 80-90 and > 90) for the spectrum of both methods.

The PCA plot score generated from both methods (NMR and FTIR) showed the same pattern. However, the ^{1}H NMR data displayed a better classification pattern than the FTIR data because the entire sample could be separated according to their respective categories without overlap (Figure 8 NMR and all PCA model analyses presented in Figure S10- Supplementary Materials 2). As for the PCA FTIR data pattern, several sample products are delineated classes into different categories, including AT, CH, DIO, OF, and RF (Figure 8 FTIR and all PCA model analyses are presented in Figure S11- Supplementary Materials 2). These results happen because the FTIR spectrum pattern variance is more significant than ^{1}H NMR, so that it can cause a more considerable matrix variable variance.[32] Interestingly, OVO and VCO have the same categorization of the FFA value at < 10. Both are located on the same PC1 (farthest negative); meanwhile, they are different in PC2; OVO PC2 is negative while VCO PC2 is positive. These results can be caused by the spectral variance pattern correlated with the chemical bonds of a free fatty acid constituent of each oil. For OVO, mainly FFA consists of oleic acid. Meanwhile, most of VCO's FFA consists of palmitic acid.[32,33]

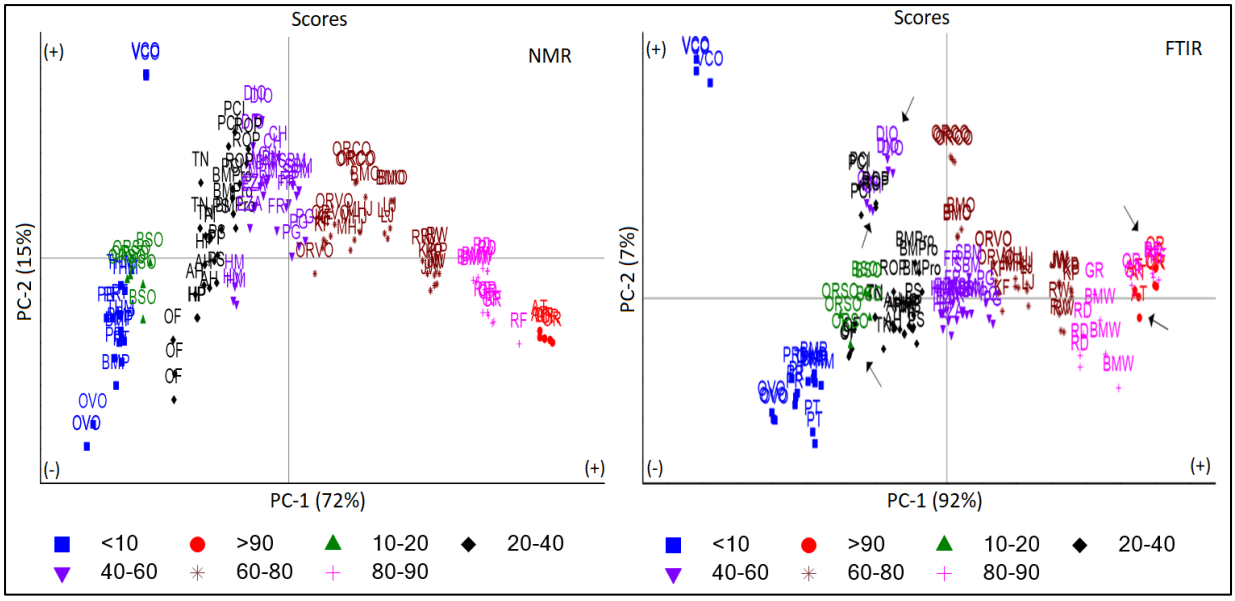

FIGURE 8 Plot scores of all samples (120 spectra) on the main components PC1 and PC2 on the selected signal ^{1}H NMR spectra and the selected band FTIR spectra based on the FFA value category (The point label according to the abbreviation section)

In contrast, BSO plot scores differ almost from the RFO product and OVO in the degree of unsaturation category but have adjacent plot scores in the FFA category. This result indicates they may have the same acid value even though their free fatty acid composition is different.[9,32,34] Therefore, this signal is suitable for classifying and authenticating commercial RFOs based on the acid value profile.

On the other hand, De la Mata et al.[35], employing FTIR and PLS-DA spectra in the entire band at 3508-650 cm^{-1} (except 2350-1870 cm^{-1}), which was derivatized, demonstrated that 100% olive oil was identified and differentiated from vegetable oil. However, up to 50% for mixed samples results in a more significant prediction error. In comparison, this finding can also visualize the grouping of the RFO based on the degree of unsaturation and the FFA value up to a total PC of 99% with a lower error prediction even using two bands (3000-3020 cm^{-1} and 1680-1780 cm^{-1}) and without derivatization spectra.

Popescu et al.[36] used NMR spectra (^{1}H, ^{13}C) combined with PCA, and were able to produce projections of olive oil that clustered close together even though they come from different

countries of origin, while walnut oil is in varied plots. Subsequently, a mixture of 1% olive oil and sunflower oil can also be detected, with a total PC variance between 91% and 92%. However, the author can show a total PC variant of up to 98% in visualizing the different RFO products and projecting the presence of adulterants, including olive oil, black seed oil, and virgin coconut oil.

In comparison to the ^{13}C NMR approach without chemometrics for the identification of adulterant vegetable oils in essential oils as described by Truzzi et al. [37], the ^{1}H NMR requires a shorter acquisition time of only 15 min per sample compared to 47 min. One of the reasons for this condition is the relaxation times of carbon atoms are significantly longer (5.6 s) than those of ^{1}H NMR (1.56 s) in the lipid component.[38,39]

Furthermore, the approach without chemometrics in ^{13}C NMR still entails manually calculating the similarity using the square ratio matrix formula. In comparison, the procedure for chemometrics is relatively simple; the entire bucketing sample spectrum data is directly imported into Unscrambler X 11.0 (see 2.5) for PCA and PLS analysis. Therefore, the time needed for analysis was relatively fast (approximately 10 min). In addition, applying chemometrics is more able to visualize groups with a confidence level of more than 95% with an acceptable error lower than 5% compared to those without chemometrics; the confidence level obtained 75% and the minimum error achieved 10% to identify the presence of adulterants in essential oil. Nevertheless, ^{13}C NMR experiments are a worthwhile alternative because they provide a lot more information than the time-consuming determination of e.g. the iodine value.

Finally, the results from this work pointed out that NMR-PCA and FTIR-PCA are suitable and more straightforward, quick and efficient methods for describing classes, differentiating RFO types, or detecting adulteration, especially adulteration with other types of oil that have a higher or lower unsaturated degree and FFA values without losing precision.

3.8 PLS model for prediction of the degree of unsaturation and free fatty acid value

A PLS model is constructed for each parameter (the degree of unsaturation and free fatty acid value). Calibration was performed with "leave one out" cross-validation. Furthermore, the prediction of the test to validate was performed (see section on Materials and Methods). **Table 2** shows the mean values for each parameter, and the results are presented in terms of the number of factors used, correlation coefficient (R^2), calibration standard error (SEC), and prediction standard error (SEP). SEC and SEP are the standard deviations for the difference between the measured and ^{1}H NMR estimated values for the samples in the

calibration and validation sets, respectively.

TABLE 2 Results of PLS modeling and prediction of the RFO properties based on both methods (^{1}H NMR and FTIR)

Parameter	Method	Value	Factor	R^2			Root Mean Square Error (RMSE)		
				Calibration	Validation	Prediction	RMSEC	RMSEV	RMSEP
Unsaturated degree	^{1}H NMR	0-90	1	0.972	0.967	0.915	3.08	3.29	4.18
	FTIR	0-90	1	0.919	0.914	0.834	5.31	5.49	5.50
FFA value	^{1}H NMR	0 - 100	2	0.988	0.986	0.982	3.49	3.76	3.12
	FTIR	0 - 100	2	0.977	0.977	0.948	4.88	5.15	5.10

The performance results indicate that both parameters show a good match based on the R^2 index with RMSEC for each model lower than SEP.[22] Furthermore, at least 92% of the variation of the output variable can be explained by the ^{1}H NMR and FTIR spectra (all PLS models and predicted analyses presented in Figure S12-S19 - Supplementary Materials 2). However, ^{1}H NMR data give more results with better reproducibility, indicated by a lower error value for both parameters.

Therefore, ^{1}H NMR replication is more promising and proven to determine the difference between each RFO product based on the degree of unsaturation and the FFA value. These findings support several previous reports[14,15,27,28] on the success of ^{1}H NMR spectroscopy in analyzing fat and oil quality parameters.

In conclusion, the spectra profiled by ^{1}H NMR and FTIR and chemometric analysis contributed to the discriminant of RFO based explicitly on the degree of unsaturation and the FFA value. Compared with other traditional techniques, ^{1}H NMR and FTIR combined with chemometrics provide a fast and economical method for RFO characterization, classification, and authentication. Both methods were successful for the projection, classification, and prediction of the distinction of the degree of unsaturation and FFA value between crude RFO, commercial RFO, and modified RFO. However, better results were achieved for ^{1}H NMR data. These results demonstrate that chemometrics is a robust characterization, classification, and authentication tool.

ETHIC STATEMENT

Our research did not include any human subjects or animal experiments.

ACKNOWLEDGEMENTS

The authors would like to thank the supporting finance of Lambung Mangkurat University (Grant No. 3894/UN8/KP/2019). The authors warmly thank Dr. Jens Schmitz, Sebastian Schmidt and Alexander Becht for their technical support during the study as well as Dr. Ludwig Höllein for editorial support during writing and preparation for submission this publication.

CONFLICT OF INTEREST

The authors declare no conflict of interest.

REFERENCES

1. Mun'im A, Andrajati R, Susilowati H. Tumorigenesis inhibition of water extract of red fruit (Pandanus conoideus Lam.) on Sprague–Dawley rat female induced by 7,12-dimetilbenz(a)antrasen (DMBA). *Indon J Pharm Sci* 3. 2006; 153–161. https://doi.org/10.7454/psr.v3i3.3407

2. Surono I, Endaryanto TA and Nishigaki T. Indonesian biodiversities from microbes to herbal plants as potential functional foods. *J. Fac. Agric. Shinshu Univ*. 2008; 44(1.2): 23–27

3. Khiong K, Adhika OA and Chakravitha M. Inhibition of NF-κB pathway as the therapeutic potential of red fruit (Pandanus conoideus Lam.) in the treatment of inflammatory bowel disease. *JKM (Jurnal Kedokteran Maranatha)*. 2009; 9 (1): 69–75

4. Rohman A, Riyanto S, Yuniarti N, Saputra WR, Utami R and Mulatsih W. Antioxidant activity, total phenolic, total flavanoid of extracts and fractions of red fruit (Pandanus conoideus Lam). *Int. Food Res. J*. 2010; 17: 97–106

5. Rohman, A, Sugeng R, & Che Man Y B. Characterizaton of red fruit (Pandanus conoideus Lam) oil. *Int. Food Res. J.* 2012;*19*(2):563–567

6. Sarungallo ZL, Hariyadi P, Andarwulan N & Purnomo EH. Characterization of chemical properties, lipid profile, total phenol and tocopherol content of oils extracted from nine clones of red fruit (Pandanus conoideus). *J. Natural Sci*. 2015; *49*(2) : 237–250.

7. Triyasmono L, Riyanto S & Rohman A. Determination of iodine value and acid value of red fruit oil by infrared spectroscopy and multivariate calibration. *Int. Food Res. J*. 2013; *20*(6), 3259–3263

8. Ropodi AI, Panagou EZ, Nychas GJE. Data mining derived from food analyses using non-invasive/non-destructive analytical techniques; determination of food authenticity, quality & safety in tandem with Computer Science Disciplines. *Trends Food Sci Technol*. 2016 ;50:11–25. https://doi.org/10.1016/j.tifs.2016.01.011

9. Rohman A, Mohd A.B. Ghazali, Anjar Windarsih, Irnawati, Sugeng Riyanto, Farahwahida M. Yusof, and Shuhaimi Mustafa.. "Comprehensive Review on Application of FTIR Spectroscopy Coupled with Chemometrics for Authentication Analysis of Fats and Oils in

the Food Products" *Molecules.* 2020; 25(22): 5485. https://doi.org/10.3390/molecules25225485

10. Monakhova YB, Kuballa T & Lachenmeier DW. Chemometric methods in NMR spectroscopic analysis of food products. *J. Anal. Chem*. 2013. https://doi.org/10.1134/S1061934813090098

11. Alcantara GB, Honda NK, Ferreira MM & Ferreira AG. Chemometric analysis applied in 1H HR-MAS NMR and FT-IR data for chemotaxonomic distinction of intact lichen samples. *Anal. Chim. Acta*. 2007; 595. https://doi.org/10.1016/j.aca.2007.03.032

12. Becht A, Schollmayer C, Monakhova YB & Holzgrabe U. Tracing the origin of paracetamol tablets by near-infrared, mid-infrared, and nuclear magnetic resonance spectroscopy using principal component analysis and linear discriminant analysis. *Anal. Bioanal. Chem*. 2021; *413*(11): 3107–3118. https://doi.org/10.1007/s00216-021-03249-z

13. Roberto de Alvarenga Junior B & Lajarim Carneiro R. Chemometrics Approaches in Forced Degradation Studies of Pharmaceutical Drugs. *Molecules.* 2019; 24 (3804): 1-24 *(Basel, Switzerland)*. NLM (Medline). https://doi.org/10.3390/molecules24203804

14. Ingallina C, Cerreto A, Mannina L, Circi S, Vista S, Capitani D, Marini F. Extra-virgin olive oils from nine italian regions: An ^{1}H NMR-chemometric characterization. *Metabolites*. 2019; *9*(4): 1-12. https://doi.org/10.3390/metabo9040065

15. Giese E, Rohn S & Fritsche J. Chemometric tools for the authentication of cod liver oil based on nuclear magnetic resonance and infrared spectroscopy data. *Anal. Bioanal. Chem*. 2019; *411*(26): 6931–6942. https://doi.org/10.1007/s00216-019-02063-y

16. Rodionova OY & Pomerantsev AL. Chemometrics: achievements and prospects. *Russ. Chem. Rev* 2006; *75*(4):271–287. https://doi.org/10.1070/rc2006v075n04abeh003599

17. Folch J, Lees M & Sloane Stanley GH. A simple method for the isolation and purification of total lipides from animal tissues. *J. Biol. Chem*. 1957; *226*(1) : 497–509. https://doi.org/10.1016/s0021-9258(18)64849-5

18. Triyasmono L, Schollmayer C, Schmitz J, Hovah E, Lombo C, Schmidt S, Holzgrabe U. Simultaneous Determination of the Saponification Value, Acid Value, Ester Value, and Iodine Value in Commercially Available Red Fruit Oil (Pandanus conoideus, Lam.) Using ^{1}H qNMR Spectroscopy. *Food Anal. Methods*. 2022; 1-13. https://doi.org/10.1007/s12161-022-02401-4

19. Holzgrabe U. Quantitative NMR spectroscopy in pharmaceutical applications. *Prog. Nucl. Magn. Reson. Spectrosc*. 2010; 57:229–240. https://doi.org/10.1016/j.pnmrs.2010.05.001

20. Savitzky A & Golay MJE. . Smoothing and Differentiation of Data by Simplified Least Squares Procedures. *Analytical Chemistry*. 1964; *36*(8). https://doi.org/10.1021/ac60214a047

21. Casale M, Oliveri P, Casolino C, Sinelli N, Zunin P, Armanino C, Lanteri S. Characterisation of PDO olive oil Chianti Classico by non-selective (UV-visible, NIR and MIR spectroscopy) and selective (fatty acid composition) analytical techniques. *Anal. Chim. Acta.* 2012; 712:56–63. https://doi.org/10.1016/j.aca.2011.11.015

22. Schönberger T, Monakhova YB, Lachenmeier DW, Walch S, Kuballa T, (NEXT) -NMR working group. EUROLAB Technical Report 01/2015. Guide to NMR Method Development and Validation-Part II: Multivariate data analysis. 2016; (01):1–20. https://doi.org/10.13140/RG.2.1.4265.1289

23. Sousa SAA, Magalhães A & Ferreira MMC. Optimized bucketing for NMR spectra: Three case studies. *Chemom. Intell. Lab. Syst.* 2013; 122: 93–102. https://doi.org/10.1016/j.chemolab.2013.01.006

24. Vu TN, Valkenborg D, Smets K, Verwaest KA, Dommisse R, Lemière F, Laukensn K. An integrated workflow for robust alignment and simplified quantitative analysis of NMR spectrometry data. *BMC Bioinform.* 2011; 12(405): 1-14. https://doi.org/10.1186/1471-2105-12-405

25. Jellema RH, Brown SD, Tauler R, Walczak B. Comprehensive Chemometrics in: Variable shift and alignment. *Chemical and Biochemical Data Analysis*, vol. 2, Elsevier, Oxford, 2009, pp. 85–108

26. Gulmine JV, Janissek PR, Heise HM, Akcelrud L. Polyethylene characterization by FTIR. *Polym. Test*. 2002; 21(5): 557-563. https://doi.org/10.1016/S0142-9418(01)00124-6

27. Guillén MD & Ruiz A. Rapid simultaneous determination by proton NMR of unsaturation and composition of acyl groups in vegetable oils. *Eur J Lipid Sci Technol*. 2003; *105*(11): 688–696. https://doi.org/10.1002/ejlt.200300866

28. Parker T, Limer E, Watson AD, Defernez M, Williamson D & Kemsley EK. 60 MHz ^{1}HNMR spectroscopy for the analysis of edible oils. *TrAC - Trends Anal. Chem.* 2014; 57:147.158. https://doi.org/10.1016/j.trac.2014.02.006

29. An Z, Jiang X, Xiang G, Fan L, He L, Zhao W. A Simple and Practical Method for Determining Iodine Values of Oils and Fats by the FTIR Spectrometer with an Infrared Quartz Cuvette. Anal. Methods, 2017; **9**: 3669-3674. https://doi.org/10.1039/C7AY00727B

30. Lievens C, Mourant D, Min He, Gunawan R, Li X, Li CZ.. An FT-IR spectroscopic study of carbonyl functionalities in bio-oils. *Fuel*. 2011;90:3417-3423. https://doi.org/10.1016/j.fuel.2011.06.001

31. Wold S, Esbensen K, Geladi P. Principal component analysis. *Chemom. Intell. Lab. Syst*. 1987; 2(1–3): 37-52p. https://doi.org/10.1007/978-0-387-87811-9_2

32. Jović O, Smolić T, Primožič I & Hrenar T. Spectroscopic and Chemometric Analysis of Binary and Ternary Edible Oil Mixtures: Qualitative and Quantitative Study. *Anal. Chem*. 2016; 88(8): 4516–4524. https://doi.org/10.1021/acs.analchem.6b00505

33. Rohman A, Irnawati, Erwanto Y, Lukitaningsih E, Rafi M, Fadzilah NA, Windarsih A, Sulaiman A & Zakaria Z. Virgin Coconut Oil: Extraction, Physicochemical Properties, Biological Activities and Its Authentication Analysis, *Food Rev. Int*. 2021;37(1): 46-66. https://doi.org/10.1080/87559129.2019.1687515

34. Lutterodt H, Luther M, Slavin M, Yin JJ, Parry, J, Gao, JM, Yu L. Fatty acid profile, thymoquinone content, oxidative stability, and antioxidant properties of cold-pressed black cumin seed oils, *LWT - Food Sci and Technology*. 2010;43(9), 1409-1413. https://doi.org/10.1016/j.lwt.2010.04.009

35. De la Mata P, Dominguez-Vidal A, Bosque-Sendra JM, Ruiz-Medina A, Cuadros-Rodríguez L, Ayora-Cañada MJ. Olive oil assessment in edible oil blends by means of ATR-FTIR and chemometrics, *Food Control*. 2012; 23(2): 449-455. https://doi.org/10.1016/j.foodcont.2011.08.013

36. Popescu R, Costinel D, Dinca OR, Marinescu A, Stefanescu I, Ionete RE. Discrimination of vegetable oils using NMR spectroscopy and chemometrics. *Food Control*. 2015; 48: 84-90. https://doi.org/10.1016/j.foodcont.2014.04.046

37. Truzzi E, Marchetti L, Benvenuti S, Ferroni A, Rossi MC, Bertelli D. Novel Strategy for the Recognition of Adulterant Vegetable Oils in Essential Oils Commonly Used in Food Industries by Applying 13C NMR Spectroscopy. J. Agric. Food Chem. 2021; 69: 8276−8286. https://doi.org/10.1021/acs.jafc.1c02279

38. Vlahov G. Application of NMR to the study of olive oils. Prog. Nucl. Magn. Reson. Spectrosc. 1999; 35: 341– 357. https://doi.org/10.1016/S0079-6565(99)00015-1

39. Alexandri E, Ahmed R, Siddiqui H, Choudhary MI, Tsiafoulis CG, Gerothanassis IP. High resolution NMR spectroscopy as a structural and analytical tool for unsaturated lipids in solution. Molecules. 2017; 1-71. https://doi.org/10.3390/molecules22101663

Chemometric analysis applied to ^{1}H NMR and FTIR data for a quality parameter distinction of Red Fruit Oil products

Liling TRIYASMONO[a,b], Curd SCHOLLMAYER[a], Ulrike HOLZGRABE[a,*]

[a]Institute for Pharmacy and Food Chemistry, University of Würzburg, , 97074 Würzburg, Germany

[b]Department of Pharmacy, Faculty of Mathematics and Natural Sciences, Lambung Mangkurat University, 70713 Banjar Baru, Indonesia

SUPPLEMENTARY INFORMATION 1

Bucketing Process

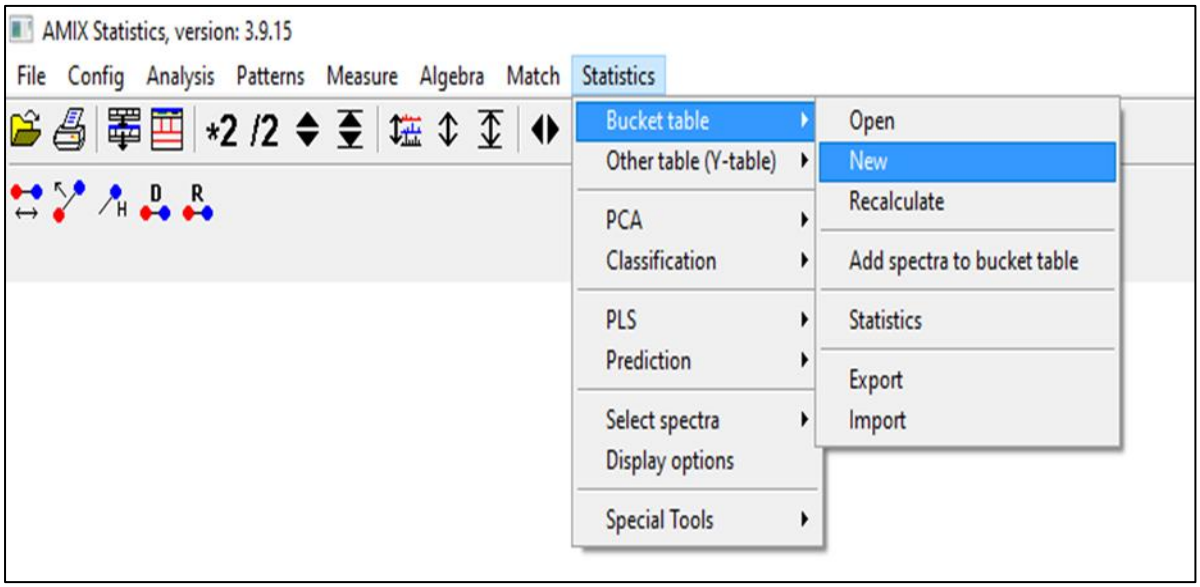

Fig. S1 The 1st step of operation bucketing data by AMIX: "AMIX-TOOLS" clicks on the toolbar, and "BUCKETS, STATISTICS" is selected in the submenu. Then, in the menu bar, the item "STATISTICS," the item "BUCKET TABLE," and the submenu item "NEW" is selected..

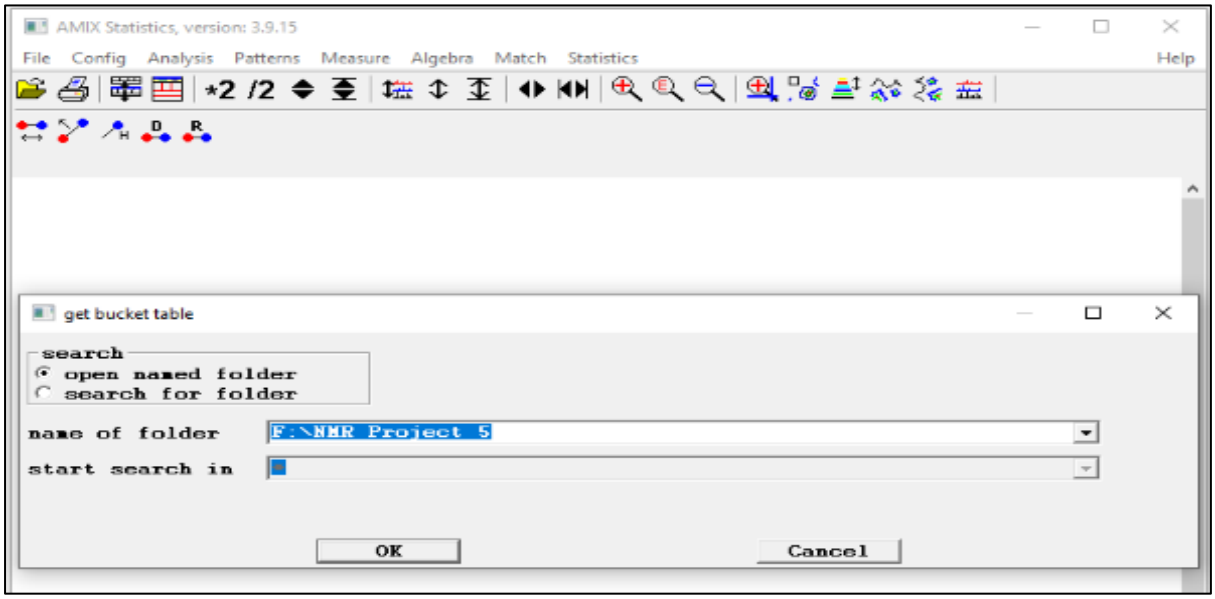

Fig. S2 The 2nd step is open the named folder. Confirm with OK

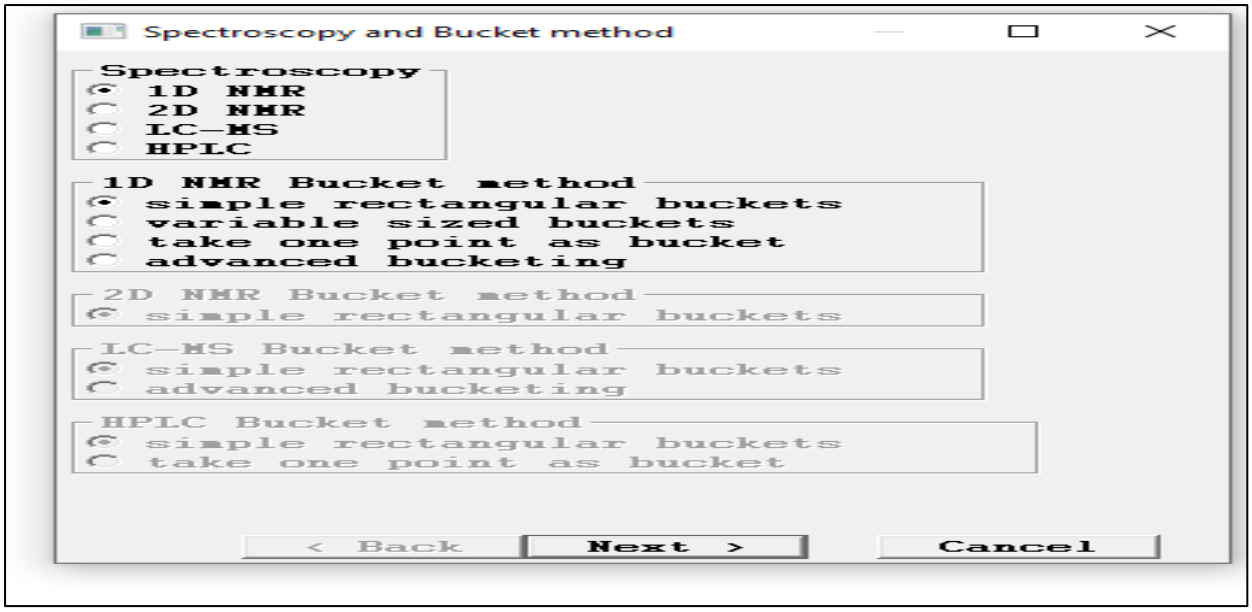

Fig. S3 The 3rd step**:** A selection window open (the points "1D" and "simple rectangular buckets" must be activated). With "NEXT," another selection window will be opened

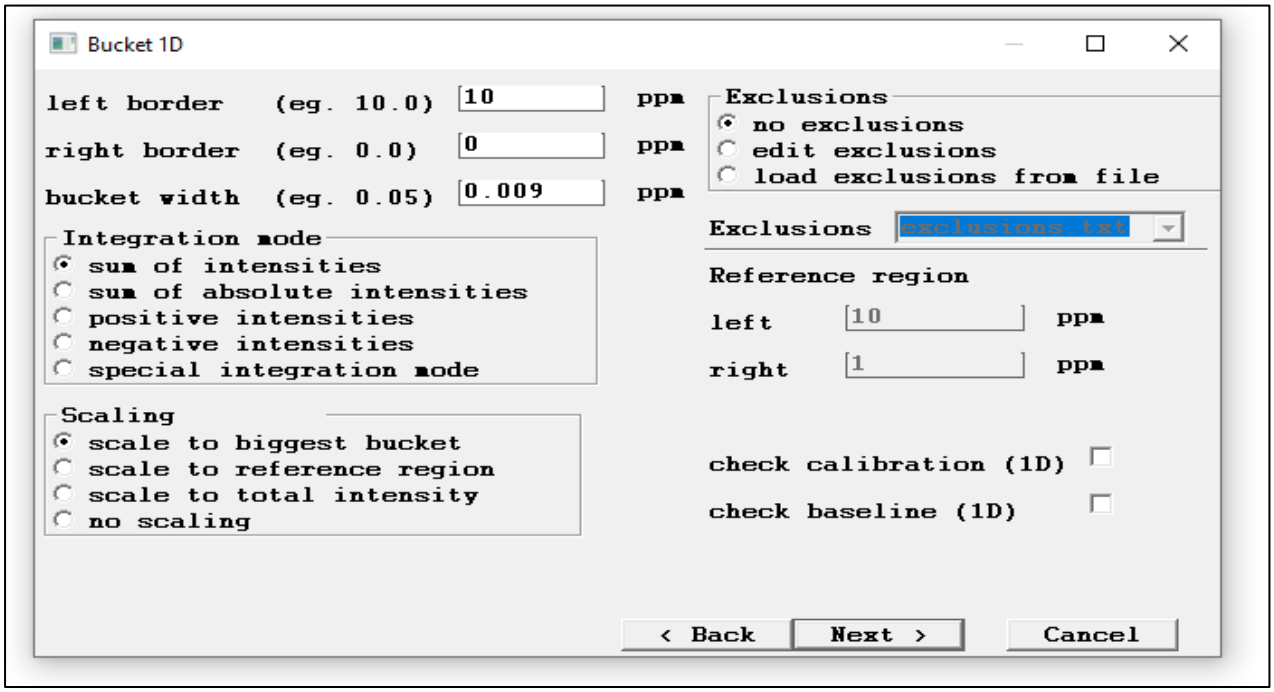

Fig. S4 The 4th step: The following points must be activated in this: left border: 10, right border: 0, bucket width: 0.009, Integration mode: sum of intensities active, Scaling: Scale to the biggest bucket, Active exclusions: no exclusion active. With "NEXT," another selection window will be opened

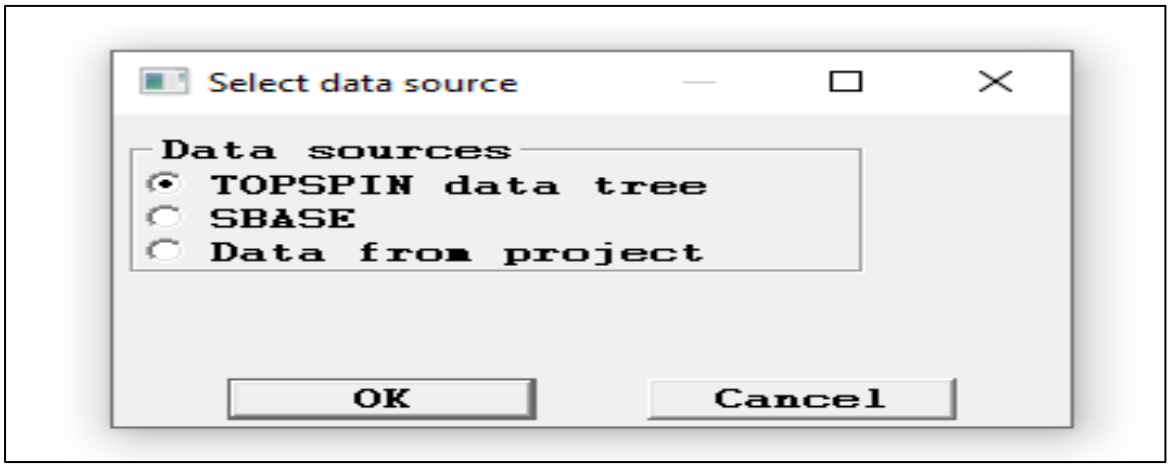

Fig. S5 The 5th step: The "TOPSPIN data tree" item must be activated there. Confirm with OK, and following, another selection window will be opened.

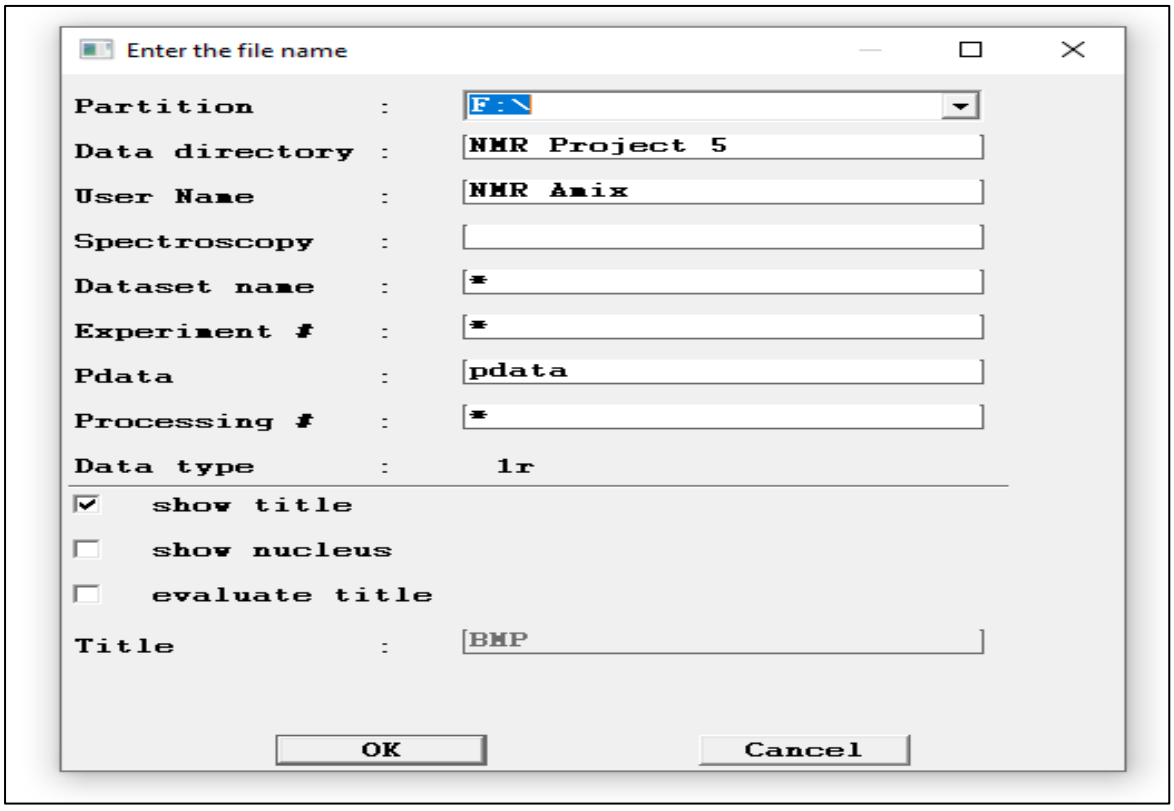

Fig. S6 The 6th step: the path to the output data is entered here, e.g., for RFO: Partition F:\ NMR Project 5; Username: NMR Amix; Confirm with OK. The data is read in and displayed in the following new window.

Fig. S7 The 7th step: All data selected in the previous step will be read alphabetically, as in the new windows display above. All data are selected with the "autoselect" button

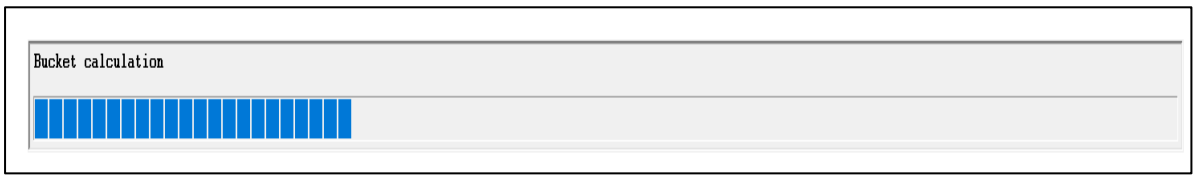

Fig. S8 The 8th step: Data is processed

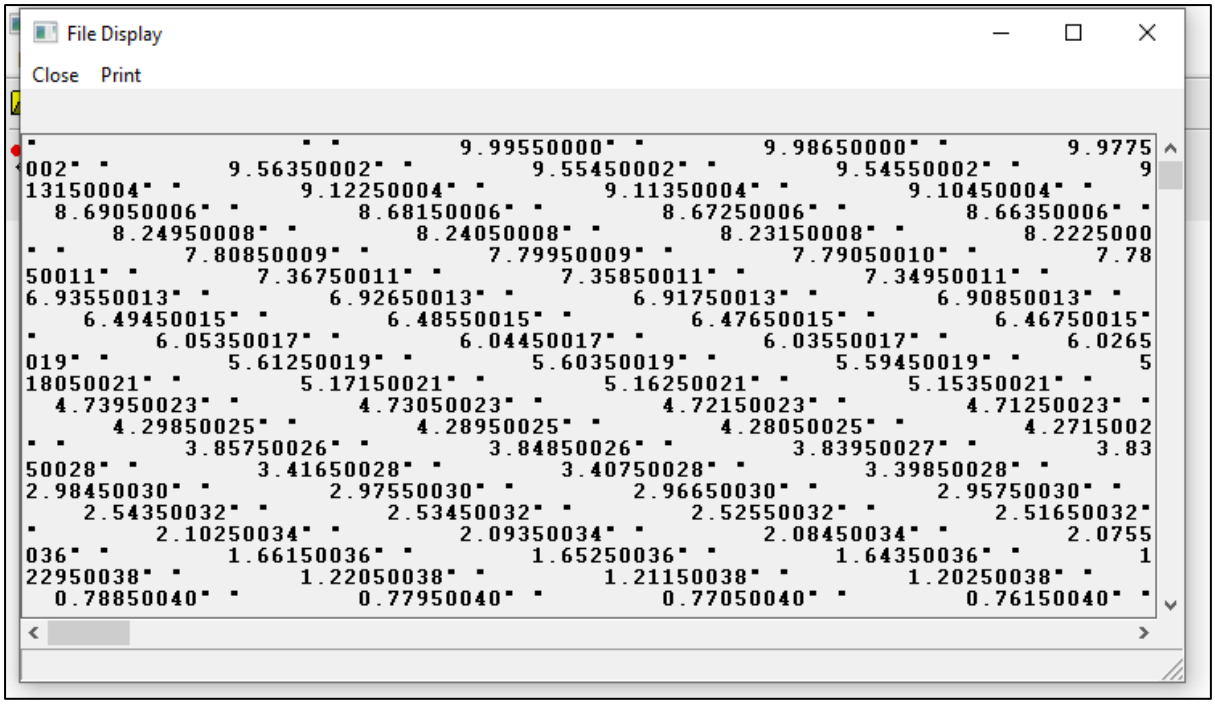

Fig. S9 The 9th step: after the data bucketing process is complete, the results will appear in the new windows display as above, which can be closed

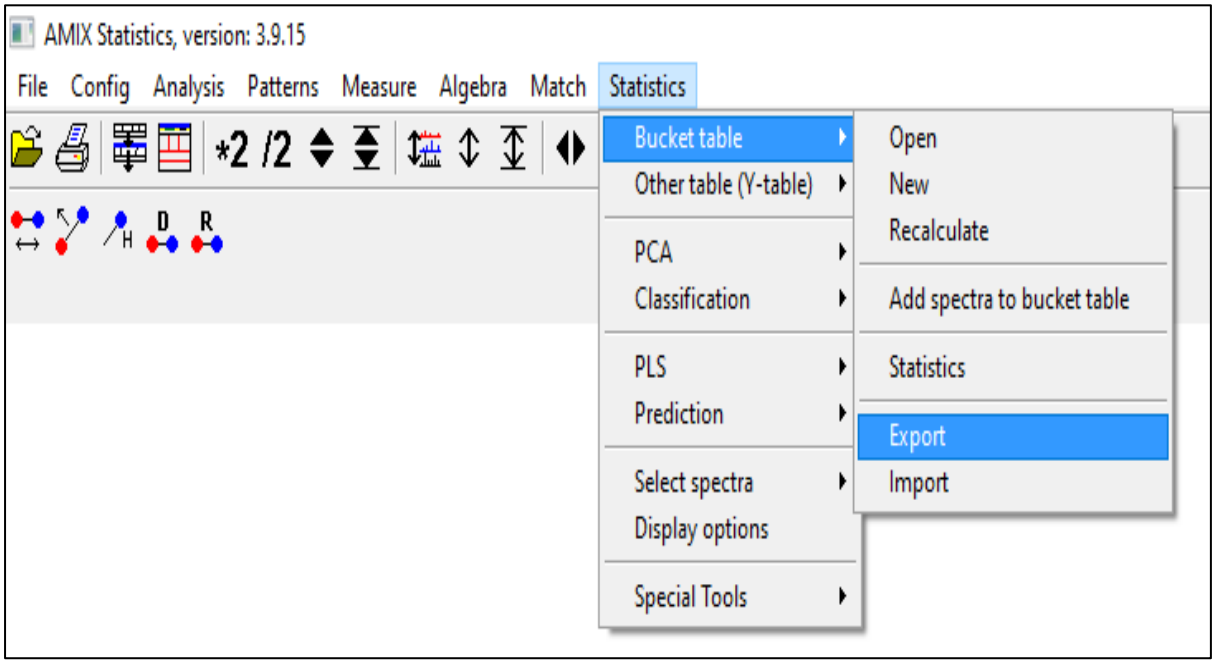

Fig. S10 The 10th step: export the data for further processing. In the menu item "statistics", "bucket table", "export". Furthermore, another next window will be appears

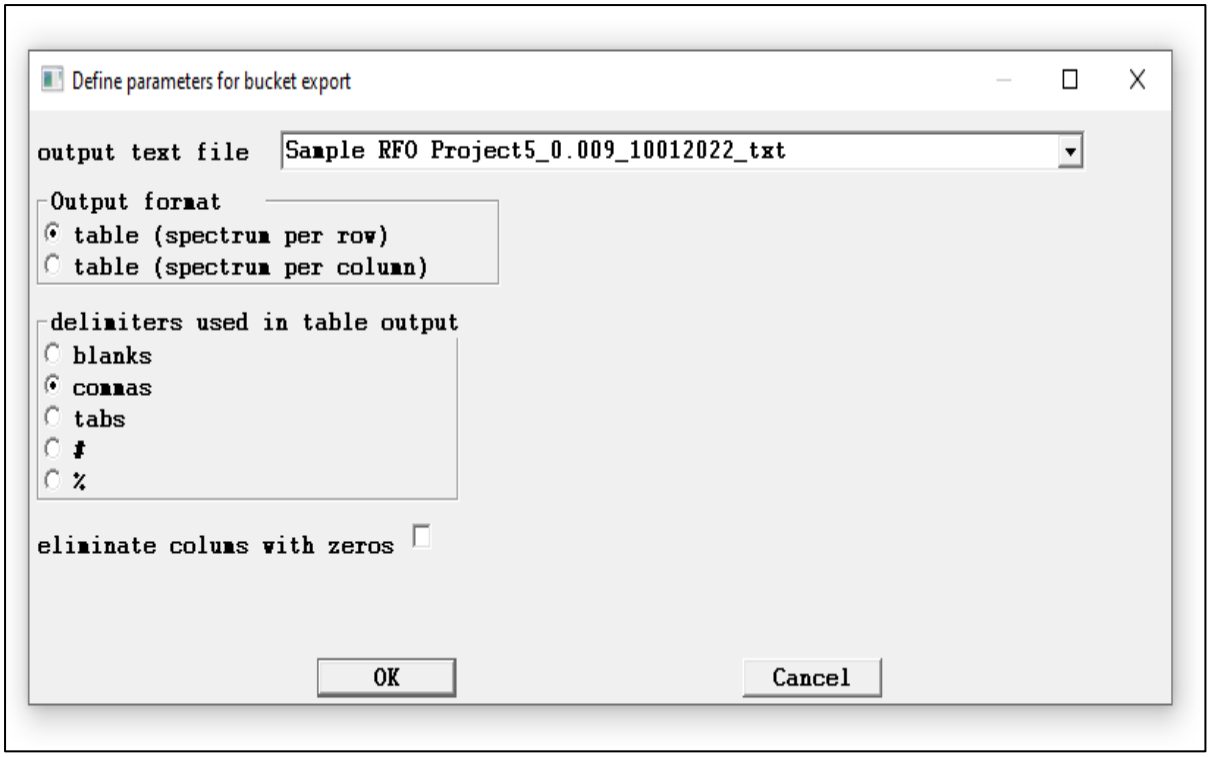

Fig. S11 The 11th step: specify the filename with; Output text File Select file name and path; Delimiters used in table output: Activate commas. Confirm with OK and end the program. For PCA and PLS analysis, bucketing results files (.txt) will be further processed to Unscramble 11.0.

Chemometric analysis applied to ^{1}H NMR and FTIR data for a quality parameter distinction of Red Fruit Oil products.

Liling TRIYASMONO[a,b], Curd SCHOLLMAYER[a], Ulrike HOLZGRABE[a,*]

[a]Institute for Pharmacy and Food Chemistry, University of Würzburg, , 97074 Würzburg, Germany

[b]Department of Pharmacy, Faculty of Mathematics and Natural Sciences, Lambung Mangkurat University, 70713 Banjar Baru, Indonesia

SUPPLEMENTARY INFORMATION 2

Table of content

11	**Figure S11** (A) Score Plot classification PC1 vs. PC2 of selection band FTIR data; (B) Plot of X-Loading with axis X-Variables (PC1) (1680 - 1780 cm^{-1}); (C) Plot Hotelling's T^2; (D) Plot Explained variance vs. PC-0 to PC-7 (calibration and validation)
12	**Figure S12** PLS calibration analyses for the degree of unsaturation on NMR data. (A) Score Plot Factor 1 vs. Factor-2 of selected signal NMR data; (B) Plot of X-Loading with axis X-Variables (Factor-1) (5.37-5.27 ppm); (C) Plot Explained Variance Factor-0 - 7 to Y-variance; (D) Plot Predicted vs. Reference Y from Factor-2 of the degree of unsaturation
13	**Figure S13** (A) Plot Predicted vs. Y Reference of the degree of unsaturation on the sample (prediction set) with calibration model Fig.12D (NMR); (B) Plot Predicted Y with a deviation of samples (Prediction test)
14	**Figure S14** PLS calibration analyses for the degree of unsaturation on FTIR data. (A) Score Plot Factor 1 vs. Factor-2 of FTIR data; (B) Plot of X-Loading with axis X-Variables (Factor-1) (2990 - 3020 cm^{-1}); (C) Plot Explained Variance Factor-0 - 7 to Y-variance; (D) Plot Predicted vs. Reference Y from Factor-1 of the degree of unsaturation
15	**Figure S15** A Plot Predicted vs. Y Reference of the degree of unsaturation sample (prediction set) with calibration model Fig.14D (FTIR); B Plot Predicted Y with a deviation of the sample (Prediction test)
16	**Figure S16** PLS calibration analyses for the FFA value on NMR data. (A) Score Plot Factor 1 vs. Factor-2 of selected signal NMR data; (B) Plot of X-Loading with axis X-Variables (Factor-1) (2.37-2.27 ppm); (C) Plot Explained Variance Factor-0 - 7 to Y-variance; (D) Plot Predicted vs. Reference Y from Factor-2 of the FFA value
17	**Figure S17** (A) Plot Predicted vs. Y Reference of the FFA number on the sample (prediction set) with calibration model Fig.16D (NMR); (B) Plot Predicted Y with a deviation of samples (Prediction test)
18	**Figure S18** PLS calibration analyses for the FFA value on FTIR data. (A) Score Plot Factor 1 vs. Factor-2 of selected band FTIR data; (B) Plot of X-Loading with axis X-Variables (Factor-1) (1680 - 1780 cm^{-1}); (C) Plot Explained Variance Factor-0 - 7 to Y-variance; (D) Plot calibration of Predicted vs. Reference Y from Factor-2 of the FFA number
19	**Figure S19** (A) Plot Predicted vs. Y Reference of the FFA number on the sample (prediction set) with calibration model Fig.18D (FTIR); (B) Plot Predicted Y with a deviation of samples (Prediction test)

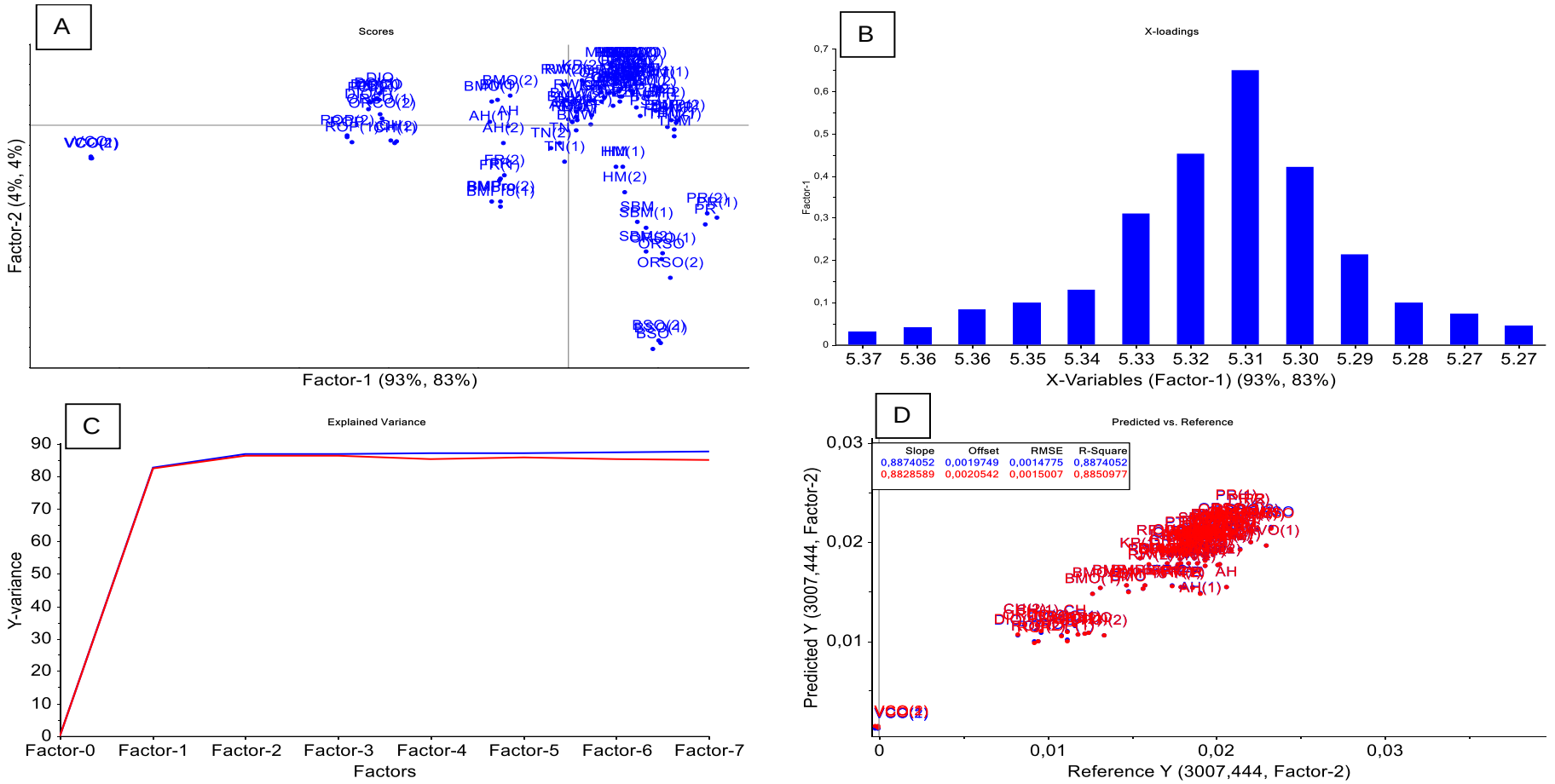

Figure S1 Comparison signal CH=CH (5.37 – 5.27 ppm) NMR and the C-H stretching band of the double bond of FTIR (3007 cm^{-1}) by the PLS model. (A) Score Plot Factor 1 vs. Factor 2 of NMR vs. FTIR data; (B) Plot of X-Loading with axis X-Variables Factor 1 (5.37-5.27 ppm); (C) Plot Explained Variance Factor 0 -7 to Y-variance; (D) Plot Predicted vs. Reference Y from Factor-2 of band 3007 cm^{-1}

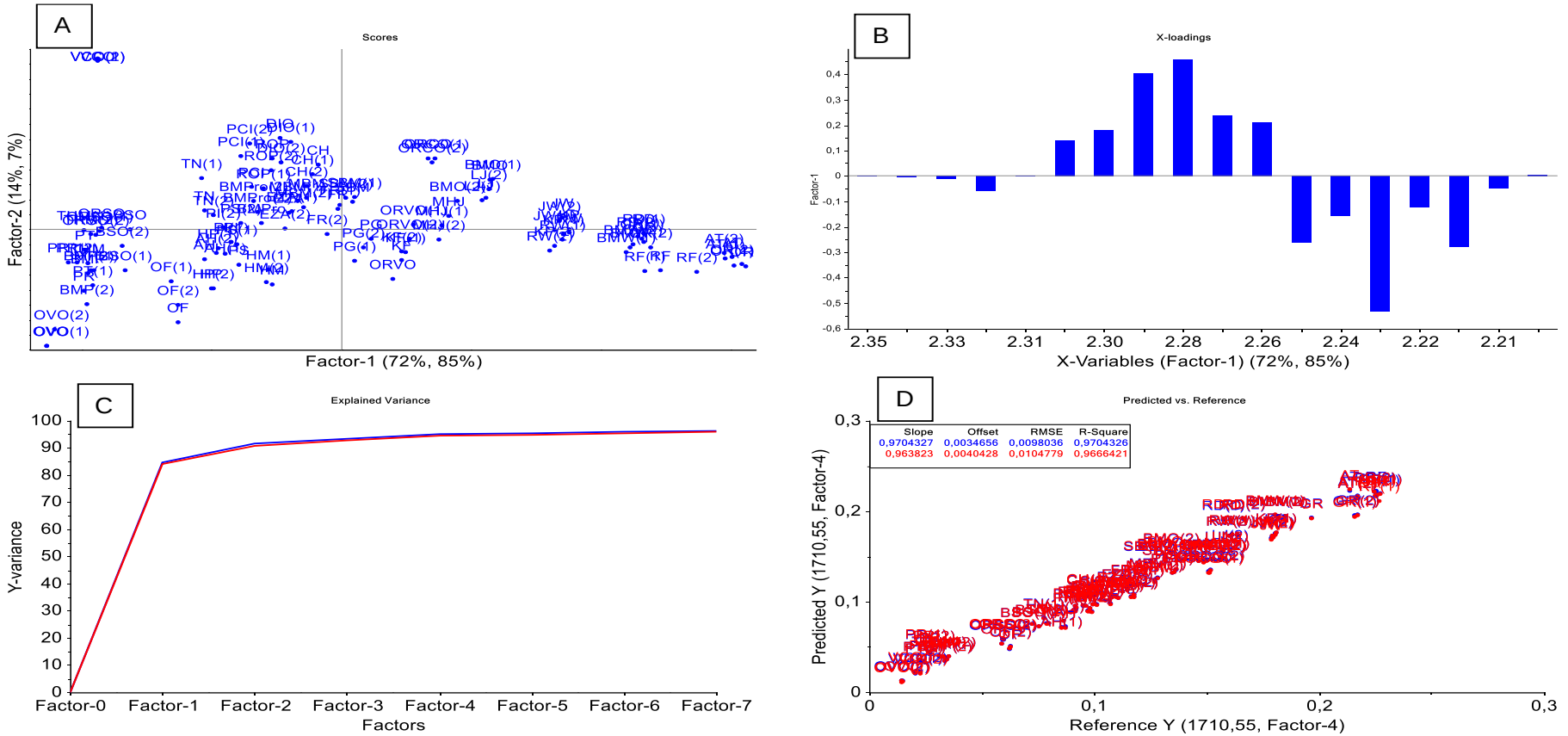

Figure S2 Comparison signal α-CH_2 (δ= 2.37-2.20 ppm) NMR and band C=O (1710 cm^{-1}) FTIR by the PLS model. (A) Score Plot Factor 1 vs. Factor 2 of NMR vs. FTIR data; (B) Plot of X-Loading with axis X-Variables Factor 1 (2.37-2.20 ppm); (C) Plot Explained Variance Factor 0 -7 to Y-variance; (D) Plot Predicted vs. Reference Y from Factor-4 of band 1710 cm^{-1}

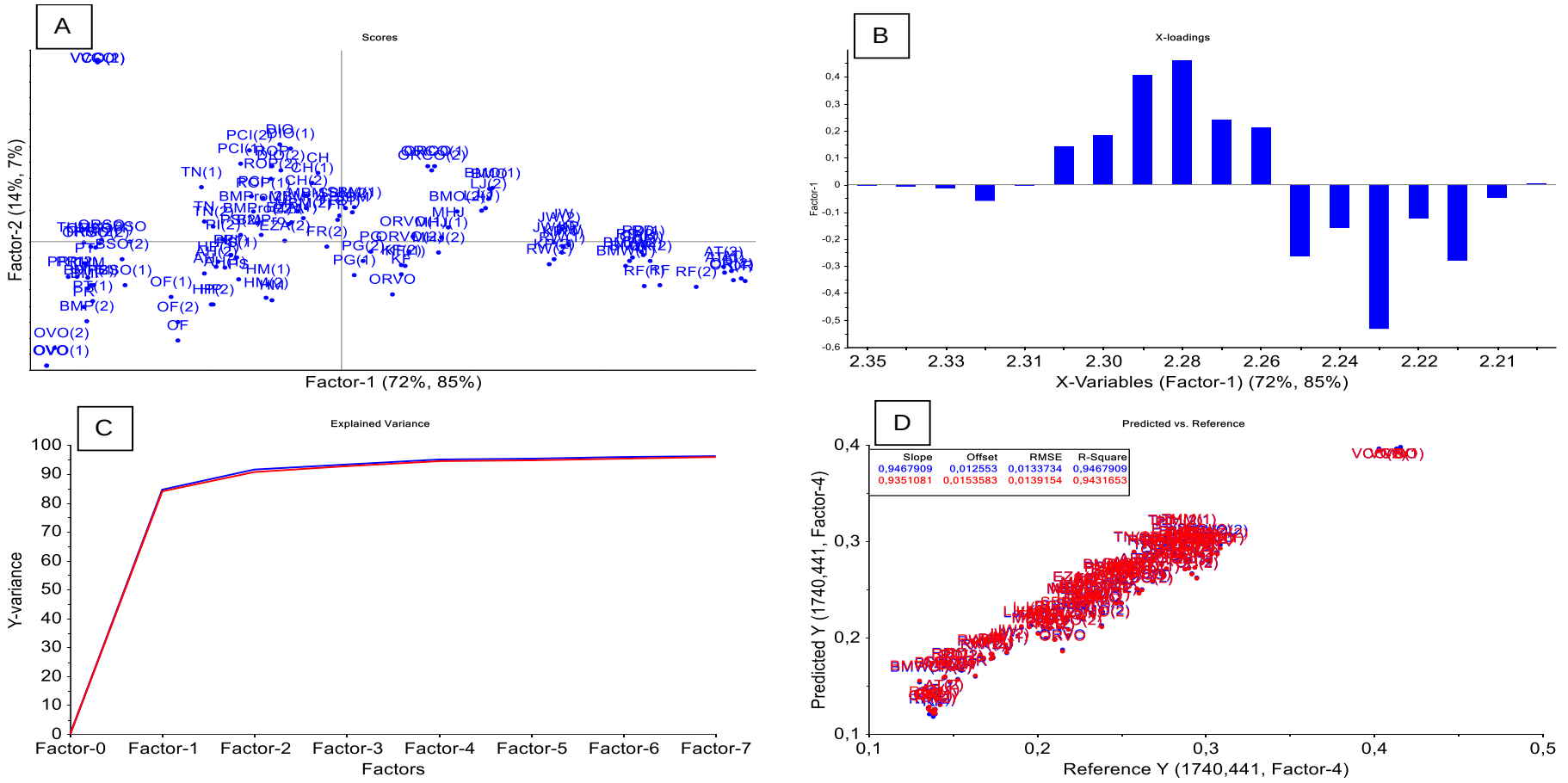

Figure S3 Comparison signal α-CH_2 (δ= 2.37-2.20 ppm) NMR and band C=O (1740 cm^{-1}) FTIR by the PLS model. (A) Score Plot Factor 1 vs. Factor 2 of NMR vs. FTIR data; (B) Plot of X-Loading with axis X-Variables Factor 1 (2.37-2.20 ppm); (C) Plot Explained Variance Factor-0 - 7 to Y-variance; (D) Plot Predicted vs. Reference Y from Factor-4 of band 1740 cm^{-1}

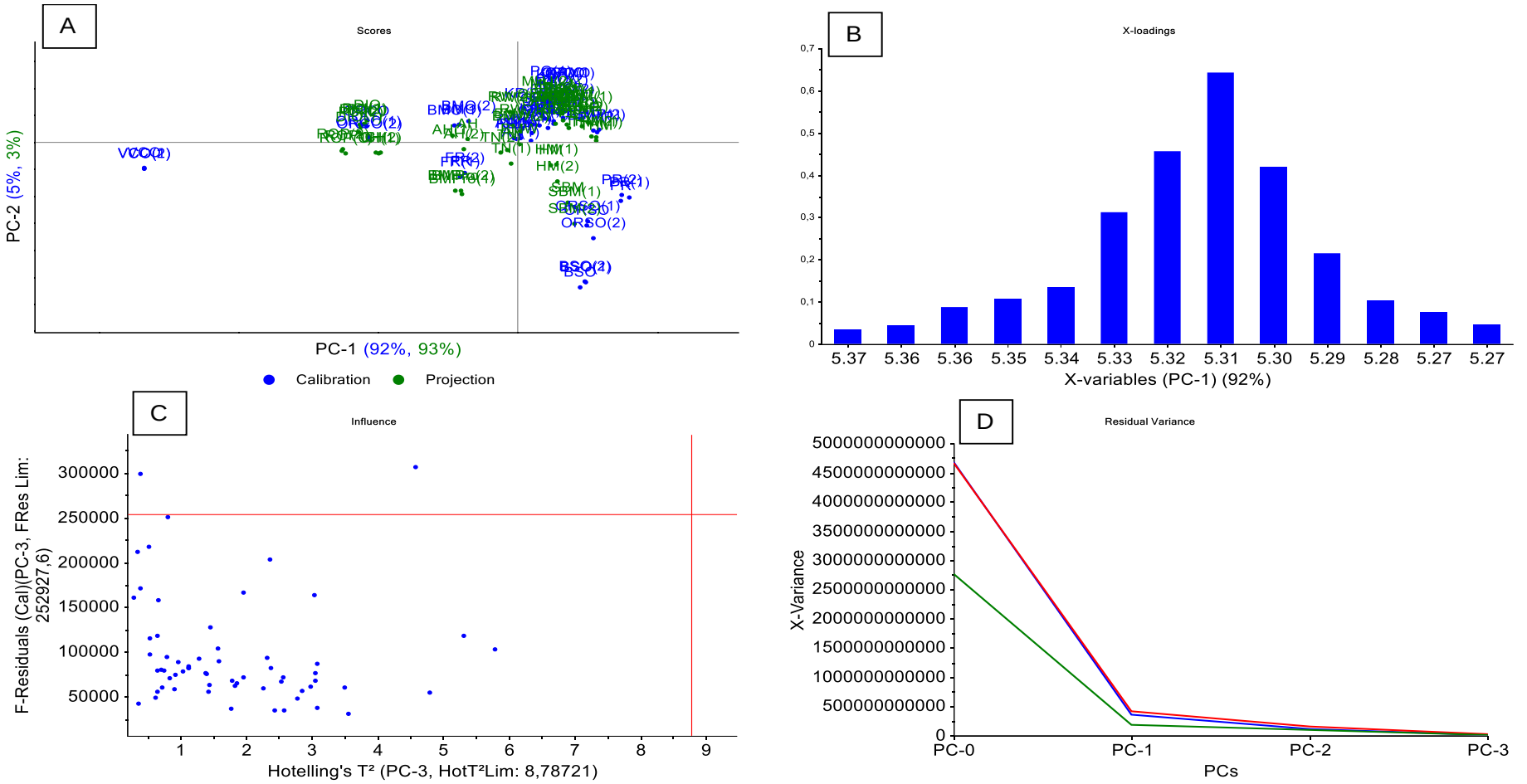

Figure S4 (A) Score Plot projection PC1 vs. PC2 (calibration and projection) of selected signals on NMR data; (B) Plot of X-Loading with axis X-Variables (PC1) (5.37-5.27 ppm); (C) Plot Hotelling's T^2; (D) Plot X variance vs. PC-0 to PC-3 (calibration, validation, and projection)

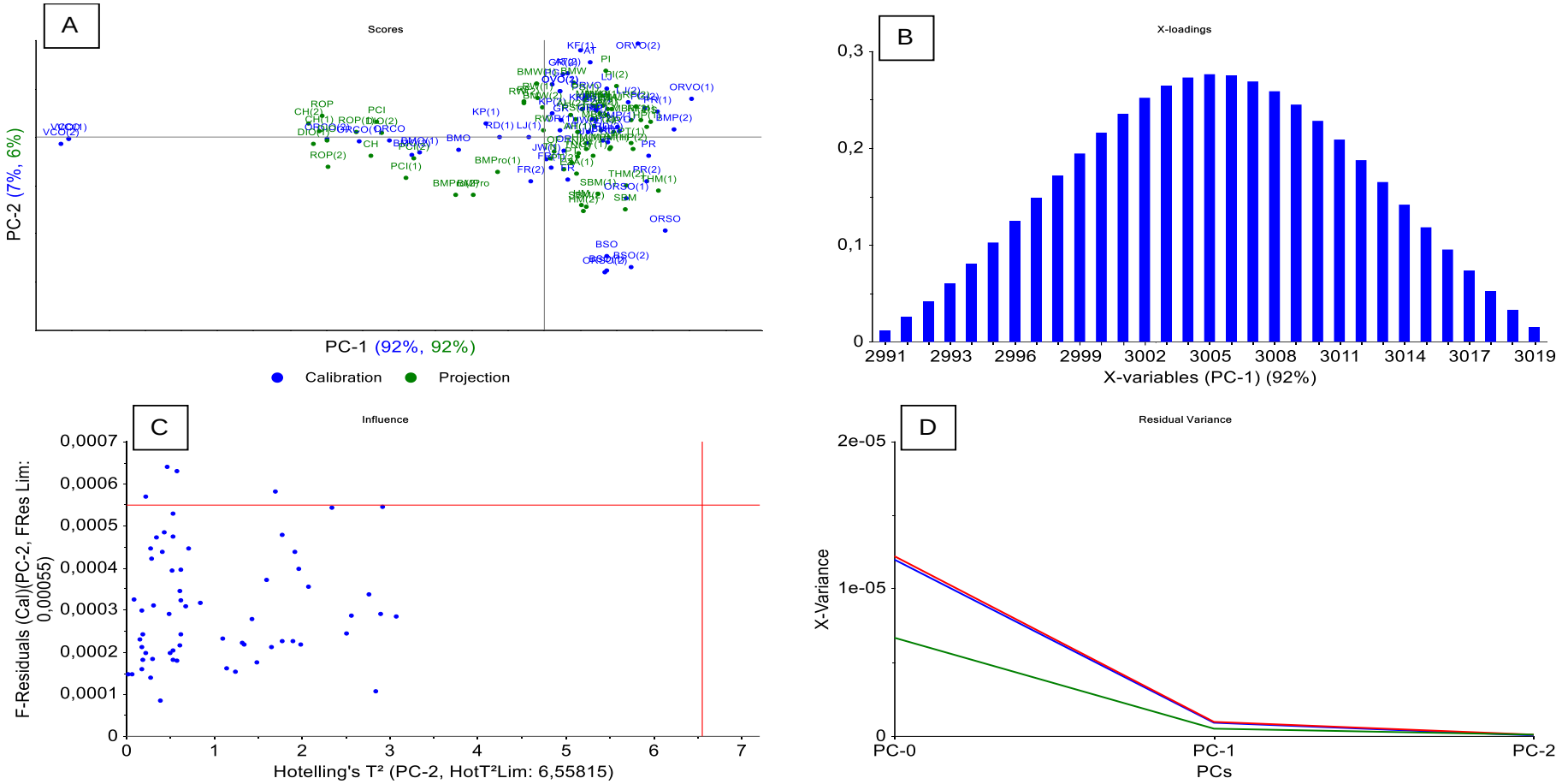

Figure S5 (A) Score Plot projection PC1 vs. PC2 of FTIR data; (B) Plot of X-Loading with axis X-Variables (PC1) (2990 - 3020 cm^{-1}); (C) Plot Hotelling's T^2; (D) Plot X variance vs. PC-0 to PC-2 (calibration, validation, and projection)

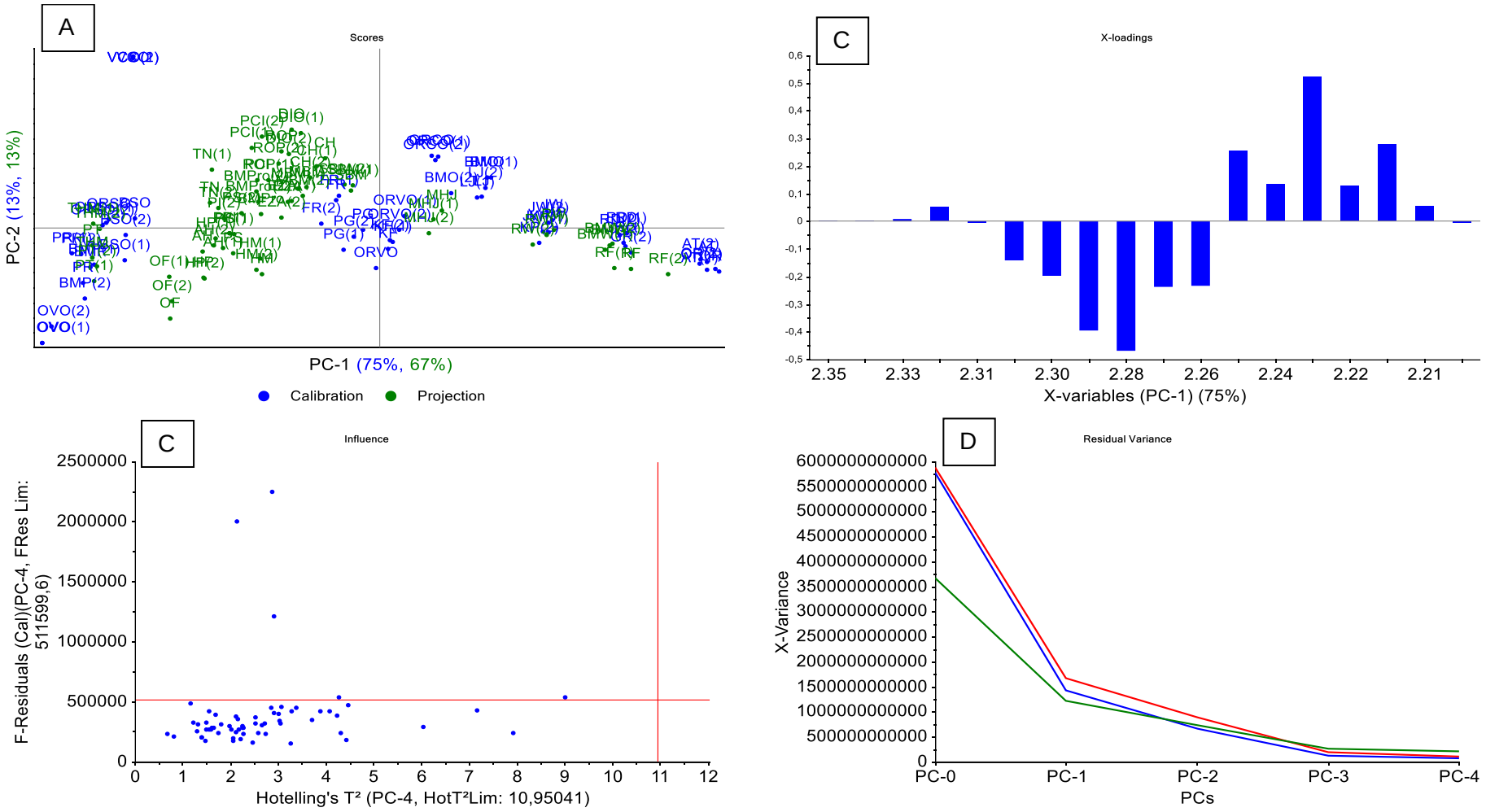

Figure S6 (A) Score Plot projection PC1 vs. PC2 (calibration and projection) of selected signals on NMR data; (B) Plot of X-Loading with axis X-Variables (PC1) (2.37-2.20 ppm); (C) Plot Hotelling's T^2; (D) Plot X variance vs. PC-0 to PC-4 (calibration, validation, and projection)

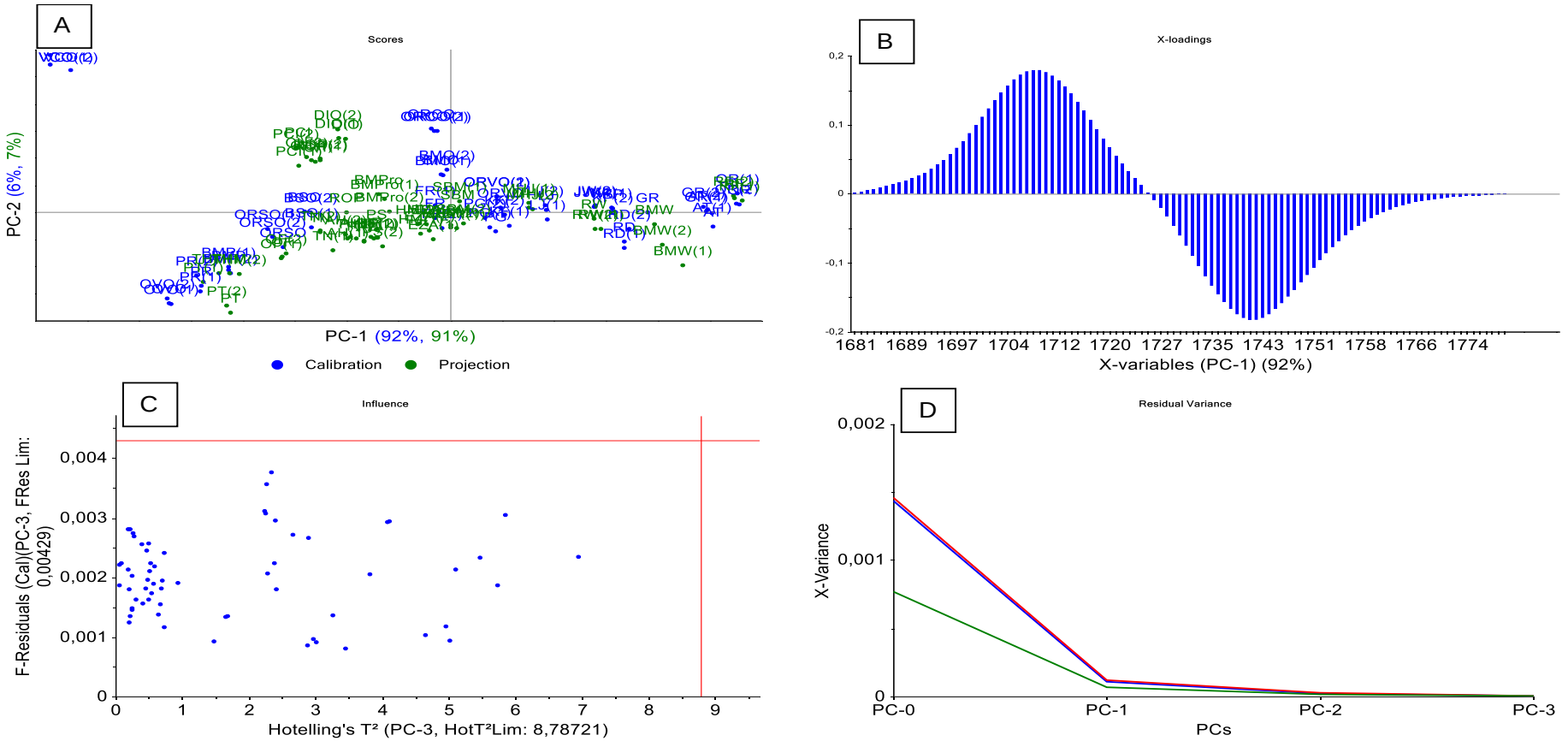

Figure S7 (A) Score Plot projection PC1 vs. PC2 (calibration and projection) of selection band on FTIR data; (B) Plot of X-Loading with axis X-Variables (PC1) (1680 - 1780 cm^{-1}); (C) Plot Hotelling's T^2; (D) Plot X variance vs. PC-0 to PC-3 (calibration, validation, and projection)

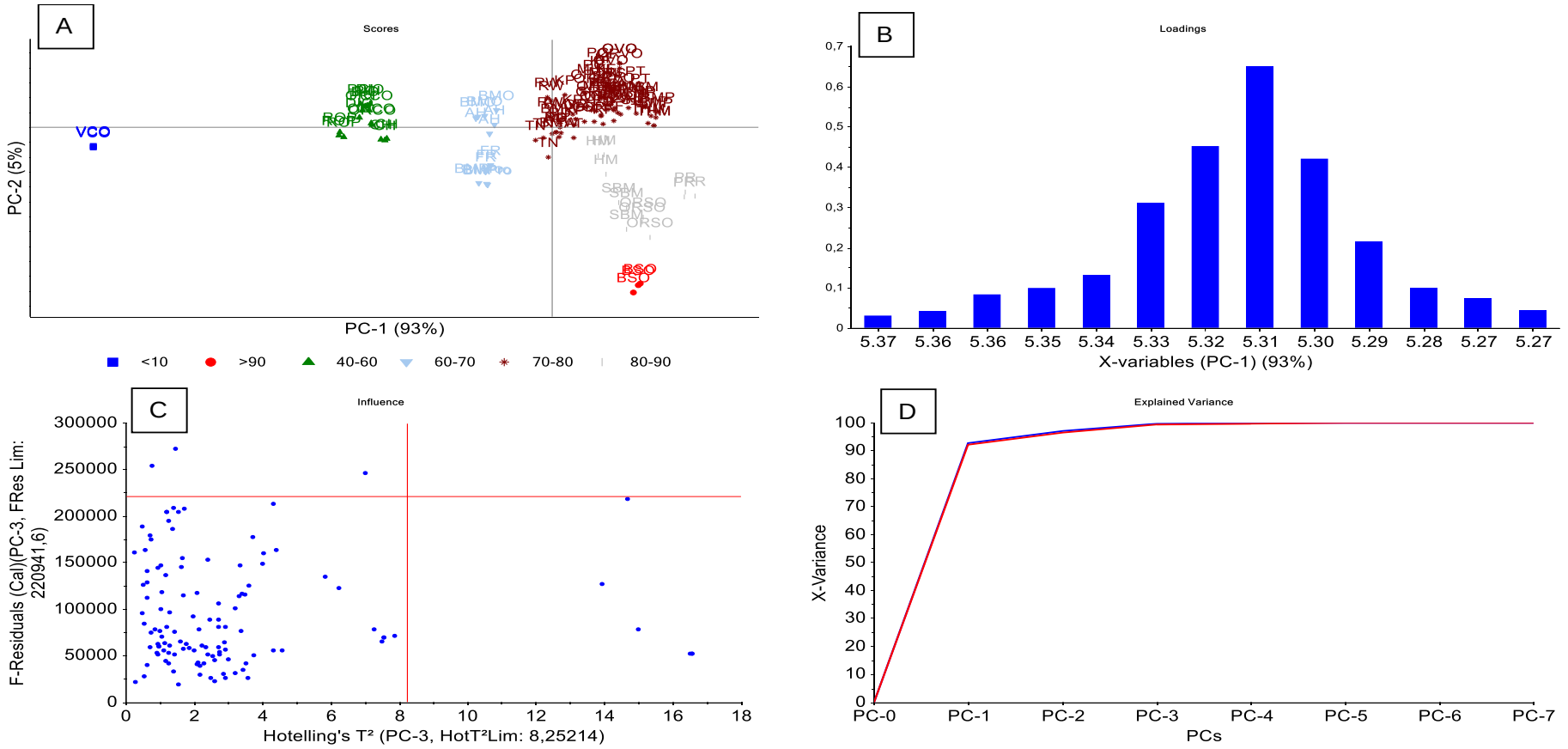

Figure S8 (A) Score Plot classification PC1 vs. PC2 of selected signal NMR data; (B) Plot of X-Loading with axis X-Variables (PC1) (5.37-5.27 ppm); (C) Plot Hotelling's T^2; (D) Plot Explained variance vs. PC-0 to PC-7 (calibration and validation)

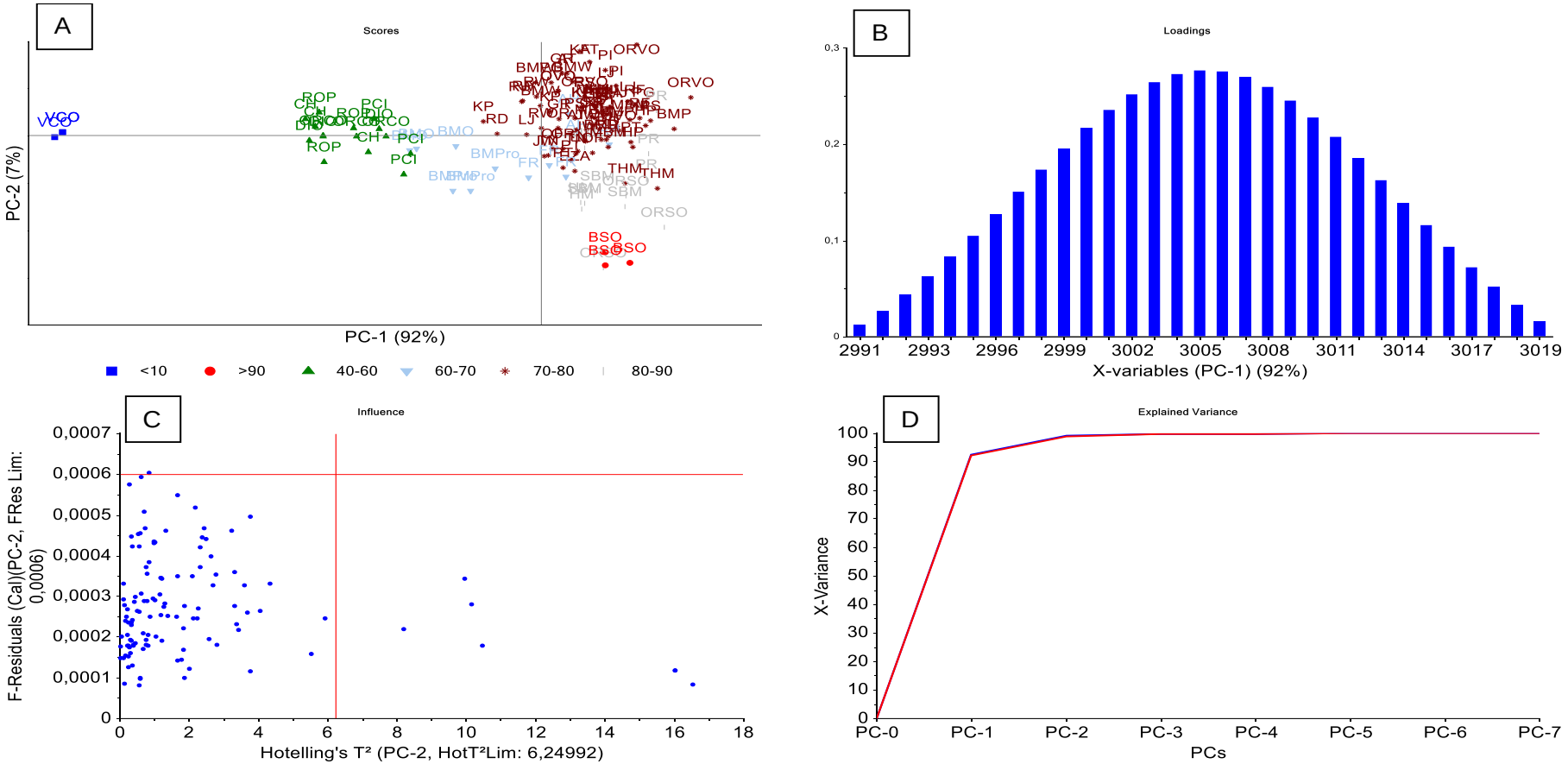

Figure S9 (A) Score Plot classification PC1 vs. PC2 of FTIR data; (B) Plot of X-Loading with axis X-Variables (PC1) (2990 - 3020 cm^{-1}); (C) Plot Hotelling's T^2; (D) Plot Explained variance vs. PC-0 to PC-7 (calibration and validation)

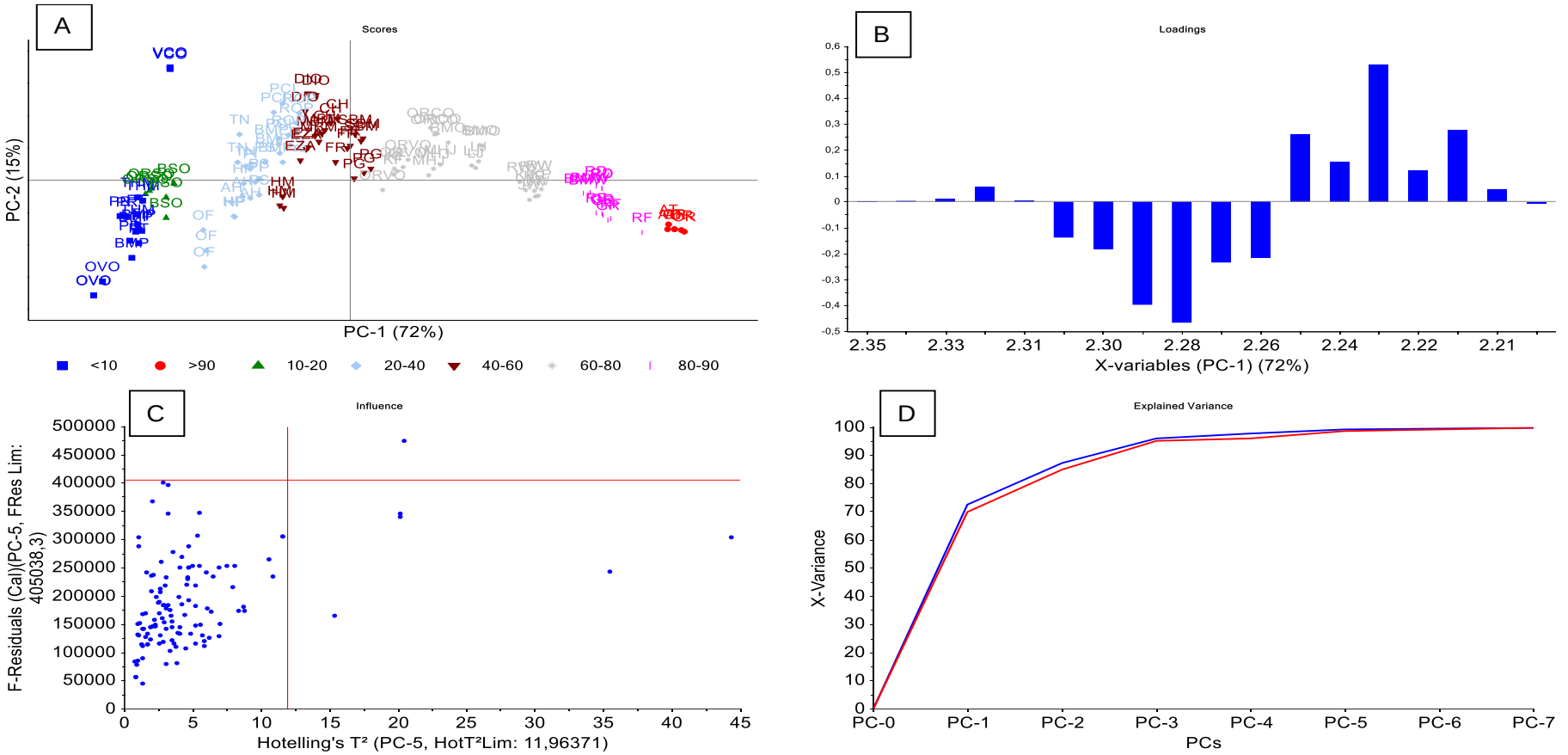

Figure S10 (A) Score Plot classification PC1 vs. PC2 of selected signal NMR data; (B) Plot of X-Loading with axis X-Variables (PC1) (2.37-2.20 ppm); (C) Plot Hotelling's T^2; (D) Plot Explained variance vs. PC-0 to PC-7 (calibration and validation)

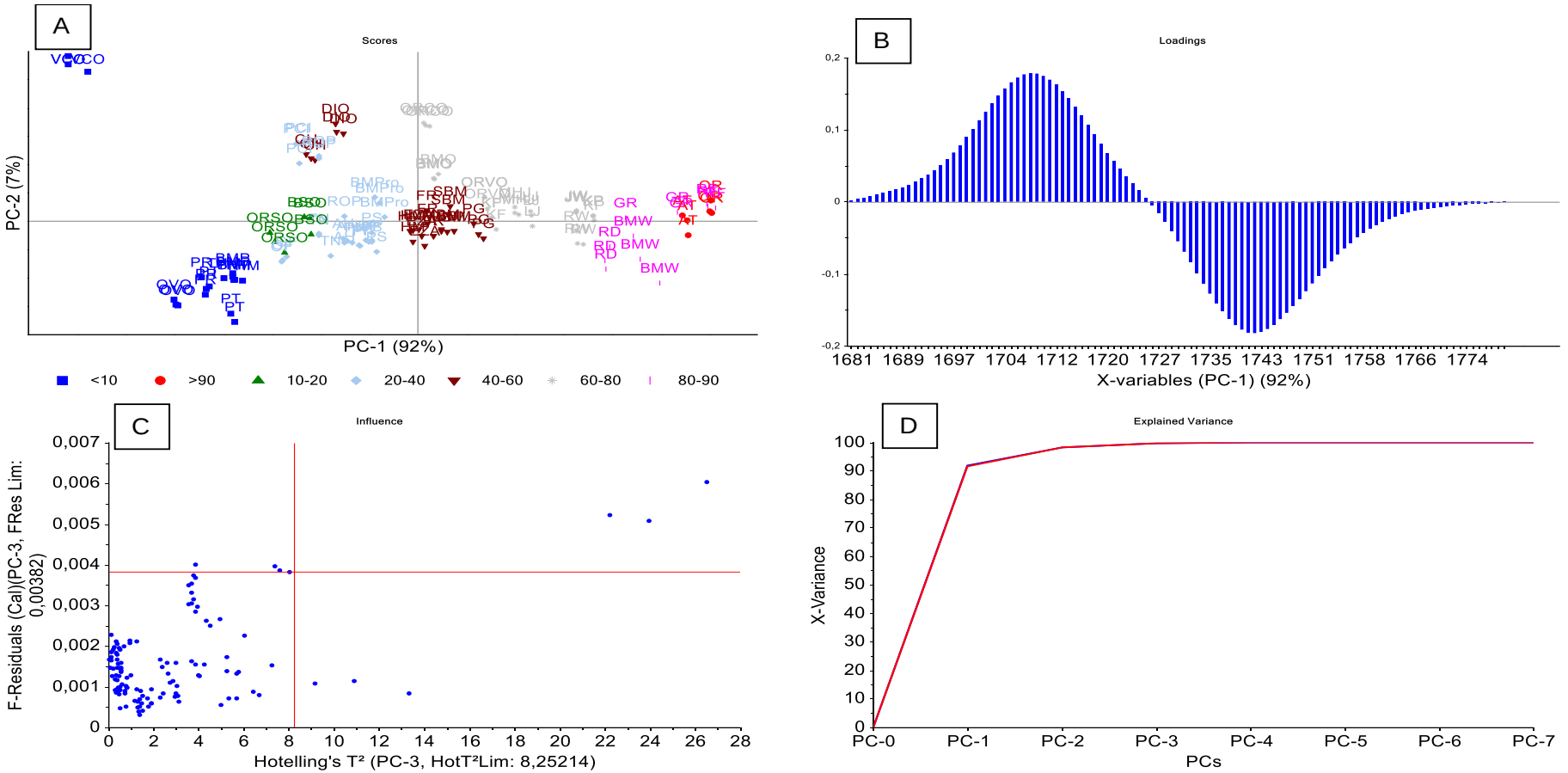

Figure S11 (A) Score Plot classification PC1 vs. PC2 of selection band FTIR data; (B) Plot of X-Loading with axis X-Variables (PC1) (1680 - 1780 cm^{-1}); (C) Plot Hotelling's T^2; (D) Plot Explained variance vs. PC-0 to PC-7 (calibration and validation)

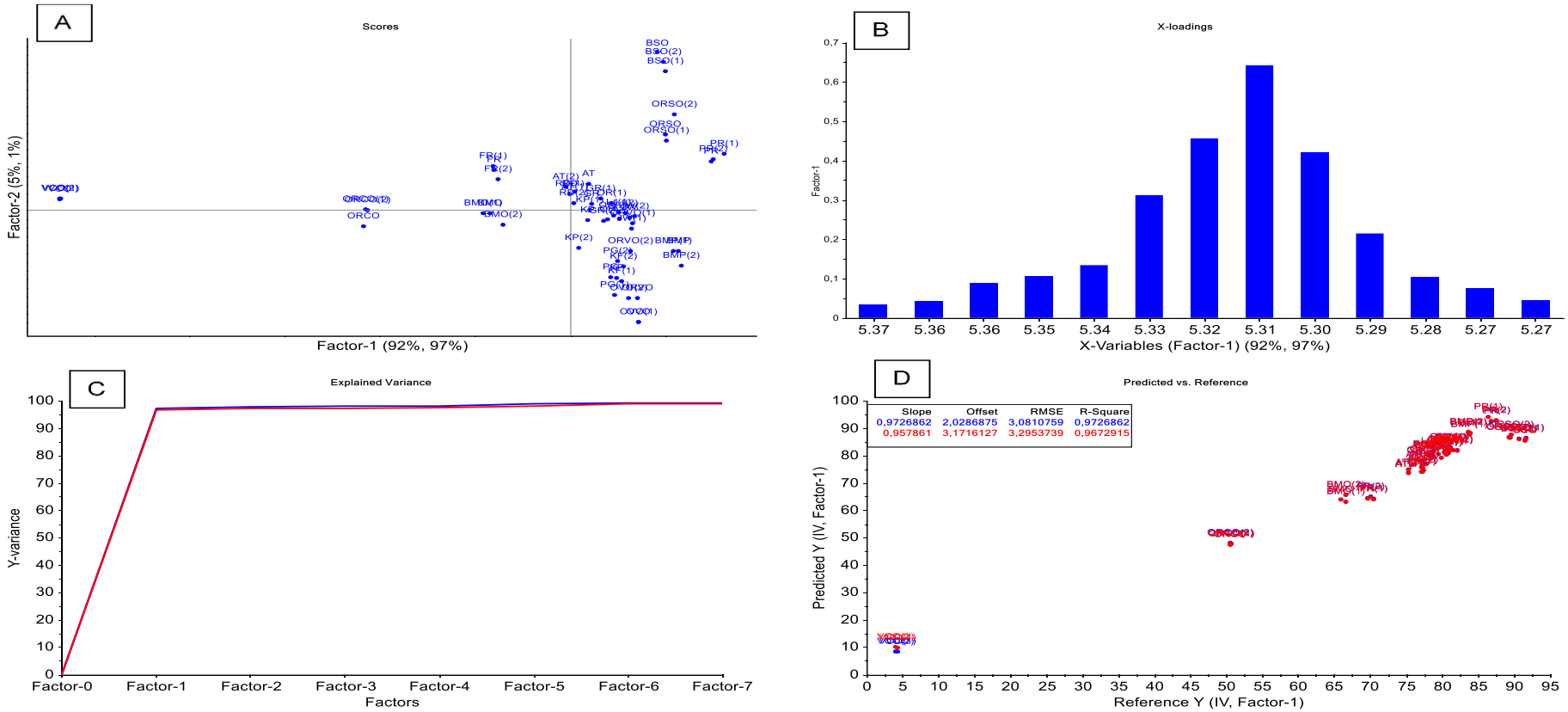

Figure S12 PLS calibration analyses for the degree of unsaturation on NMR data. (A) Score Plot Factor 1 vs. Factor-2 of selected signal NMR data; (B) Plot of X-Loading with axis X-Variables (Factor-1) (5.37-5.27 ppm); (C) Plot Explained Variance Factor-0 - 7 to Y-variance; (D) Plot Predicted vs. Reference Y from Factor-2 of the degree of unsaturation

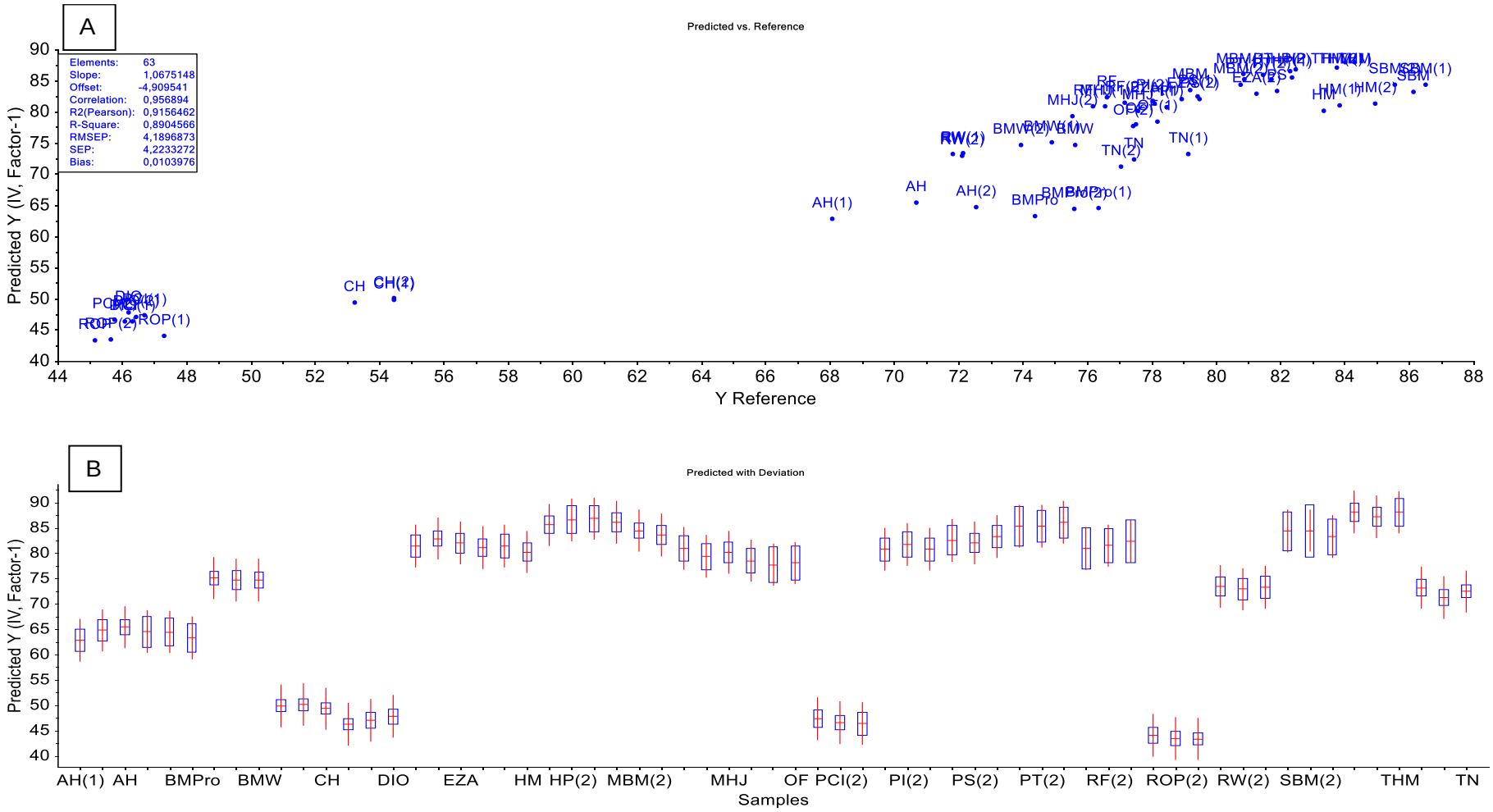

Figure S13 (A) Plot Predicted vs. Y Reference of the degree of unsaturation on the sample (prediction set) with calibration model Fig.12D (NMR); (B) Plot Predicted Y with a deviation of samples (Prediction test)

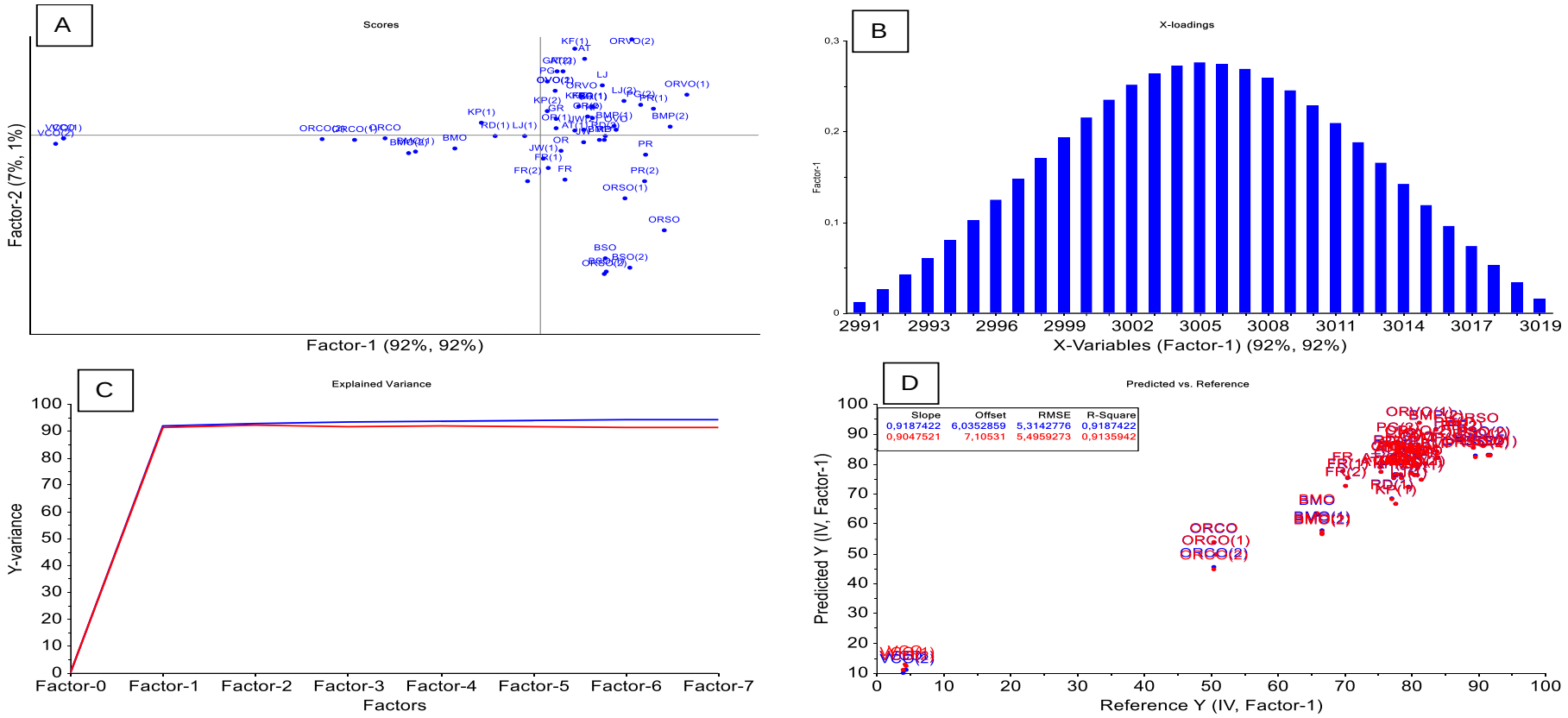

Figure S14 PLS calibration analyses for the degree of unsaturation on FTIR data. (A) Score Plot Factor 1 vs. Factor-2 of FTIR data; (B) Plot of X-Loading with axis X-Variables (Factor-1) (2990 - 3020 cm^{-1}); (C) Plot Explained Variance Factor-0 - 7 to Y-variance; (D) Plot Predicted vs. Reference Y from Factor-1 of the degree of unsaturation

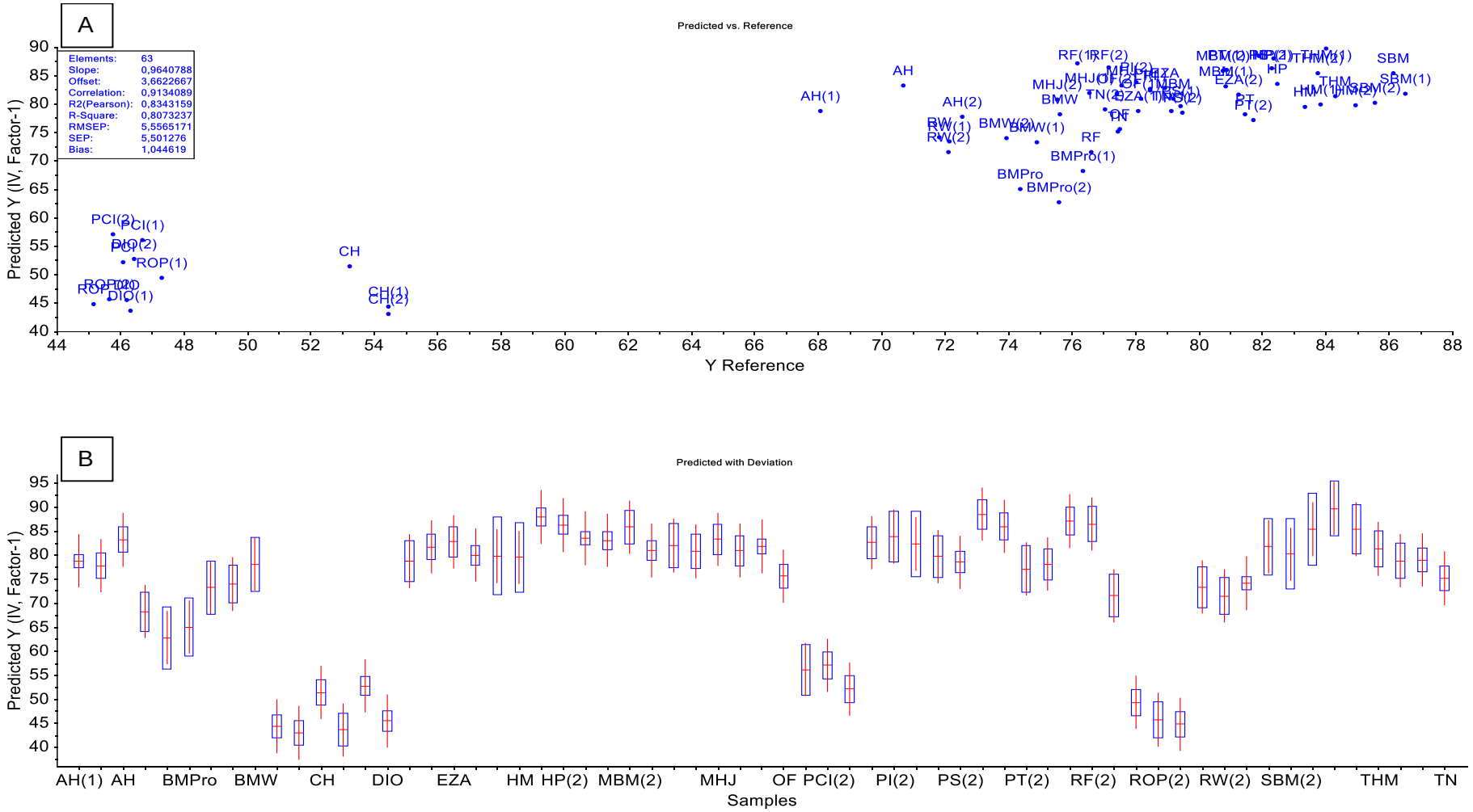

Figure S15 A Plot Predicted vs. Y Reference of the degree of unsaturation sample (prediction set) with calibration model Fig.14D (FTIR); B Plot Predicted Y with a deviation of the sample (Prediction test)

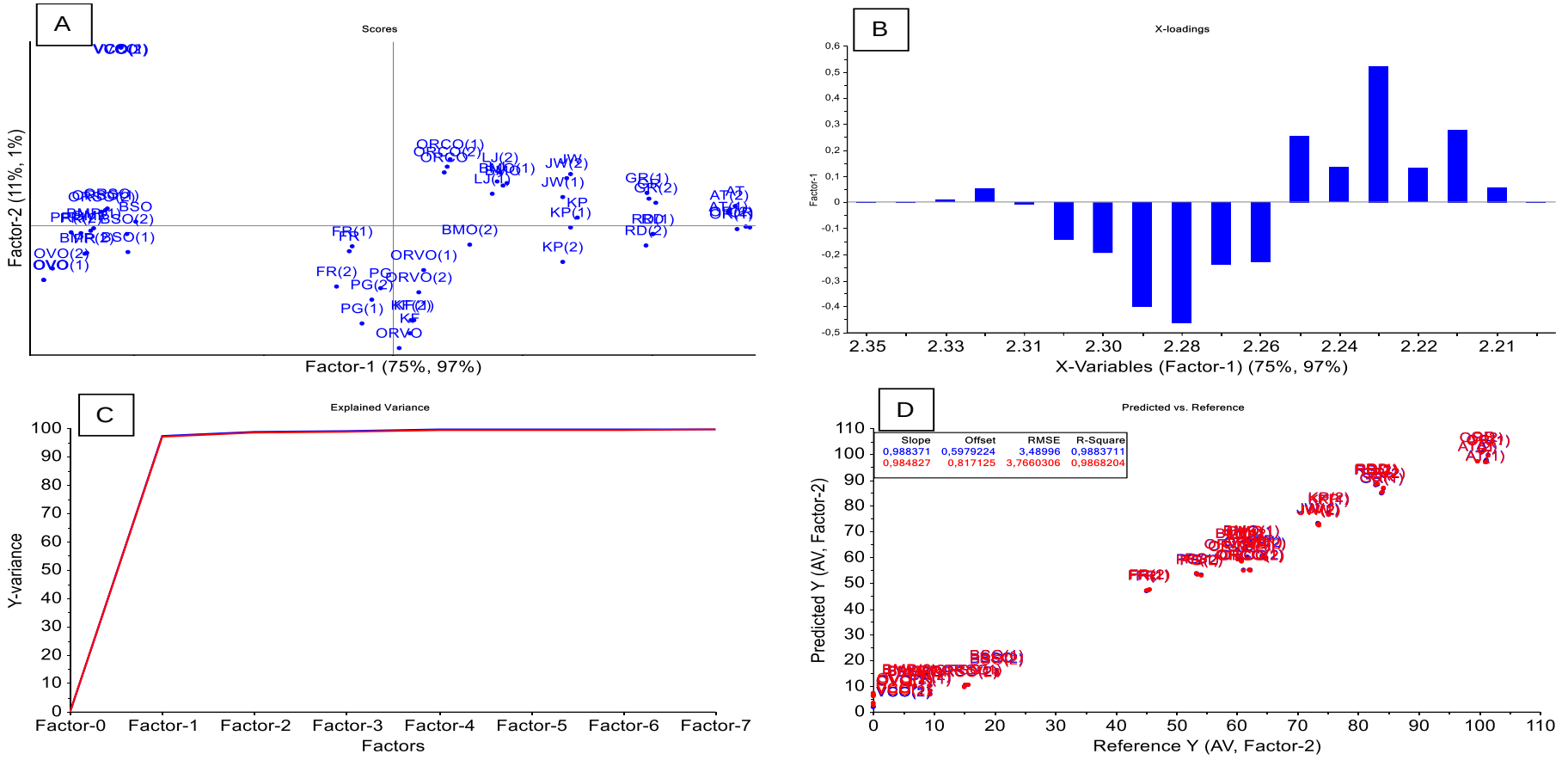

Figure S16 PLS calibration analyses for the FFA value on NMR data. (A) Score Plot Factor 1 vs. Factor-2 of selected signal NMR data; (B) Plot of X-Loading with axis X-Variables (Factor-1) (2.37-2.27 ppm); (C) Plot Explained Variance Factor-0 - 7 to Y-variance; (D) Plot Predicted vs. Reference Y from Factor-2 of the FFA value

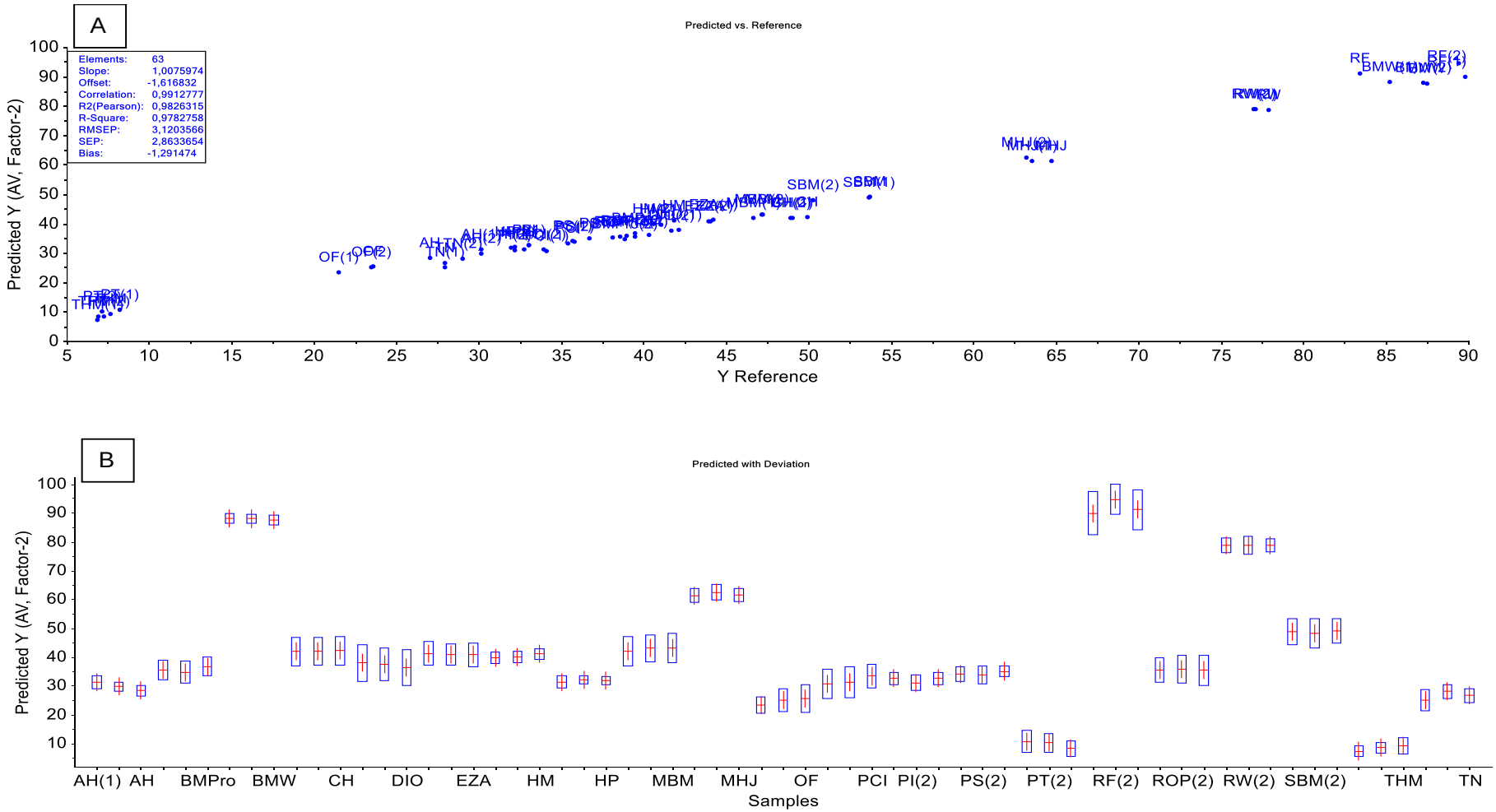

Figure S17 (A) Plot Predicted vs. Y Reference of the FFA value on the sample (prediction set) with calibration model Fig.16D (NMR); (B) Plot Predicted Y with a deviation of samples (Prediction test)

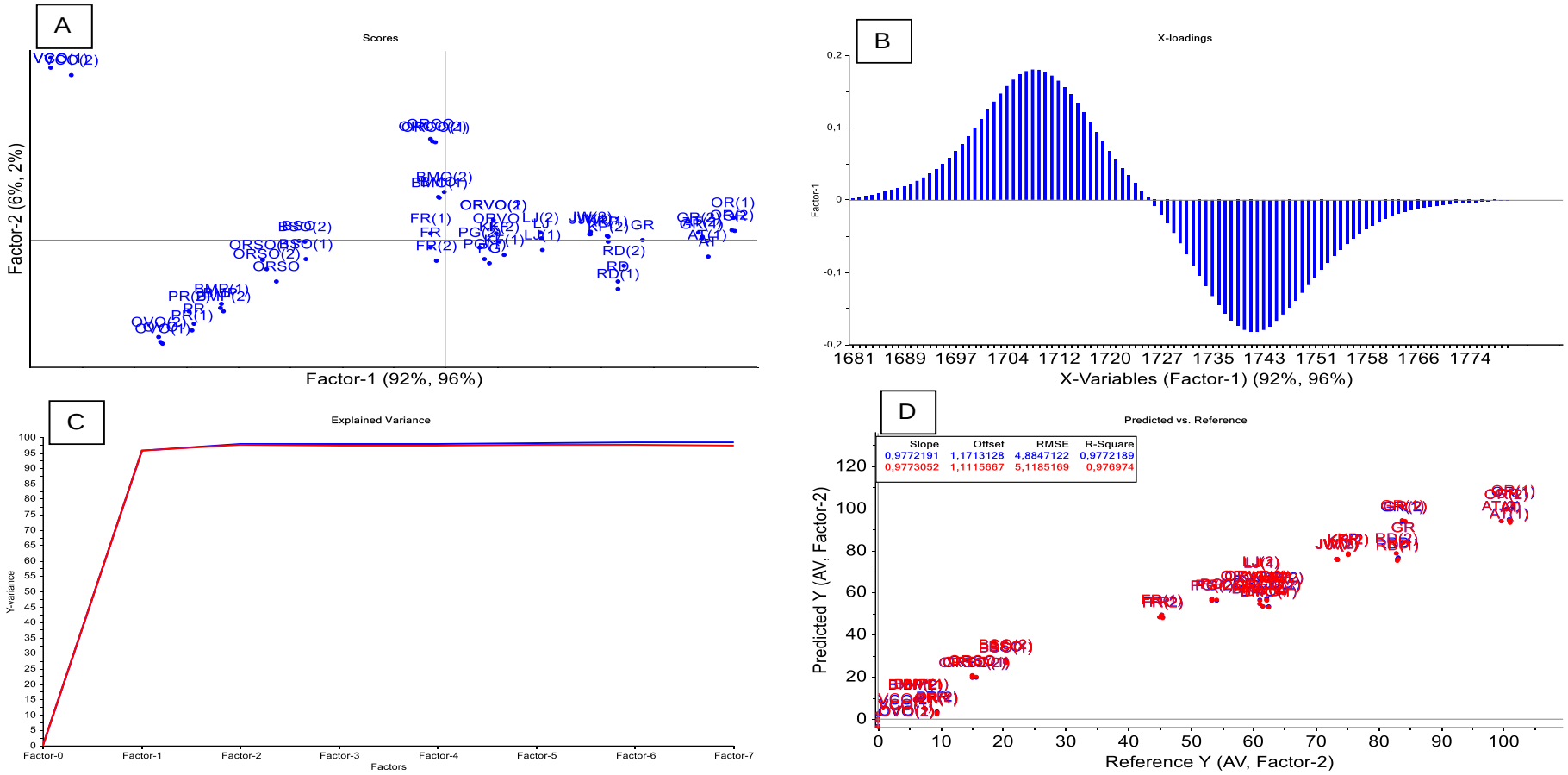

Figure S18 PLS calibration analyses for the FFA value on FTIR data. (A) Score Plot Factor 1 vs. Factor-2 of selected band FTIR data; (B) Plot of X-Loading with axis X-Variables (Factor-1) (1680 - 1780 cm^{-1}); (C) Plot Explained Variance Factor-0 - 7 to Y-variance; (D) Plot calibration of Predicted vs. Reference Y from Factor-2 of the FFA value

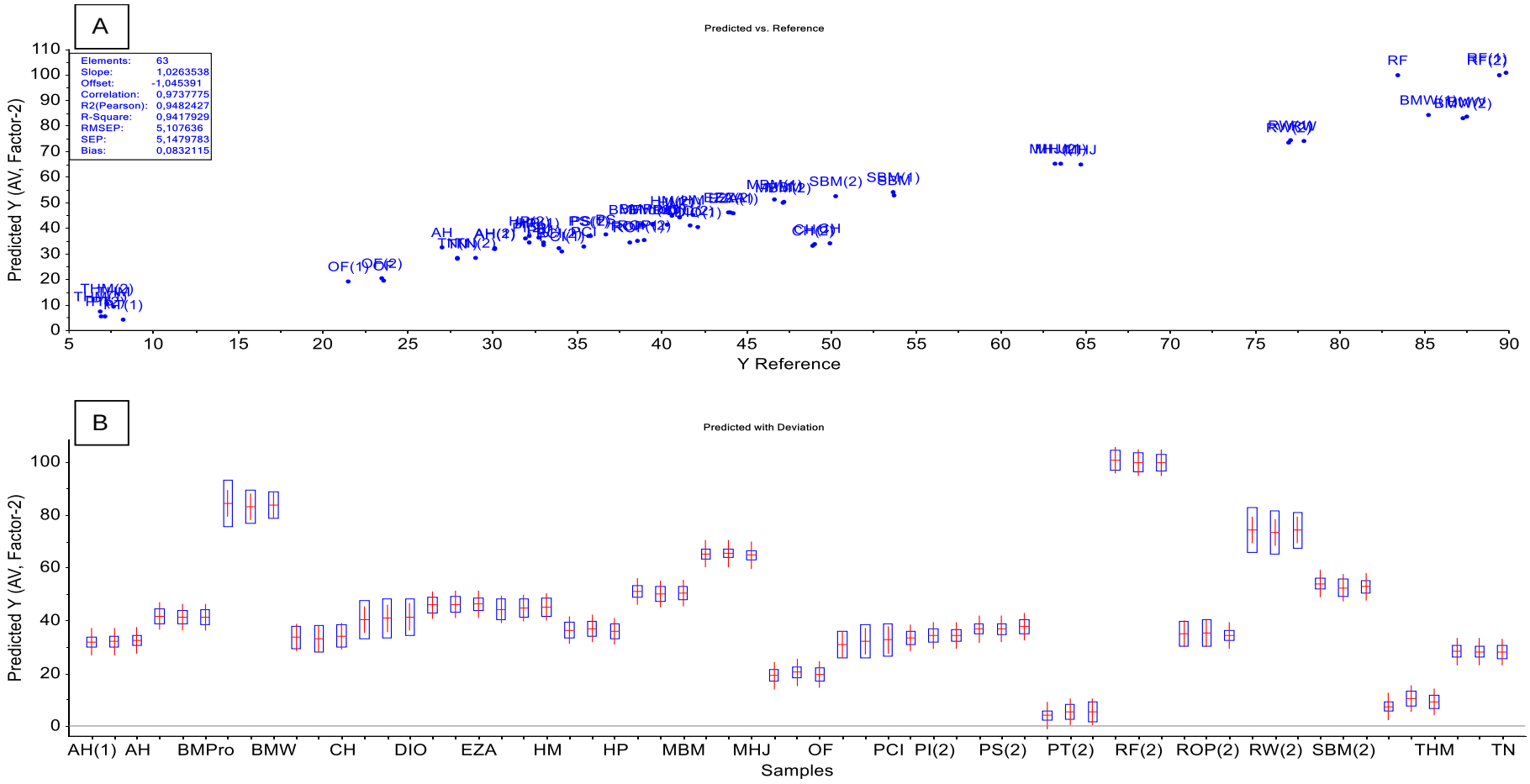

Figure S19 (A) Plot Predicted vs. Y Reference of the FFA value on the sample (prediction set) with calibration model Fig.18D (FTIR); (B) Plot Predicted Y with a deviation of samples (Prediction tes)

3.3 Quantitative ^{1}H NMR Spectroscopy Combined with Chemometrics as a Profiling and Estimation Tool for Unsaturated Fatty Acid Composition in Red Fruit Oil and its commercial products[1]

[1]This chapter was submitted and under review for publication in *Eur.J. Lipid Sci.Technol*. (2022). For details see chapter 7.1 List of publications

Liling Triyasmono, Curd Schollmayer, Ulrike Holzgrabe

Abstract

A fast and straightforward procedure based on ^{1}H NMR spectroscopy combined with chemometrics was developed to assess the unsaturated fatty acid content in red fruit oil (RFO). This oil is obtained from the fruit of Pandanus conoideus, Lam., and has the potential as a source of essential unsaturated fatty acids for low-fat diets. Forty samples (crude RFO, a mixture of crude RFO with olive oil, virgin coconut oil, black seed oil, and 33 commercial products RFO) were previously analyzed by ^{1}H NMR spectroscopy. Here, a principal component analysis (PCA) was used as a visualization grouping, and the partial least square (PLS) was used to predict the composition of PUFA, Total UFA, and MUFA. The selected signals showed characteristics at δ = 2.80 - 2.71 ppm for PUFA and δ = 2.10 - 1.90 ppm for Total UFA and MUFA. Furthermore, the satisfactory quality of the PCA plot is shown by 99% of the total PC obtained, so each sample was successfully grouped according to its PUFA and Total UFA values. PLS also provided excellent results in the calibration model, validation, and prediction for PUFA, Total UFA, and MUFA based on a small root mean square error (RMSE) value and the coefficient of determination (R^2) value more than 0.90 for all models. The study demonstrates the potential of quantitative ^{1}H NMR using internal standards combined with chemometrics. It can routinely be applied for quality monitoring and authentication of RFO products, mainly based on their unsaturated fatty acid compositions.

Practical application: This study proves that the value of PUFA, Total UFA, and MUFA in oil, primarily crude RFO and commercial RFO products, can be determined by the quantitative ^{1}H

NMR spectroscopy method using the internal standards. At the same time, these parameters (PUFA, Total UFA and MUFA) play an essential role in assessing oil quality. Therefore, this method is helpful in fast analysis without the derivatization process and has high accuracy and precision. In addition, the combination with chemometrics makes the process more efficient for visualizing grouping based on the composition of unsaturated fatty acids as well as predicting the amount of PUFA, MUFA, and total UFA, so that it will be more beneficial in quality assurance and detection of adulterants in commercial RFO with other edible oils.

Keywords: ^{1}H NMR, PUFA, Total UFA, MUFA, RFO, PCA, PLS

Abbreviations

RFO, Red Fruit Oil, PUFA, Polyunsaturated fatty acids, Total UFA, Total unsaturated fatty acids, MUFA, Mono unsaturated fatty acids, SFA, Saturated fatty acid, FA, Fatty acid, PCA, Principal component analysis, PLS, Partial least Square, RMSEC, Root mean square error calibration, RMSEV, Root mean square error validation, RMSEP, Root mean square Prediction, FFA, Free fatty acid, OR, Crude RFO (Original RFO), BSO, Black Seed Oil (Habattusauda), OVO, Olive Oil, VCO, Virgin Coconut Oil, ORCO, Crude RFO plus VCO, ORVO, Crude RFO plus Olive Oil, Crude RFO plus Black Seed Oil (Habbatusauda), AT, ATHAKU, BMO, Buah Merah Oil Papua, BMP, Buah Merah Papua, FR, Fira Herbalindo Buah Merah, GR, Golden Red, JW, Jaya Wijaya, KF, KF Minyak Buah Merah, KP, King Pandanus, LJ, Loh Jinawi, PG, Premium Gold, PR , Pro Jep Buah Merah, RD, REDOTEN, AH, Agro Herbal Husada, BMPro, BMPro Minyak Buah Merah, BMW, Buah Merah Wamena, CH, Cahaya Minyak Buah Merah, DIO, DioDes Minyak Buah Merah, EZA, Essensa Naturale Buah Merah, HM, Herbal Food Buah Merah, HP, Herbal Produk Buah Merah, MBM, Minyak Buah Merah, MHJ, Mahesa Herbal Jogja, OF, Oil Fit, PCI, PCI Buah Merah, PI, Papua Indonesia Minyak Buah Merah, PS, Planta Sehat, PT, Papua Tropika MBM, ROP, Red Oil Papua, RW, Redwin, SBM, Sari Buah Merah Made, THM, Tani Home Industri Buah Merah, TN, Tamba Sanjiwani Natur, RF, FIRA PAPUA.

1. Introduction

Low-lipid diets are a health food icon and are relatively popular today. Those diets focus on the abundant consumption of several fruits, vegetables, and olive oil as the primary source of lipids. In addition, consuming olive oil can reduce the risk of coronary artery disease.[1] Pandanus conoideus, Lam. is one of the potential plants from the Papua region, Indonesia, which can be used as a source of functional oil because of its high content of antioxidant compounds, fat-soluble vitamins, and high MUFA which is comparable to olive oil.[2,3] In addition, due to the relatively high proportion of unsaturated fatty acids, the oil is susceptible to oxidation. This fact contributes to the co-evolution of its high antioxidant content. However, the potential of RFO as a source of essential fatty acids is still underutilized.

Oil composition analysis based on standard method is mainly carried out by means of chromatographic techniques such as gas chromatography (GC). Although GC is the method of choice, it requires esterification to form methyl ester compounds.[4] Complex sample handling and the need for expensive derivatizing agents are disadvantages of using GC for fatty acid analysis. In addition, samples cannot be recovered after the experiment. Furthermore, several methods have also been reported, including Fourier Transform Infrared (FTIR)[5,6] and High Performances Liquid Chromatography (HPLC).[7,8] However, the methods have not been entirely accepted as standard methods until now.

High-resolution nuclear magnetic resonance (NMR) spectroscopy is gaining popularity as a lipid analysis method. NMR spectra provide structure information and the qualitative and quantitative composition of lipid molecules even in complex mixtures.[9,10] NMR spectroscopy has several advantages compared with general chromatographic analysis (e.g., GC and HPLC). For example, the NMR measurement maintains the integrity of the oil. Furthermore, the obtained spectral data from one single measurement can be used for further analysis, including the determination of the oil's acid number, saponification number, and iodine number.[11-13] Therefore, this method can speed up the quality control process without derivatization.

Recently, different results on vegetable oil composition with ^{1}H NMR have been published.[14-17] These reports describe approaches for the calculation of fatty acid (FA) percentages for different oils using ^{1}H NMR spectra. Unfortunately, the FA value of each oil is obtained by varying mathematical formula approaches, depending on the differences of the signal selected for integration and the type of sample studied. In addition, Ingalina et al.[18] developed a method for the characterization of extra virgin olive oil based on the FA composition using ^{1}H NMR combined with chemometrics from 9 regions in Italy, mainly utilizing 19 signals between δ = 0.60 - 9.94 ppm. The correctness of the classification obtained consistently reaches more than 84% and 90% based on region categories.

Triyasmono et al.[12] have succeeded in developing a quantitative study of ^{1}H NMR spectroscopy to simultaneously determine the acid value, saponification value, ester value, and iodine value of RFO and its commercial products. Furthermore, the reliability of the ^{1}H NMR quantification technique by using an internal standard provides the opportunity to expand its application, including the determination of the composition of unsaturated fatty acid (UFA) in RFO. Therefore, this work aims to apply the quantitative ^{1}H NMR method using an internal standard to obtain PUFA, Total UFA, and MUFA values in a short time without losing precision. It also included a study of the ^{1}H NMR spectra followed by chemometrics to classify and predict each RFO product based on PUFA, Total UFA, and MUFA to facilitate quality assurance and authentication.

2. Experimental Section

2.1. Chemical reagents and Standarts

Linoleic acid standard (99.9%) and dimethyl sulfone ($DMSO_2$) internal standard (TraceCERT®, 99.99 %) NMR grade were purchased from Merck (Darmstadt, Germany), hexadeuterium dimethylsulfoxide (DMSO-d_6, 99.9 % D), tetramethylsilane (TMS) and NMR tube Boro 400-5-7 from Deutero (Kastellaun, Germany); deuterated chloroform ($CDCl_3$, 99.8 % D) were purchased from Eurisotop (Saarbrücken, Germany).

2.2. Samples

This study used several types of oil. First, crude RFO is produced from an extraction process[3] of red fruit obtained from Papua, Indonesia. In this context, the crude RFO is interpreted as the original RFO (OR). Second, three other types of edible oil, including Virgin Coconut Oil (VCO), Olive Oil (OVO), and Black seed oil (BSO). Third, 33 commercial products of RFO from various factories were obtained from the Indonesian herbal market. Three modified RFO samples were obtained by binary mixing system, namely: each 150 mg OR was mixed with 100 mg BSO, OVO, and VCO oil, respectively. The modified RFO products are called ORSO, ORVO, and ORCO. Furthermore, the samples were grouped into two components: calibration and prediction. **Table 1** shows a list of samples and their specifications.

Table 1 Listing of all investigated sample RFO in this study

Sample	Code	Type	Specification	Quantity
1	OR	Original RFO (crude RFO)	Calibration	3
2	ORCO	OR + VCO	Calibration	3
3	ORVO	OR + OVO	Calibration	3
4	ORSO	OR + BSO	Calibration	3
5	OVO	commercial OVO	Calibration	3
6	VCO	commercial VCO	Calibration	3
7	BSO	commercial BSO	Calibration	3
8	AT	commercial	Calibration	3
10	BMP	commercial	Calibration	3
11	FR	commercial	Calibration	3
12	GR	commercial	Calibration	3
13	JW	commercial	Calibration	3
14	KF	commercial	Calibration	3
15	KP	commercial	Calibration	3
16	LJ	commercial	Calibration	3
17	PG	commercial	Calibration	3
18	PR	commercial	Calibration	3
19	RD	commercial	Calibration	3
20	AH	commercial	Prediction Test	3
21	BMPro	commercial	Prediction Test	3
22	BMW	commercial	Prediction Test	3
23	CH	commercial	Prediction Test	3

Table 1 continued

Sample	Code	Type	Specification	Quantity
24	DIO	commercial	Prediction Test	3
25	EZA	commercial	Prediction Test	3
26	HM	commercial	Prediction Test	3
27	HP	commercial	Prediction Test	3
28	MBM	commercial	Prediction Test	3
29	MHJ	commercial	Prediction Test	3
30	OF	commercial	Prediction Test	3
31	PCI	commercial	Prediction Test	3
32	PI	commercial	Prediction Test	3
33	PS	commercial	Prediction Test	3
34	PT	commercial	Prediction Test	3
35	ROP	commercial	Prediction Test	3
36	RW	commercial	Prediction Test	3
37	SBM	commercial	Prediction Test	3
38	THM	commercial	Prediction Test	3
39	TN	commercial	Prediction Test	3
40	RF	commercial	Prediction Test	3

2.3. NMR spectroscopy

The sample preparation was carried out according to Triyasmono et al.[12] Briefly: 833.3 mg RFO and 3.33 mg $DMSO_2$ were weighed into a 2.0 ml volumetric flask. Next, an amount of the solvent mixture $CDCl_3$: DMSO-d_6 (5:1 v/v) containing 0.1% TMS (Tetramethylsilane) was added to 2.0 ml, and the tube was vortexed for 10 seconds. Then, 600 µL of this solution was put into a 5 mm diameter NMR tube (Boro 400-5-7, Deutero, Kastellaun, Germany).

Quantitative ^{1}H NMR analyses was performed employing a Bruker 400 MHz instrument (Avance III 400 MHz, Bruker BioSpin GmbH, Rheinstetten, Germany), equipped with the Bruker B-ACS 60 robotic autosampler (which allows fully automated analysis of up to 60 samples at once) and a 5 mm Z-gradient PABBI inverse probe. For accurate quantification, the T1 value of each sample was measured to ensure complete relaxation between scans, according to Holzgrabe[19] and Triyasmono et al.[12] Furthermore, the one-dimensional (1D) ^{1}H NMR spectra used for quantifications were recorded using the zg30 pulse sequence, no

rotation, with a spectral width 30.0 ppm, 160 k time-domain size, 32 scans, acquisition time 6.81 s, receiver gain was set 4, digital resolution 0.147 Hz, and the relaxation delay (d1) 9 s. The spectra were processed using a line broadening of 0.3 Hz. Chemical shifts were referenced to TMS at δ = 0.00 ppm.

The total time required to obtain each spectrum is approximately 15 minutes. Data were automatically obtained using ICON-NMR TopSpin 3.6.4 (Bruker BioSpin, Rheinstetten, Germany). Each sample was measured in triplicate. Furthermore, the resulting spectra were processed manually with TopSpin 4.0 (Bruker BioSpin GmbH, Rheinstetten, Germany), including a phasing and baseline correction

2.4. Evaluation of assignment signal by linoleic acid standard

The standard addition method was performed to ensure that the selected RFO ^{1}H NMR spectra signal correlated with the quantification of the UFA components,[18] as follows: five sample series consisting of 250 mg RFO without linoleic acid and 250 mg RFO plus linoleic acid (10, 20, 40 and 80 mg), respectively. Each sample was measured in triplicate. Furthermore, the correlation of the effect of adding linoleic acid and the signal integral at δ = 2.80 - 2.71 ppm and δ = 2.10 - 1.90 ppm, as well as the PUFA, Total UFA, and MUFA values, can be assessed by statistical regression analysis using Microsoft® Excel® 2019 MSO (Version 2204 Build 16.0.15128.20158) 64-bit software.

2.5. Determination of PUFA, Total UFA, and MUFA using relative method

The calculation of the relative percentages of PUFA, total UFA, and MUFA was performed by using the different signal integrals (D, F, and H) of the ^{1}H NMR RFO spectrum and its assignment to the TAG structure (**Figure 1**) as the relative method equation.[20]

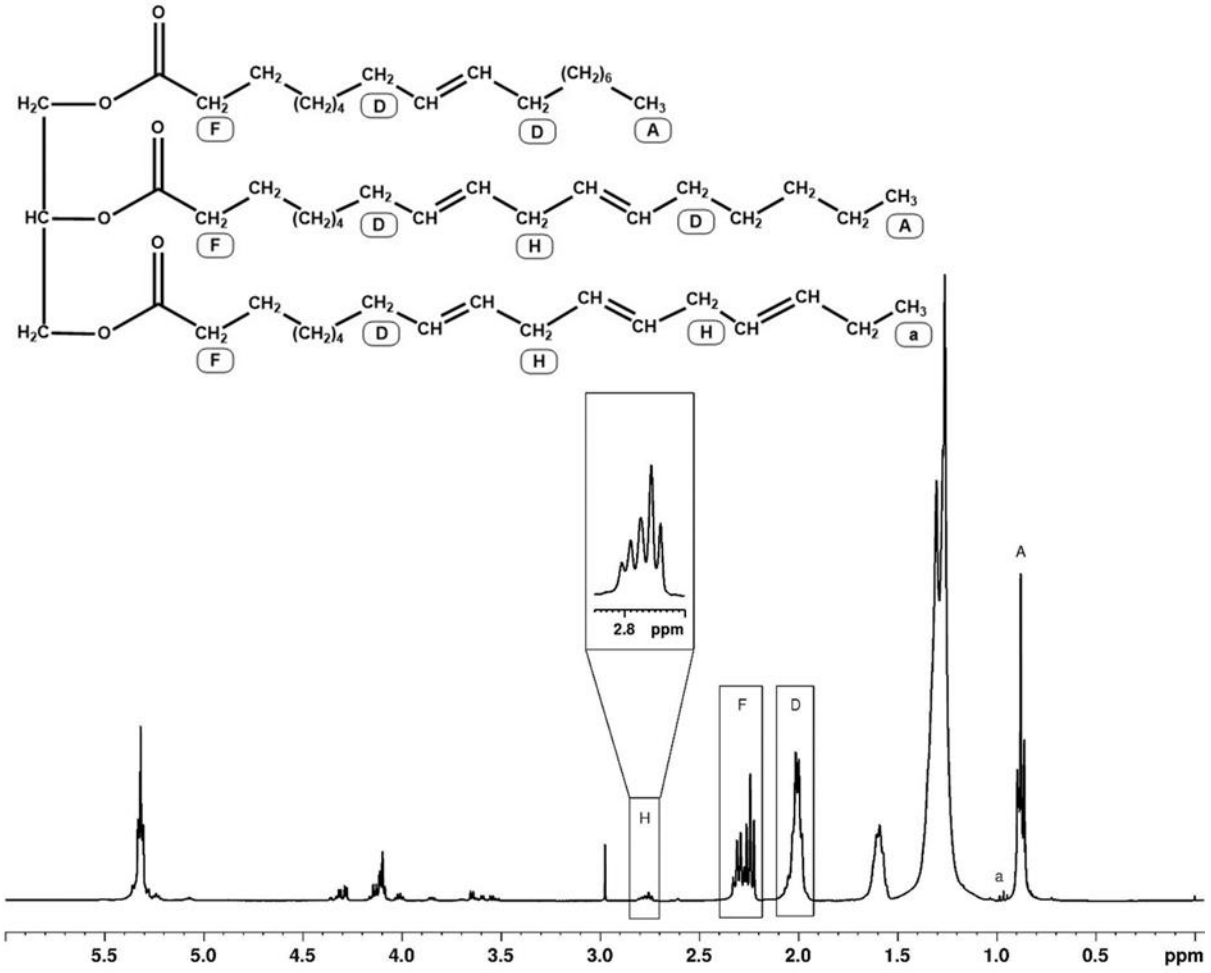

Figure 1. Representative ^{1}H NMR spectrum of RFO and its assignment to the TAG structure shows the characteristic signal; A -C$\underline{H}_3$ group signal at the terminal chains for most fatty acids, a is apart signal from -C$\underline{H}_3$ group terminal of ω-3 unsaturated fatty acids. D -C$\underline{H}_2$-CH=CH- signal, F α-C$\underline{H}_2$ signal, H bis-allylic (-C=C-C$\underline{H}_2$-C=C-) signal. All ^{1}H NMR shifts at 400 MHz in the mixture of $CDCl_3$: DMSO-d_6 (5:1 v/v) containing TMS 0.1 %.

This approach has also been reported by Knothe & Kenar[11] and Hama et al.[16]; the relative amount of PUFA can be calculated by integrating the signal of the α-C$\underline{H}_2$ (F) at δ= 2.37 - 2.20 ppm and the signal at δ = 2.80 – 2.71 ppm (H), which can be assigned to the bis-allylic (-CH=CH-C$\underline{H}_2$-CH=CH-). The signal of the α-C$\underline{H}_2$ group consists of two doublets in all types of fatty acids. The signals corresponding to the bis-allylic (-CH=CH-C$\underline{H}_2$-CH=CH-) group doublets were only present in PUFA. Therefore, PUFAs can be quantified by the equation below:

PUFA = (H/F) x 100% (1)

The allylic (-C<u>H</u>$_2$-CH=CH-) multiplets (D) at δ = 2.10 – 1.90 ppm is present in all unsaturated fatty acids. The relative amount of MUFA is related to the signal integral of the allylic (-C<u>H</u>$_2$-CH=CH) (D) with two α-C<u>H</u>$_2$ signals (F). Therefore, the Total UFA is represented by the equation below:

$$\text{Total UFA} = (D/2F) \times 100\% \quad (2)$$

The relative MUFA content can be calculated from equation:

$$\text{MUFA} = \text{Total UFA} - \text{PUFA} \quad (3)$$

2.6. Determination of PUFA, Total UFA, and MUFA using Internal standard method

For the calculation, using the standard internal approach, the following signals were used for quantitative analysis, including $DMSO_2$ (δ = 2.98 ppm), PUFA (δ = 2.80-2.71 ppm), and Total UFA (δ = 2.10-1.90 ppm). The acquisition was carried out under the conditions mentioned above (see **2.3**), according to the equation formula of quantitative NMR discussed by Holzgrabe[19], Bharti & Roy[21], and development by Skiera et al.[22] and Triyasmono et al.[12] Hence, each UFA value was calculated by the equations below:

$$PUFA_{NMR} = \frac{M_{PUFA}}{m_s} \cdot \frac{m_{DMSO_2} \cdot P_{DMSO_2}}{M_{DMSO_2}} \cdot \frac{N_{DMSO_2}}{N_s\ (2)} \cdot \frac{I_{CH_2\ (\text{bis allylic})}\ (2.80\text{-}2.71\ \text{ppm})}{I_{DMSO_2}\ (2.98\ \text{ppm})} \cdot 100\% \quad (4)$$

$$\text{Total UFA}_{NMR} = \frac{M_{\text{Total UFA}}}{m_s} \cdot \frac{m_{DMSO_2} \cdot P_{DMSO_2}}{M_{DMSO_2}} \cdot \frac{N_{DMSO_2}}{N_s\ (2)} \cdot \frac{\frac{1}{2} \cdot I_{CH_2\ (\text{allylic})}\ (2.10\text{-}1.90\ \text{ppm})}{I_{DMSO_2}\ (2.98\ \text{ppm})} \cdot 100\% \quad (5)$$

$$MUFA_{NMR} = \text{Total UFA}_{NMR} - PUFA_{NMR} \quad (6)$$

m_s denotes the sample weight in mg, *P* the purity, M the molecular weight in g/mol, N_s the number of protons signal, and I the ^{1}H NMR integral area, according to Triyasmono et al.[12]

2.7. Comparison of the results using internal standard with relative methods

A statistical regression was applied to compare the results of the PUFA, Total UFA, and MUFA RFO values from both methods (internal standard and relative method) of quantitative ^{1}H NMR. Data were processed using Microsoft® Excel® 2019 MSO (Version 2204 Build 16.0.15128.20158) 64-bit software. The correlation between both methods can be assessed based on the coefficient of determination (R^2) and precision (standard error).

2.8. Pre-processing and multivariate data analysis

The NMR data underwent several pre-treatment and transformation treatments before chemometric analysis. First, the bucketing process on ^{1}H NMR spectra with the bucket width of 0.009 ppm was applied using Amix 3.9.15 software (Bruker BioSpin GmbH, Rheinstetten, Germany). Furthermore, the results of the bucketing are saved in txt format to build a data matrix. The final ranges signal used for PCA and PLS are the signal at δ = 2.80 - 2.71 ppm and δ = 2.10 - 1.90 ppm.

Furthermore, chemometric analysis was performed by importing the entire bucketing data matrix into Unscramble X 11.0 (CAMO Software USA, Oslo, Norway). First, the PCA method was applied. The score plot is a projection of the starting point towards the main component and can be used to classify according to PUFA content and Total UFA content. While loading represents a unique vector of the data covariance matrix (or correlation matrix), it can be used to identify data variables. In addition, PLS analysis was applied to construct the model calibration using a spectral matrix X (^{1}H NMR spectra) and a quantitative matrix Y (the percentage of PUFA, Total UFA, and MUFA). Finally, PLS calibration was applied to predict the percentage of the composition of PUFA, Total UFA and MUFA in RFO commercial products.

The calibration models were built using nineteen samples (in triplicate), twenty-one commercial samples (in triplicate) were used to test their class identities, as shown in **Table 1**. The leave-one-out cross-validation procedure was used to verify the calibration and

prediction model. The models were evaluated considering the coefficient of correlation for cross-validation and prediction and the root means square error for cross-calibration, validation, and prediction (RMSEC, RMSEV and RMSEP).[23]

3. Results and discussion

3.1. Evaluation of assignment signal by linoleic acid standard

^{1}H NMR spectra of all samples were measured and the signals assigned to the protons of the RFO. Therefore, the selection of signals for the quantification of PUFA, Total UFA, and MUFA can be assessed. **Figure 2A** shows a change of the signal at δ = 2.80-2.71 ppm upon addition of linoleic acid. Furthermore, based on regression analysis statistics, a linear relationship was found between the integral of the signal of the allylic protons at δ = 2.80 - 2.71 ppm (R^2 = 0.996) and the amount of added linoleic acid (**Figure 2B**). This means that the signal at δ = 2.80 - 2.71 ppm on the RFO as a -CH=CH-C$\underline{H}_2$-CH=CH- signal, agreed with the assignment reported by Alexandri et al.[24]

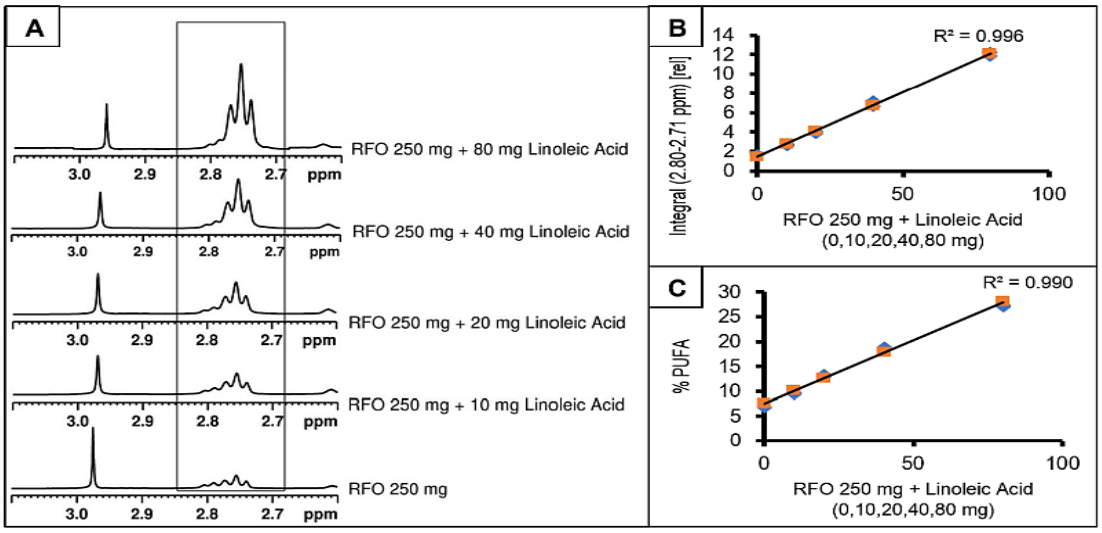

Figure 2. (**A**) Stacked Plot ^{1}H NMR Spectra (from bottom to top) of an RFO 250 and RFO 250 mg with linoleic acid (10,20,40 and 80 mg), respectively. (**B**) Linear correlation between RFO with linoleic acid addition versus integral of ^{1}H NMR RFO (δ= 2.80-2.71 ppm). (**C**) Linear correlation between RFO with % PUFA by qNMR calculation. (Orange plot: predicted-Y; blue plot: actual value).

Consequently, the addition of a certain amount of linoleic acid to the RFO resulted in a proportional increase in the relative amount of PUFA (**Figure 2C**). Thus, selecting a signal at δ = 2.81 - 2.70 ppm as the PUFA quantification signal is appropriate and is in line with the assignment which been reported previously.[11,16]

The addition of linoleic acid also affects the -C$\underline{H}_2$-CH=CH- signal at δ = 2.10 - 1.90 ppm **(Figure 3A)**. Accordingly, by the regression analysis, the correlation between the addition of linoleic acid and the integral of signal at δ = 2.80 - 2.71 ppm is linear (R^2 = 0.996) (**Figure 3B**) and is in accordance with finding reported in the literature for other FA mixtures,[24,25] and it is found in all UFA's.[11,16]

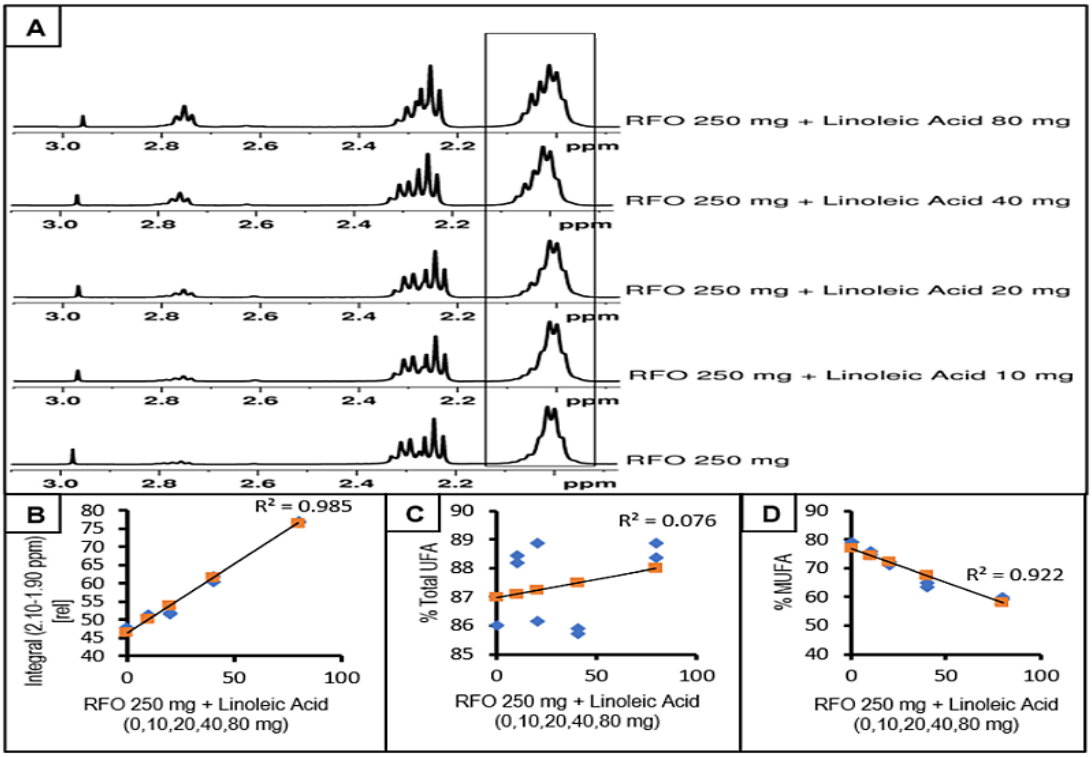

Figure 3. (**A**) Stacked Plot ^{1}H NMR Spectra (from bottom to top), especially on selected signal Allylic -C$\underline{H}_2$ (δ = 2.10-1.90 ppm) of an RFO 250 and RFO 250 mg with Linoleic acid (10,20,40 and 80 mg), respectively. (**B**) Linear correlation between RFO with linoleic acid addition versus Integral of ^{1}H NMR RFO (δ= 2.10-1.90 ppm). (**C**) Nonlinear correlation between RFO with linoleic acid addition versus % Total UFA by qNMR calculation. (**D**) Negative linear correlation between RFO with linoleic acid addition versus % MUFA by qNMR estimate. (Orange plot: predicted-Y; blue plot: actual value).

As expected, there was a proportional decrease in the number of MUFAs (**Figure 3D**). It means that linoleic acid (a double UFA) will reduce the relative amount of MUFA and increase the relative PUFA in RFO. On the other hand, as shown in **Figure 3C**, the actual plot value (blue plot) obtained is different from the predicted-Y value (orange plot) because the residuals of both values are relatively large. These results prove that there is no linear correlation between the Total UFA content with the addition of linoleic acid. Therefore, it can be stated that the relative total UFA in the RFO remains constant (Total UFA = MUFA + PUFA).

Hence, the signal at δ = 2.10 – 1.90 ppm can be used for the calculation of the Total UFA and MUFA, which was also suggested by Castejon et al.[15] and Hama et al.[16] for other oils.

3.2. Comparison of PUFA, Total UFA, and MUFA determination using relative and internal standards method on ^{1}H NMR spectra.

PUFA, Total UFA, and MUFA were determined for 19 RFO samples (calibration sample / **Table 1**) using both a relative and an internal standards method. A statistical regression was applied to evaluate the correlation between both equation methods (see equations 1-6 on method **2.5** & **2.6**). **Table 2** summarizes the results. The findings of the internal standard method are similar to the ones obtained by the relative method indicated by R^2 above 0.90 and low standard error (all regression models are presented in **Figure 1** Supplementary Information S1).

Table 2. Regression analysis for the determination of PUFA, Total UFA and MUFA using relative and internal standard methods in the RFO ^{1}H NMR spectra

Parameter	Equation	Regression Statistic		
		Multiple R	R^2	Standard error
PUFA	y= 1.02x - 0.276	0.997	0.995	0.55
Total UFA	y= 0.95x + 3.34	0.989	0.979	2.82
MUFA	y= 0.94x + 3.62	0.990	0.981	2.70

Therefore, the quantitative ^{1}H NMR method using the standard internal has strong potential as an alternative for determining PUFA, Total UFA, and MUFA. Furthermore, the percentage of PUFA, Total UFA and MUFA from 19 RFO sample calibration sets are presented in **Table 3**.

Table 3. The percentage of PUFA, Total UFA and MUFA from 19 RFO sample by relative and internal standard method

Sample Code	Signal (ppm)	PUFA (%)		Signal (ppm)	Total UFA (%)		MUFA (%)	
		Internal standard (Equation 4)	Relative method (Equation 1)		Internal standard (Equation 5)	Relative method (Equation 2)	Internal standard (Equation 6)	Relative method (Equation 3)
AT		8.51 ± 0.23	8.75 ± 0.24		85.13 ± 2.16	87.19 ± 2.22	78.87 ± 2.04	76.81 ± 1.99
BMO		6.47 ± 0.07	6.56 ± 0.08		69.82 ± 0.33	70.50 ± 0.31	63.99 ± 0.24	63.32 ± 0.26
BMP		14.47 ± 0.18	14.19 ± 0.13		88.05 ± 1.60	86.32 ± 1.20	72.05 ± 1.01	73.78 ± 1.41
FR		15.27 ± 0.17	15.38 ± 0.17		66.89 ± 0.59	67.09 ± 1.20	51.99 ± 0.88	51.79 ± 0.76
GR		6.72 ± 0.11	7.04 ± 0.09		83.72 ± 0.50	87.64 ± 0.18	81.02 ± 0.13	77.10 ± 0.41
JW		7.04 ± 0.12	7.15 ± 0.13		87.57 ± 1.17	88.79 ± 1.31	81.72 ± 1.21	80.50 ± 1.07
KF		8.11 ± 0.09	7.86 ± 0.09		93.38 ± 0.88	90.75 ± 0.40	82.62 ± 0.47	85.25 ± 0.92
KP		6.44 ± 0.05	6.59 ± 0.06		82.27 ± 0.37	83.66 ± 0.23	77.27 ± 0.25	75.88 ± 0.40
LJ		7.15± 0.11	7.49 ± 0.12		84.95 ± 0.65	88.89 ± 0.88	81.62 ± 0.79	77.67 ± 0.56
PG	2.81-2.70	7.07± 0.11	7.25 ± 0.11	2.10-1.90	83.59 ± 1.42	85.62 ± 2.25	78.67 ± 2.24	76.64 ± 1.38
PR		20.82 ± 0.27	22.29 ± 0.19		85.63 ± 0.69	90.79 ± 0.43	69.66 ± 0.49	64.50 ± 0.43
RD		7.55 ± 0.01	7.85 ± 0.03		74.18 ± 0.32	77.00 ± 0.27	69.44 ± 0.27	66.62 ± 0.33
OR		6.72 ± 0.05	6.66 ± 0.03		86.30 ± 0.46	84.87 ± 0.52	78.10 ± 0.56	79.53 ± 0.40
ORCO		4.17 ± 0.03	3.78 ± 0.02		52.96 ± 0.29	47.98 ± 0.11	43.79 ± 0.14	48.78 ± 0.26
ORVO		7.77 ± 0.19	7.85 ± 0.09		88.65 ± 3.00	90.86 ± 0.61	83.18 ± 0.72	80.97 ± 2.81
ORSO		27.00 ± 0.94	25.0 ± 0.32		79.53 ± 1.86	74.59 ± 0.06	48.22 ± 0.92	53.16 ± 0.91
OVO		7.75 ± 0.25	7.81 ± 0.07		82.20 ± 1.77	84.81 ± 0.48	77.34 ± 0.65	74.74 ± 1.52
VCO		0.40 ± 0.01	0.38 ± 0.01		4.18 ± 0.05	3.97 ± 0.03	3.58 ± 0.02	3.78 ± 0.03
BSO		33.18 ± 0.14	32.32 ± 0.13		70.16 ± 0.58	68.21 ± 0.29	35.16 ± 0.19	37.11 ± 0.44

The percentage of PUFA, Total UFA, and MUFA for OR are in the range of the previous RFO authentication results by Rohman et al.[2] and Sarungallo et al.[3] In addition, the PUFA, Total UFA, and MUFA of OVO and BSO products are also in accordance with the value of their product claims.

Considering the good accuracy and reliability of the PUFA, Total UFA, and MUFA results for this calibration sample set, so these results can be used as a model to classify and predict PUFA, Total UFA, and MUFA in other RFO samples (prediction test / **Table 1**) by chemometric.[23]

3.2. Spectral data for multivariate analysis

As explained in the previous section, the signal at δ = 2.80 - 2.71 ppm and δ = 2.10 - 1.90 ppm were selected for the classification and prediction of PUFA, Total UFA, and MUFA. For this reason, **Figure 4** displays the results of a bucketing process of all samples ^{1}H NMR spectra. The bucketing process by bucket width 0.009 ppm gave satisfactory results, including the reliability of the chemical shift and the signal intensity, because they were the same as in the original spectra for each sample (enlarged). It is obtained by summing up the intensities inside each bucket so that every area from the signal spectrum is used instead of the individual intensity.[26] This methodology was effectively applied in some publications dealing with gingko and wine preparations.[27,28]

As can be seen in **Figure 4**, differences in signal intensity at δ = 2.80 - 2.71 ppm (H) can be observed, which correlates to PUFA content. Likewise, the signal at δ = 2.10 - 1.90 ppm (D) also shows a variation in intensity correlating with Total UFA.[16] Based on these findings, two ^{1}H NMR variable matrices will be used to delineate classes and predict PUFA (-CH=CH-C<u>H</u>$_2$-CH=CH-) and Total UFA (-C<u>H</u>$_2$-CH=CH-). It consists of 120 lines (sample spectra) and 11 variables (relative intensity) for PUFA and 120 lines (sample spectra) and 23 variables (relative intensity) for Total UFA, respectively.

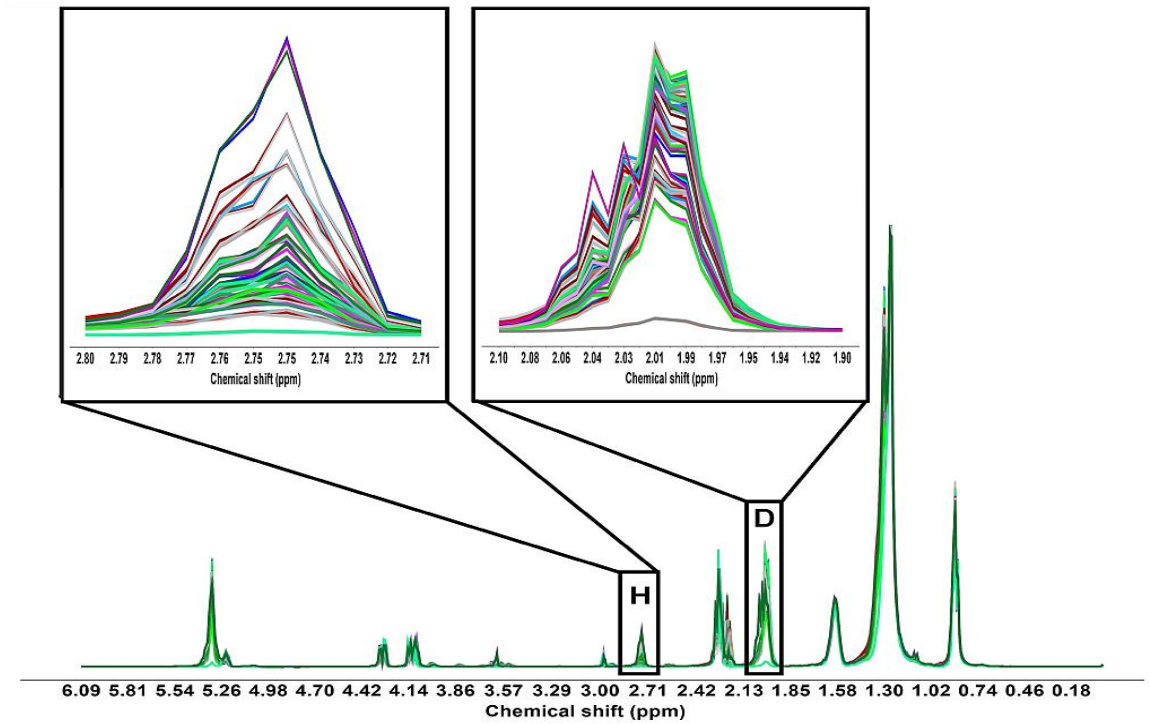

Figure 4. Bucketing results of all ^{1}H NMR spectra samples (δ = 0.00 -6.70 ppm) with enlargement spectral range at δ = 2.80 - 2.71 ppm (H) and δ = 2.10 - 1.91 ppm (D). The spectra are color-coded to the brand.

3.3. PCA for visualization grouping PUFA and Total UFA

Based on the calculation of PUFA and Total UFA content using a calibration model (**Table 3**), all sample spectra can be categorized based on their respective value range, which consist of <1, 5-10, 10-20, 20-25, 25-30, and >30 for PUFA and <10, 30-40, 40-50, 60-70 and 70-90 for Total UFA. As shown in the PCA results (**Figure 5** and **Figure 6**), the OVO, VCO, and BSO used for the comparison and as OR adulterant (ORVO, ORCO, ORSO) in the calibration model. It aims to provide an overview of the variable matrix changes in OR because of the oil adulterant effect. These results can provide a visualization grouping pattern that follows the PUFA content for each RFO product and can be one of the parameters for characterization and authentication.

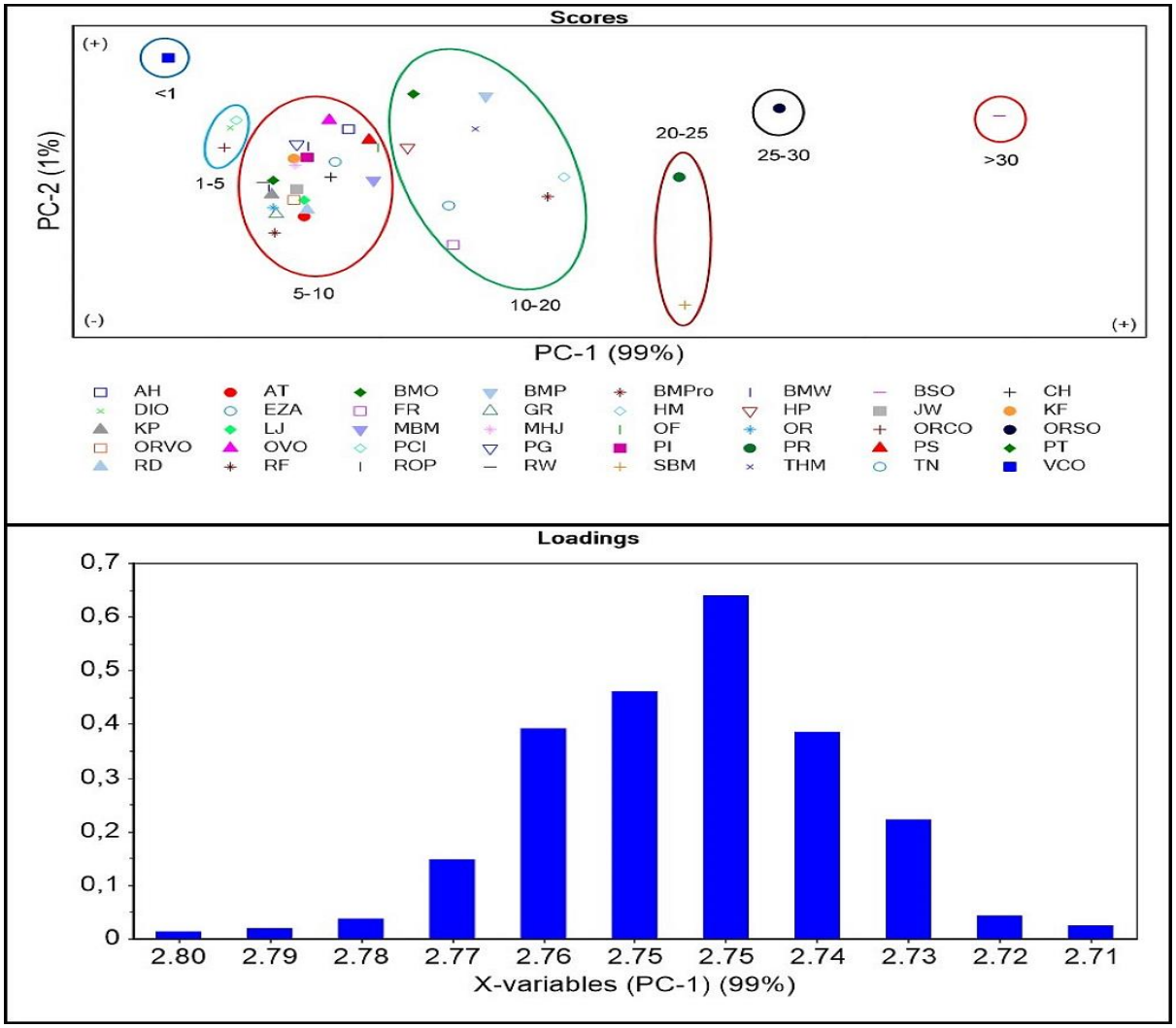

Figure 5. Plot score classification of all samples (120 spectra) on the main components (PC1 and PC2) and loading plot X-variable (PC1) on the selected signal ^{1}H NMR spectra based on the PUFA value category.

For PUFA, the PCA score plot performed for all samples was successfully described with 99% X-variable variance (see **Figure 5** and all PCA model analyses presented in **Figure S2-** Supplementary Information): BSO and ORSO on the farthest positive PC1 axis, respectively. These results reveal the effect of varying the intensity of the -CH=CH-C$\underline{H}_2$-CH=CH- signal (δ = 2.80 – 2.71 ppm) due to high PUFA content, these is in line with previous research.[29] According to the literature, BSO has a high linoleic acid content (approximately 50%).[30]

VCO (<1) is separated far from BSO; this indicates the difference in the intensity of the two matrix variables due to PUFA content. These results imply that VCO has almost no PUFA (see

Table 3), as previously reported by Suryani et al.[31] Similarly, sample groups that contained VCO were also located close to VCO (PCI, DIO, and ORCO) (1-5). Interestingly, most RFO products gave the same plot score as OVO and ORVO, located between the VCO and BSO score plots. According to Rohman et al.[2] and Sarungallo et al.[3] most RFOs have minimal PUFA and most fatty acid components are oleic acid (MUFA). The crude RFO contains about 4-10% PUFA.

Furthermore, 11 RFO products were successfully classified into sample group that had PUFA values more than OR, including BMP, BMPro, FR, HM, HP, PT, THM, and TN (10-20), followed by PR and SBM (20-25). This points to the fact that another oil with high PUFA content has been added to RFO products, for example, BSO, which is commonly added in some edible oils. This is confirmed by the finding that these products are also located closer to the ORSO and BSO score plot. Finally, these results indicate that the composition of PUFA in the sample can be grouped well into seven categories (<1, 1-5, 5-10, 10-20, 20-25, 25-30, and > 30). This finding shows that this PCA model is effective and fast for authentication and visualization of grouped RFO products' quality based on their PUFA values.

The PCA score of Total UFA displays a visualization grouping pattern different from PUFA (see **Figure 6** and all PCA model analyses presented in **Figure S3**- Supplementary Information). BSO is located on the farthest negative PC2, and VCO is on the farthest negative PC1, whereas most RFO products have the same score plot as OVO, the farthest positive PC1 and PC2. These results prove that the Total UFA content of most RFO products oils is similar to OVO, where the total UFA value of OVO ranges from 70 to 90%.[32] In addition, these results indicate that VCO and BSO as oil adulterants can be successfully classified differently from most RFO products. Both oils have a Total UFA values different from OVO and OR. According to Suryani et al.[31] VCO is dominated by saturated fatty acids (SFA) and contains almost no UFA. Whereas the Total UFA of BSO was lower than that of OR and OVO[30] and is reported to be 60-80% Total UFA, crude RFO contains about 70-90% of Total UFA.[2,3]

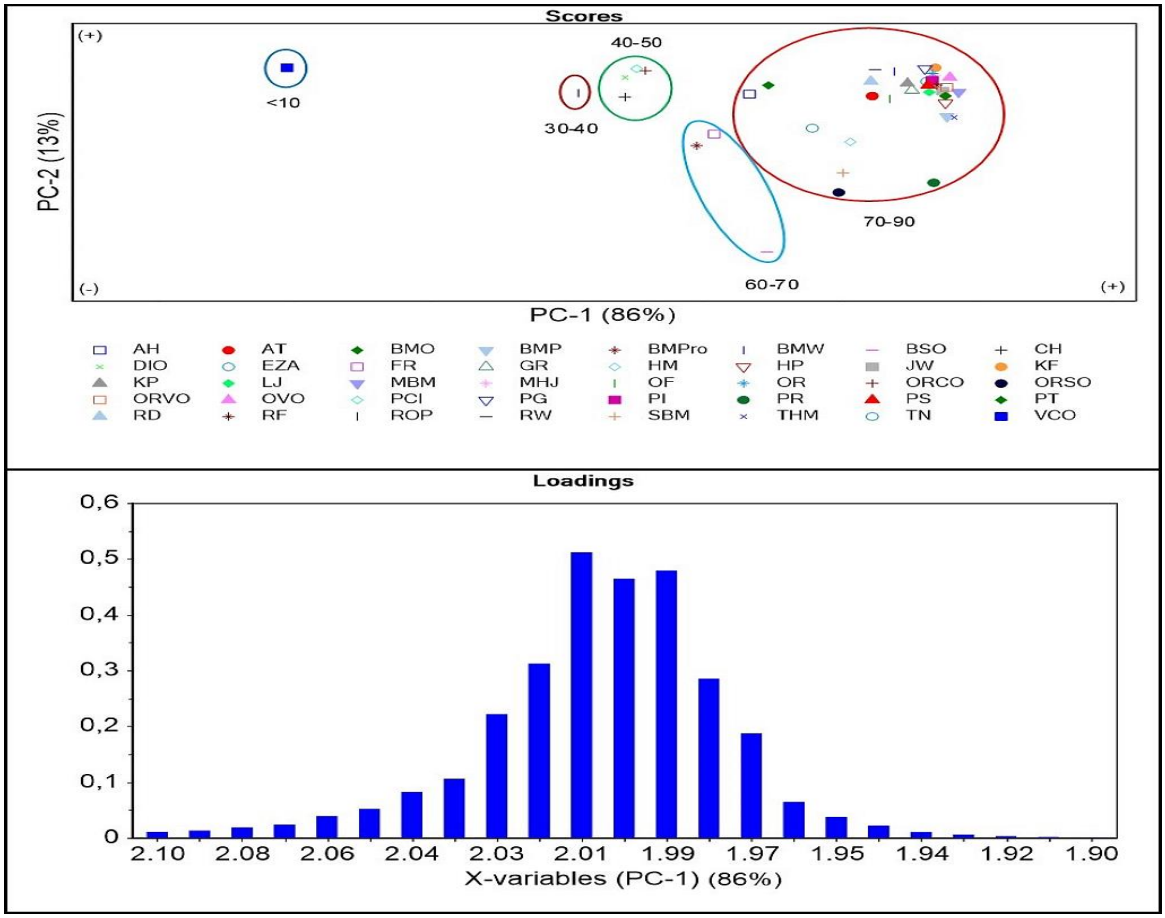

Figure 6. Plot score classification of all samples (120 spectra) on the main components (PC1 and PC2) and loading plot X-variable (PC1) on the selected signal ^{1}H NMR spectra based on the Total UFA value category.

In fact, HM, ORSO, PR, and SBM are closer to the BSO score plot, even if in different categories of Total UFA value, indicating that the Total UFA value of these oils is lower than OR because of the presence of BSO, although this is not significant. On the other hand, BMPro and FR are located in the same Total UFA value category as BSO although they are relatively far from each other. These results can be caused by the fact, that the Total UFA value for BMPro and FR is significantly lower than for OR, which was influenced by the presence of BSO and VCO.

Subsequently, five products (ORCO, DIO, CH, PCI, and ROP) can be classified as close to the VCO score plot with a Total UFA value lower than OR, OVO, and BSO, indicating that some RFO products have been contaminated with other oils containing a higher amount of

SFA (VCO). This results in a reduction of the relative PUFA and MUFA value in RFO, which additionally causes the Total UFA value to decrease. This can be derived from the PUFA and MUFA values of ORCO in **Table 3**. Finally, the total PC formed 99%, with the x-variable (PC1) 86% of the variance explained. These results demonstrated that the visualization of grouped RFO based on Total UFA could disclose adulteration of RFO products with other oils, so this finding also proves useful for authentication.

3.4. PLS for prediction of PUFA, Total UFA and MUFA

The possibility of predicting PUFA, Total UFA, and MUFA content from ^{1}H NMR spectra was investigated, considering their importance to human health and their predominance in RFO. PLS performed well on the ^{1}H NMR spectra in the two selected matrices of variables (**Table 4**), with a total number of corresponding variables of 99% (all PLS model analyses presented in **Figure S4**-**S9**- Supplementary Information). The PLS models were compared in terms of error in calibration (RMSEC), cross-validation (RMSECV), and error of prediction (RMSEP).[23]

Table 4 Results of PLS modeling and prediction of PUFA, Total UFA, and MUFA

Parameter	Spectral range (ppm)	Value	Factor	R^2			Root Mean Square Error (RMSE)		
				Calibration	Validation	Prediction	Calibration	Validation	Prediction
PUFA	2.80-2.71	0-32	1	0.994	0.992	0.930	0.60	0.66	1.35
Total UFA	2.10-1.90	0-90	1	0.963	0.962	0.963	3.87	3.99	3.74
MUFA	2.10-1.90	0-85	2	0.970	0.969	0.955	3.33	3.49	3.10

Based on the results, the low error in the calibration, validation, and prediction model in addition to good correlation coefficients for all three shows that the model can be used to predict PUFA, total UFA, and MUFA with high accuracy. Furthermore, the ^{1}H NMR data showed valid results in determining the number of PUFA, Total UFA, and MUFA in each RFO sample (all PLS model analyses presented in **Figure S4**-**S9**- Supplementary Information). Therefore, the prediction of PUFA, Total UFA, and MUFA compositions suitable for VCO, OVO, BSO, and OR can indicate the potential authenticity of an RFO product or the presence or absence of adulterants as the addition of other oils on purpose, as has been discussed by Giese et al.[33] for cod oil and Ravaglia et al.[29] for edible oils.

It should also be emphasized that the quantitative ^{1}H NMR using a standard internal can be performed significantly faster. In addition, the association with chemometrics makes the process more efficient. The proposed quantitative ^{1}H NMR method is promising. However, further method developments should be carried out using more samples and extended to other oil matrices to obtain a more robust model.

4. Conclusion

With a standard internal calculation approach, ^{1}H NMR spectroscopy can determine PUFA, Total UFA, and MUFA on the RFO. The signals at δ = 2.80-2.71 ppm, corresponding to the -CH=CH-C<u>H</u>$_2$-CH=CH- signal, and at δ = 2.10 - 1.90 ppm, associated with the -C<u>H</u>$_2$-CH=CH- group, were included in the models for the determination of PUFA, Total UFA and MUFA, respectively. Furthermore, combining ^{1}H NMR spectroscopy and chemometrics using PCA effectively grouped RFO products based on the PUFA and Total UFA categories. In addition, the PLS model successfully predicted the PUFA, Total UFA, and MUFA content in each RFO product. This quick and easy procedure can be used routinely for quality monitoring and authentication of RFO products, mainly based on their unsaturated fatty acid components.

Acknowledgements

The authors would like to thank the supporting finance of Lambung Mangkurat University (Grant No. 3894/UN8/KP/2019) and Institut for Pharmacy and Food Chemistry, Wuerzburg University, Germany for the resources. The authors warmly thank Dr. Jens Schmitz, Dr. Alexander Becht for their technical support during the study as well as Dr. Ludwig Höllein for editorial support during writing and preparation for submission this publication.

Conflict of Interest

The authors declare no conflict of interest.

Author Contributions

L.T.: Conceptualization, Methodology, Validation, Formal analysis, Investigation, Data curation, Writing – original draft, Visualization. C.S.: Methodology, Data curation, Visualization, Writing – review & editing. U.H.: Supervision, Conceptualization, Methodology, Writing – review & editing, Funding acquisition and resources.

Ethic Statement

Our research did not include any human subjects or animal experiments.

Data Availability Statement

The data that supports the findings of this study are available in the supplementary material of this article.

References

[1] M. Dimitriou, L.S. Rallidis, E.V. Theodoraki, I.P. Kalafati, G. Kolovou, G.V. Dedoussis, *Public Health Nutr*. 2016, 1081,19.

[2] A. Rohman, S. Riyanto, Y.B. Che Man, *Int. Food Res. J*. 2012, 563,19.

[3] Z. L. Sarungallo, P. Hariyadi, N. Andarwulan, E. H. Purnomo, *J. Natural Sci*. 2015, 237, 49.

[4] H.H. Chiu, C.H. Kuo, *J. Food Drug Anal*. 2020, 60, 28.

[5] B. Li, H. Wang, Q. Zhao, J. Ouyang, Y. Wu, *Food Chem*. 2015, 25, 181.

[6] A. Rohman, Y.B. Che Man, A.F. Nurrulhidayah, *Int. J. Food Prop*. 2015, 1086, 18.

[7] J.S. Amaral, S.C. Cunha, M.R. Alves, J.A. Pereira, R.M. Seabra, B.P.P. Oliveira, *J Agric Food Chem*. 2004, 7964, 52.

[8] J. Qian, C. Zhao, H. Zhu, J. Tong, X. Zhao, H. Yang, H. Guo, *J Food Meas. Charact*. 2021, 2716, 15.

[9] M. Elyashberg, *TrAC Trends Anal. Chem*. 2015, 88, 69.

[10] R. Sacchi, F. Addeo, L. Paolillo, *Magn. Reson. Chem*. 1997, 133, 35.

[11] G. Knothe, J. A. Kenar, *Eur. J. Lipid Sci. Technol*. 2004, 88, 106.

[12] L. Triyasmono, C. Schollmayer, J. Schmitz, E. Hovah, C. Lombo, S. Schmidt, U. Holzgrabe, *Food Anal. Methods*. 2022, 1.

[13] G. Vigli, A. Philippidis, A. Spyros, P. Dais, *J. Agric. Food Chem*. 2003, 5715, 51.

[14] A. Barison, C.W. da Silva, F.R. Campos, F. Simonelli, C.A. Lenz, A.G. Ferreira, *Magn Reson Chem*. 2010, 642, 48.

[15] D. Castejón, P. Fricke, M. I. Cambero, A. Herrera, *Nutrients*. 2016, 1, 8.

[16] J. R. Hama, V. Fitzsimmons-Thoss, *Food Anal. Methods*. 2022, 1,1.

[17] J. Sedman, L. Gao, D. García-González, S. Ehsan, F.R. van de Voort, *Eur. J. Lipid Sci. Technol*. 2010, 439, 112.

[18] C. Ingallina, A. Cerreto, L. Mannina, S. Circi, S. Vista, D. Capitani, F. Marini, *Metabolites*. 2019, 1, 9.

[19] U. Holzgrabe, *Prog. Nucl. Magn. Reson. Spectrosc*. 2010, 229, 57.

[20] V. Thoss, P.J. Murphy, R. Marriott, T. Wilson, *RSC Adv*. 2012, 5314, 2.

[21] S.K Bharti, R. Roy, *TrAC- Trends. Analyt. Chem*. 2012, 5, 35.

[22] C. Skiera, P. Steliopoulos, T. Kuballa, B. Diehl, U. Holzgrabe, *J. Pharm. Biomed. Anal*. 2014, 43, 93.

[23] T. Schönberger, Y. B. Monakhova, D. W. Lachenmeier, S. Walch, T. Kuballa, *Guide to NMR Method Development and Validation-Part II: Multivariate data analysis*. EUROLAB Technical Report 01/2015, Brussels. 2015.

[24] E. Alexandri, R. Ahmed, H. Siddiqui, M. I. Choudhary, C. G. Tsiafoulis, I. P. Gerothanassis, *Molecules*. 2017, 2, 22, 1663.

[25] M. D. Guillén, A. Ruiz, *Eur. J. Lipid Sci. Technol*. 2003, 502, 105.

[26] R.H. Jellema, in*: Comprehensive Chemometrics,* Vol. 2 (Eds: S.D. Brown, R. Tauler, B. Walczak), Elsevier, Oxford 2009, Ch. 2.06.

[27] S. Agnolet, J.W. Jaroszewski, R. Verpoorte, D. Staerk, *Metabolomics*. 2010, 292, 6.

[28] L. Jang-Eun, H. Geum-Sook, V.D.B. Frans, L. Cherl-Ho, H. Young-Shick, *Anal. Chim. Acta*. 2009, 71, 648.

[29] L. M. Ravaglia, A. B. C. Pizzotti, G. B. Alcantara, *J. Food Sci. Technol*. 2019, 507, 56.

[30] H. Lutterodt, M. Luther, M. Slavin, J.J. Yin, J. Parry, J.M. Gao, L. Yu, *LWT - Food Sci. Tech*. 2010, 1409, 43.

[31] S. Suryani, S. Sariani, F. Earnestly, M. Marganof, R. Rahmawati, S. Sevindrajuta, A. Fudholi, *Processes*. 2020, 1, 8.

[32] M. El Riachy, A. Hamade, R. Ayoub, F. Dandachi, L. Chalak, *Front in Nutr*. 2019, 1, 6.

[33] E. Giese, S. Rohn, J. Fritsche, *Bioanal. Chem*. 2019, 6931, 411.

Quantitative ^{1}H NMR Spectroscopy Combined with Chemometrics as a Profiling and Estimation Tool for Unsaturated Fatty Acid Composition in Red Fruit Oil and its commercial products

Liling TRIYASMONO[1,2], Curd SCHOLLMAYER[1], Ulrike HOLZGRABE[1,*]

[a]Institute for Pharmacy and Food Chemistry, University of Würzburg, , 97074 Würzburg, Germany

[b]Department of Pharmacy, Faculty of Mathematics and Natural Sciences, Lambung Mangkurat University, 70713 Banjar Baru, Indonesia

SUPPLEMENTARY INFORMATION

Table of content

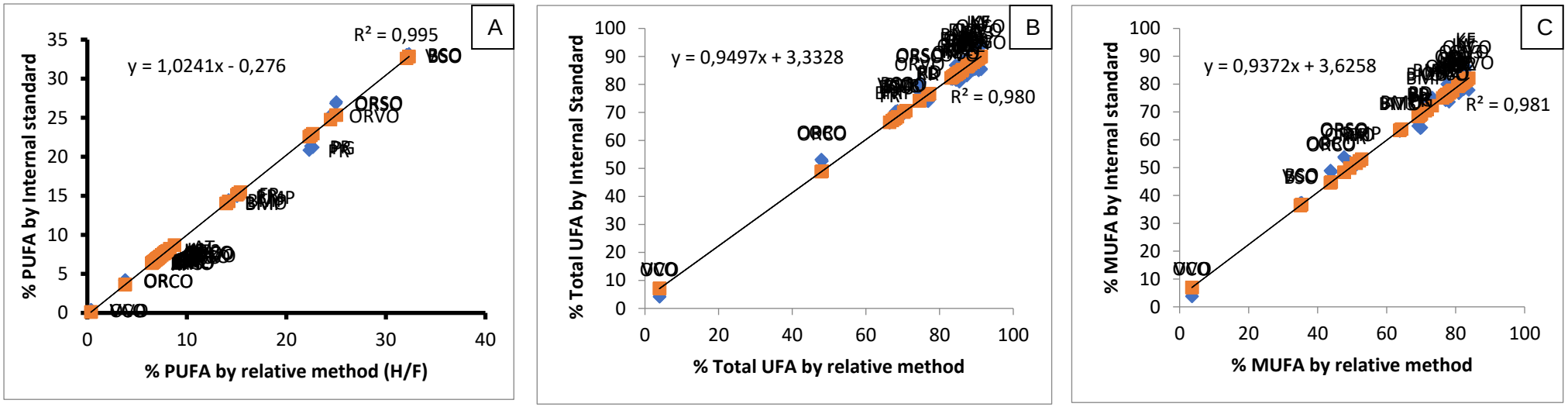

Figure S1. Plot score regression analysis between calculation by relative method vs internal standard method. (A) % PUFA, (B) % Total UFA. (C) % MUFA.

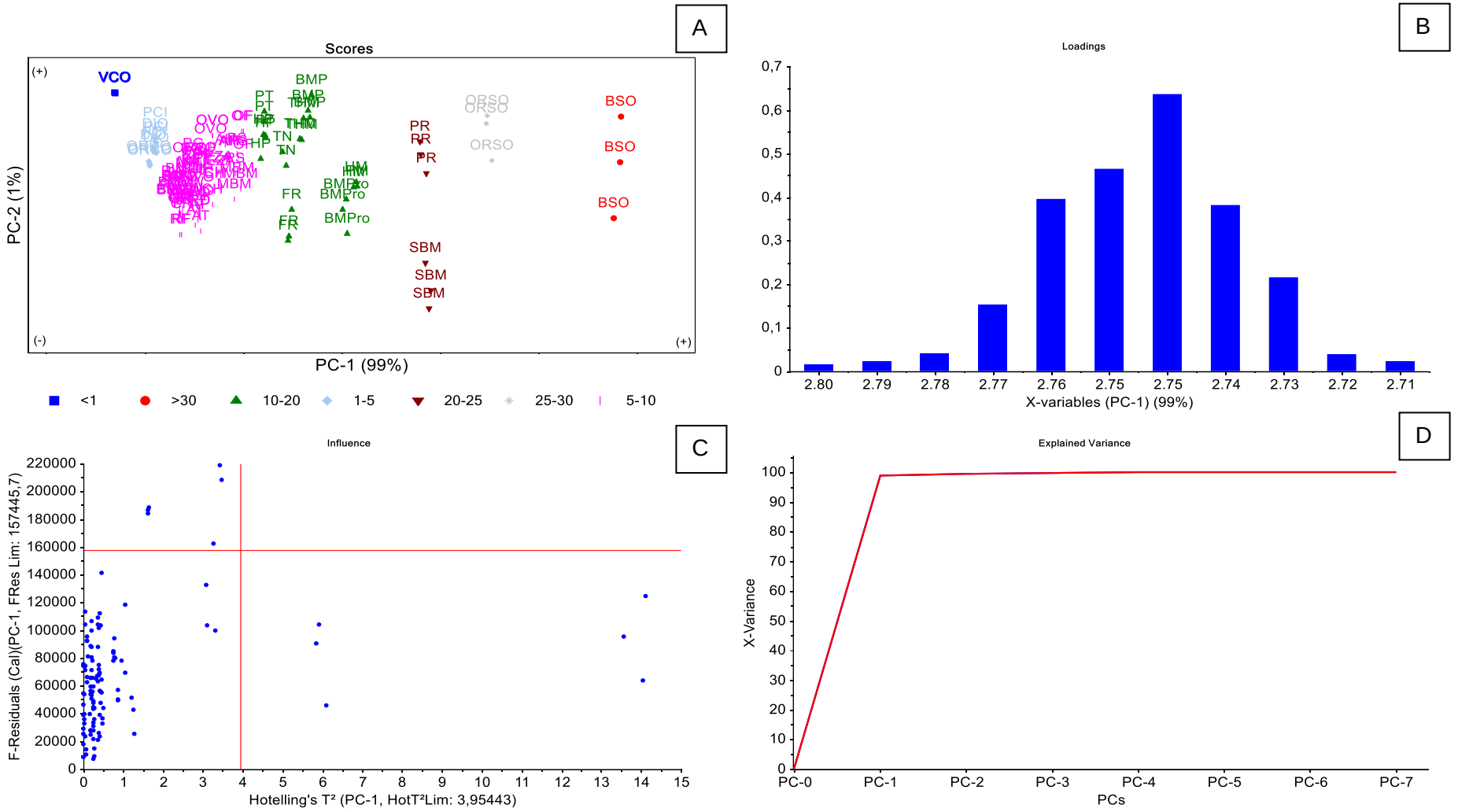

Figure S2 (A) Score Plot classification PC1 vs. PC2 of selected signal NMR data; (B) Plot of X-Loading with axis X-Variables (PC1) (2.80-2.71 ppm); (C) Plot Hotelling's T^2; (D) Plot Explained variance vs. PC-0 to PC-7 (calibration and validation)

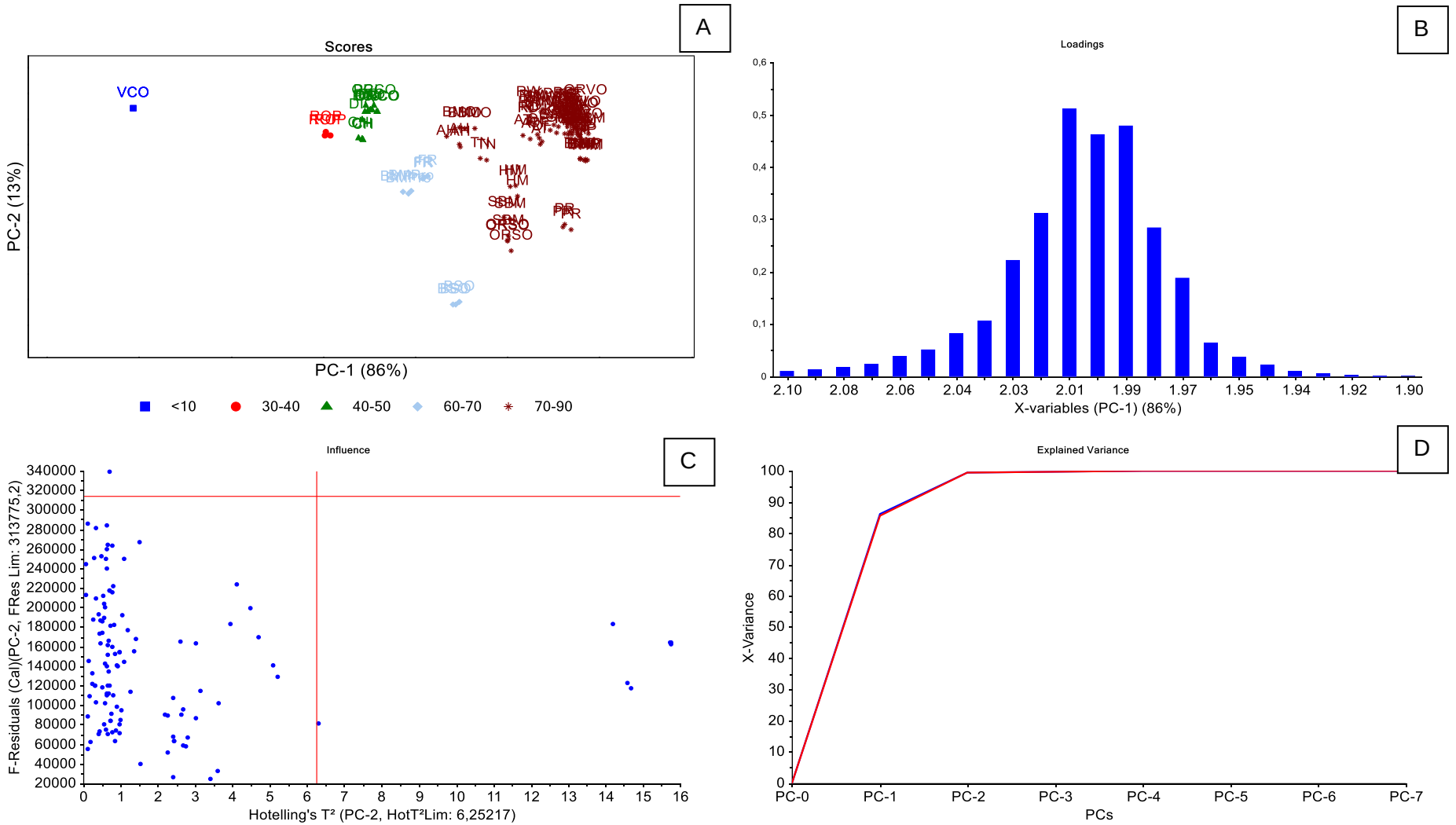

Figure S3 (A) Score Plot classification PC1 vs. PC2 of selected signal NMR data; (B) Plot of X-Loading with axis X-Variables (PC1) (2.10-1. (C) Plot Hotelling's T^2; (D) Plot Explained variance vs. PC-0 to PC-7 (calibration and validation)

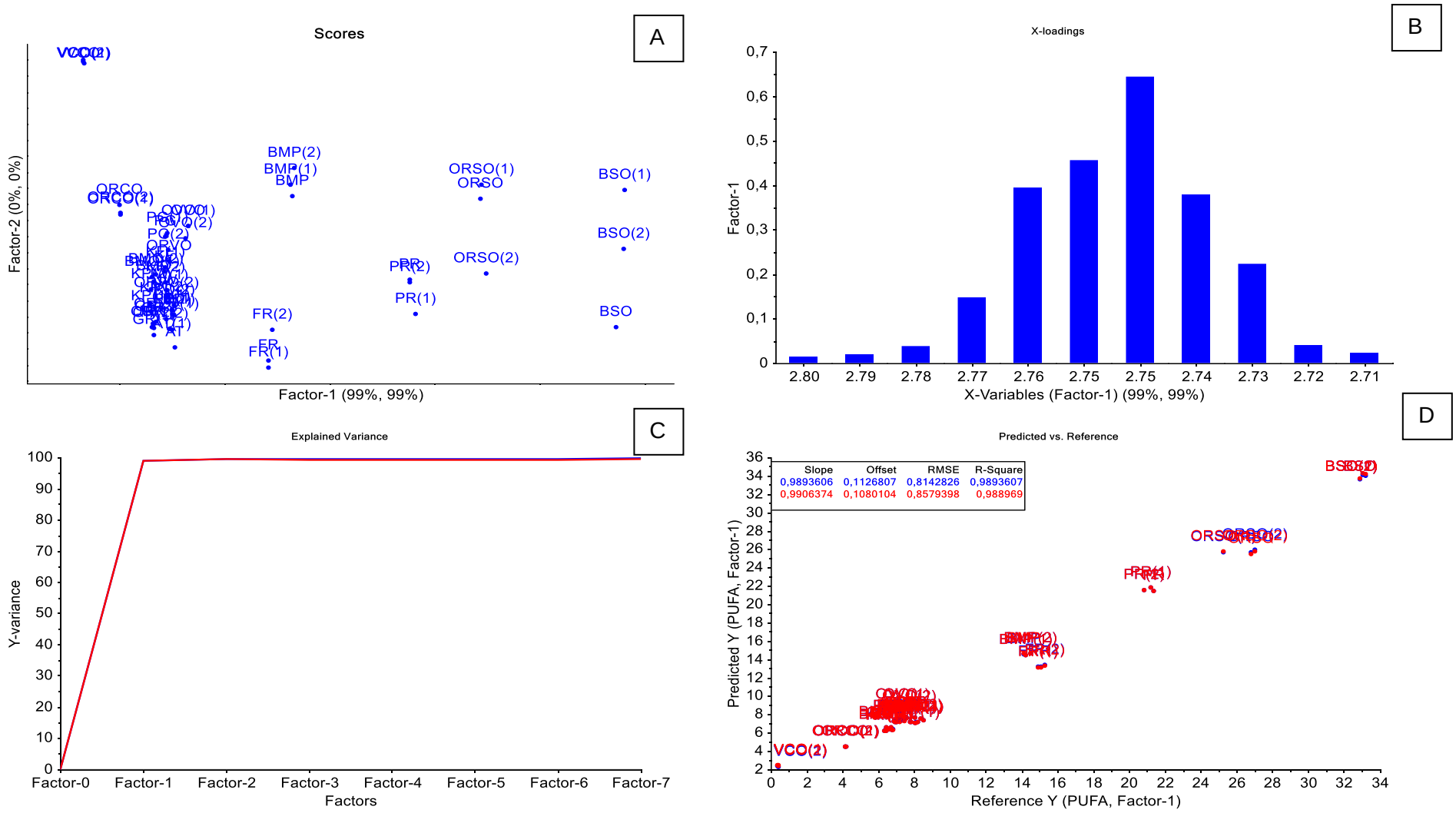

Figure S4 PLS calibration analyses for the PUFA composition on NMR data. (A) Score Plot Factor 1 vs. Factor-2 of selected signal NMR data; (B) Plot of X-Loading with axis X-Variables (Factor-1) (2.80-2.71 ppm); (C) Plot Explained Variance Factor-0 - 7 to Y-variance; (D) Plot Predicted vs. Reference Y from Factor-1 of the PUFA composition

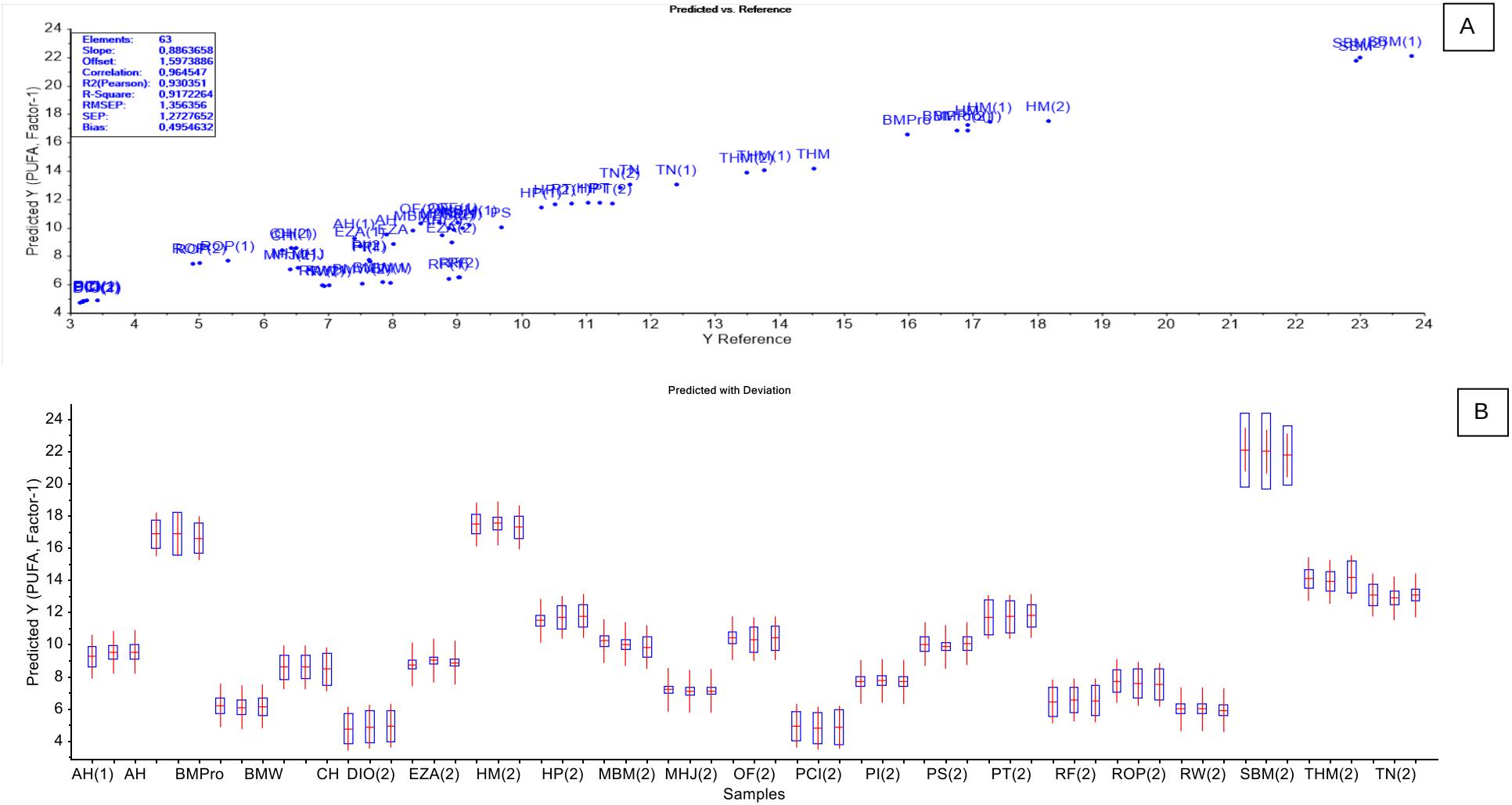

Figure S5 (A) Plot Predicted vs. Y Reference of the degree of unsaturation on the sample (prediction set) with calibration model **Figure S4** D (NMR); (B) Plot Predicted Y with a deviation of samples (Prediction test)

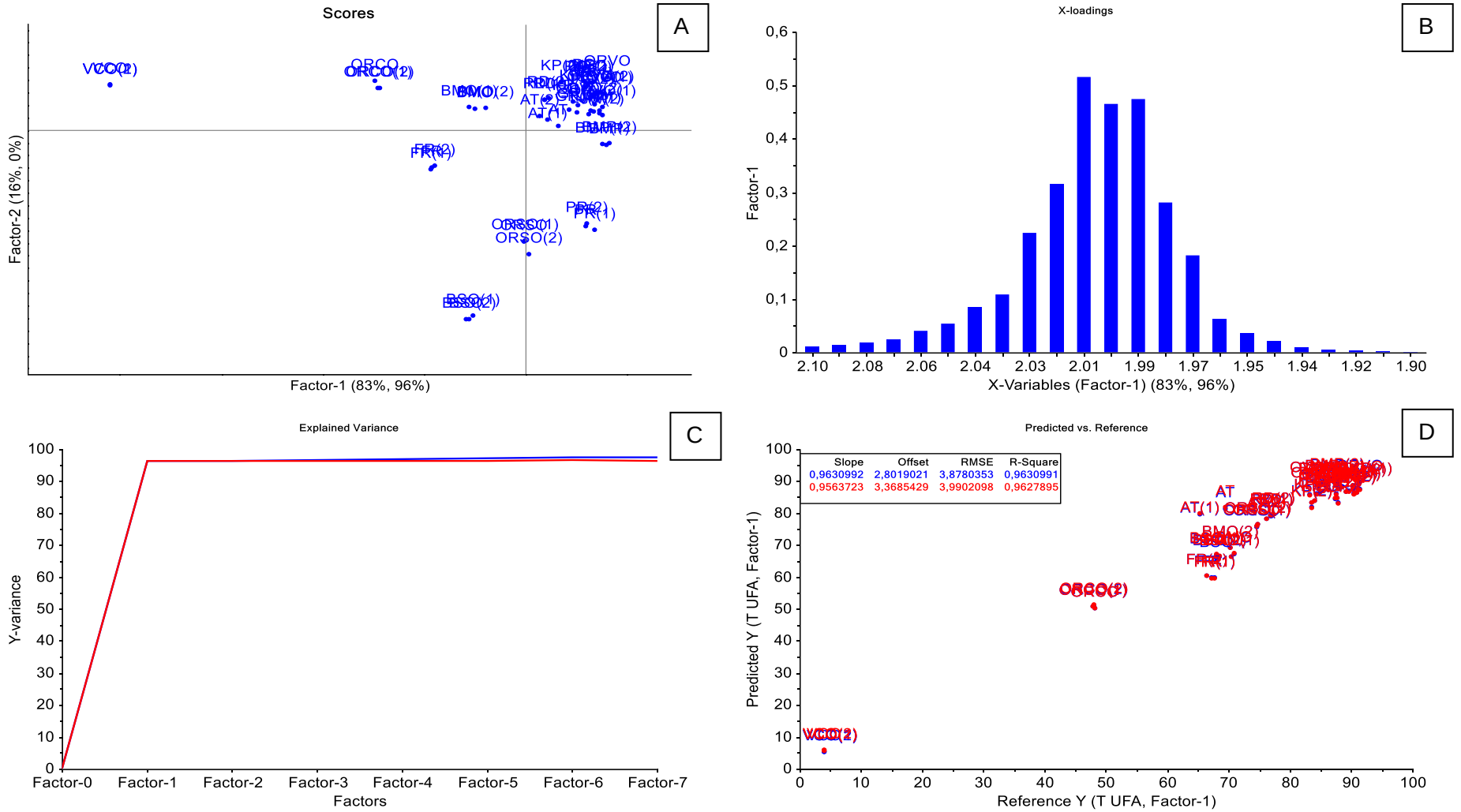

Figure S6 PLS calibration analyses for the total UFA composition on NMR data. (A) Score Plot Factor 1 vs. Factor-2 of selected signal NMR data; (B) Plot of X-Loading with axis X-Variables (Factor-1) (2.10-1.90 ppm); (C) Plot Explained Variance Factor-0 - 7 to Y-variance; (D) Plot Predicted vs. Reference Y from Factor-1 of the total UFA composition

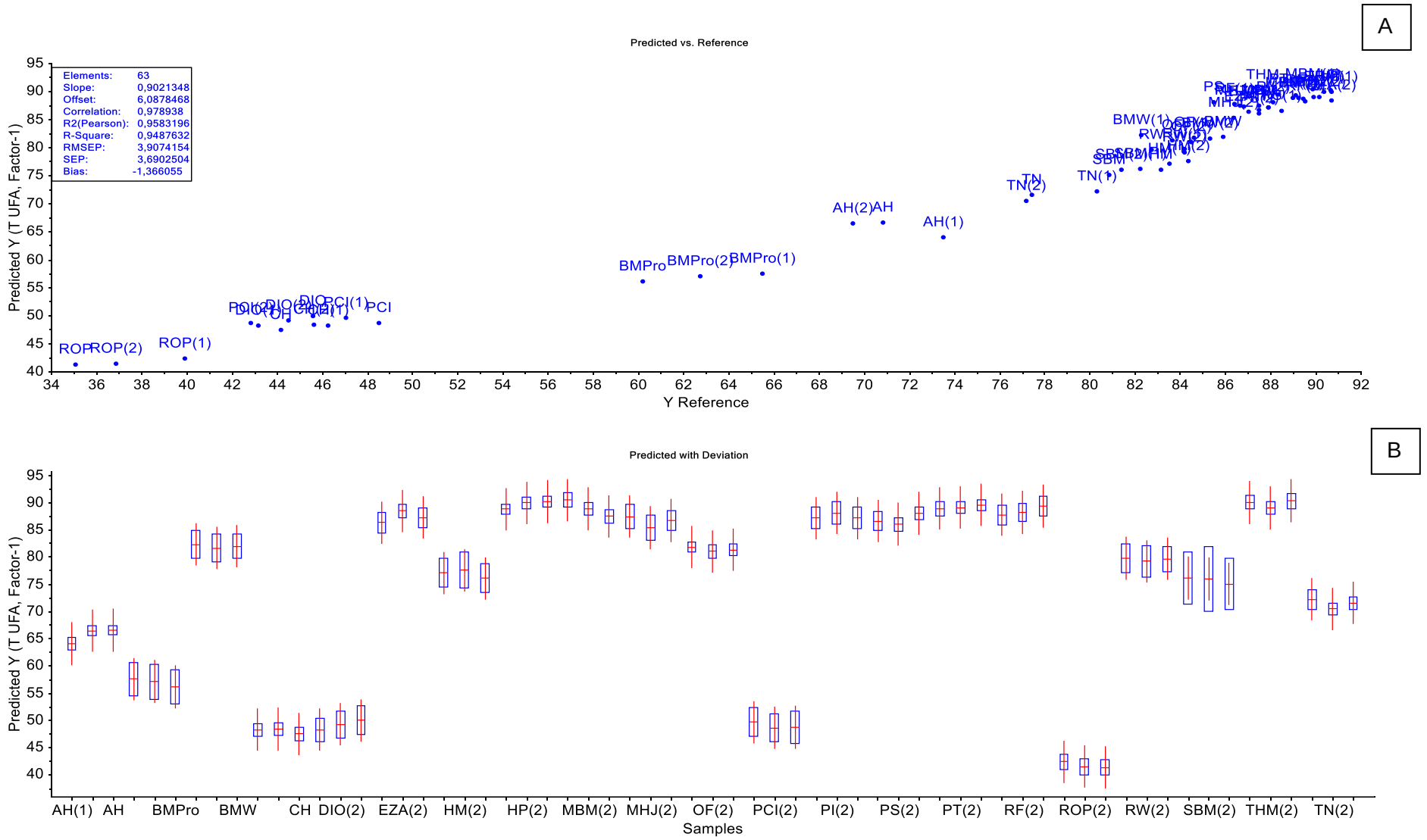

Figure S7 (A) Plot Predicted vs. Y Reference of the degree of unsaturation on the sample (prediction set) with calibration model **Figure S6** D (NMR); (B) Plot Predicted Y with a deviation of samples (Prediction test)

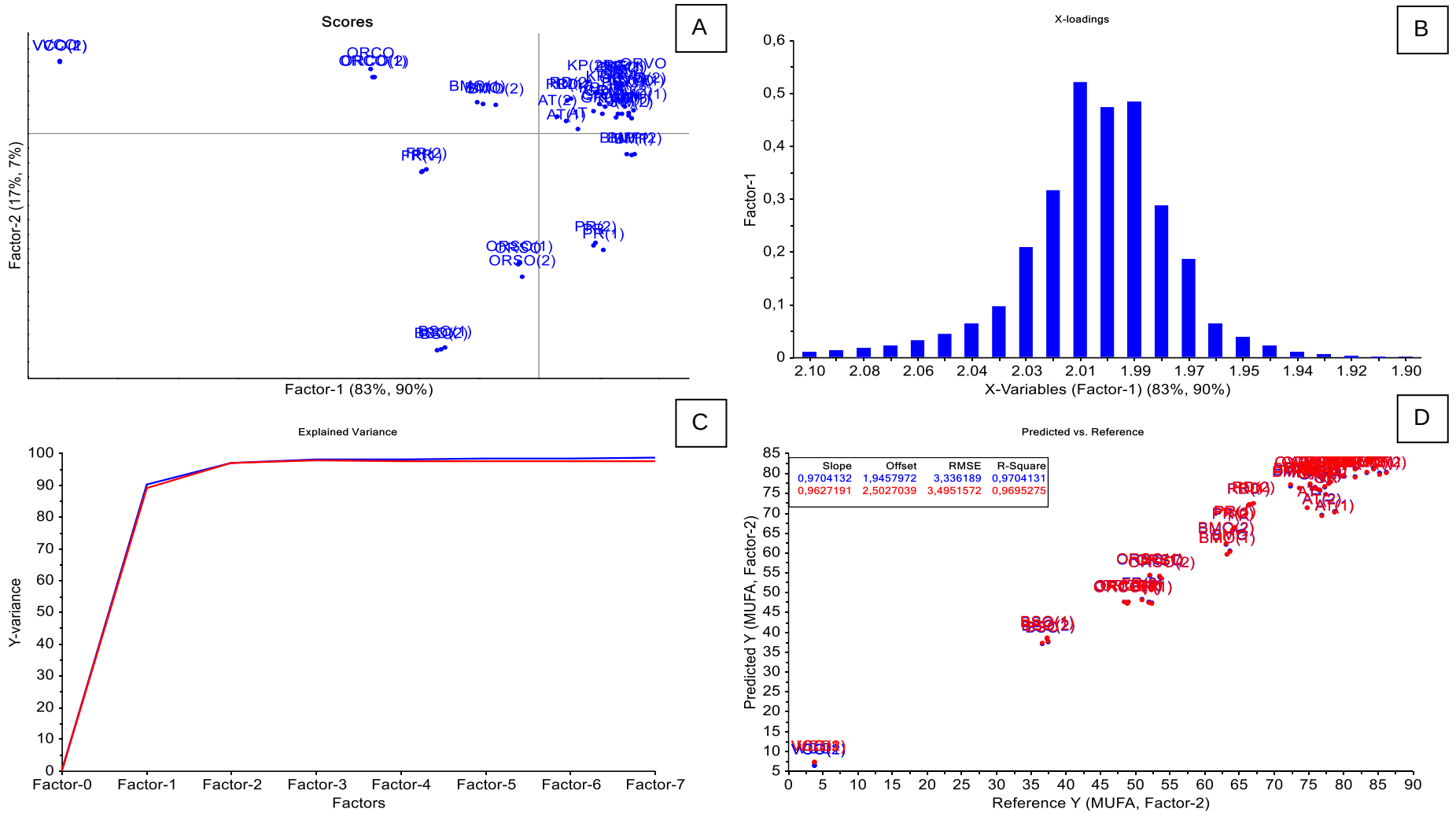

Figure S8 PLS calibration analyses for the MUFA composition on NMR data. (A) Score Plot Factor 1 vs. Factor-2 of selected signal NMR data; (B) Plot of X-Loading with axis X-Variables (Factor-1) (2.10-1.90 ppm); (C) Plot Explained Variance Factor-0 - 7 to Y-variance; (D) Plot Predicted vs. Reference Y from Factor-2 of the MUFA composition

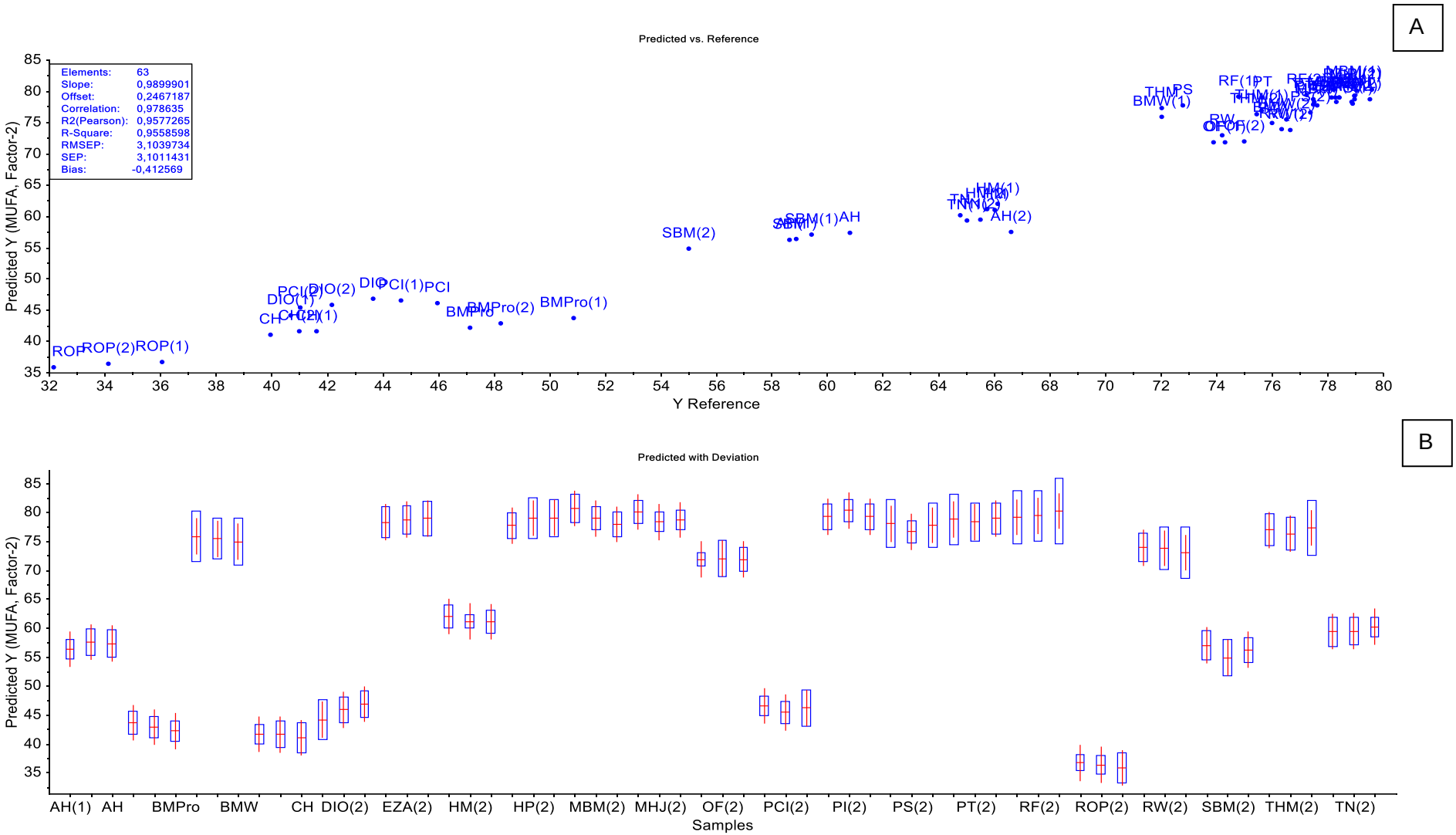

Figure S9 (A) Plot Predicted vs. Y Reference of the degree of unsaturation on the sample (prediction set) with calibration model **Figure S8** D (NMR); (B) Plot Predicted Y with a deviation of samples (Prediction test)

4. FINAL DISCUSSION

The main idea of this thesis was to examine the quality of the oil by measuring the quantitative ^{1}H NMR spectrum so that it can replace or make an alternative to conventional methods used in pharmaceutical and food chemical analysis without losing precission and accuray, especially in the oil of red fruits (RFO).

4.1 Simultaneous determination of the Saponification Value, Acid Value, Ester Value, and Iodine Value in commercially available Red Fruit Oil (*Pandanus conoideus*, Lam.) using ^{1}H qNMR spectroscopy

Conventionally, the saponification value (SV) and the acid value (AV) are determined by the acid-base titration method; the ester value (EV) is calculated from these two values. Such titration methods rely on observing visual endpoints, which may be difficult, especially in the case of red fruit oil (RFO), where the solution is already red. The iodine number (IV) is generally used to estimate the degree of unsaturation of oils and fats. This determination is based on the addition of monoiodine bromide to the double bond reaction in fatty acids. This procedure consists of several steps and is also time-consuming.

Based on the results that have been obtained, the ^{1}H NMR method has succeeded in answering problems, including the selection of the ^{1}H NMR quantitative method using internal standards, which is able to provide valid and satisfactory results. The primary step taken with selecting $DMSO_2$ as the internal standard is the right choice because its signal at = 2.98 ppm does not overlap with sample and/or solvent components. It is close to the analyte's resonance, thus minimizing the impact of pulse resonance.[1,2] Furthermore, $DMSO_2$ can be easily obtained with high purity and has good stability and solubility in the solvent system.[3] A good signal separation was achieved using a mixture of $CDCl_3$ and DMSO-d_6 (5:1, v/v) because the specific protons of the methylene -CH_2 group at = 2.37-2.27 ppm and 2.27-2.20 ppm are visible. The beneficial effect of adding DMSO-d_6 to $CDCl_3$ is the NMR complex formation between DMSO and the fatty acid moiety.[4,5]

The triplets of the α-CH_2 signals at δ = 2.27-2.20 ppm of the FFA are slightly high field shifted in comparison to the corresponding signal of TAG which is a multiplet. This is in accordance with the data reported by Nieva-Echevarría et al.[6] and Kan et al.[7] Comparison of ^{1}H NMR spectra between RFO, oleic acid, and palmitic acid standards were carried out to confirm the signal (-CH=CH-) assignment to IV calculation because there is a linear relation between IV and the number of olefinic protons.[8] The -CH=CH- signals resonate at δ = 5.37-5.27 ppm in both RFO and oleic acid.

The method's robustness also shows satisfactory results, as evidenced by the results of the validation that meet the requirements based on the ICH guidelines. Furthermore, the strong correlation between the determined value of the classical method and the ^{1}H NMR method with an R^2 value > 0.98 and a small error indicates that the accuracy and precision of the NMR method are high.

4.2 The chemometric analysis of ^{1}H NMR and FT-IR spectra data for a quality parameters distinction of Red Fruit Oil products.

For multivariate data analysis, it is mandatory to have a sample preparation that generates reproducible spectra. Spectra preprocessing technique is essential to get a reliable variable matrix. Appropriate preprocessing of the spectra was obtained by bucketing for NMR spectra and second-order smoothing polynomials through 25 points (Savitzky-Golay method) without spectra derivation for FTIR spectra. The essential signals for modeling the degree of unsaturation are the signal at δ= 5.37–5.27 ppm (^{1}H NMR) and the band at 3000-3020 cm^{-1} (FTIR). The FFA profile is represented by the signal at δ= 2.37-2.20 ppm (^{1}H NMR) and the band at 1680-1780 cm^{-1} (FTIR), respectively.

PCA allows the visualization grouping of both methods with > 98% for the degree of unsaturation and > 88% full PC for FFA values. Unfortunately, PCA projections on FTIR show a significant grouping variability, for example, the distance differences between product replication. The lower reproducibility observed in the FTIR results depends on the manual

placement of the sample on the diamond cell ATR unit, as has been discussed by Jovic et al.[9] Therefore, the triple clustering projection for FTIR shows unsatisfactory results. It is important to emphasize that replicate clustering is preferable when ^{1}H NMR is used.

In addition, the PLSR model provides an acceptable coefficient of determination (R^2) and errors in calibration, prediction, and cross-validation. The performance results indicate that both parameters show a good match based on the R^2 (coeffisien of determenitaion) and RMSEC for each model lower than SEP.[10] Furthermore, at least 92% of the variation of the output variable can be explained by the ^{1}H NMR and FTIR spectra. Therefore, ^{1}H NMR replication is more promising and proven to determine the difference between each RFO product based on the degree of unsaturation and the FFA value. These findings support several previous reports[11-14] on the success of ^{1}H NMR spectroscopy in analyzing fat and oil quality parameters.

The spectra profiled by ^{1}H NMR and FTIR and chemometric analysis contributed to the visualization grouping of RFO based explicitly on the degree of unsaturation and the FFA value. Compared with other traditional techniques, ^{1}H NMR and FTIR combined with chemometrics provide a fast and economical method for RFO characterization, classification, and authentication.

4.3 Quantitative ^{1}H NMR Spectroscopy Combined with Chemometrics as a Profiling and Estimation Tool for Unsaturated Fatty Acid Composition in Red Fruit Oil and its commercial products

According to the NMR protocol reported by Maninna et al.[15], each signal intensity of the selected ^{1}H NMR spectra that correlated with the determination of PUFA and Total UFA was measured and submitted to chemometric analysis. A complete assignment of the desired RFO signal spectrum for calculating PUFA, Total UFA, and MUFA was obtained by addition of linoleic acid. The selected signals were necessary and showed strong characteristics at δ = 2.81-2.70 ppm for PUFA and δ = 2.10-1.90 ppm for total UFA and MUFA. Subsequently,

applying comparison of both methods (internal standard with relative method) indicates that the results of the determination of PUFA, Total UFA, and MUFA using internal standard method are similar to the relative method based on R^2 above 0.90 and low standard error results of regression statistic. Therefore, the quantitative method of ^{1}H NMR by means of the usage of the internal standard has strong potential as an alternative for determining PUFA, Total UFA, and MUFA. In addition, the use of internal standards also provides added value because it can be a more practical and uniform calculation formula compared to the relative method.

Furthermore, the satisfactory quality of the PCA plots was indicated by the full 99% PC being able to visualize the grouping of each variable. As for the excellent PLS quality achieved in the calibration model, validation and prediction for PUFA, Total UFA, and MUFA in the whole sample are based on a small root mean error square and a determination coefficient (R^2) of more than 0.90 for all models. This finding is in line with expected results because a proton shift of the studied fatty acids in the signal region is characteristic for the -C$\underline{H}_2$-CH=CH- signal and -CH=CH-C$\underline{H}_2$-CH=CH- of the PUFA and MUFA structures[14]. Therefore, the prediction of PUFA and MUFA compositions suitable for VCO, OVO, BSO, and RFO may indicate the potential authenticity of an RFO product or the presence or absence of adulterants as the addition of other oils on purpose, as has been discussed by Giese et al. [12] and Ravaglia et al.[14]

It should also be emphasized that the ^{1}H NMR experiment can be performed significantly faster. In addition, the association with PCA and PLS makes the process easier and effective. The proposed ^{1}H NMR method is promising, but further development should be carried out to obtain a more robust model, use more samples, and extend this study to other edible oils.

4.4 Overall Conclusion

In general, NMR spectroscopy is a fast and non-destructive technique for which only simple and small sample preparation is required. Contrary to classical wet chemistry methods, the ^{1}H

NMR measurement requires only a small solvent volume and no toxic chemicals such as IBr. The major profit of the NMR method is time-saving. The measurement of one sample by ^{1}H NMR spectroscopy takes about 15 minutes. At first glance, this seems quite lengthy compared to the titration procedure. However, it must be considered that NMR experiments can be run automatically (autosampler). From one ^{1}H NMR spectra, different analytical parameters of fats or oils can be obtained simultaneously, including AV, SV, EV, and IV, as well as distribution of the main unsaturated fatty acid contents. These parameters are important in the assessment of oil quality. In addition, adulteration of RFO with another edible oil can also be disclosed using chemometrics methods. As expected, PCA gave satisfactory and fast results for visualization grouping quality RFO based on unsaturated degree, FFA and unsaturated fatty acid content. PLS also succeeded in proving the prediction of the value of these parameters (unsaturated degree, FFA, polyunsaturated fatty acid, monounsaturated fatty acid and total unsaturated fatty acid contents) on each product accurately and precisely. With regard to time cost, it should be mentioned, that the data of entire NMR spectra can automatically be loaded to the chemometrics software, such as the Unscramble. Hence the PCA and PLS calculations are very fast (approximately 10 min).

However, despite these benefits, NMR spectroscopy has not been widely used and has not been established in routine analysis of fats and oils. One reason might be that, until recently, NMR spectroscopy was not part of the classic laboratory equipment that performs lipid analysis. The technique required investment and maintenance costs and a skilled operator. Because the quality parameters with the classical method can be less sensitivity and time consuming, especially in samples with unique characteristics, it seems reasonable to replace the method with a directly determinable NMR method as described in this thesis. In the future the application of the less expensive and smaller benchtop NMR instruments should be checked in order to disseminate the NMR method for quality evaluation.

References

1. Fulmer GR, Miller AJM, Sherden NH, Gottlieb HE, Nudelman AB, Stoltz M, Bercaw JE, Goldberg KI NMR. 2010. Chemical shifts of trace impurities: Common laboratory solvents, organics, and gases in deuterated solvents relevant to the organometallic chemist. *Organometallics* 29(9):2176–2179. https://doi.org/10.1021/om100106e
2. Giraudeau P, Tea I, Remaud GS, Akoka S. 2014. Reference and normalization methods: Essential tools for the intercomparison of NMR spectra. *J. Pharm. Biomed. Anal*. 93:3-16. https://doi.org/10.1016/j.jpba.2013.07.020
3. Wells RJ, Cheung J, Hook JM. 2004. Dimethylsulfone as a universal standard for analysis of organics by QNMR. *Accredit. Qual. Assur*. 9(8): 450–456. https://doi.org/10.1007/s00769-004-0779-0
4. Abraham RJ, Byrne JJ, Griffiths L, Perez M. 2006. ^{1}H chemical shifts in NMR: Part 23, the effect of dimethyl sulphoxide versus chloroform solvent on ^{1}H chemical shifts. *Magn. Reson. Chem*. 44(5): 491–509. https://doi.org/10.1002/mrc.1747
5. Beyer T, Schollmayer C & Holzgrabe, U. 2010. The role of solvents in the signal separation for quantitative ^{1}H NMR spectroscopy. *J. Pharm. Biomed. Anal*. 52(1): 51–58. https://doi.org/10.1016/j.jpba.2009.12.007
6. Nieva-Echevarría B, Goicoechea E, Manzanos MJ, Guillén MD. 2014. A method based on ^{1}H NMR spectral data useful to evaluate the hydrolysis level in complex lipid mixtures. *Food Res*. *Int.* 66: 379–387. https://doi.org/10.1016/j.foodres.2014.09.031
7. Kan RO. 1964. A Correlation of Chemical Shifts with Inductive Effect Parameters. *J. Am. Oil Chem. Soc*. 86(23): 5180–5183. https://doi.org/10.1021/ja01077a029
8. Miyake Y, Yokomizo K, Matsuzaki N. 1998. Determination of unsaturated fatty acid composition by high-resolution nuclear magnetic resonance spectroscopy. *J. Am. Oil Chem. Soc.* 75: 1091–1094

9. Jović O, Smolić T, Primožič I, Hrenar T. 2016. Spectroscopic and Chemometric Analysis of Binary and Ternary Edible Oil Mixtures: Qualitative and Quantitative Study. *Anal. Chem.* 88(8): 4516–4524. https://doi.org/10.1021/acs.analchem.6b00505
10. Schönberger T, Monakhova YB, Lachenmeier DW, Walch S, Kuballa T, (NEXT) -NMR working group. EUROLAB Technical Report 01/2015. 2016. Guide to NMR Method Development and Validation-Part II: Multivariate data analysis. (01):1–20. https://doi.org/10.13140/RG.2.1.4265.1289
11. Ingallina C, Cerreto A, Mannina L, Circi S, Vista S, Capitani D, Marini F. 2019. Extra-virgin olive oils from nine italian regions: An ^{1}H NMR-chemometric characterization. *Metabolites.* 9(4): 1-12. https://doi.org/10.3390/metabo9040065
12. Giese E, Rohn S, Fritsche J. 2019. Chemometric tools for the authentication of cod liver oil based on nuclear magnetic resonance and infrared spectroscopy data. *Anal. Bioanal. Chem.* 411(26): 6931–6942. https://doi.org/10.1007/s00216-019-02063-y
13. Parker T, Limer E, Watson AD, Defernez M, Williamson D, Kemsley EK. 2014. 60 MHz ^{1}HNMR spectroscopy for the analysis of edible oils. *TrAC - Trends Anal. Chem.* 57: 147.158. https://doi.org/10.1016/j.trac.2014.02.006
14. Ravaglia LM, Pizzotti ABC, Alcantara GB. 2019. NMR-based and chemometric approaches applicable to adulteration studies for assessment of the botanical origin of edible oils**.** *J. Food Sci. Technol.* 56(1): 507–511. https://doi.org/10.1007/s13197-018-3485-3
15. Mannina L, Marini F, Gobbino M, Sobolev AP, Capitani D. 2009. NMR and chemometrics in tracing European olive oils: the case study of Ligurian samples. *Talanta*. 80: 2141–2148. https://doi.org/10.1016/j.talanta.2009.11.021

5. SUMMARY

Today's priority in pharmaceutical and food analysis is to have analytical methods available with optimal speed and effectiveness without losing precision and accuracy. One continuously developing and promising method to overcome this challenge is quantitative nuclear magnetic resonance (qNMR) spectroscopy. Although the cost of NMR equipment is relatively high and requires operator experience, the qNMR method has many advantages over other analytical methods. ^{1}H NMR spectroscopy is a reliable qualitative method because it produces structural information. Additionally, the proportionality of signal intensity to the number of nuclei can be obtained with appropriate experimental NMR parameters, allowing its use for quantification.

In this thesis, a new approach of a qNMR method has been investigated to demonstrate the reliability and importance of this method as an alternative solution for analyzing oil quality parameters, especially in RFO, which has particular characteristics (red color). This study also includes the chemometric evaluation of spectral data for authentication, visual grouping, and prediction of RFO quality based on the degree of unsaturation, FFA value, and unsaturated fatty acid content.

The analytical measurement procedure of NMR spectroscopy begins with optimization of the analytical acquisition parameters, including effect of solvent, effect of sample concentration, selection of appropriate internal standards, determination of T1, and method validation. Furthermore, the results of the method development were interpreted to RFO samples evaluation, which began with determining the assignment of signal spectra for the determination of AV, SV, EV, and IV simultaneously with: the hydrolysis approach and standard addition of palmitic acid.

For the simultaneous determination of the AV, EV, IV, and SV in RFO with ^{1}H NMR spectroscopy, dimethyl sulfone ($DMSO_2$) was a suitable internal standard because it gaves a single signal which does not overlapp with the analyte signals. After deciphering the appropriate NMR parameters, diagnostic signals for quantification were determined including

internal standard at δ = 2.98 ppm, SV at δ= 2.37-2.20 ppm, AV at δ = 2.27-2.20 ppm, EV at δ = 2.37-2.27 ppm, and IV at δ = 5.37-5.27 ppm. The validated method produces good linearity and precision. The qNMR results for the respective fat values also are in accordance with the results of standard methods.

The application of chemometrics to ^{1}H NMR and FTIR spectra was also successfully carried out to develop an effective and efficient analytical method for quality assurance of RFO based on the degree of unsaturation and the value of free fatty acids. Necessary signals for modeling the degree of unsaturation are signals at δ = 5.37–5.27 ppm (^{1}H NMR) and bands at 3000-3020 cm^{-1} (FTIR). The FFA profiles are represented by signals at =2.37-2.20 ppm (^{1}H NMR) and bands at 1680-1780 cm^{-1} (FTIR). Pre-processing of both spectroscopic data (NMR & FTIR) is an important step to obtain a reliable variable matrix. For NMR spectra using 0.009 ppm bucketing while for FTIR spectra by means of second-order smoothing polynomials through 25 points (Savitzky-Golay method) without spectra derivation gave a satisfactory results. Therefore, PCA successfully demonstrated the visualization grouping of both methods with > 98% total PC for the degree of unsaturation and >88% total PC for the FFA value. In addition, the PLSR model also produces a good coefficient of determination (R^2) of more than 0.90, with a low RMSE (Calibration, Validation and Prediction).

Furthermore, the application of the ^{1}H NMR method using internal standards for quantifying the unsaturated fatty acid component in RFO also showed the potential of the method. Assignment of the signal responsible for quantification was shown with strong characteristics at δ = 2.80-2.71 ppm for PUFA and δ = 2.10 - 1.90 ppm for Total UFA and MUFA. By chemometric approach, each sample was successfully grouped according to its PUFA and Total UFA values and predicted for the unsaturated fatty acid component value of commercial RFO. This finding provides a very simple method for the quality assurance and authentication of RFO.

Therefore, it has been demonstrated in various projects that the development of a quantitative ^{1}H NMR spectroscopy method combined with a chemometric approach allows in-depth

findings and contributes to a clear added value as a reliable alternative to the compendial method (titration and GC spectroscopy) on simultaneous quantification and identification of the parameters AV, EV, IV, SV and an unsaturated fatty acid content for quality assurance and authentication of oil.

6. ZUSAMMENFASSUNG

In der pharmazeutischen und Lebensmittelanalytik geht es heute vorrangig darum, Analysemethoden mit optimaler Geschwindigkeit und Wirksamkeit zur tend zühaben ohne dabei an Präzision und Genauigkeit zu verlieren. Eine sich ständig weiterentwickelnde und vielversprechende Methode zur Bewältigung dieser Herausforderung ist die quantitative Kernspinresonanz-Spektroskopie (qNMR). Obwohl die Kosten für die NMR-Ausrüstung relativ hoch sind und Erfahrung des Bedieners erfordern, hat die qNMR-Methode viele Vorteile gegenüber anderen Analysemethoden. Die ^{1}H-NMR-Spektroskopie ist eine zuverlässige qualitative Methode, da sie Strukturinformationen liefert. Auf Grund der Proportionalität der Signalintensität zur Anzahl der Kerne (mit geeigneten experimentellen NMR-Parametern) kann quantifiziert werden.

In dieser Dissertation wurde ein neuer Ansatz der quantitativen NMR-Spektroskopie untersucht, um die Zuverlässigkeit und Bedeutung dieser Methode als alternative Lösung für die Analyse von Ölqualitätsparametern zu demonstrieren, insbesondere bei RFO, das besondere Merkmale (rote Farbe) aufweist. Diese Studie umfasst auch die chemometrische Auswertung von Spektraldaten zur Authentifizierung, visuellen Gruppierung und Vorhersage der RFO-Qualität auf der Grundlage des Ungesättigungsgrads, des freie Fettsäuren-Werts und des Gehalts an ungesättigten Fettsäuren.

Das analytische Messverfahren der NMR-Spektroskopie beginnt mit der Optimierung der analytischen Aufnahmeparameter, einschließlich der Auswirkung des Lösungsmittels, der Auswirkung der Probenkonzentration, der Auswahl geeigneter interner Standards, der Bestimmung von T1 und der Methodenvalidierung. Darüber hinaus wurden die Ergebnisse der Methodenentwicklung auf die Auswertung der RFO-Proben übertragen, die mit der Bestimmung der Zuordnung der Signalspektren für die Bestimmung von Säurezahl, Esterzahl, Jodzahl, Verseifungszahl gleichzeitig mit dem Hydrolyseansatz und der Standardaddition von Palmitinsäure begann.

Für die gleichzeitige Bestimmung von Säurezahl, Esterzahl, Jodzahl, und Verseifungszahl in RFO mit ^{1}H-NMR-Spektroskopie war Dimethylsulfon ($DMSO_2$) ein geeigneter interner Standard, da er ein einzelnes Signal liefert, das sich mit den Signalen der Analyten interferiert. Nach der Optimierung der NMR-Parameter wurden diagnostische Signale für die Quantifizierung erhalten, darunter der interne Standard bei δ = 2.98 ppm, Verseifungszahl bei δ = 2.37 - 2.20 ppm, Säurezahl bei δ = 2.27 - 2.20 ppm, Esterzahl bei δ = 2.37 - 2.27 ppm und Jodzahl bei δ = 5.37 - 5.27 ppm. Die validierte Methode weist eine gute Linearität und Präzision auf. Die qNMR-Ergebnisse für die jeweiligen Fettwerte stimmen ebenfalls mit den Ergebnissen der Standardmethoden überein.

Die Verwendung der Chemometrie auf ^{1}H-NMR und FTIR-Spektren war eine wirksame und effiziente Auswertemethode für die Qualitätssicherung von RFO auf der Grundlage des Ungesättigtheitsgrads und des Werts der freien Fettsäuren zu entwickeln. Die für die Modellierung des Ungesättigtheitsgrads erforderlichen NMR-Signale sind bei δ = 5.37 - 5.27 ppm (^{1}H NMR) und IR-Banden bei 3000-3020 cm^{-1} (FTIR). Die freie Fettsäuren-Profile werden durch Signale bei δ = 2.37 - 2.20 ppm (^{1}H NMR) und Banden bei 1680 - 1780 cm^{-1} (FTIR) dargestellt. Die Aufbereitung der beiden spektroskopischen Datensätze (NMR und FTIR) ist ein wichtiger Schritt, um eine zuverlässige variable Matrix zu erhalten. Bei den NMR-Spektren führte die Verwendung von 0.009 ppm ‘‘Bucketts“ und bei den FTIR-Spektren die Verwendung von Glättungspolynomen zweiter Ordnung über 25 Punkte (Savitzky-Golay-Methode) ohne Spektrenableitung zu zufriedenstellenden Ergebnissen. Daher zeigte die PCA erfolgreich die Visualisierungsgruppierung beider Methoden mit > 98% Gesamt-PC für den Grad der Ungesättigtheit und >88% Gesamt-PC für den FFA-Wert. Darüber hinaus ergibt das PLSR-Modell einen guten Bestimmtheitsgrad (R^2) von über 0.90 mit einem niedrigen RMSE (Kalibrierung, Validierung und Vorhersage).

Darüber hinaus zeigte die Anwendung der ^{1}H-NMR-Methode unter Verwendung interner Standards zur Quantifizierung der ungesättigten Fettsäurekomponente in RFO ebenfalls das Potenzial der Methode. Die Zuordnung des für die Quantifizierung verantwortlichen Signals

wurde bei δ = 2.80 - 2.71 ppm für mehrfach ungesättigte Fettsäure und δ = 2.10 – 1.90 ppm für insgesamt ungesättigte Fettsäure und einfach ungesättigte Fettsäure gezeigt. Mit dem chemometrischen Ansatzes wurde jede Probe erfolgreich nach ihren Gehalte an mehrfach ungesättigten Fettsäuren und für den Gesamtgehalt an ungesättigten Fettsäuren gruppiert und der Gehalt an ungesättigten Fettsäurekomponente des kommerziellen RFO vorhergesagt. Dieses Ergebnis bietet eine sehr einfache Methode für die Qualitätssicherung und Authentifizierung von RFO.

In verschiedenen Projekten konnte somit gezeigt werden, dass die Entwicklung einer quantitativen ^{1}H-NMR-Spektroskopie-Methode in Kombination mit einem chemometrischen Ansatz tiefgreifende Erkenntnisse ermöglicht und zu einem deutlichen Mehrwert als zuverlässige Alternative zur Kompendienmethode (Titration und GC-Spektroskopie) bei der gleichzeitigen Quantifizierung und Identifizierung der Parameter von Säurezahl, Esterzahl, Jodzahl, Verseifungszahl und des Gehalts an ungesättigten Fettsäuren zur Qualitätssicherung und Authentifizierung von Öl beiträgt.

7. APPENDIX

7.1. List of publications

Research papers

1. Triyasmono L, Schollmayer C, Schmitz J, Hovah E, Lombo C, Schmidt S, Holzgrabe U. Simultaneous determination of the Saponification Value, Acid Value, Ester Value, and Iodine Value in commercially available Red Fruit Oil (*Pandanus conoideus*, Lam.) using ^{1}H qNMR spectroscopy. *Food Anal. Method* (2022), 1-13.
2. Triyasmono L, Schollmayer C, Holzgrabe U. Chemometric analysis applied to ^{1}H NMR and FTIR data for a quality parameter distinction of Red Fruit (*Pandanus conoideus*, Lam.) Oil products. (accepted to *Phytochem. Anal*. (2022))
3. Triyasmono L, Schollmayer C, Holzgrabe U. Quantitative ^{1}H NMR Spectroscopy Combined with Chemometrics as a Profiling and Estimation Tool for Unsaturated Fatty Acid Composition in Red Fruit Oil and its commercial products. (submitted and under review) to *Eur. J. Lipid Sci. Technol*. (2022))

7.2. Documentation of authorship

In this section, the individual contribution for each author to the publications reprinted in this thesis is specified. Submitted manuscripts are handled, accordingly.

Julius-Maximilians-
UNIVERSITÄT
WÜRZBURG

Fakultät für
CHEMIE UND
PHARMAZIE

Erklärung zur Autorenschaft

Simultaneous determination of the Saponification Value, Acid Value, Ester Value, and Iodine Value in commercially available Red Fruit Oil (*Pandanus conoideus*, Lam.) using ^{1}H qNMR spectroscopy

Detaillierte Darstellung der Anteile an der Veröffentlichung (in %)
Angabe Autoren/innen (ggf. Haupt- / Ko- / korrespondierende/r Autor/in) mit Vorname Nachname (Initialen)

Autor/in 1 (LT) Autor/in 2 (CS), Autor/in 3 (JS), Autor/in 4 (EH), Autor/in 5 (CL), Autor/in 6 (SS), Autor/in 7 (UH)

Autor	LT	CS	JS	EH	CL	SS	UH	∑ in Prozent
Studydesign	7						3	10%
Experimentelle Arbeit	20	3		1	1	1		26%
Datenanlysis-und Interpetration	20	2	2	1	1	1	2	29%
Verfassen der Veröffentlichung	20	1	1			1	2	25%
Korrektur der Veröffentlichung			1				4	5%
Koordination der Veröffentlichung							5	5%
Summe	67	6	4	2	2	3	16	100%

Julius-Maximilians-
UNIVERSITÄT
WÜRZBURG

Fakultät für
CHEMIE UND
PHARMAZIE

Die Mitautoren der in dieser (teil-)kumulativen Dissertation verwendeten Manuskripte sind sowohl über die Nutzung als auch über die angegebenen Eigenanteile informiert und stimmen dem zu.

Liling Triyasmono

Autor/in 1 (LT)

Hauptautor/in

☒ Verweis: E-Mail hinterlegt

Curd Schollmayer

Autor/in 2 (CS)

Koautor/in

☒ Verweis: E-Mail hinterlegt

Jens Schmitz

Autor/in 3 (JS)

Koautor/in

☒ Verweis: E-Mail hinterlegt

Emilie Hovah

Autor/in 4 (EH)

Koautor/in

☒ Verweis: E-Mail hinterlegt

Cristian Lombo

Autor/in 5 (CL)

Koautor/in

☒ Verweis: E-Mail hinterlegt

Sebastian Schmidt

Autor/in 6 (SS)

Koautor/in

☒ Verweis: E-Mail hinterlegt

Ulrike Holzgrabe

Autor/in 7 (UH)

Korrespondenzautor/in

☒ Verweis: E-Mail hinterlegt

Würzburg, 01.12.2022 _____

Prof. Dr. Ulrike Holzgrabe

Julius-Maximilians-
UNIVERSITÄT
WÜRZBURG

Fakultät für
CHEMIE UND
PHARMAZIE

Erklärung zur Autorenschaft

Chemometric analysis applied to ^{1}H NMR and FTIR data for a quality parameter distinction of Red Fruit (*Pandanus conoideus*, Lam.) Oil products

Detaillierte Darstellung der Anteile an der Veröffentlichung (in %)

Angabe Autoren/innen (ggf. Haupt- / Ko- / korrespondierende/r Autor/in) mit Vorname Nachname (Initialen)

Autor/in 1 (LT) Autor/in 2 (CS), Autor/in 3 (UH)				
Autor	**LT**	**CS**	**UH**	**∑ in Prozent**
Studydesign	7		3	10%
Experimentelle Arbeit	20	3		23%
Datenanlysis-und Interpetration	23	5	2	30%
Verfassen der Veröffentlichung	20	2	5	27%
Korrektur der Veröffentlichung			5	5%
Koordination der Veröffentlichung			5	5%
Summe	70	10	20	100%

Julius-Maximilians-
UNIVERSITÄT
WÜRZBURG

Fakultät für
CHEMIE UND
PHARMAZIE

Die Mitautoren der in dieser (teil-)kumulativen Dissertation verwendeten Manuskripte sind sowohl über die Nutzung als auch über die angegebenen Eigenanteile informiert und stimmen dem zu.

Liling Triyasmono	Curd Schollmayer	Ulrike Holzgrabe
Autor/in 1 (LT)	Autor/in 2 (CS)	Autor/in 3 (UH)
Hauptautor/in	**Koautor/in**	**Korrespondenzautor/in**
☒ Verweis: E-Mail hinterlegt	☒ Verweis: E-Mail hinterlegt	☒ Verweis: E-Mail hinterlegt

Würzburg, 01.12.2022 _____

Prof. Dr. Ulrike Holzgrabe

Julius-Maximilians-
UNIVERSITÄT
WÜRZBURG

Fakultät für
CHEMIE UND
PHARMAZIE

Erklärung zur Autorenschaft

Quantitative ^{1}H NMR Spectroscopy Combined with Chemometrics as a Profiling and Estimation Tool for Unsaturated Fatty Acid Composition in Red Fruit Oil and its commercial products

Detaillierte Darstellung der Anteile an der Veröffentlichung (in %)

Angabe Autoren/innen (ggf. Haupt- / Ko- / korrespondierende/r Autor/in) mit Vorname Nachname (Initialen)

Autor/in 1 (LT) Autor/in 2 (CS), Autor/in 3 (UH)				
Autor	**LT**	**CS**	**UH**	**∑ in Prozent**
Studydesign	7		3	10%
Experimentelle Arbeit	23	2		25%
Datenanlysis-und Interpetration	25	3	2	30%
Verfassen der Veröffentlichung	17	2	6	25%
Korrektur der Veröffentlichung			5	5%
Koordination der Veröffentlichung			5	5%
Summe	72	7	21	100%

Julius-Maximilians-
UNIVERSITÄT
WÜRZBURG

Fakultät für
CHEMIE UND
PHARMAZIE

Die Mitautoren der in dieser (teil-)kumulativen Dissertation verwendeten Manuskripte sind sowohl über die Nutzung als auch über die angegebenen Eigenanteile informiert und stimmen dem zu.

Liling Triyasmono	Curd Schollmayer	Ulrike Holzgrabe
Autor/in 1 (LT)	Autor/in 2 (CS)	Autor/in 3 (UH)
Hauptautor/in	**Koautor/in**	**Korrespondenzautor/in**
☒ Verweis: E-Mail hinterlegt	☒ Verweis: E-Mail hinterlegt	☒ Verweis: E-Mail hinterlegt

Würzburg, 01.12.2022 _____

Prof. Dr. Ulrike Holzgrabe